

## AN ABSTRACT OF THE THESIS OF

Kenneth Edward Milligan III for the degree of Doctor of Philosophy in Pharmacy  
presented on October 10, 2001. Title: Marine Algal Secondary Metabolites of Unique  
Structure and Biomedicinal or Agrichemical Potential.

# Redacted for Privacy

Abstract approved: \_\_\_\_\_

William H. Gerwick

This thesis describes investigations of marine algal secondary metabolites, with particular interest in their biomedical and agrichemical potential. Invaluable in such pursuits have been the access and application of advanced spectroscopic techniques, such as NMR, and the ability to assess the biological activity of the algal samples in a variety of diverse protocols, through in-house evaluation and industrial collaborations.

As an in-house bioassay, a survey of algal extracts for molluscicidal activity has led to the isolation of the previously reported chondrocole C (*Portieria bornemanni*), tanikolide (*Lyngbya majuscula*), and debromoaplysiatoxin (*L. majuscula*).

Debromoaplysiatoxin is 100 times more potent than niclosamide, the commercially utilized molluscicide.. Such activity may make debromoaplysiatoxin an attractive agent for molluscan biological control to prevent the spread of schistosomiasis in artificial waterways such as irrigation channels and rice paddies.

The isolation of chondrocole C led to further chemical investigations of *P. bornemanni*. A total of six related polyhalogenated monoterpenes were isolated from

this collection. While four of these compounds were previously reported, taviochtodene represents the newest member of this class of secondary metabolites. Previously, this alga has yielded compounds with great potential anticancer utility, but naturally and synthetically elusive. The discovery of this class of chemistry potentially locates new geographic territory to search for such anticancer metabolites.

While there has been little reported biological activity attributed to the malyngamides, they form the most prevalent class of secondary metabolites isolated from *Lyngbya majuscula*. To this list we have added malyngamides L, Q, and R. Of particular note, malyngamides Q and R were the first malyngamides to have been reported with altered stereochemistry at the vinyl chloride carbon. Subsequently, and in part stimulated by this finding, this alternate stereochemistry has been defined for some newly reported malyngamides.

Also from *L. majuscula*, tortugin and lyngbyabellin B were isolated as toxic cyclic depsipeptides. Both of these compounds displayed relatively potent biological activity (brine shrimp and antifungal). Each possessing particular structural motifs previously seen in invertebrate secondary metabolites, they lend further evidence for cyanobacteria as the producer of many of the polyhalogenated compounds often attributed to *de novo* invertebrate biosynthesis.

<sup>(c)</sup>Copyright by Kenneth E. Milligan III

October 10, 2001

All Rights Reserved

MARINE ALGAL SECONDARY METABOLITES OF UNIQUE STRUCTURE AND  
BIOMEDICINAL OR AGRICHEMICAL POTENTIAL

by

Kenneth Edward Milligan III

A THESIS

submitted to

Oregon State University

in partial fulfillment of

the requirements for the

degree of

Doctor of Philosophy

Presented October 10, 2001

Commencement June 2002

Doctor of Philosophy thesis of Kenneth Edward Milligan III presented on October 10, 2001.

APPROVED:

Redacted for Privacy

---

Major Professor, representing Pharmacy

Redacted for Privacy

---

Dean of College of Pharmacy

Redacted for Privacy

---

Dean of Graduate School

I understand that my thesis will become part of the permanent collection of Oregon State University libraries. My signature below authorizes release of my thesis to any reader upon request.

Redacted for Privacy

---

Kenneth Edward Milligan III, Author

## ACKNOWLEDGMENTS

First, I would like to thank Dr. William H. Gerwick, my major professor, for his guidance, mentorship, patience, and friendship, and for inviting me into his laboratory to fulfill my academic aspirations. My thanks also go to the members of my committee, Dr. George Constantine, Dr. Philip Proteau, Dr. Ajoy Velayudhan, and Dr. Joseph Spatafora for their insight, suggestions, time, and assistance in the completion of my program.

For all the assistance I have received from the College of Pharmacy office staff, faculty, and administration, I am very grateful. I would also like to thank Ika Fifita for all of the effort and care he showed for myself and all the students of the College of Pharmacy during his tenure here. I am also grateful for the help of Rodger Kohnert (Dept. Chemistry NMR), Brian Arbogast (Dept. of Chemistry EIHMS), and the laboratory of Dr. Victor Hsu (600 MHz NMR). I must also recognize the Graduate School for their useful advice and kindness while constructing this thesis.

I feel fortunate to have shared this experience with all the members of Dr. Gerwick's laboratory, past and present; I wish I had the space to list each of you by name with my special thanks. I need to specifically mention Dr. Brian Marquez, Dr. Thomas Williamson, and Jim Rossi for their friendship and all that I have learned from each of them. I would also like to thank all of my friends from the pharmacy building and from around Corvallis.

Last, and certainly not least, I am thankful beyond words for the support of my family, both in Corvallis and Rhode Island, and my wife, Shelley. All your love has buoyed me in all my pursuits. Thank you.

## CONTRIBUTION OF AUTHORS

Chapter II. Many of the molluscicidal screening assays were performed by Evan Mix, who, while attending Corvallis High School worked in our laboratory. Tanikolide was isolated and characterized by Dr. I.P. Singh while a Post-Doctoral Fellow in Dr. Gerwick's laboratory.

Chapter IV. Min Wu, co-author on the work describing malyngamide L, isolated and characterized malyngamides J and K. Dr. Michael Davies-Coleman facilitated and participated in the original collections which yielded malyngamides Q and R and shared in the scholarship of that paper during a visit to OSU.

Chapter III, IV, and V. Most of the sophisticated NMR experiments present in these chapters have been either accomplished by, programmed by, or inspired by Dr. Brian L. Marquez and Dr. R. Thomas Williamson.

## TABLE OF CONTENTS

CHAPTER I.	GENERAL INTRODUCTION	1
	Marine Natural Products Chemistry	3
	The Algal Divisions	6
	Human Uses of Algae	12
	Thesis Statement	18
	General Thesis Content	18
	References	22
CHAPTER II.	MOLLUSCICIDAL ACTIVITY IN MARINE ALGAL EXTRACTS; A SURVEY AND CHEMICAL INVESTIGATION OF PROMISING MOLLUSCICIDAL ALGAL EXTRACTS	
	Abstract	25
	Introduction	26
	Results and Discussion	37
	Experimental	59
	References	63
CHAPTER III.	HALOGENATED MONOTERPENES ISOLATED FROM THE FIJIAN RED ALGA <i>PORTIERLA HORNEMANNI</i> .	
	Abstract	65
	Introduction	66
	Results & Discussion	74
	Experimental	97
	References	100



## TABLE OF CONTENTS (CONTINUED)

### CHAPTER IV. ISOLATION AND STRUCTURE ELUCIDATION OF THREE NEW MALYNGAMIDES FROM THE MARINE CYANOBACTERIUM, *LYNGBYA MAJUSCULA*.

Abstract	101
Introduction	102
Results and Discussion	113
Experimental	146
References	153

### CHAPTER V. THE ISOLATION AND STRUCTURE ELUCIDATION OF LYNGBYABELLIN B AND TORTUGIN: SUPPORT FOR THE CYANOBACTERIAL ORIGIN OF SEVERAL MOLLUSCAN CYCLIC DEPSIPEPTIDES

Abstract	153
Introduction	154
Results and Discussion	164
Experimental	193
References	199

### CHAPTER VI. SUMMARY 201

### BIBLIOGRAPHY 215

## LIST OF FIGURES

Figure	Page
I.1. Selected natural product drugs in common use.	2
I.2. Facts about the ocean that stimulated the pursuit of marine natural products chemistry.	6
I.3. Selected examples of marine natural products with potential medicinal or research utility.	8
I.4. The chemical structures of marine natural products with potential medicinal or research utility.	9
I.5. A comparison of the characteristics of the four major divisions of algae.	11
II.1. The five spp. of schistosomiasis causing trematodes.	27
II.2. The schistosome life cycle.	29
II.3. Methods used, or proposed, to control the spread of schistosomiasis.	31
II.4. Praziquantel (27), oxamniquine (28), and metrifonate (29), three chemotherapeutic agents used to treat schistosomiasis infection, and niclosamide (30), the most common commercially utilized molluscicidal agent.	35
II.5. Schistosomiasis "The Scourge of Developing Nations". Irrigation Systems & Dams can result in stagnant water, recycling of wastewater, and increased water temperature and have led to marked increases in schistosomiasis transmission in some instances.	35
II.6. The molluscicidal bioassay protocol, (A) add 9900 µl of H <sub>2</sub> O to scintillation vial, (B) add 100 µl of premade test solution, (C) add a pair of <i>B. glabrata</i> snails, (D) lightly cap and allow 24 hr then examine for snail toxicity.	38
II.7.a. The taxonomic distribution of algal extracts represented in the molluscicidal screening assay.	43

## LIST OF FIGURES (CONTINUED)

Figure	Page
II.7.b. The molluscicidal activity of algal crude extracts at 50 ppm.	43
II.8. Division breakdown of molluscicidal extracts at 100 and 50 ppm.	45
II.9. Molluscicidal Cyanobacteria Crude Extracts at 100 and 50 ppm.	46
II.10. Molluscicidal Chlorophyte crude extracts at 100 and 50 ppm.	46
II.11. Molluscicidal Rhodophyte crude extracts at 100 and 50 ppm.	47
II.12. Molluscicidal Phaeophyte crude extracts at 100 and 50 ppm.	47
II.13. The isolation of the molluscicide chondrocole C ( <b>31</b> ).	50
II.14. The isolation of the molluscicide tanikolide ( <b>32</b> ).	50
II.15. Graphical representation of <b>20</b> on TLC.	52
II.16. The isolation of the molluscicide debromoaplysiatoxin ( <b>20</b> ) and the inactive lyngbic acid ( <b>33</b> ).	54
II.17. Molluscicidal Activity of debromoaplysiatoxin ( <b>20</b> ) and PME ( <b>34</b> ). Calculated errors are; for <b>20</b> , +/- 13.7% at 5 nM and +/- 22.4% at 6.7 nM; for <b>34</b> , +/- 22.4% for 100 and 800 nM concentrations and +/- 35.4% at 400 nM.	56
II.18. Molluscicidal Activity of debromoaplysiatoxin ( <b>20</b> , DBX) and PMA ( <b>34</b> ) in the presence of PKC Inhibitor (MPKCI). All deviations = 0 except for DBX w/MPKCI, which = +/- 22.3).	57
II.19. Molluscicidal Activity of debromoaplysiatoxin ( <b>20</b> , DBX) at 1 and 2 hr.	57
III.1. The four major skeletal arrangements isolated from <i>Portieria</i> and <i>Ochtodes</i> spp.	67
III.2. Representative ochtadanes isolated from <i>Portieria</i> and <i>Ochtodes</i> spp. Structures <b>43a</b> & <b>43b</b> and <b>44a</b> & <b>44b</b> are stereoisomers that have yet to have their stereochemistries fully elucidated.	68
III.3. Dimethyloctanes isolated from <i>Portieria</i> and <i>Ochtodes</i> spp.	69

## LIST OF FIGURES (CONTINUED)

Figure	Page
III.4. Chondrocoles isolated from <i>Portieria</i> and <i>Ochtodes</i> spp.	70
III.5. Mass spectral isotope cluster patterns observed for halogenated compounds.	70
III.6. GC/MS of chondrocole C.	75
III.7. $^1\text{H}$ NMR of chondrocole C.	77
III.8. $^{13}\text{C}$ NMR of chondrocole C.	78
III.9. HMBC of chondrocole C.	79
III.10. Proposed long-range correlations for chondrocole C using the chemical shift assignments as in the literature.	81
III.11. HSQC of chondrocole C.	82
III.12. Long-range correlations observed for chondrocole C with revised chemical shift assignment.	83
III.13. GC/MS of taviochtodene.	84
III.14. $^1\text{H}$ NMR spectrum of taviochtodene.	85
III.15. HSQC of taviochtodene.	87
III.16. HMBC of taviochtodene.	88
III.17. Key HMBC correlations used to define taviochtodene (65).	89
III.18. Hypothetical compound ( $m/z = 216$ ) demonstrating the empirical observations that, in GC/MS, structural data can be obtained for halogenated compounds even when the halogen is too labile for mass spectral detection.	96
IV.1. The lyngbic acids.	104
IV.2. The pyrrolidone-type subclass of malyngamides.	105

## LIST OF FIGURES (CONTINUED)

Figure	Page
IV.3. The cyclohexyl malyngamides	106
IV.4. Non-standard malyngamides.	107
IV.5. Common structural motifs of malyngamide amino portion.	108
IV.6. Malyngamide biogenesis (80).	111
IV.7. LREIMS of malyngamide L (80).	114
IV.8. $^1\text{H}$ NMR spectrum of malyngamide L (80).	115
IV.9. $^{13}\text{C}$ NMR spectrum of malyngamide L (80).	116
IV.10. $^1\text{H}$ - $^1\text{H}$ COSY of malyngamide L (80).	117
IV.11. DEPT of malyngamide L (80).	118
IV.12. Partial structures of malyngamide L (80).	119
IV.13. LRFABMS of malyngamide Q (70).	122
IV.14. $^1\text{H}$ NMR spectrum of malyngamide Q (70).	124
IV.15. $^{13}\text{C}$ NMR of malyngamide Q (70).	125
IV.16. HMQC spectrum of malyngamide Q (70).	126
IV.17. $^1\text{H}$ - $^1\text{H}$ COSY of malyngamide Q (70).	127
IV.18. HMBC spectrum of malyngamide Q (70).	128
IV.19. Partial Structures of Malyngamide Q (70).	129
IV.20. LRFABMS of malyngamide R (71).	133
IV.21. $^1\text{H}$ NMR spectrum of malyngamide R (71).	134
IV.22. $^{13}\text{C}$ NMR spectrum of malyngamide R (71).	135
IV.23. HMQC spectrum of malyngamide R (71).	136

## LIST OF FIGURES (CONTINUED)

Figure	Page
IV.24. HMBC spectrum of malyngamide R (71).	137
IV.25. Suppression of signals arising from $^1\text{H}$ - $^{12}\text{C}$ by Bird Sandwich NMR pulse sequence allowing observation of $^3\text{J}_{\text{H}4'-\text{H}5'} \text{ } ^1\text{H}$ - $^{13}\text{C}$ coupling = 16 Hz, and therefore defining the C4'-C5' olefin as trans.	138
IV.26. Malyngamide R (71) with important NOE correlations shown.	138
IV.27. DPGFSE NOE spectra of malyngamide R (71).	140
IV.28. HSQMBBC spectra highlighting the long range heteronuclear coupling between H-6 and C-4 & 7 of malyngamide R (71).	142
IV.29. HSQMBBC correlations for malyngamide R (71), F (76), and I (78), confirming the geometry of the vinyl chloride.	144
V.1. Cyanobacterial cyclic peptides.	155
V.2. Examples of the dolastatins, invertebrate derived secondary metabolites.	157
V.3. Structural units shared by the dolastatins and cyanobacterial secondary metabolites.	158
V.4. The molluscan derived secondary metabolite dolabellin (108) appears to be closely related to the <i>L. majuscula</i> metabolites lyngbyabellin A (95) and B (96) and hectochlorin (97).	159
V.5. $\beta$ -hydroxy and amino octynoic acids found in some cyanobacterial cyclic peptides.	160
V.6. Secondary metabolites isolated from marine invertebrates which either bear strong resemblance to cyanobacterial compounds or have also been isolated from a cyanobacterial source.	162
V.7. LREIMS of lyngbyabellin B (96).	165

## LIST OF FIGURES (CONTINUED)

Figure	Page
V.8. $^1\text{H}$ NMR spectrum of lyngbyabellin B (96).	166
V.9. $^{13}\text{C}$ NMR spectrum of lyngbyabellin B (96).	167
V.10. HSQC spectrum of lyngbyabellin B (96).	168
V.11. $^1\text{H}$ - $^1\text{H}$ HSQC-TOCSY spectrum of lyngbyabellin B (96).	169
V.12. HSQC spectrum of lyngbyabellin B (96).	170
V.13. $^1\text{H}$ - $^{15}\text{N}$ -PEP- HSQC-TOCSY spectrum of lyngbyabellin B (96).	171
V.14. Partial structures of lyngbyabellin B (96).	174
V.15. Key HMBC correlations used in the sequencing of partial structures A-G of lyngbyabellin B (96).	174
V.16. FABMS of tortugin (101).	178
V.17. $^1\text{H}$ NMR spectrum of tortugin (101).	180
V.18. $^{13}\text{C}$ NMR spectrum of tortugin (101).	181
V.19. HSQC-TOCSY of tortugin (101).	182
V.20. HSQC of tortugin (101).	183
V.21. HMBC of tortugin (101).	184
V.22. $^1\text{H}$ - $^{15}\text{N}$ PEP-HSQC-TOCSY of tortugin (101). The correlations representing the non-NMe amino acid residues of the two conformers are contained within the boxes.	185
V.23. Partial structures of tortugin (101).	188
V.24. Assembling the partial structures of tortugin (101).	188

## LIST OF FIGURES (CONTINUED)

Figure	Page
V.25. The four stereoisomers of HMPA, the synthesis of L-allo and D-allo-HMPA, and the synthesis of menthyl carbonates for GC/MS analysis (MCC = Menthoxycarbonyl chloride).	191
V.26. GC/MS analysis of MCC derivatized HMPAs and tortugin ( $t_R$ = retention time). <b>A.</b> L and D-HMPA-MCC ( $t_R$ 20.70 and 20.95, respectively). <b>B.</b> L-HMPA-MCC ( $t_R$ 20.70). <b>C.</b> L-allo-HMPA-MCC ( $t_R$ 20.37). <b>D.</b> D-allo-HMPA-MCC ( $t_R$ 20.80). <b>E.</b> HMPA-MCC (from tortugin, $t_R$ 20.70). <b>F.</b> Tortugin HMPA-MCC and L-allo-HMPA-MCC coinjection. <b>G.</b> Tortugin HMPA-MCC and D-allo-HMPA-MCC coinjection. <b>H.</b> Tortugin-HMPA-MCC and L/D-HMPA-MCC coinjection. Notice the increase in L-HMPA. <b>I.</b> Tortugin-HMPA-MCC and L-HMPA-MCC coinjection.	192
VI.1. Newly reported secondary metabolites from marine algae presented within this thesis.	203
VI.2. Molluscicidal metabolites isolated from marine algal extracts.	205
VI.3. The chemical shift re-assignment of chondrocole C.	206
VI.4. Hypothetical compound (mw = 216) supporting empirical observation that structural data can be obtained for halogenated compounds even when the halogen is too labile for mass spectral detection.	207
VI.5. HSQMBBC spectra highlighting the long range heteronuclear coupling between H-6 and C-4 & 7 of malyngamide R.	209
VI.6. Malyngamide biogenesis.	210
VI.7. The molluscan derived secondary metabolite dolabellin appears to be closely related to the <i>L. majuscula</i> metabolites lyngbyabellin A and B and hectochlorin.	211
VI.8. Examples of cyanobacterial secondary metabolites possessing unusual octanoic and octynoic acid residues.	212



## LIST OF TABLES

Table	Page
II.1. Crude algal extracts examined in molluscicidal survey.	39
III.1. NMR Data for taviochtodene (65).	90
III.2. Chemical shift comparisons for ochtodenes and chondrocoles which are structurally similar to taviochtodene (65). *denotes that assignments are reversed in literature. <sup>a</sup> NMR experiment run in C <sub>6</sub> D <sub>6</sub> , all others were accomplished in CDCl <sub>3</sub> .	92
IV.1 NMR data for malyngamide L (80).	120
IV.2 NMR data for malyngamide Q (70) and R (71).	132
V.1. NMR Data for lyngbyabellin B (96).	172
V.2. NMR Data for tortugin (101).	186

## LIST OF ABBREVIATIONS

Amo	Amino methyl octynoic acid
Ahp	3-amino-6-hydroxy-2-piperidone
Ala	Alanine
Ara-A	Adenine arabinoside
Ara-C	Cytosine arabinoside
br	broad
bs	broad singlet
CIMS	Chemical ionization mass spectroscopy
COSY	$^1\text{H}$ - $^1\text{H}$ Correlation spectroscopy
d	doublet
Dhoa	Dihydroxy octynoic acid
Dhoaa	Dihydroxy octanoic acid
DPFGSE	Double pulsed field gradient spin echo
ED	Effective dosage
EIMS	Electron impact mass spectroscopy
EtOAc	Ethyl acetate
FABMS	Fast atom bombardment mass spectroscopy
FDAA	<i>N</i> $\alpha$ -(2,4-dinitro-5-fluoro-phenyl)- <i>L</i> -alaninamide
GC	Gas chromatography
GC/MS	Gas chromatography/mass spectroscopy
Gly	Glycine
HMBC	Heteronuclear multiple bond correlation

## LIST OF ABBREVIATIONS (CONTINUED)

HMQC	Heteronuclear multiple quantum coherence
HMPA	Hydroxy methyl pentanoic acid
HPLC	High pressure liquid chromatography
HRMS	High resolution mass spectroscopy
HSQC	Heteronuclear single quantum coherence
HSQMBC	Heteronuclear single quantum multiple bond coherence
Ile	Isoleucine
IR	Infrared
Leu	Leucine
LD	Lethal dose
m	multiplet
MCC	Menthoxy carbonyl chloride
Me	Methyl
MeOH	Methanol
MS	Mass spectroscopy
NMR	Nuclear magnetic resonance
NOESY	Nuclear overhauser effect spectroscopy
NPHPLC	Normal phase high pressure liquid chromatography
NRPS	Non-ribosomal peptide synthetase
Phe	Phenylalanine
PKS	Polyketide synthase

## LIST OF ABBREVIATIONS (CONTINUED)

q	Quartet
ROESY	Rotating frame overhauser effect spectroscopy
RPHPLC	Reversed phase high pressure liquid chromatography
RT	Room temperature
s	Singlet
SPE	Solid phase extraction
t	Triplet
TLC	Thin layer chromatography
TOCSY	Total correlation spectroscopy
$t_R$	Retention time
UV	Ultraviolet
Val	Valine
VLC	Vacuum liquid chromatography

## DEDICATION

This thesis is dedicated to all my friends and family who have helped and supported me throughout this adventure and to my beautiful wife, Shelley, who has been my strength.

# MARINE ALGAL SECONDARY METABOLITES OF UNIQUE STRUCTURE AND BIOMEDICINAL OR AGRICHEMICAL POTENTIAL

## CHAPTER I.

### GENERAL INTRODUCTION

The use of natural products for ceremonial and medicinal benefit predates written history. Presumably deduced by observations of human health within hunter-gatherer and early agrarian cultures, the medicinal power of natural materials was passed orally through early healers until written pharmacopoeias were established.<sup>1,2</sup> This pursuit of natural products chemistry is present in every culture, and has aided or led to the discoveries of salicylic acid (1), vinblastine (2), digitoxin (3), and many other commonly known modern medicinal products (Figure I.1).<sup>1,2</sup> Particularly steadfast in exploring and utilizing the healing properties present in nature, practitioners of Traditional Chinese Medicine (TCM), Ayurvedic Medicine (India), and examples within the Ebers Papyri (Egypt), and various tribal 'prescriptions' demonstrate a rich history of success treating their patients using natural products.<sup>1,2,3</sup> Such remedies typically exist in crude form as combinations of ingredients. Modern Western Medicine has only recently begun to unravel the mysteries held within these ancient medicines. An obvious display of the respect held for these practitioners is the International Cooperative Biodiversity Group (ICBG) initiated by the NCI and NIH to explore the uses of natural products in the pharmacopoeia of the modern

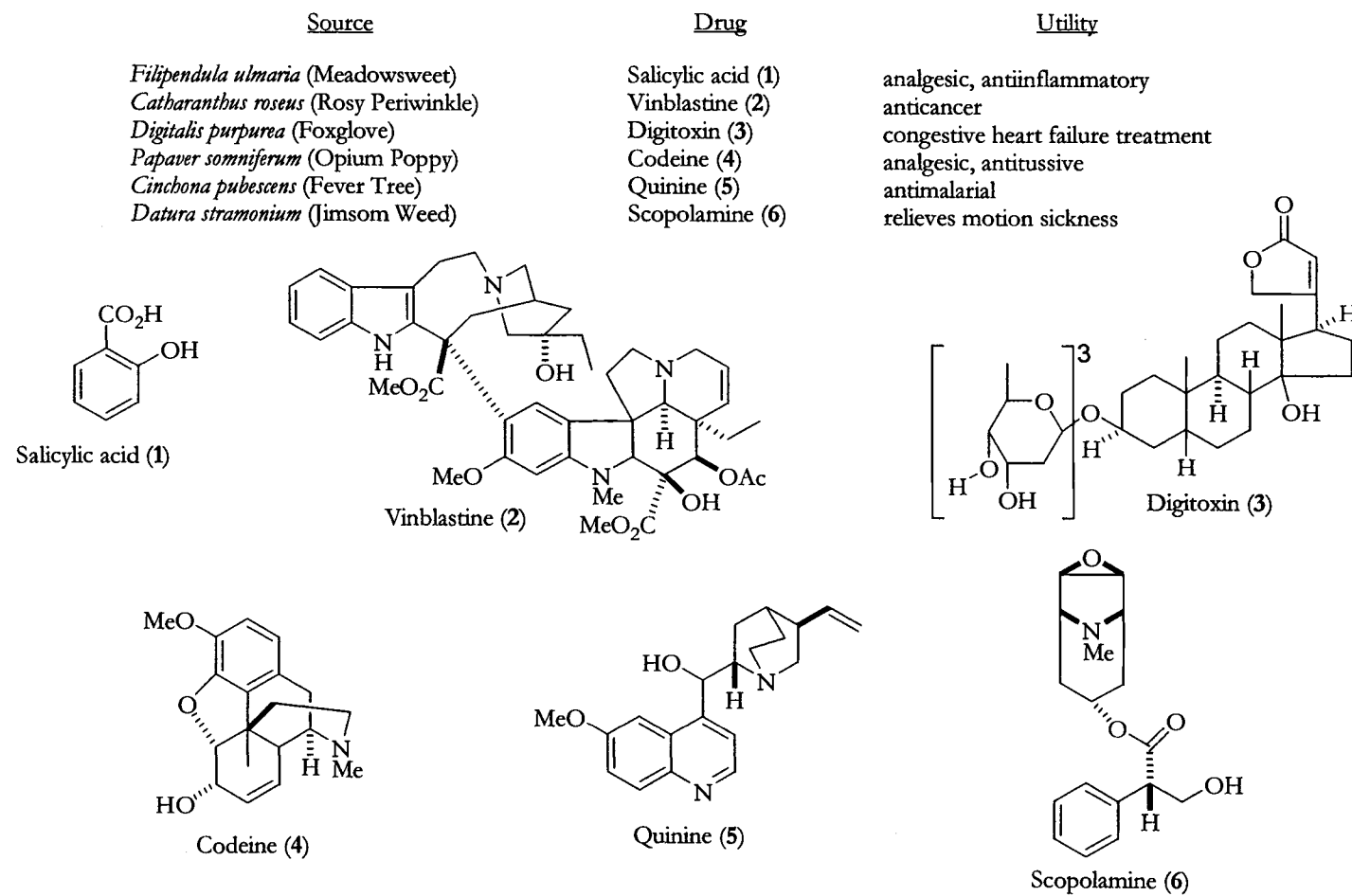


**Figure I.1.** Selected natural product drugs in common use.

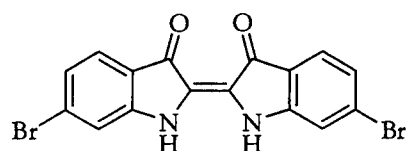
“Shaman”, and investigations undertaken by the Natural Products Branch of the NCI.<sup>4</sup>

The ICBG and NCNPDDG (National Cooperative Natural Products Drug Discovery Group) programs supported through collaboration between the NIH, NCI, pharmaceutical companies, and natural products scientists are an effort to increase the already substantial use of natural products (terrestrial and marine) in pharmaceutical therapy. Recently, it has been reported that natural products, derivatives of natural products, and synthetic molecules inspired by or modeled upon natural products comprise 39% of the newly approved drugs from 1984-1994.<sup>5</sup> This same study observed that 61% of the available anticancer therapies (1989-1995) were of that same demographic as well. Further examination of both the terrestrial and marine worlds, and the continued investigation of non-western pharmacopoeia will doubtless provide many more medicinally beneficial natural products.

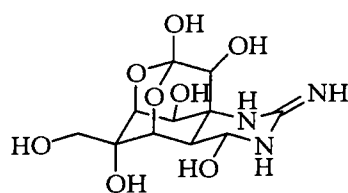
#### MARINE NATURAL PRODUCTS CHEMISTRY

Historically, the first commercially valuable marine natural product is Tyrian Purple (7), an ancient Phoenician dye produced from the mollusc, *Murex brandaris*, around 1600 BCE.<sup>6</sup> Tyrian purple also has the distinction of being the first marine natural product to have its structure successfully deduced. The powerful toxicity of tetrodotoxin (8) (recently recognized as a sodium channel blocker)<sup>7,8</sup> is also supposed to have been recognized in antiquity, as depictions of its source, the puffer fish *Tetraodon stellatus*, can be found in Pharonic tombs of Egypt dating to around 2700 BCE.<sup>6</sup> The toxicity of marine fish, molluscs, echinoderms, and coelenterates is also

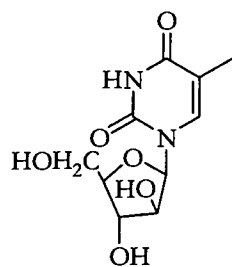




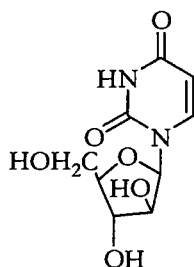
Tyrian Purple (7)



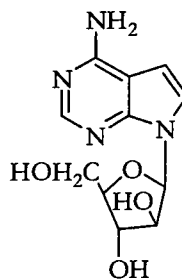
Tetrodotoxin (8)



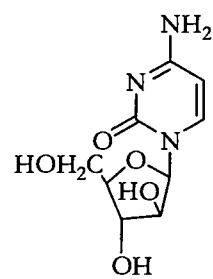
Spongothymidine (9)



Spongouridine (10)



Ara-A (11)

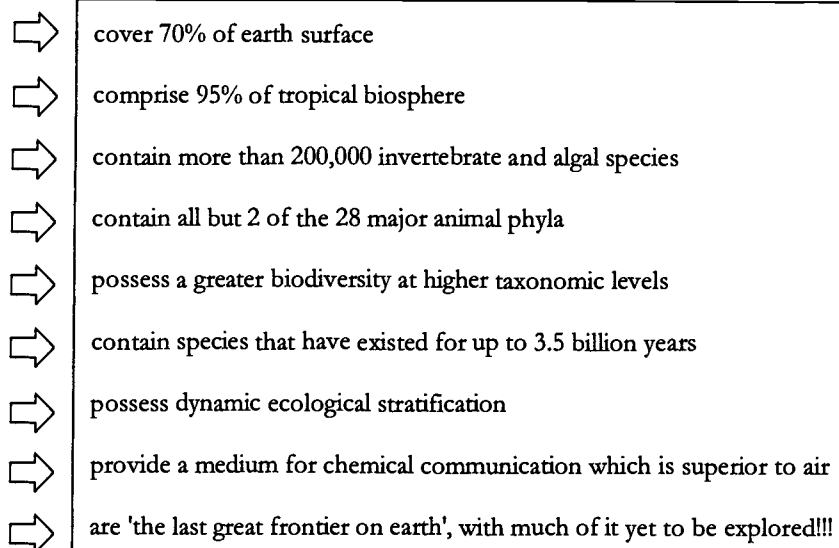


Ara-C (12)

commented upon in records of the early Hellenic, Assyrian, Persian, Indian, and Babylonian cultures.<sup>6</sup> However, ensuing epochs and the lack of written records for many cultures intimately associated with the oceans left few records of marine natural product utility.<sup>1,2,6</sup> Technology, the search for novel scientific niches, a heightened understanding of the ocean and its components, and the potential for profit, both financial and medicinal, served to alter the landscape of marine natural products research in the 20<sup>th</sup> century.

Figure I.2 highlights certain key facts concerning the marine environment that began to pique the interest of natural product scientists. These factors provided explorers with an alternative to exploring a terrestrial environment that had been the subject of 5000 years of natural products pursuit. Making this unexplored frontier accessible was the advent of technology that enabled underwater respiration (SCUBA). Lending further impetus to marine expeditions was the discovery by Bergmann of spongothymidine (9) and spongouridine (10), metabolites incorporating arabinose instead of ribose, from the marine sponge *Cryptotethia crypta*.<sup>9</sup> From the structures of 9 and 10, Ara-A (11) and Ara-C (12) were synthesized into two of the most successful commercial marine natural products. Ara-C is used to treat non-Hodgkin's lymphoma and acute myelocytic leukemia, whereas Ara-A a pharmaceutical that treats herpes infections.<sup>9,10</sup> These occurrences combined to give academic birth to the field of marine natural products chemistry in the early 1970s.<sup>11,12,13</sup> Available avenues of funding were developed through the NIH, NCI, NOAA, National Sea Grant College program, and NAIAD (National Institute of Allergic and Infectious Diseases), as well as through collaboration with pharmaceutical companies.<sup>6,11-13</sup>

**OCEANS...**

- 
- ⇒ cover 70% of earth surface
  - ⇒ comprise 95% of tropical biosphere
  - ⇒ contain more than 200,000 invertebrate and algal species
  - ⇒ contain all but 2 of the 28 major animal phyla
  - ⇒ possess a greater biodiversity at higher taxonomic levels
  - ⇒ contain species that have existed for up to 3.5 billion years
  - ⇒ possess dynamic ecological stratification
  - ⇒ provide a medium for chemical communication which is superior to air
  - ⇒ are 'the last great frontier on earth', with much of it yet to be explored!!!

**Figure I.2.** Facts about the oceans that stimulated the pursuit of marine natural products chemistry.<sup>2,6,11-13</sup>

Despite a mere three decades of existence, marine natural products chemistry has described the isolation of over 10,000 new compounds,<sup>2</sup> quite a few of which hold important promise as drug leads or molecular probes (Figure I.3 and Figure I.4). Apart from the tangible profitability that a new pharmaceutical product delivers, the pursuit of marine natural products has resulted in the description of numerous fascinating organisms and associations, and attaches academic and financial value to a still largely unknown natural resource.

#### THE ALGAL DIVISIONS

The algae are a diverse group of organisms, ranging in size from single-celled cyanobacteria (blue-green algae) to the great brown algae of the kelp forests, and are typically divided into four major divisions, brown (Phaeophyceae), red (Rhodophyta), green (Chlorophyta), and blue-green (Cyanobacteria). The classification of algae is not based upon visible color, but is predominately dependent on the type of chlorophyll, accessory pigments, storage proteins, and cell wall composition employed by the alga (Figure I.5).<sup>14,15,16</sup> The taxonomic structure for algae is an often disputed topic, as despite their photosynthetic capabilities they lack the appropriate characteristics to be truly considered plants, and they show little phylogenetic relatedness between divisions.<sup>14,15,16</sup> Also, difficulties exist in describing the cyanobacteria as bacteria or as algae. Cyanobacteria, while capable of photosynthesis, lack organized organelles (thus being prokaryotes) and apparently utilize some of the biosynthetic machinery extant in bacteria and fungi. For taxonomic purposes herein, the cyanobacteria will be referred to as "algae."

<u>Source</u>	<u>Drug</u>	<u>Utility</u>	<u>Status</u>
<i>Dolabella auricularia</i> (Sea Hare)	Dolastatin-10 (13)	Anticancer	Phase II clinical trials
<i>Ecteinascidia turbinata</i> (Sea Squirt)	Ecteinascidin 743 (14)	Anticancer	Phase II clinical trials (Europe)
<i>Bugula neritina</i> (Bryozoan)	Bryostatin-1 (15)	Anticancer	Phase II clinical trials
<i>Lissodendoryx</i> sp. (Sponge)	Discodermolide (16)	Anticancer	Preclinical development
<i>Discodermia dissoluta</i> (Sponge)	Halichondrin B (17)	Anticancer/immunosuppressant	Advanced preclinical
<i>Portieria hornemanni</i> (Red alga)	Halomon (18)	Anticancer	Advanced preclinical
<i>Jaspis</i> spp. (Sponge)	Jasparamide/Jaspakinolide (19)	Anticancer/antifungal/molecular probe	Advanced preclinical/commercially available
<i>Lyngbya majuscula</i> (Blue-green alga)	Debromoaplysiatoxin (20)	Molecular probe	Commercially available
<i>Lyngbya majuscula</i> (Blue-green alga)	Curacin A (21)	Antimitotic/molecular probe	Preclinical trials

**Figure I.3.** Selected examples of marine natural products with potential medicinal or research utility.<sup>2,4,6,11-13,30</sup>

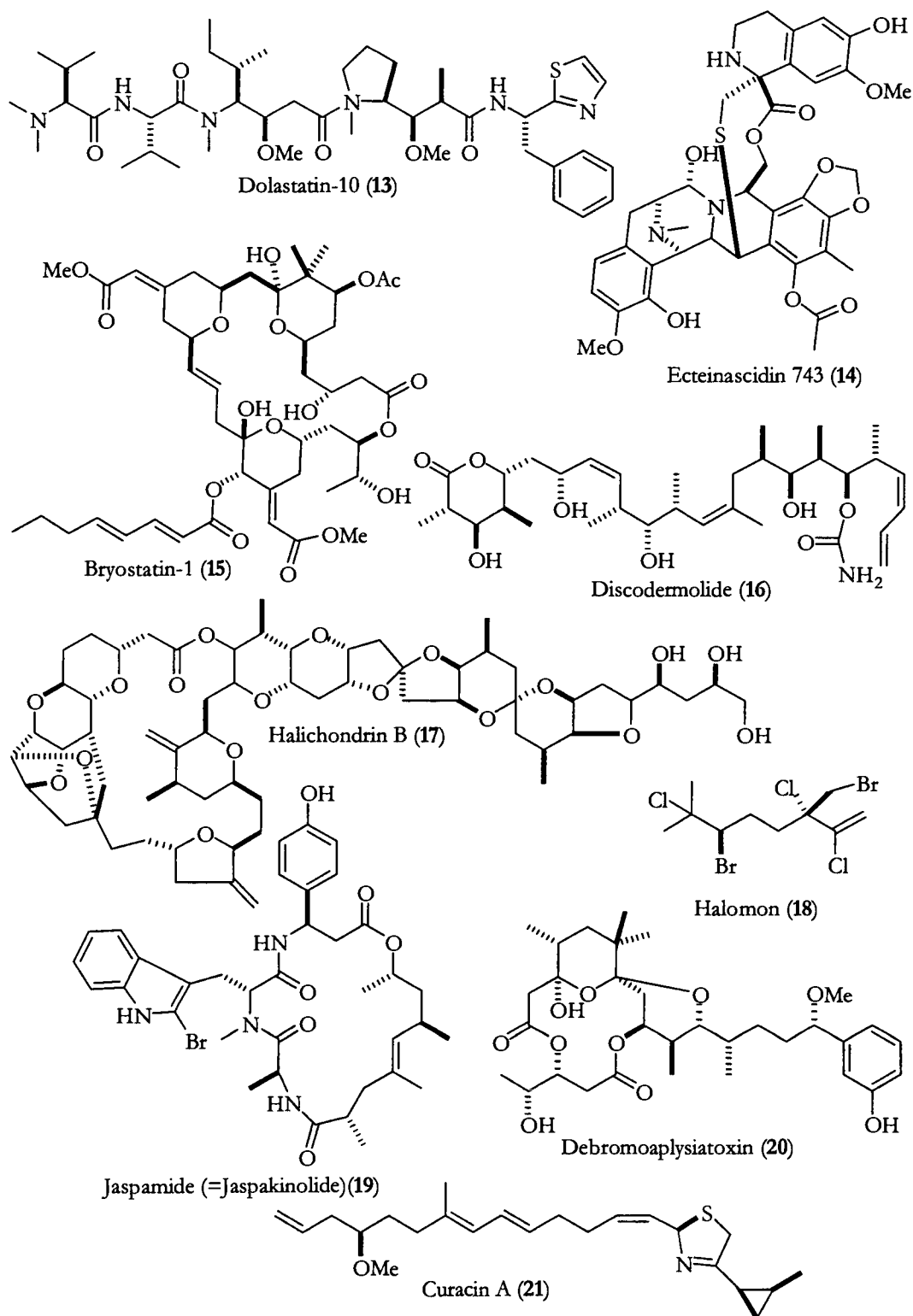


**Figure I.4.** The chemical structures of marine natural products with potential medicinal or research utility.<sup>2,4,6,11-13</sup>

Their environmental plasticity is dramatic, as algae can be found from the depths of the oceans (200-300 m) to the partially dry intertidal regions of the shore, and from terrestrial soils, freshwater rivers, lakes, and even swimming pools to mountaintops, hot springs, and snow fields.<sup>14,15</sup> Equally varied are the types of organisms which prey upon algae, and thus, algal survival has been made possible by a variety of defenses, including structural, temporal, spatial, and chemical.<sup>17,18,19</sup> Structural defense can be observed most clearly in calcified red and green algae, their bodies being rendered impregnable to many predators by a tough calcium carbonate exterior. Other algae have a life cycle which is opposite that of their predators, and thus displaces them temporally from danger.<sup>19</sup> An intricate method of temporal defense is the utilization of a life cycle which consists of an alternation of generations. The red alga *Porphyra* sp., as well as many other red and brown algae, have heteromorphic gametophyte and sporophyte stages with the large and leafy sporophyte present in the winter season, shielded in time from the voracious molluscs present in the summer season.<sup>20,21</sup> In situations such as this, the smaller gametophyte stage overlaps with the periods of highest predation. However, this small size increases the probability of being located in protected microhabitats, inaccessible to predators much larger than itself; this is an example of spatial protection.<sup>19</sup> The production of secondary metabolites which are distasteful or toxic to predators can also convey protection.<sup>17,18,19</sup> These chemical defenses represent molecules sculpted by time and evolution as potent weapons of survival for the organism, that can be utilized and manipulated by man in our defense or treatment of disease.

<u>Division</u>	<u>Chlorophyll</u>	<u>Accessory Pigments</u>	<u>Cell Wall</u>	<u>Storage Product</u>	<u>Habitat</u>
Cyanophyta	a	phycoerythrin, phycocyanin	peptidoglycan	glycogen	marine & freshwater, adaptable therein
Rhodophyta	a,d	phycoerythrin, phycocyanin, zeaxanthin	cellulose	floridean starch	marine & freshwater, temperate/tropical, to depth of ~200 m
Chlorophyta	a,b	lutein	cellulose, pectin	starch	marine & freshwater, mostly freshwater, cosmopolitan (freshwater), polar & tropical (marine), often intertidal
Phaeophyta	a,c	fucoxanthin	cellulose	laminarin	mostly marine, high intertidal

**Figure I.5** A comparison of the characteristics of the four major divisions of algae.<sup>16,34</sup>



Algae are ancient organisms instrumental in the formation of the earth's atmosphere, and as primary producers, contribute to the current atmospheric oxygen load.<sup>14,15</sup> They also form the base of the marine food web, supplying an immediate source of nutrients to filter feeders and herbivorous marine animals.<sup>14,15</sup> Apart from these primary nutrient roles, the algae are of extreme importance to two key structural features of the oceans; the intertidal zone and coral reefs. In intertidal and coral reef zones, algae transform a two dimensional rock formation into a 3-D habitat, thus fostering ecosystem maintenance and development.<sup>14,15</sup> Continuing biological, ecological, and marine natural product investigations, algae may also someday be responsible for the next generation of pharmaceuticals.

#### HUMAN USES OF ALGAE

Ancient healers recognized the value of algae as a potent natural pharmacy. The medicinal qualities of algae are extolled in the Ebers Papyrus (ancient Egypt), ayurvedic medicine (India), and traditional Chinese medicine, as well as in some tribal customs (the Inuit treat sore joints with an application of green algae) and Japanese folk medicine.<sup>1-3,22</sup> Such ancient medicinal uses of seaweed includes the promotion of bone formation [*Undaria* spp. (Wakame)], and treatments for parasites (*Digenea* spp.), gout and goiter (*Laminaria* spp.), sexually transmitted diseases (Dumontiaceae), and cancer.<sup>22,23,24</sup> Brown algae, specifically *Laminaria* spp. and *Sargassum* spp., were used by Egyptian, Chinese, Japanese, and ayurvedic medical practitioners to treat cancer, and were particularly mentioned in the Ebers Papyrus for their efficacy in treating breast cancer.<sup>21-25</sup> The traditional use of *Digenea* spp. as an antiparasitic led to the discovery of

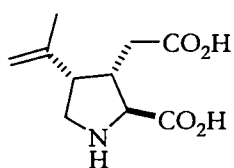
kainic acid (22), a small molecule used in treatments of roundworm, whipworm, and tapeworm infections, and as a biochemical tool due to its potent neurotoxicity.<sup>2,3,5</sup>

Modern uses of algae and algal products are more common than many would suspect. Polysaccharides of brown and red algae are used extensively in science and the food industry, in products such as agar, toothpaste, gelatin, and ice cream.<sup>16,21-26</sup> The commercialization of such products produces an annual revenue of approximately \$250 million.<sup>16</sup> Carageenan is one such commercially important polysaccharide that also has folk-medicine applications as an anticoagulant and cancer-fighting agent.<sup>26</sup>

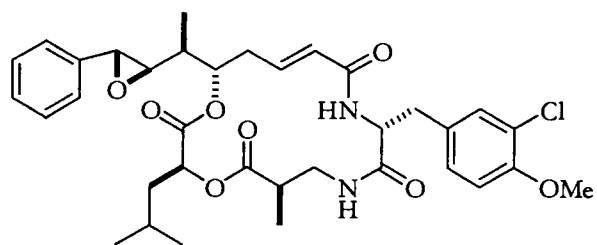
Antiviral Dumontiaceae (red algae) carbohydrates, including carageenan and dextran sulfate, among others, were found effective (pre- and post-infection) against herpes I and II in human clinical trials, both topically and orally, with no observed side effects.<sup>21-26</sup> Despite these promising results, Dumontiaceae-derived compounds have not yet cleared the high hurdles of the drug approval process, and thus have been relegated to the ranks of alternative medicines.<sup>21-26</sup>

#### FRESHWATER ALGAE

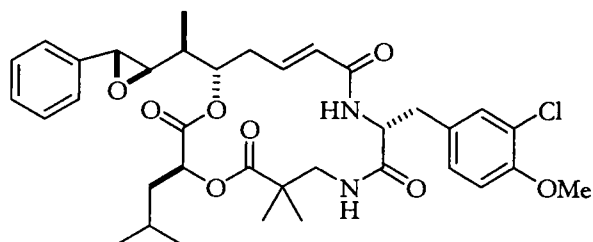
Another hopeful development is the isolation of a protein from the freshwater cyanobacterium *Nostoc ellipsosporum* that may also play a role in the fight against a sexually transmitted virus. Cyanoviran-N (CV-N), a small uncomplicated protein (101 amino acids) whose function in nature, if any, is still unknown, acts in the laboratory as a “fusion inhibitor” of the human immuno-deficiency virus (HIV).<sup>27</sup> CV-N forms an irreversible complex with the gp120 surface-receptor molecule of HIV, stripping the virus of its ability to penetrate and infect cells.<sup>27</sup> The CV-N binding site of gp120



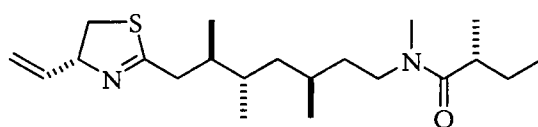
Kainic Acid (22)



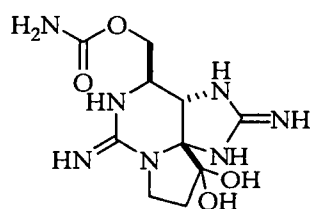
Cryptophycin 1 (23)



Cryptophycin 52 (24)



Kalkitoxin (25)



Saxitoxin (26)

may be a common retrovirus motif, as this complex (and subsequent cessation of viral activity) is observed in all laboratory strains of HIV, including HIV-2, SIV (simian), and FIV (feline).<sup>27</sup> CV-N is unaffected by heating, freezing, thawing, acidification, and denaturing, adding to its attractiveness as a medical treatment.<sup>27</sup>

Despite these advantages, the formation of antibodies against foreign proteins like CV-N limits its potential therapeutic utility; thus, CV-N is likely to be most useful as a barrier to infection.<sup>27,28</sup> Using biotechnological tools, the genetic code responsible for the production of CV-N could be spliced into *Lactobacillus*, a common, necessary, and beneficial microbe of the vaginal mucosa. The resulting culture—which would be administered in suppository form—would create a fortified infection barrier, having the advantages of both the low pH produced by lactic acid (secreted by *Lactobacillus*) and the fusion-inhibiting action of CV-N.<sup>27,28</sup>

The cryptophycins, secondary metabolites found in the same genus of freshwater cyanobacteria responsible for CV-N, have been shown to possess antifungal and anticancer activity.<sup>29</sup> The active molecules are small, cyclic depsipeptides originally isolated from *Nostoc* spp. following antifungal activity. However, they may have more potential utility in the anticancer realm.<sup>29</sup> Cryptophycin 1 (23) is an extremely potent antimetabolic agent that binds nearly irreversibly to tubulin (a cytoplasmic protein), thus inhibiting microtubule dynamics and preventing the uncontrolled proliferation of cells that characterizes cancer.<sup>29</sup> The action of cryptophycin 1 is similar to that of vinblastine (2), a drug derived from the Madagascar rosy periwinkle, and used to treat breast and testicular cancer and Hodgkin's disease.

Both compounds act at the vinca alkaloid site, but the former is an even more potent stabilizer of microtubule dynamics. In fact, it is the most powerful such agent yet found. In animal tests, analogs of cryptophycin 1 have “cured” some types of tumors.<sup>29</sup> One such analog, cryptophycin 52 (24) has advanced to Phase II clinical trials, and may someday be a new cancer treatment.

#### MARINE ALGAE

Like their freshwater cousins, marine blue-green algae are also a source of potentially powerful pharmaceuticals. Curacin A (21) is a lipopeptide isolated from a sample of *Lyngbya majuscula* collected on the southwestern Caribbean island of Curaçao.<sup>30</sup> An extract containing curacin A displayed striking toxicity to goldfish, brine shrimp, and snails—as well as cancer cells. The pure isolate of curacin A destroyed cancer cells by inhibiting microtubule formation, similar to the action of colchicine.<sup>30</sup> However, curacin A has not progressed on the “drug pipeline” due to problems with stability and solubility. Research is currently underway to alleviate these problems and further test this powerful chemical. Incidentally, the discovery of curacin A has yielded ecological as well as pharmaceutical benefits. The mangrove swamps from which the curacin A producing alga had been collected were destined to be replaced by a coastal resort development. Because of curacin A’s great pharmaceutical potential, however, the development was cancelled and the mangrove habitat was preserved.<sup>31</sup>

Kalkitoxin (25), another product of *L. majuscula*, is a potent toxin to brine shrimp, rat neurons, and goldfish, an inhibitor of fertilized sea-urchin-embryo cell

division, and an antagonist of hepatocarcinoma proliferation in vitro.<sup>32</sup> Kalkitoxin is among the most potent neurotoxins ever discovered. Like topiramate (a pharmaceutical used in the treatment of epileptic seizures) and lidocaine (an analgesic), kalkitoxin acts as a sodium-ion channel blocker.<sup>32</sup> Saxitoxin (26), a very potent dinoflagellate neurotoxin responsible for numerous closings of the shellfish industry of the northwest U.S. coast, acts at the same site, but is one-tenth as potent. Such potency suggests kalkitoxin could have great potential as a molecular probe.

Algae such as *L. majuscula* afford us the opportunity to study and manipulate the biosynthetic machinery that creates such potent secondary metabolites. Curacin A and kalkitoxin are both products of mixed biogeneses, combining aspects of the polyketide synthase and non-ribosomal peptide synthetase pathways.<sup>33</sup> Both pathways have been shown to possess clustered genetic machinery composed of modules, creating its products on a metabolic assembly line. Efforts are underway at Oregon State University and the University of Minnesota to probe and manipulate these pathways in cultured specimens to better understand the organisms and the biosynthetic pathways, and to potentially create even more potent chemicals.

Apart from their ability to seed our atmosphere with oxygen, and their necessary functions as valuable members of coral reef communities, algae present us with a chemical cornucopia of potential pharmaceuticals. With this inherent wealth of metabolic machinery, they provide us with a template which can be manipulated through culture techniques and the burgeoning power of molecular biology to create the next generation of pharmaceuticals to combat human diseases. Such tremendous value could lead one to envision the farming of these organisms to the detriment of

their natural ecosystems, and, by extension, to all ecosystems. However, as exemplified by the power of curacin A to protect a stretch of Curaçao's mangroves, knowledge of the diversity extant within our oceans, the understanding of the relatedness and dependence of all organisms upon each other, and the potential medicinal treasures, made possible only by such diversity, can serve to protect rather than endanger.

#### THESIS STATEMENT

Algae are sessile organisms often encountered in areas of intense species diversity and herbivory.<sup>17-19</sup> As such, many have developed methods of defense most suitable for their local habitats. Chemical defense seems to be the defense of choice for smaller slow growing algae.<sup>17-19</sup> Since such secondary metabolites have been honed by evolutionary forces to be biologically active compounds, they represent a downstream stage of the "natural drug discovery process." The investigation of the secondary metabolites present in natural systems has two valuable outcomes, 1) an enhanced understanding and appreciation for the natural environment, with a heightened awareness of the intricate processes that are present yet barely understood and 2) a contribution to the drug discovery process by uncovering both biologically active and inactive secondary metabolites produced by biosynthetic pathways that, while originally protecting more primitive organisms, may lead to the next generation of pharmaceuticals which aid humans. As such, the overarching hypothesis of this work is that marine algae produce metabolites, which can be isolated and chemically

defined, that will enhance the understanding of marine algae and their products and will play a necessary 'front line' role in drug discovery efforts.

## GENERAL THESIS CONTENT

The focus of this thesis is the isolation and structure elucidation of secondary metabolites from marine algae (macrophytes and cyanobacteria). Three components have proven invaluable in this pursuit; a library of crude extracts representing algae collected from locations circumnavigating the globe, the ability to examine the biological activity of these samples (both in-house and through extensive academic and industrial collaborations), and the application and, when necessary, creation of technology to properly identify the structure of the component of interest. In the shadow of this general introduction can be seen a common braid that weaves itself through each chapter in an attempt to unravel, identify, and qualify what is extant in nature. The goal of all such work is a contribution to the drug discovery process, the scientific archive, and our general understanding of existing natural processes.

As such, after this general introduction, the thesis begins with a survey of algal extracts for molluscicidal activity against *Biomphalaria glabrata*, the intermediate host for the schistosomiasis causing worm, *Schistosoma mansoni*. One method of disease prevention (especially in artificial waterways such as irrigation channels) is to control the population of the snail. Currently, niclosamide is the commercially utilized molluscicide. Pursuing activity discovered through this survey, tanikolide, chondrocole C, and debromoaplysiatoxin were purified and identified as the active constituents of their respective extracts. Debromoaplysiatoxin possessed more



potency than niclosamide, and may have utility in efforts to stop the spread of schistosomiasis.

The re-discovery of chondrocole C as a molluscicidal secondary metabolite inspired the work described in Chapter III. In total five polyhalogenated monoterpenes were isolated from a collection of *Portieria hornemanni*, with one of them being the newly described compound, taviochtodene. The small size and chemical shift similarities within this structure class called for extensive utilization of mass spectrometry (especially GC/MS) and NMR experiments to accurately determine chemical structures. *P. hornemanni* is the original source for halomon, a rare and highly potent secondary metabolite with anticancer potential, that has not proceeded down the drug pipeline because of its scarcity and synthetic complexity. A close chemical relative of halomon, 2-dechlorohalomon (slightly less active in cancer studies than halomon) was among the isolated compounds.

Moving from the red algae to cyanobacteria, Chapter IV details the discovery of three new malyngamides. The malyngamides are the most prominent class of *Lyngbya majuscula* secondary metabolites. To this list have been added malyngamides L, Q, and R. While malyngamide L shares many characteristics of the standardly encountered cyclohexyl-type malyngamide, malyngamides Q and R offered some intriguing differences. Firstly, they are structurally similar to malyngamides A and B, members of the less common pyrrolidone-type subclass of malyngamides. Also, malyngamides Q and R were the first malyngamides discovered with an alternative geometric stereochemistry at the vinyl-halide carbon.

*Lyngbya majuscula* secondary metabolites are also the topic of the penultimate chapter, Chapter V. A Dry Tortugas sample of *L. majuscula* yielded two toxic cyclic depsipeptides, lyngbyabellin B and tortugin. Lyngbyabellin B, toxic to brine shrimp and *Candida albicans*, is a dichlorinated compound resembling the molluscan-derived metabolite dolabellin. Tortugin, displaying activity against brine shrimp, incorporates a seldom encountered terminal acetylene residue which has most commonly been observed in a series of molluscan secondary metabolites.

A summary of the presented work on marine algal natural products chemistry appears in the concluding Chapter VI. Specifically highlighted are the topics running through each chapter that tie them together as one work. Also summarized is the attempt of this work to unravel, identify, and qualify what is extant in nature in the hopes of contributing to the drug discovery process, the scientific archive, and our general understanding of existing natural processes.

## REFERENCES

- 1 Cox, P.A. and Balick, M.J. *Scientific American* **1994**, *4*, 82-87.
- 2 McConnell, O.J.; Longley, R.E.; Koehn, F.E. *The Discovery of Natural Products with Therapeutic Potential*; Gullo, V.P., Ed.; Butterworth-Heinemann: Boston, **1994**; pp. 109-174.
- 3 Arasaki, S. and Arasaki, R. *Low Calorie, High Nutrition Vegetables from the Sea to help you look and feel better*, Japan Publications, Inc., Tokyo, **1983**; p. 136.
- 4 National Cancer Institute Cancer Web, Questions and Answers About NCI's Natural Products Branch, <http://www.graylab.ac.uk/cancernet/600733.html>, (accessed August 2001).
- 5 Cragg, G.M.; Newman, D.J.; Snader, K.M. *J. Nat. Prod.* **1997**, *60*, 52-60.
- 6 Kelecom, A. *An. Acad. Bras. Ci.* **1999**, *71*, 249-263.
- 7 Tsuda, K. and Kawamura, M. *J. Pharm. Soc. Japan* **1952**, *72*, 771.
- 8 Kao, C.Y.; Levinson, S.R. *Tetrodotoxin, Saxitoxin, and the Molecular Biology of the Sodium Channel*, Kao, C.Y.; Levinson, S.R., Eds.; The New York Academy of Sciences: New York, **1986**.
- 9 Bergmann, W. and Feeney, R.J. *J. Org. Chem.* **1951**, *16*, 981-987.
- 10 Scheuer, P.J. *Med. Res. Rev.* **1989**, *9*, 535.
- 11 Wallace, R.W. *Molecular Medicine Today* **1997**, *4*, 291-295.
- 12 Hay, M.E. and Fenical, W. *Oceanography* **1996**, *9*, 10-20.
- 13 El Sayed, K.A.; Dunbar, D.C.; Bartyzel, P.; Zjawiony, J.K.; Day, W.; Hamann, M.T. In *Biologically Active Natural Products: Pharmaceuticals*, Cutler, S.J. and Cutler, H.G., Eds.; CRC Press: New York, **2000**, pp. 233-252.
- 14 Abbott, I.A. and Dawson, E.Y. In *How to Know the Seaweeds*, 2<sup>nd</sup> Ed., WCB McGraw-Hill: Boston, **1978**, pp. 1-19.
- 15 O'Clair, R.M. and Lindstrom, S.C. In *North Pacific Seaweeds*, Plant Press: Alaska, **2000**, pp. 1-8.

- 16 Dixon, G.H. In *Crop Protection Agents from Nature*; Copping, L.G. Ed.; SCI Publications: London, **1996**, pp. 114-216.
- 17 Hay, M.E. *J. Exp. Mar. Biol. Ecol.* **1996**, *200*, 103-134.
- 18 Hay, M.E. In *Ecological Roles of Marine Natural Products*, Paul, V.J., Ed., Comstock Publishing Associates: Ithaca, **1996**, pp. 93-117.
- 19 Cronin, G. and Hay, M.E. *Oecologia* **1996**, *105*, 361-368.
- 20 Littler, M.M. and Littler, D.S. *Am. Nat.* **1980**, *116*, 25-44.
- 21 Conway, E. and Cole, K. *Phycologia* **1977**, *16*, 205-216.
- 22 Gray, G. *Can. Med. Assoc. J.* **1996**; *155*, 1613-1614.
- 23 Hatch, M.T.; Ehresmann, D.W.; Deig, F.E. *Mar. Algae Pharm. Sci.* **1979**, 343-363.
- 24 Neushul, D.E. *Hydrobiologia* **1990**, *204/205*, 99-104.
- 25 Richards, C.S. *Antimicrob. Agents Chemother.* **1978**, *14*, 24-35.
- 26 Thomson, A.W. and Fowler, E.F. *Agents and Actions.* **1981**, *11*, 265-273.
- 27 Boyd, M.R.; Gustafson, K.R.; McMahon, J.B.; Shoemaker, R.H.; O'Keefe, B.R.; Mori, T.; Gulakowski, R.J.; Wu, L.; Rivera, M.I.; Laurencot, C.M.; Currens, M.J.; Cardellina, J.H.; Buckheit, R.W.; Nara, P.L.; Pannell, L.K.; Sowder, R.C.; Henderson, L.E. *Antimicrob. Agents Chemother.* **1997**, *41*, 1521-1530.
- 28 Blakeslee, D. *JAMA Newslne* [Online] October 27, **1998**.
- 29 Panda, D.; Himes, R.H.; Moore, R.E.; Wilson, L.; Jordan, M.A. *Biochemistry* **1997**, *36*, 12948-12953.
- 30 Gerwick, W.H.; Proteau, P.J.; Nagle, D.G.; Hamel, E.; Blokhin, A.; Slate, D.L. *J. Org. Chem.* **1994**, *59*, 1243-1245.
- 31 Wu, M.; Okino, T.; Nogle, L.M.; Marquez, B.L.; Williamson, R.T.; Sitachitta, N.; Berman, R.W.; Murray, T.F.; McGough, K.; Jacobs, R.; Colsen, K.; Asano, T.; Yokokawa, T.; Shioiri, T.; Gerwick, W.H. *J. Am. Chem. Soc.* **2000**, *122*, 12041-12042.

- 32 Simonetti, J. *Rodale's Scuba Diving* 1997, 8.
- 33 Tan, L.T.; Sitachitta, N.; Gerwick, W.H. *Alkaloids*, in press.
- 34 Sze, P. *A Biology of the Algae*, 3<sup>rd</sup> Ed., WCB McGraw-Hill: Boston, 1998.

## CHAPTER II.

MOLLUSCICIDAL ACTIVITY IN MARINE ALGAL EXTRACTS; A SURVEY AND  
CHEMICAL INVESTIGATION OF PROMISING MOLLUSCICIDAL ALGAL  
EXTRACTS

## ABSTRACT

Schistosomiasis is a parasitic disease endemic in many of the world's developing nations, and victimizes hundreds of millions of people. The causative trematode, *Schistosoma* spp., has proven quite adaptive to commonly administered therapies, developing refractile resistance at an alarming pace. In response to a lack of potential new and affordable pharmaceutical alternatives, the World Health Organization is advocating the search for toxins that specifically target the freshwater snail, *Biomphalaria glabrata*, which serves as the obligate intermediate host for the schistosome larvae, as a method of disease control. As marine algae are thought to employ at least some of their myriad secondary metabolites in combating predation, with aquatic molluscs being dominant herbivores and potential targets, it is possible that the chemical extracts of marine algae possess compounds that are toxic to freshwater snails. Therefore, this chapter reports the screening of marine algal crude extracts for their toxicity to *B. glabrata*. Following analysis of the results, the active constituents of some of the most highly potent extracts were isolated in a bioassay guided manner, yielding the previously discovered chondrocole C, tanikolide, and debromoaplysiatoxin.

## INTRODUCTION

Schistosomiasis, also known as bilharziasis, is a disease that afflicts 200-300 million people, in regions spanning the globe.<sup>35-39</sup> A further five to six million people remain at high risk of contracting the disease, as it is endemic in 74 countries.<sup>35-43</sup> Children and some agricultural laborers bear the greatest burden of disease among demographic groups due to age or occupation related activities increasing the probability of contact with the schistosome.<sup>40-42</sup> Such high-risk populations are especially prevalent in countries with rapidly developing infrastructures, such as Egypt and China, where public works projects have played a role in the epidemiology of schistosomiasis.<sup>38-41</sup>

While schistosomiasis is typically not life threatening, the effects are often chronic and can lead to disability, representing a significant drain on both the human and economic resources of affected countries.<sup>38</sup> As a public health issue, schistosomiasis is a worldwide concern, and ranks second only to malaria in socio-economic and human health importance in tropical nations.<sup>35-39</sup>

The disease is caused by one of five schistosome species (Figure II.1); *S. mansoni*, *S. japonicum*, *S. mekongi*, and *S. intercalatum* which cause intestinal schistosomiasis, and *S. haematobium* which is responsible for urinary schistosomiasis. These differences in disease manifestation are due to the habits of the individual trematode species for location of egg deposition.<sup>37-40</sup>

<u>Species</u>	<u>Location</u>	<u>Type of Schistosomiasis</u>
<i>S. mansoni</i>	Africa, Eastern Mediterranean, Caribbean, South America	Intestinal
<i>S. japonicum</i> and <i>S. mekongi</i>	South-East Asia and Western Pacific	Oriental or Asiatic Intestinal
<i>S. intercalatum</i>	Central Africa	Intestinal
<i>S. haematobium</i>	Africa and Eastern Mediterranean	Urinary

**Figure II.1.** The five spp. of schistosomiasis causing trematodes.<sup>40</sup>



## THE DISEASE

Disease symptoms and complications are primarily the result of immune responses to antigens secreted by the schistosome eggs.<sup>45,46</sup> In acute schistosomiasis, Katayama fever, a sudden high influx of antigen, which typically coincides with egg deposition, causes symptoms such as epidermal rash, asthma, fever, diarrhea, and malaise. Extremely heavy infections can also result in death. Fever and diarrhea also accompany chronic schistosomiasis, as does hepatosplenomegaly, liver fibrosis, hepatoportal hypertension, and esophageal lesions.<sup>45,46</sup> Children also have reduced growth rates as a result of the chronic form of this disease. Urinary schistosomiasis has the additional complications of pyelonephritis, hydronephritis, and bladder fibrosis, which can lead to ureter obstruction and/or kidney failure. Liver, bladder, and intestinal cancer are also a potential result of severe chronic schistosomiasis.<sup>45,46</sup>

## TRANSMISSION

Schistosomiasis is caused by parasitic trematodes that live and reproduce in the blood of mammals.<sup>35-46</sup> Within the mammalian host, the female deposits eggs in the veins surrounding the bladder or intestines, depending on the infecting species.<sup>45</sup> The eggs are released into the environment when the mammal excretes or defecates. If within, or near, a body of water, or in cases of waterways polluted by wastewater, the eggs hatch and proceed to the next stage of their life cycle (Figure II.2).<sup>39-42,46</sup>

When delivered to water the eggs hatch into their first larval form, the miracidia.<sup>35-39</sup> The miracidia is a free-swimming larva capable of infecting only the intermediate host, the snail. In the laboratory, miracidia have been shown to be

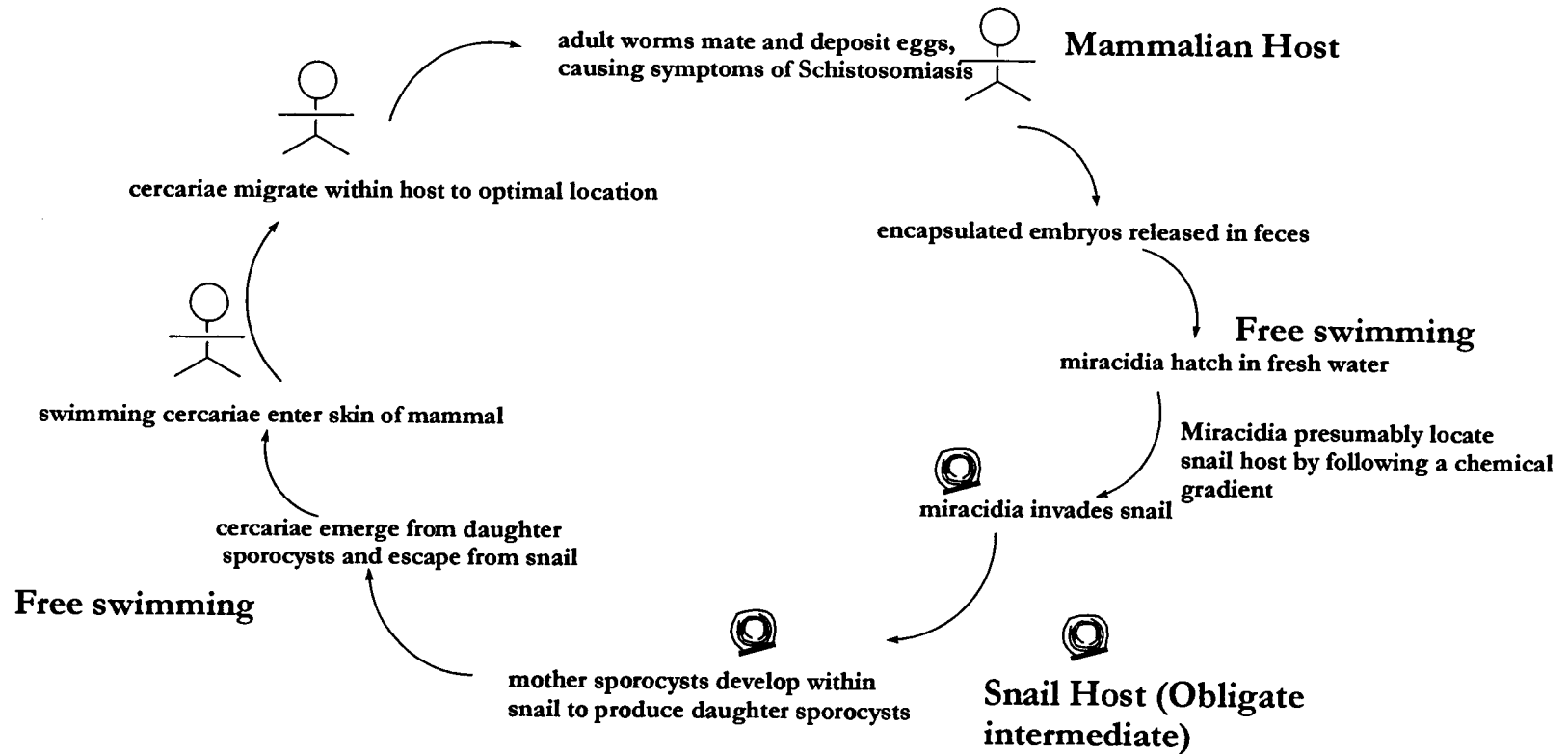


Figure II.2. The life cycle of *Schistosoma* spp.

negatively photo-tactic, thus facilitating the location of snails crawling along the bottom of the waterway.<sup>47,48</sup> It also appears that the miracidia respond to exuded metabolites of the snail, thus finding their host by traversing along a chemical gradient. The nature of the sensory chemical(s), however, is yet to be discovered.<sup>47-54</sup> Within the snail, the miracidia undergoes metamorphosis, forming numerous cercariae.<sup>35-39</sup>

The cercariae emerge from the host as pathogenic parasites that exhibit positive photo-taxis, presumably increasing the probability of encountering mammals in shallow water.<sup>47,48</sup> The infective larvae penetrate the exposed skin of their mammalian host then mature and reproduce. Each day hundreds of eggs are produced by the female; many causing the symptoms typically encountered, and the rest being released into waterways by the mammal, thus perpetuating the cycle of infection.<sup>35-39</sup>

## METHODS OF CONTROL

There exist three areas of focus for the control of schistosomiasis, all used in various degrees and levels of success, and which target different aspects of the disease or transmission of the disease. Figure II.3 highlights the methods of control currently utilized.<sup>37-41,47-49</sup>

The most common form of control is treatment of the patient after having been infected by the trematode, or by application of immunization programs. Figure II.4 shows the current drugs used to treat schistosomiasis. While praziquantel (27) is the current drug of choice, and has been highly successful, refractile resistance to 27 is becoming alarmingly prevalent.<sup>37,38,40-42</sup> Such resistance suggests an adaptive ability of

<u>Method of Control</u>		<u>Difficulties with Treatment</u>
<b>Treatment;</b> in human, post-infection		
Chemotherapy; praziquantel	⇒	Costly, Refractile resistance
Immunization	⇒	Not yet possible, Risk of spreading other diseases
<b>Pre-Infection;</b> preventing interaction of man & pathogenic schistosome		
Environmental Infrastructure; Improve sanitation	⇒	Economically costly, Encysting stages of life cycle
<b>Pre-Activation;</b> inhibiting contact between schistosome larvae and obligate intermediate host		
Molluscicides; Niclosamide (remove host snails)	⇒	Remigration of snails, Environmental toxicity
Aquatic Controls; Dry canals ("drown schistosomes")	⇒	Costly, Difficult to implement
Biological Control; Species Introduction	⇒	Potential environmental disaster, Adaptability of schistosome
<i>Marisa cornuarietis</i>		
Molluscan competitor		

**Figure II.3.** Methods used, or proposed, to control the spread of schistosomiasis.<sup>37-41,47-49</sup>

the schistosome that may necessitate renewed interest in the development of new anti-schistosomiasis drugs. An additional problem encountered with pharmaceutical treatment of schistosomiasis is that it is often a cost prohibitive solution in areas where it is most needed. Other useful pharmaceuticals employed in the treatment of schistosomiasis are oxamniquine (28) and metrifonate (29).<sup>37-40</sup> The use of immunization programs is a goal of many affected countries, but has not yet seen broad application. It has, however, received intense interest from the WHO, and shown potential utility.<sup>40</sup>

A second method attempts to limit the interaction of humans and schistosomes, thus preventing infection. As the spread of the disease is assisted by waterways being polluted by human waste, or the waterways themselves serving as the primary conduits of waste, some countries are attempting to improve their sanitation infrastructure. This, however, is an extremely costly venture further exacerbated by large populations living in distant and decentralized regions.<sup>36-42</sup>

The third method of control is aimed at disrupting the successful completion of the schistosome life cycle; thus blocking the activation of human pathogenicity.<sup>37-40</sup> This effort has witnessed three focal points of attack, molluscicidal, environmental, and biological methods of control. Used as a molluscicidal agent, niclosamide (30) has been introduced into many waterways, resulting in death of many snails and other, non-target, invertebrates.<sup>35-43</sup> Problems encountered using niclosamide include environmental toxicity and the re-migration of snails after inoculation with the compound.<sup>48</sup> Also, 30 is a very stable molecule, resistant to changes in pH and

temperature, thus stimulating concern for environmental accumulation.<sup>48</sup> Of course, in many areas the cost of niclosamide limits its utility.

Attempts have also been made to alter the environment of the schistosome by draining waterways, and thus “drowning” the snails and schistosomes in air.<sup>37-40,48,49</sup> This method has had very limited success due to the ability of the schistosomes to form encysting bodies which yield viable trematodes upon reintroduction of water and snails.<sup>48</sup> There are also obvious financial problems associated with this method, as the resources needed to accomplish it are extraordinary, and the disruption of the waterways results in significant economic hardship for many of the affected areas.

Biological controls have proven only slightly more successful. The introduction of a competitor to *B. glabrata*, the mollusc *Marisa cornuarietis*, has limited the viability of *B. glabrata* by competing for its resources.<sup>48,49</sup> Exotic species introduction, however, is a troublesome initiative to support, as ecological disasters appear to occur as a frequent result of such endeavors.<sup>51</sup>

#### SCHISTOSOMIASIS; ‘THE SCOURGE OF DEVELOPING NATIONS’

Schistosomiasis has been called ‘the scourge of developing nations’.<sup>49</sup> This moniker is due to the dramatic rise in disease incidence that accompanies public works projects, specifically water resource development, such as dam building and the creation of irrigation systems.<sup>49</sup> The construction of dams and man-made lakes, usually for hydroelectric power, results in stagnant water that has a higher temperature than if it were allowed to flow freely.<sup>48-50</sup> The fecundity of both the snail and worm is much more robust under such stagnant and warm conditions.<sup>49,50</sup> Therefore, a

population explosion could be expected which would lead to an increased incidence of disease in the immediate vicinity of the stagnant water, as well as in those regions that receive this water. As a confounding consequence, irrigation systems derive their resources from the dammed and man-made lakes, thereby delivering the snails and worms to regions that typically would have a decreased likelihood of schistosomiasis incidence. These irrigation systems are often supporting rice paddies, and other crops that require immersion or floating techniques, thus significantly increasing the exposure of the workers in the fields with the infective organism.<sup>50</sup> Figure II.5 highlights a few worldwide examples of the effects of developing infrastructure upon schistosomiasis incidence.<sup>49</sup> Aside from public works projects, civil strife (resulting in mass population movements into or out of endemic areas) and "off-track tourism" are also responsible for the increased incidence of schistosomiasis.<sup>48,49</sup>

#### THE POTENTIAL USE OF CHEMICAL ECOLOGY AS A METHOD OF CONTROL

Laboratory experiments have proven the effectiveness of snail-conditioned water (SCW) in the attraction of miracidia.<sup>51-58</sup> While the chemical structure of this/these chemoattractants has yet to be fully explored, size exclusion filtration and hydrolysis experiments have suggested that the compound(s) possess a molecular weight below 1000 da and are of a peptide nature.<sup>51-54,58</sup> Analyses of SCW by HPTLC and free amino acid analysis have described a chemically-rich effluent of various neutral fatty acids, free fatty acids, and free amino acids.<sup>53</sup> While these free amino acids may be partially active as chemoattractants, the fully active component appears to be a small oligopeptide due to loss of chemoattractant activity after hydrolysis.<sup>53</sup> A

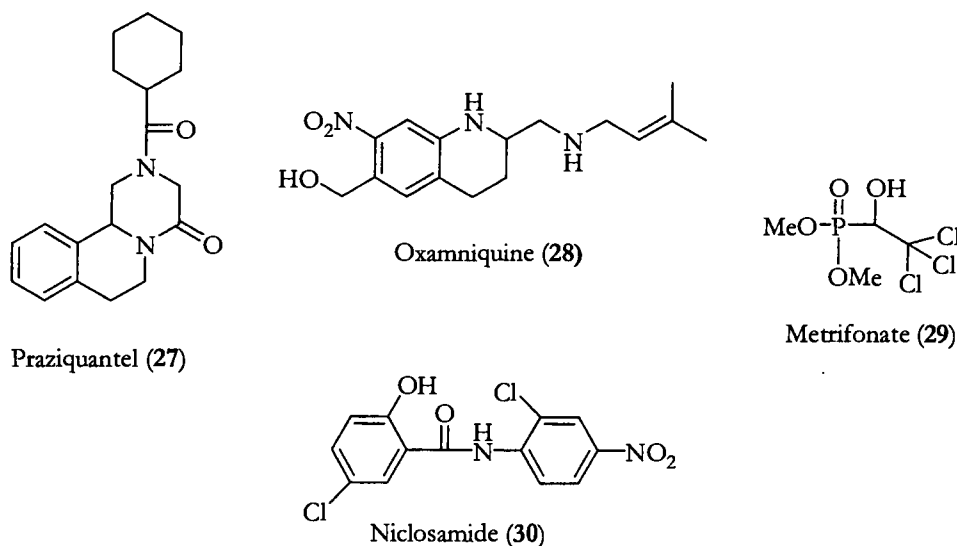


**Figure II.4.** Praziquantel (27), oxamniquine (28), and metrifonate (29), three chemotherapeutic agents used to treat schistosomiasis infection, and niclosamide (30), the most common commercially utilized molluscicidal agent.

#### Schistosomiasis The Scourge of Developing Nations

Aswan Dam, Egypt (prevalence leaped from 6-60% 3 yrs after completion)

Lake Volta, Ghana (90% prevalence two years after filling of lake)

Zambezi River, Zambezi (damming led to prevalence of 70% in children)

Kainji Lake, Nigeria (prevalence increased from 30% to 45% in 2 yrs after damming)

**Figure II.5.** Schistosomiasis The Scourge of Developing Nations . Irrigation Systems & Dams can result in stagnant water, recycling of wastewater, and increased water temperature and have led to marked increases in schistosomiasis transmission in some instances.<sup>49</sup>



detailed understanding of the specific chemical components of snail effluent is lacking and the potential for non-peptidic chemoattractants, as well as multiple chemoattractants, remains possible. Detailed analysis of this complex interaction between miracidia and snail would provide a powerful tool to control schistosomiasis, allowing the manipulation of their chemical ecology to short-circuit the life cycle of the trematode. Such a control system would mimic the attractive qualities of SCW (taking advantage of the chemosensory aspect of host location) from a location near the bottom of a waterway (using the negative photo-taxis of the miracidia to aid control), leading the miracidia into the mimic, where they could then be destroyed. By removing large numbers of miracidia from the waterway disease incidence would be decreased dramatically.

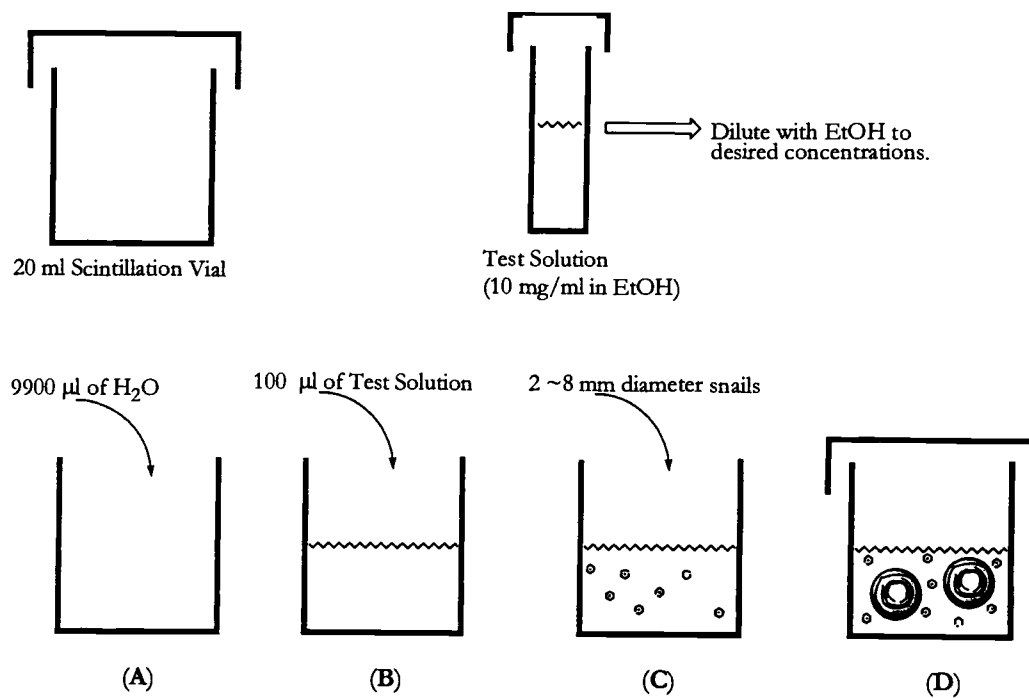
In the treatment of established ecosystems, the ecologically optimal course of action will use control methods other than the introduction of foreign species or molluscicidal agents. However, in artificial waterways such as irrigation channels and rice paddies, the use of molluscicides could represent the best, and most efficient, solution presently available. While niclosamide has been used effectively for decades, further research into molluscicides could develop an alternative that would be more potent and selective and less expensive, thus decreasing the contraction of schistosomiasis in developing nations.

## RESULTS AND DISCUSSION

Marine algae have proven themselves to be dynamic producers of secondary metabolites of structural novelty and potent biological activity. While yet difficult to prove categorically, it is believed that many of these secondary metabolites participate in the chemical defense of algae against herbivorous predators. As molluscs are dominant marine herbivores, algal survival would seem to indicate defensive capabilities against these predators. By extension, the potential exists that algal secondary metabolites could display molluscicidal activity against the freshwater snail, *Biomphalaria glabrata*, evolutionary "cousins" of marine molluscs. To begin exploring this, a panel of marine algal extracts was screened for toxicity to *B. glabrata*. The objective of this screening effort was two-fold, 1) to provide support for the hypothesis that marine algae produce molluscicidal secondary metabolites, and 2) to define algal extracts of high potency, enabling the isolation and structure elucidation of new molluscicidal components that could be useful in the treatment of snail infested waterways.

### MOLLUSCICIDAL SCREENING

Using the previously described molluscicidal assay (Figure II.6), a total of 90 algal samples were examined for activity against *B. glabrata* (Table II.1).<sup>59</sup> Algal samples tested were derived from tropical locations ranging in depth from 0-30 m. All four major algal divisions (red, brown, green, blue-green) were represented to varying degrees (Figure II.7.a), predominantly based on the availability of extract. The most commonly tested algae in the survey were cyanobacteria and red algae.

Molluscicidal Bioassay Protocol

**Figure II.6.** The molluscicidal bioassay protocol, (A) add 9900  $\mu$ l of  $H_2O$  to scintillation vial, (B) add 100  $\mu$ l of premade test solution, (C) add a pair of *B. glabrata* snails, (D) lightly cap and allow 24 hr then examine for snail toxicity.

**Table II.1.** Crude algal extracts examined in molluscicidal survey.

Gerwick Lab #	Organism	Type	Stock #	Depth Collected	Location Collected
1 MNS-8/Apr/97-02	<i>Lyngbya</i>	BG	WG-EXT-1058	2 meters	Madagascar
2 MNA-5/Apr/97-02	<i>Lyngbya</i>	BG	WG-EXT-1062	1-3 meters	Madagascar
3 MNT-6/Apr/97-01	<i>Lyngbya majuscula</i>	BG	WG-EXT-1083	6-7 meters	Madagascar
4 MSL-1/Apr/97-08	Blue green	BG	WG-EXT-1133	0-1 meters	Madagascar
5 MNS-8/Apr/97-03	<i>Lyngbya majuscula</i>	BG	WG-EXT-1153	2-3 meters	Madagascar
6 MNA-5/Apr/97-01	<i>Schizothrix</i>	BG	WG-EXT-1144	1-4 meters	Madagascar
7 MNA-5/Apr/97-03	sea grass/epiphytic blue green	BG	WG-EXT-1081	0-1 meters	Madagascar
8 MSL-1/Apr/97-08	Blue green	BG	WG-EXT-1133	0-1 meters	Madagascar
9 VTI-10/Feb/97-01	<i>Lyngbya</i>	BG	WG-EXT-1040	3-4 meters	Fiji
10 VYI-6/Feb/97-04	<i>Lyngbya/Schizothrix</i>	BG	WG-EXT-1064	2-3 meters	Fiji
11 VYI-5/Feb/97-02	<i>Lyngbya/Schizothrix</i>	BG	WG-EXT-1066	0-2 meters	Fiji
12 VYI-3/Feb97-01	<i>Schizothrix-Lyngbya</i>	BG	WG-EXT-1139	3-5 meters	Fiji
13 MAM-10/Apr/95-01	<i>Lyngbya</i>	BG	WG-EXT-1203		Madagascar
14 PNVB-6/Sep/98-02	<i>Lyngbya majuscula</i>	BG	WG-EXT-1209	0-1 meters	Papa New Guinea
15 PNHV-11/Sep/98-01	Blue-green algae	BG	WG-EXT-1215	0-1 meters	Papa New Guinea
16 PNSB-5/Sep/98-02	<i>Lyngbya</i>	BG	WG-EXT-1220	0-1 meters	Papa New Guinea
17 APO-22/Nov/98-01	<i>Lyngbya mix</i>	BG	WG-EXT-1245	0-1 meters	Japan
18 PNHL-9/Sep/98-02	<i>Lyngbya majuscula</i>	BG	WG-EXT-1232	5-8 meters	Papa New Guinea
19 PNFP-8/Sep/98-05	Blue-green	BG	WG-EXT-1242	0-1/3 meters	Papa New Guinea
20 PNHL-9/Sep/98-08	blue green algae	BG	WG-EXT-1255	0-1 meters	Papa New Guinea
21 PNSM-4/Sep/98-01	blue green algae	BG	WG-EXT-1257	0-1 meters	Papa New Guinea
22 PNLI-10/Sep/98-04	blue green algae	BG	WG-EXT-1261	0-1 meters	Papa New Guinea
23 VTI-11/Feb/97-02	<i>Schizothrix-lyngbya</i>	BG	WG-EXT-1189	11-12 meters	Fiji
24 HBP-14/Mar/98-01	<i>Lyngbya</i>	BG	WG-EXT-1205		Japan
25 MLK-2/Apr/97-01	<i>Laurencia</i>	R	WG-EXT-1074	0-1 meters	Madagascar
26 MSL-1/Apr/97-10	red algae	R	WG-EXT-1075	0-1 meters	Madagascar
27 ZAK-27/Mar/97-05	<i>Spiridea cupressina</i>	R	WG-EXT-1080	drift	South Africa
28 ZAK-27/Mar/97-01	<i>Gelidium</i>	R	WG-EXT-1082	drift	South Africa
29 ZAK-27/Mar/97-03	<i>Rhodophyllis neptans</i>	R	WG-EXT-1085	drift	South Africa

**Table II.1 (Continued).** Crude algal extracts examined in molluscicidal survey.

Gerwick Lab #	Genus	species	Stock #	Depth Collected	Location Collected
30 ZAR-28/Mar/97-01	<i>Gigartina minima</i>	R	WG-EXT-1089	0-1 meters	South Africa
31 ZAT-26/Mar/97-03	red algae	R	WG-EXT-1091	0-1 meters	South Africa
32 ZAK-27/Mar/97-06	<i>Plocamium corallorhiza</i>	R	WG-EXT-1077	0 meters	South Africa
33 MSL-1/Apr/97-04	<i>Laurencia</i>	R	WG-EXT-1128	0-2 meters	Madagascar
34 MSL-1/Apr/97-05	red algae	R	WG-EXT-1129	0-1 meters	Madagascar
35 ZAC-25/Mar/97-01	<i>Gigartina</i> type	R	WG-EXT-1098	0-1 meters	South Africa
36 MSL-1/Apr/97-07	<i>Halimena</i>	R	WG-EXT-1126	0-2 meters	Madagascar
37 MSL-1/Apr/97-06	red algae	R	WG-EXT-1135	0-2 meters	Madagascar
38 VYI-5/Feb/97-07	red algae	R	WG-EXT-1099	2-3 meters	Fiji
39 VSS-7/Feb/97-01	<i>Asparagopsis taxiformis</i>	R	WG-EXT-1152	6-7 meters	Fiji
40 VYI-2/Feb/97-07	<i>Galaxaura</i>	R	WG-EXT-1161	3-5 meters	Fiji
41 VYI-2/Feb/97-05	red algae	R	WG-EXT-1163	3-5 meters	Fiji
42 VTI-6/Feb/97-01	<i>Portieria hornemanni</i>	R	WG-EXT-1177	2-3 meters	Fiji
43 VYI-6/Feb/97-02	red algae	R	WG-EXT-1179	2-3 meters	Fiji
44 VTI-11/Feb/97-05	<i>Halimena</i>	R	WG-EXT-1180	3-4 meters	Fiji
45 MFM-31/Mar/97-01	red algae	R	WG-EXT-1143	0-1 meters	Madagascar
46 MFM-31/Mar/97-03	<i>Chondrococcus</i>	R	WG-EXT-1145	0-1 meters	Madagascar
47 MSL-1/Apr/97-03	<i>Rhodopeltis</i> types	R	WG-EXT-1151	2-3 meters	Madagascar
48 MDS-3/Apr/97-03	<i>Halymenia</i>	R	WG-EXT-1155	0-1 meters	Madagascar
49 VTI-10/Feb/97-02	<i>Titanophora weberae</i>	R	WG-EXT-1183	4-7 meters	Fiji
50 MSL-1/Apr/97-02	<i>Bostrychia</i>	R	WG-EXT-1200	0-1 meters	Madagascar
51 PNSB-5/Sep/98-01	<i>Chondococcus hornemannae</i>	R	WG-EXT-1221	3-10 meters	Papa New Guinea
52 PNSB-4/Sep/98-04	<i>Ceratodictyon</i>	R	WG-EXT-1222	1-2 meters	Papa New Guinea
53 PNSB-4/Sep/98-05	<i>Halymenia</i>	R	WG-EXT-1223	0-1 meters	Fiji
54 VSS-7/Feb/97-02	red algae	R	WG-EXT-1186	2-3 meters	Fiji
55 VYI-5/Feb/97-08	<i>plocamium?</i>	R	WG-EXT-1187	2-3 meters	Fiji
56 VYI-5/Feb/97-06	red algae	R	WG-EXT-1188	2-3 meters	Papa New Guinea
57 PNVB-6/Sep/98-06	<i>Peyssonelia</i>	R	WG-EXT-1236	10 meters	Papa New Guinea

**Table II.1 (Continued).** Crude algal extracts examined in molluscicidal survey.

Gerwick Lab #	Genus	species	Stock #	Depth Collected	Location Collected
58 PNSB-4/Sep/98-03	red algae	R	WG-EXT-1239	0-1 meters	Papa New Guinea
59 PNSB-4/Sep/98-02	<i>Halymenia</i>	R	WG-EXT-1249	0-1 meters	Papa New Guinea
60 PNVB-6/Sep/98-03	<i>Coralina red alga</i>	R	WG-EXT-1251	10 meters	Papa New Guinea
61 PNSM-4/Sep/98-03	Red algae	R	WG-EXT-1252	0-1 meters	Fiji
62 VYI-5/Feb/97-05	<i>Peysonnellia coulifera</i>	R	WG-EXT-1191	2-3 meters	Fiji
63 VYI-2/Feb/97-03	<i>Plocamium</i>	R	WG-EXT-1192	3-5 meters	Fiji
64 VYI-11/Feb/97-08	<i>Zellera tawallina</i>	R	WG-EXT-1193	3-7 meters	Fiji
65 VYI-5/Feb/97-03	<i>Vidalia obtusiloba</i>	G	WG-EXT-1199	2-3 meters	Fiji
66 VTI-11/Feb/97-03	<i>Flabaultia tegetiformis</i>	G	WG-EXT-1201	3-4 meters	Fiji
67 MLK-2/Apr/97-02	filamentous green	G	WG-EXT-1073	0-2 meters	Madagascar
68 ZAM-28/Mar/97-03	<i>Halimeda cuneata</i>	G	WG-EXT-1061	0-2 meters	South Africa
69 MDS-3/Apr/97-01	<i>Codium (encrusting)</i>	G	WG-EXT-1097	0-1 meters	Madagascar
70 ZAM-28/Mar/97-02	<i>Caulerpa filiformis</i>	G	WG-EXT-1092	3-4 meters	South Africa
71 VTI-11/Feb/97-04	<i>Halimeda discoidea</i>	G	WG-EXT-1100	3-4 meters	Fiji
72 VYI-2/Feb/97-02	<i>Tydemania expeditionis</i>	G	WG-EXT-1172	13-14 meters	Fiji
73 VTI-11/Feb/97-07	<i>Boodlea coacta</i>	G	WG-EXT-1173	3-4 meters	Fiji
74 VTI-9/Feb/97-03	<i>Avrainvillea</i>	G	WG-EXT-1174	13-14 meters	Fiji
75 VTI-3/Feb/97-07	<i>Dictyosphaeria versleysii</i>	G	WG-EXT-1176	2 meters	Fiji
76 MNS-8/Apr/97-01	<i>Halimeda "crinkly"</i>	G	WG-EXT-1147	0-1 meters	Madagascar
77 VYI-3/Feb/97-04	<i>Chlorodesmis</i>	G	WG-EXT-1182	2 meters	Fiji
78 PNTD-8/Sep/98-02	<i>Avrainvillea</i>	G	WG-EXT-1217	26-30 meters	Papa New Guinea
79 VYI-4/Feb/97-03	<i>Halimeda</i>	G	WG-EXT-1184	2-3 meters	Fiji
80 PNNI-7/Sep/98-03	<i>Tydemanea expeditionalis</i>	G	WG-EXT-1225	13-14 meters	Papa New Guinea
81 PNWB-3/Sep/98-01	<i>Halimeda maculosa</i>	G	WG-EXT-1228	1-4 meters	Papa New Guinea
82 VYI-3/Feb/97-03	<i>Tydemania expeditionis</i>	G	WG-EXT-1198	16-17 meters	Fiji
83 ZAT-26/Mar/97-02	<i>Zonaria subarticulata</i>	B	WG-EXT-1088	0-1 meters	South Africa
84 VYI-5/FEB/97-04	<i>Padina minor</i>	B	WG-EXT-1115	2-3 meters	Fiji
85 VYI-4/Feb/97-06	<i>Padina minor</i>	B	WG-EXT-1168	2-3 meters	Fiji

**Table II.1 (Continued).** Crude algal extracts examined in molluscicidal survey.

Gerwick Lab #	Genus	species	Stock #	Depth Collected	Location Collected
86 VYI-2/Feb/97-04	<i>Laminaria catenata</i>	B	WG-EXT-1171	3-5 meters	Fiji
87 VYI-3/Feb/97-06	<i>Turbinaria</i>	B	WG-EXT-1181	2 meters	Fiji
88 ZAR-28/Mar/97-03	<i>Ecklonia biminciata</i>	B	WG-EXT-1150	0-2 meters	South Africa
89 VSS-7/Feb/97-03	<i>Padina gymnospora</i>	B	WG-EXT-1185	3 meters	Fiji
90 PNVB-6/Sep/98-05	<i>Lobophora</i>	B	WG-EXT-1226	10 meters	Papa New Guinea

Legend

BG = blue-green

R = red

G = green

B = brown

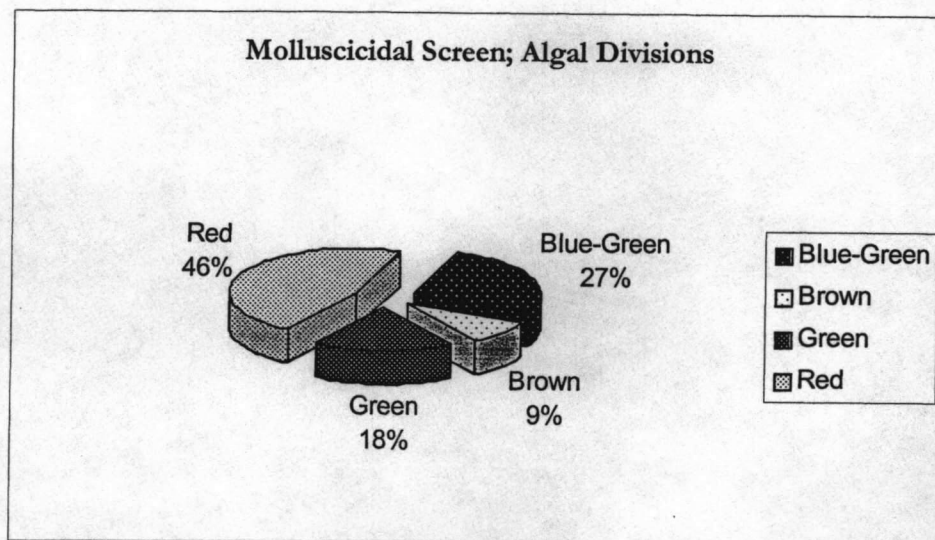


**Figure II.7.a.** The taxonomic distribution of algal extracts represented in the molluscicidal screening assay.

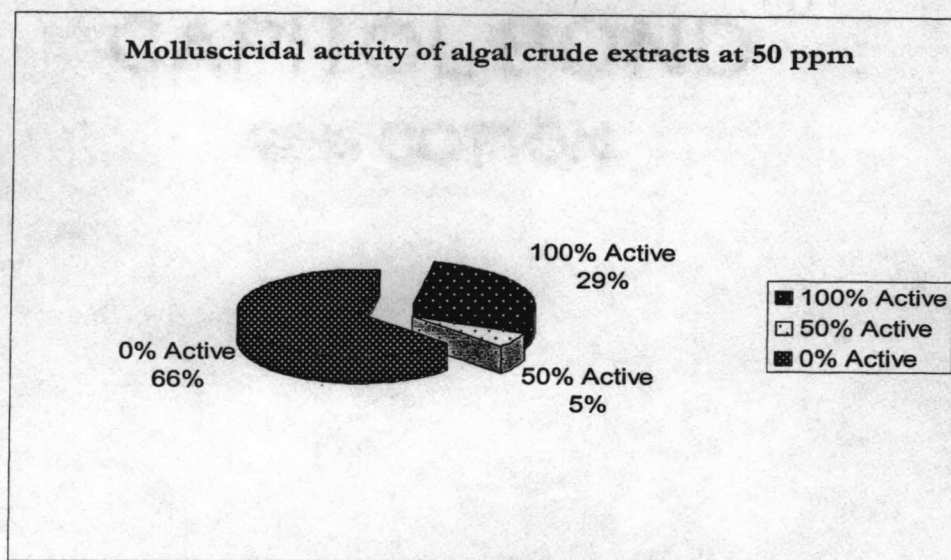


**Figure II.7.b** The molluscicidal activity of algal crude extracts at 50 ppm..



Overall, 46% of tested extracts caused molluscan lethality at 100 ppm, and 34% were toxic at 50 ppm (Figure II.7.b). Figure II.8 describes the overall percentage of molluscicidal activity of each of the divisions. The cyanobacteria displayed the highest percentage of active extracts, with 58% and 46% of their members toxic at 100 and 50 ppm, respectively (Figure II.9). Strong toxicity was also observed in extracts of Chlorophytes (56% at 100 ppm and 44% at 50 ppm; Figure II.10) and extracts of the Rhodophyta (45% at 100 ppm and 29% at 50 ppm; Figure II.11). Phaeophyceans were responsible for the least molluscicidal extracts, with only 1 in 8 being toxic at either concentration (Figure II.12).

The lack of activity in the brown algal extracts may be partially due to the small sample size examined. It is also possible that, while lacking statistical relevance, the low percentage of molluscicidal extracts for this division, as well as the high activity rates observed for other divisions, reflects divergent methods of predator defense. It has been theorized that algae can prevent predation in a number of ways, among them chemical, structural (calcification), and photosynthetic (growth). The primary tenet of this theory is the optimal allocation of resources by the algae to those methods of defense that will yield the highest probability of survival. Algae which optimize their photosynthetic capacity, and thus grow in a rapid manner, and also often to large sizes, are able to avoid being decimated by predators by outgrowing them (such as some brown algae). Those that grow more slowly are believed to protect themselves by producing a tough exterior (calcified red and green algae, for example) or by being chemically defended (cyanobacteria, green and red algae).

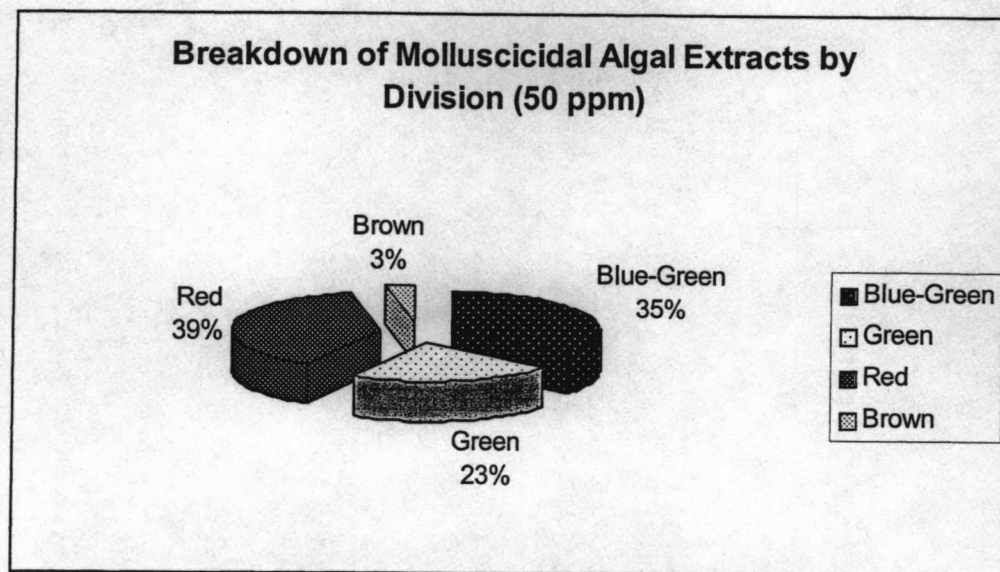
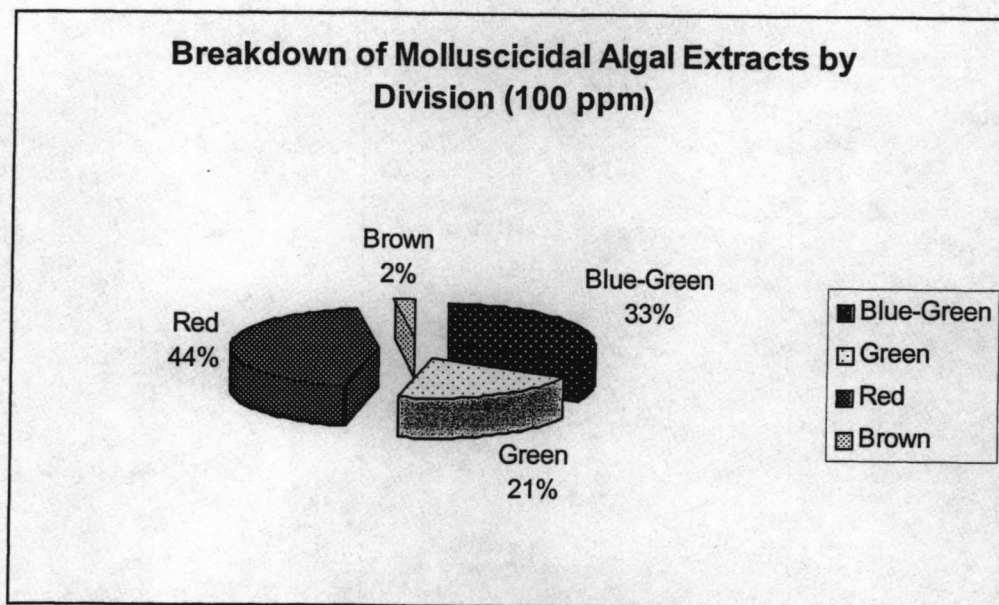


**Figure II.8.** Division breakdown of molluscicidal extracts at 100 and 50 ppm.

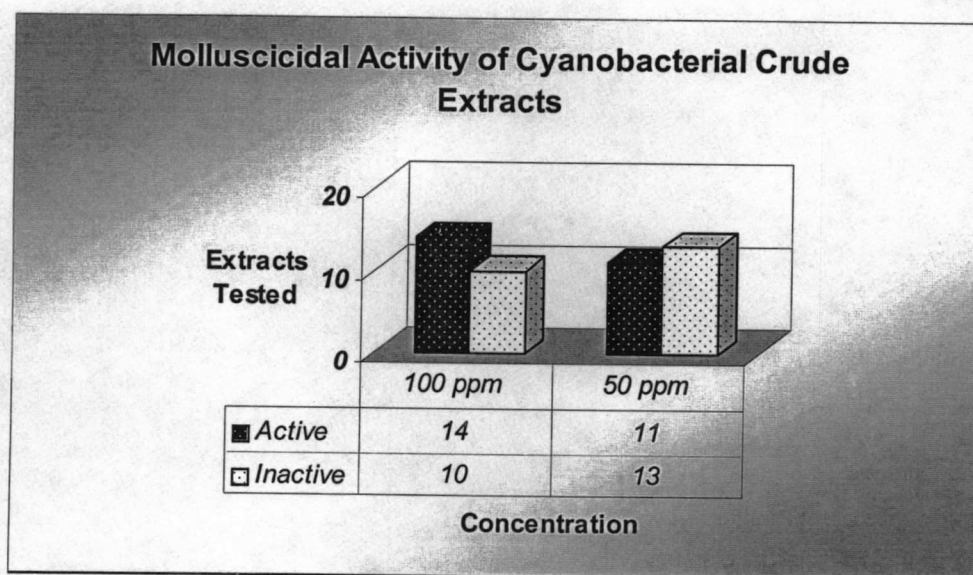


**Figure II.9.** Molluscicidal Cyanobacteria Crude Extracts at 100 and 50 ppm.

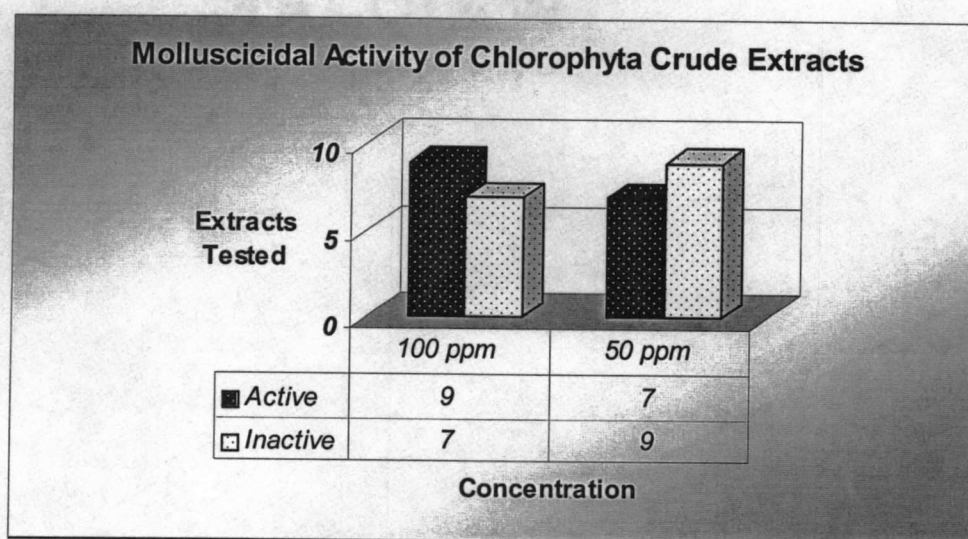


**Figure II.10.** Molluscicidal Chlorophyte crude extracts at 100 and 50 ppm.



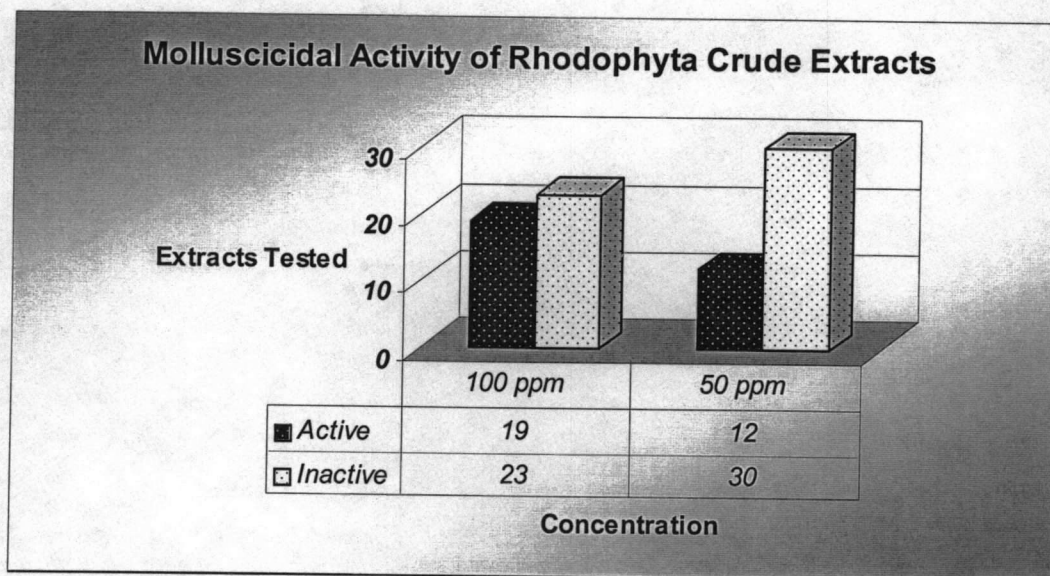


**Figure II.11.** Molluscicidal Rhodophyte crude extracts at 100 and 50 ppm.

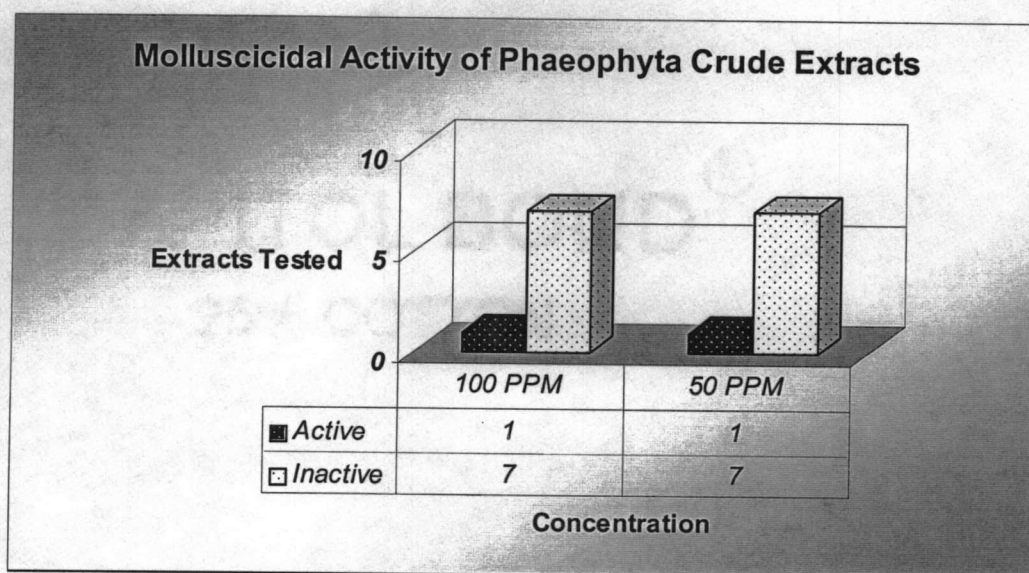


**Figure II.12.** Molluscicidal Phaeophyte crude extracts at 100 and 50 ppm.

The results of this survey support the hypothesis that marine algae produce secondary metabolites that are toxic to snails, including freshwater representatives. Further investigation is required to definitively link *B. glabrata* toxicity to compounds that function in nature to protect algae from their natural molluscan predators. It is reasonable, however, that such a correlation exists.

As an additional observation, the high potency of molluscicidal marine algal extracts suggests that the 50 ppm test concentration may prove more efficient in initial assessments of activity. Typically, a concentration of 100 ppm is used to identify extracts worthy of further pursuit. However, the observed 34% lethality of extracts at 50 ppm provides a more restrictive, and therefore, more appealing threshold than the 46% observed when algal samples are tested at 100 ppm.

#### THE CHEMICAL INVESTIGATION OF PROMISING MOLLUSCICIDAL ALGAL EXTRACTS

The robust activity of marine algal extracts in the molluscicidal screening assay afforded many candidates for further investigation. Of these, three were identified as possessing the greatest promise of successful isolation of the molluscicidal constituent, a Fijian *Portieria hornemanni* (Rhodophyta) and two Malagasy *Lyngbya majuscula* extracts (cyanobacteria).

Remarkable molluscicidal activity was observed when an extract of *P. hornemanni* was examined. While the typical molluscicidal assay is run for 24 hr, the extract of *P. hornemanni* was 100% lethal to snails within 0.5 hr at 100, 50, and 25 ppm. Full toxicity was also observed at 10 and 1 ppm, but only at the 24 hr time-point. The

potency at the upper three concentrations resulted in the expulsion of hemolymph (snail blood) by the snail into the water. This bleeding commenced prior to snail death and continued briefly afterwards.

Guided by biological activity (at 25 ppm), the extract was subjected to successive rounds of chromatography utilizing VLC and solid phase extraction, and final purification through HPLC (Figure II.13). All of the molluscicidal activity of this extract was due to a single non-polar major compound. Using the standard assortment of spectroscopic experiments, the molluscicidal compound was identified as the known metabolite chondrocole C (**31**, discussed further in Chapter III of this thesis).<sup>60</sup> Interestingly, chondrocole C retained the extreme potency of its crude extract at 100, 50, and 25 ppm, but was non-lethal at concentrations below 25 ppm, yielding fully live snails after 24 hr. Despite this apparent lack of activity after 24 hr, at 10 ppm **31** caused the exuding of hemolymph during hour one. While this observation coincided with rapid snail death when assaying the crude extract and active fractions, nearly full recovery of the snails could be observed at the end of the first hour when **31** was tested. Possible explanations for the lack of concentration of activity, as compared to the crude extract, include increased degradation of **31** in pure form when exposed to the assay environment or multiple compounds acting synergistically. Both of these conclusions are tenable, as **31** is acid sensitive and only one of numerous compounds present in this extract that are structurally, and perhaps toxicologically, similar (see Chapter III).

Molluscicidal activity (full lethality at 1-100 ppm) was also observed in a pair of Malagasy *L. majuscula* crude extracts. In one, collected off Nosy Tanikely, Madagascar

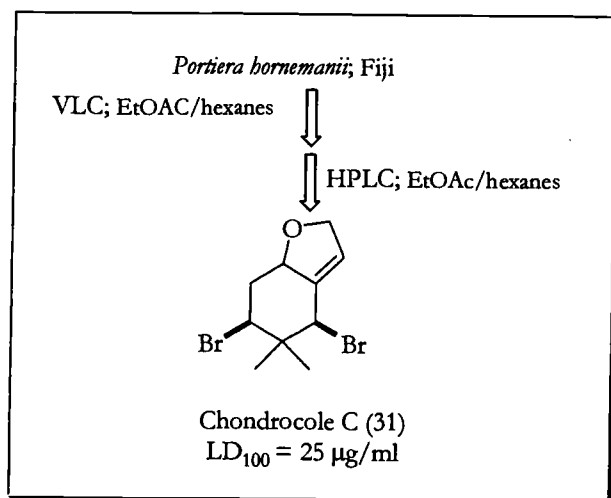


Figure II.13. The isolation of the molluscicide chondrocole C (31).

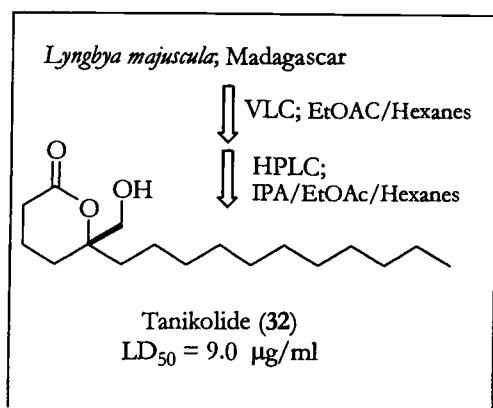


Figure II.14. The isolation of the molluscicide tanikolide (32).

(and referred to herein as Extract-MNT), bioassay guided fractionation lead to the isolation and structure elucidation of tanikolide (**32**, Figure II.14).<sup>61</sup> Tanikolide, however, only accounted for a portion of the toxicity observed in the crude extract, with an LD<sub>50</sub> of 9 ppm compared to the full toxicity at 1 ppm of its parent extract. Continued examination of the fractions of Extract-MNT for the remainder of its molluscicidal activity resulted in the isolation of a second toxic compound, a lyngbic acid (**33**).<sup>62</sup> While toxicity to brine shrimp has been observed previously for **33**, molluscicidal activity was unknown.<sup>62</sup> Lyngbic acids are components of the tail of the non-molluscicidal malyngamides, the most frequently encountered of *Lyngbya* spp. secondary metabolites (Chapter IV). To validate the molluscicidal activity of **33**, three previously, and independently, isolated samples of **33**, and the Extract-MNT **33**, were tested in the same assay. However, the results of this assay created more questions than answers. While three of the samples, including **33** derived from Extract-MNT, were lethal to *B. glabrata*, one was completely inactive. Comparisons of 1-D <sup>1</sup>H NMR spectra could not define a single characteristic that would distinguish them from each other, and the result remained a curiosity until the molluscicidal component of another Malagasy *L. majuscula* (Extract-MNA) was defined, as described below.

Extract-MNA was toxic to snails at concentrations as low as 0.1 ppm, a highly robust activity for a crude extract. After each chromatographic step the biological activity appeared to coincide with a somewhat polar and minor compound presenting a 'lemon-yellow' char when treated with heat and H<sub>2</sub>SO<sub>4</sub> on TLC (Figure II.15). Fractionation was also concentrating the molluscicidal activity; final purification yielded a compound that was fully lethal at an astoundingly potent 0.004 ppm. The



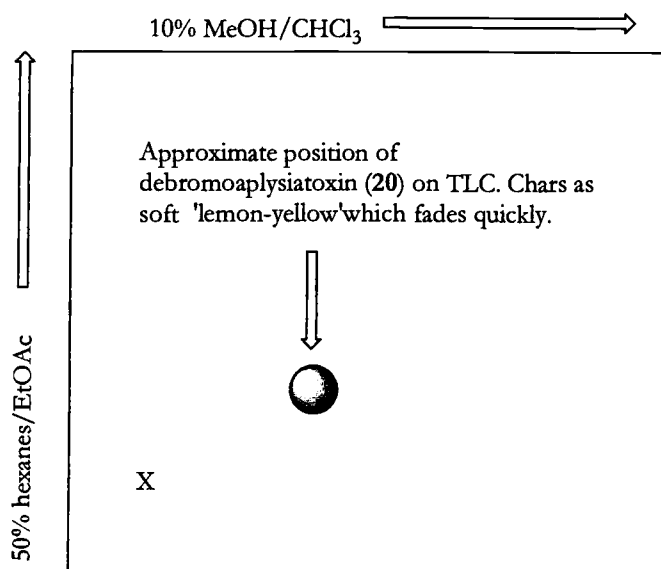
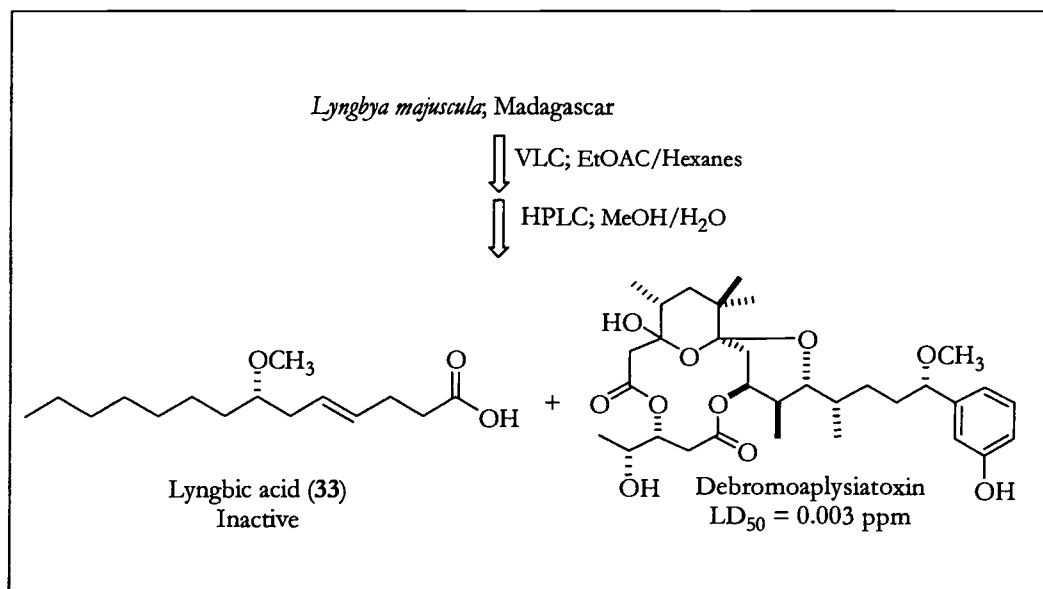


Figure II.15. Graphical representation of **20** on TLC.

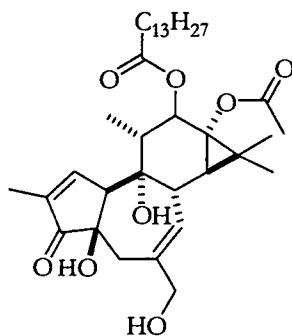
activity quickly decreased at lower concentrations, with an LD<sub>50</sub> established at 0.003 ppm and no activity at 0.002 ppm, after a 24 hr incubation.

Familiar resonances in the 1-D <sup>1</sup>H NMR spectra suggested that the molluscicidal compound of Extract-MNA was the known *L. majuscula* metabolite, debromoaplysiatoxin (**20**, Figure II.16), a fact confirmed by HPLC co-injection with a standard solution of **20**.<sup>63</sup> As mentioned above, debromoaplysiatoxin has a relatively conspicuous polarity and charring pattern on TLC. The polarity range coincides very closely with lyngbic acid. In extracts with only a minor component of debromoaplysiatoxin, it is conceivable that the tailing char of a fatty acid such as **33** could obscure the visualization of **20**. HPLC co-injections confirmed this, with **20** present as an extremely minor contaminant of the lyngbic acid preparation of Extract-MNT as well as the other two samples of lyngbic acid that displayed molluscicidal activity. Consistent with this scenario, **20** was not present in the lyngbic acid preparation that was inactive against *B. glabrata*. The potency of **20** accounts for most of the activity of Extract-MNT, thus providing a satisfying conclusion to the anomalous results that were encountered.

Debromoaplysiatoxin, one of the best known *L. majuscula* metabolites, is commercially valuable as a molecular probe due to its ability to activate the protein kinase C (PKC) pathway.<sup>64</sup> Functioning in a manner similar to a phorbol ester, the ability of **20** to stimulate the PKC pathway can lead to the promotion of tumors. In order to determine if PKC pathway stimulation by **20** was the cause of its molluscicidal activity, a series of whole animal pharmacological experiments was undertaken.



**Figure II.16** The isolation of the molluscicide debromoaplysiatoxin (20) and the inactive lyngbic acid (33).



Phorbol 12-Myristate 13-Acetate (34, PMA)

An assessment of the relative molluscicidal potencies of debromoaplysiatoxin and the phorbol ester, phorbol 12-myristate 13-acetate (**34**) showed debromoaplysiatoxin to be 80x more potent, with an LD<sub>50</sub> of 5.0 nM as compared to 400 nM for **34** (Figure II.17). To determine the involvement of the PKC pathway in the toxicity exhibited by **20** and **34** against snails, they were assayed in the presence of the PKC pathway inhibitor, MPKCPI (myristoylated protein kinase C peptide inhibitor). The molluscicidal assay was run as before but with the addition of a 2 hr pre-incubation period of the antagonist. The antagonist was added at two concentrations, equimolar and 2x molar excess, according to the LD<sub>50</sub> of the PKC activator being tested. After the 2 hr incubation, the test sample was added and the 24 hr test period initiated. As a control, the inhibitor was tested and found to possess no molluscicidal activity.

As expected, the inhibition of the PKC pathway abrogated the molluscicidal effects of PMA at both concentrations (Figure II.18). However, while not dead, the snails were visibly effected. When antagonizing the molluscicidal effects of debromoaplysiatoxin, the inhibitor had only mixed success. Successful at inhibiting toxicity at 10 nM (twice the LD<sub>50</sub> of **20**), at equimolar concentrations (5 nM), debromoaplysiatoxin retained its lethality to the snails despite the presence of the PKC inhibitor (Figure II.18). Therefore, the molluscicidal activity of debromoaplysiatoxin, and **34**, is most likely due to their activity as PKC activators. The residual activity of debromoaplysiatoxin in the presence of the PKC antagonist, and the decreased health of the snails even in the presence of the antagonist, may hint at additional mechanisms

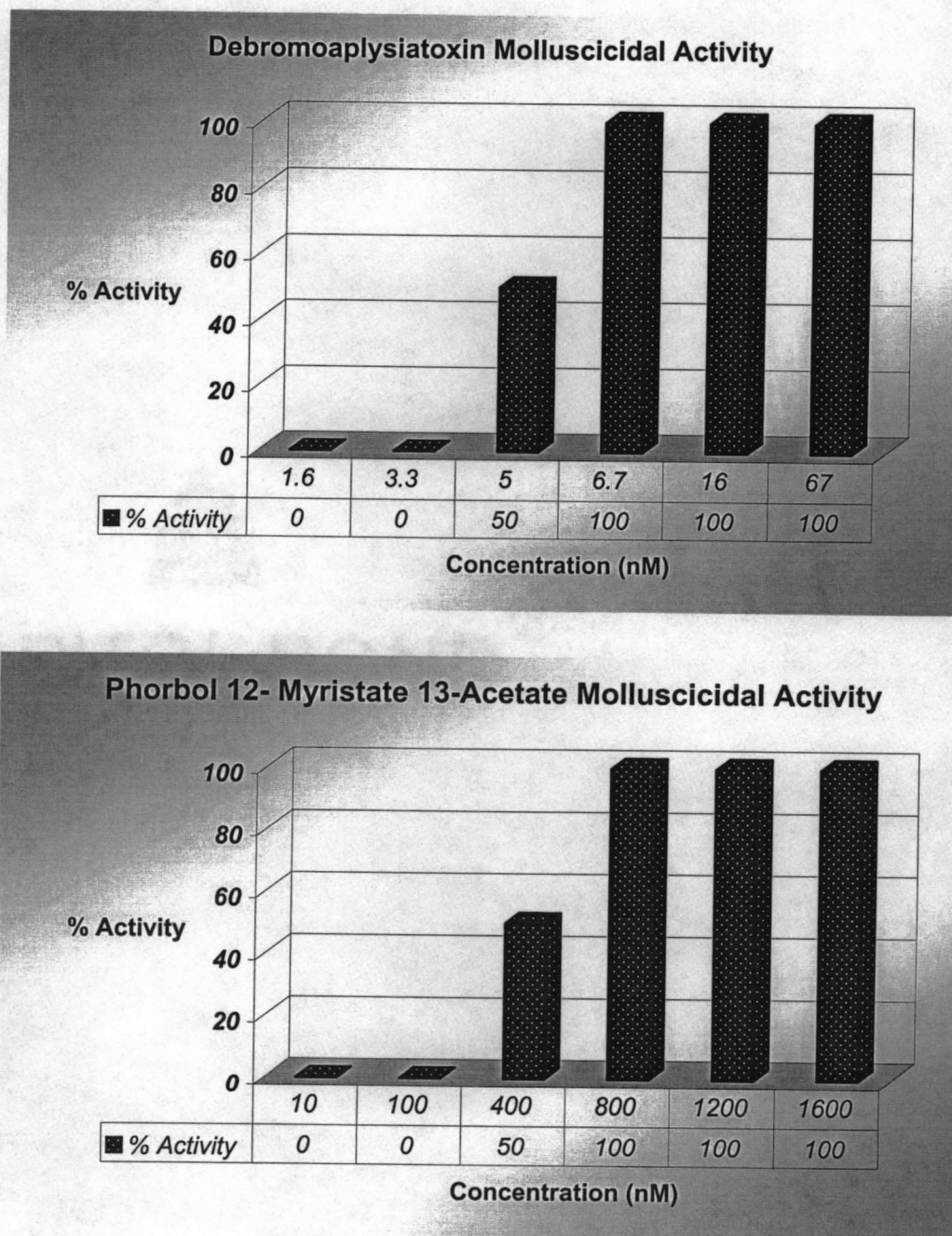


**Figure II.17.** Molluscicidal Activity of debromoaplysiatoxin (**20**) and PME (**34**). Calculated errors are; for **20**,  $\pm 13.7\%$  at 5 nM and  $\pm 22.4\%$  at 6.7 nM; for **34**,  $\pm 22.4\%$  for 100 and 800 nM concentrations and  $\pm 35.4\%$  at 400 nM.

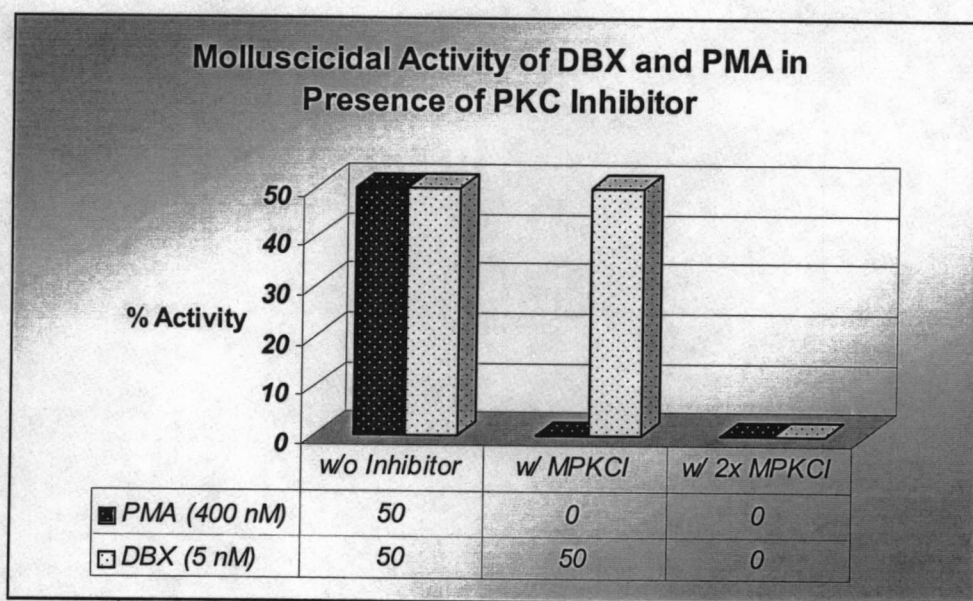


**Figure II.18.** Molluscicidal Activity of debromoaplysiatoxin (**20**, DBX) and PMA (**34**) in the presence of PKC Inhibitor (MPKCI). All deviations = 0 except for DBX w/MPKCI, which =  $\pm 22.3$ .

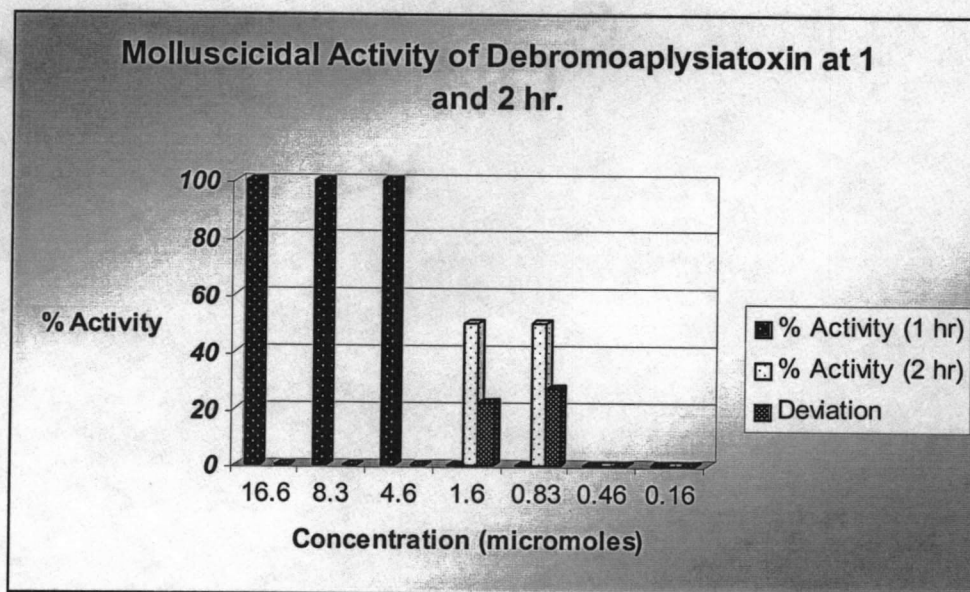


**Figure II.19.** Molluscicidal Activity of debromoaplysiatoxin (**20**, DBX) at 1 and 2 hr.

of molluscicidal activity, such as the potential for a different binding site or target. The tropical plant *Jatropha curcas* (Euphorbiaceae) has also been shown to produce metabolites which function as phorbol esters and molluscicides.<sup>65</sup> Perhaps this apparent snail sensitivity to PKC pathway activation could be exploited in the creation of new molluscicides.

Despite the fact that debromoaplysiatoxin is a tumor promoter, it could still be valuable in controlling the spread of schistosomiasis, as it has a few advantages over niclosamide. The first advantage is potency; niclosamide is fully lethal to snails in 2 hr at 1.5 mg/L,<sup>9</sup> or 4.6  $\mu$ M, whereas debromoaplysiatoxin is equally active in less than 1 hr at the same molarity and 50% toxic at 1.6  $\mu$ M in 2 hr (Figure II.19). Also, a difficulty in working with debromoaplysiatoxin in the laboratory is its propensity to degrade, especially in the presence of acid. This may be a benefit if used as a molluscicidal. While niclosamide accumulates in the soils, debromoaplysiatoxin will be degraded relatively quickly by microbial esterases. Resistance to niclosamide has also been noted in *Bulinus truncatus* in the field and laboratory samples of *Biomphalaria glabrata*; hence, a fundamentally new agent would be of value.

The utility of a compound such as debromoaplysiatoxin would be best in artificial waterways such as rice paddies and irrigation channels where a stable and natural ecosystem would not be decimated. Taking advantage of the rapid action and degradation of **20**, a waterway could be inoculated periodically, presumably without risk to human or livestock (assuming time is allowed for **20** to degrade). Used in such a manner, debromoaplysiatoxin or one of its pharmaceutical derivatives could greatly assist in the effort to control the spread of schistosomiasis.

## EXPERIMENTAL

## GENERAL

NMR spectra were recorded on Bruker DRX 300 MHz spectrometer. Mass spectra were recorded on a Kratos MS50TC mass spectrometer. UV spectra were recorded on a Hewlett Packard 8452A diode array spectrophotometer while FT-IR spectra were recorded on a Nicolet 510 spectrophotometer. HPLC separation was accomplished with a Waters M-6000A pump, a Rheodyne 7010 injector, and a Waters Lambda-Max 480 spectrophotometer or a Waters RI detector. Optical rotation measurements were recorded on a Perkin-Elmer Model 141 polarimeter. Phorbol 12-Myristate 13-Acetate (34, PMA) CAS 16561-29-8. FisherBiotech Cat. #BP685-1. Myristoylated Protein Kinase C Peptide Inhibitor (MPKCI) Promega Corporation Cat. #V5691. Authentic debromoaplysiatoxin source supplied by Dr. Kerry McPhail, OSU.

## BIOLOGICAL MATERIAL

The marine red alga, *Portieria hornemanni*, was collected by hand from shallow water (2-3 m) on 6 February 1997 at Taveuni Island, Fiji, and stored at -20°C in IPA until workup. Original collections were made by G. Hooper and M. Graber. A voucher sample is available from WHG as collection number VTI-6 FEB 97-1.

The marine cyanobacterium, *Lyngbya majuscula*, was collected by hand from shallow water (6-7 m) on 6 April, 1997 at Nosy Tanikely, Madagascar, and stored at -20°C in IPA until workup. Original collections were made by W. Gerwick, G.



Hooper, and E. Gerwick. A voucher sample is available from WHG as collection number MNT-6 APR 97-1.

The marine cyanobacterium, *Lyngbya majuscula*, was collected by hand from shallow water (1-3 m) on 5 April 1997 at Nosy Be, Madagascar and stored at  $-20^{\circ}\text{C}$  in IPA until workup. Original collections were made by W. Gerwick, G. Hooper, and E. Gerwick. A voucher sample is available from WHG as collection number MNA-5 APR 97-1.

#### EXTRACTION AND ISOLATION OF CHONDROCOLE C (**31**)

The IPA preserved alga was extracted with  $\text{CH}_2\text{Cl}_2/\text{MeOH}$  (2:1) two times to give a crude extract of 1.5 g. A portion of this (1.3 g) was fractionated using vacuum liquid chromatography (VLC) on Si gel with a stepwise gradient of hexanes/EtOAc and EtOAc/MeOH to give six fractions. Because fraction two (eluted 0%-10% hexanes/EtOAc) possessed toxicity to *B. glabrata* (at 25 ppm), it was subjected to RP-Solid Phase Extraction (5mm Varian SEP Cartridge) with a 60-100% MeOH/ $\text{H}_2\text{O}$  gradient. Molluscicidal activity was observed in fraction two (60-70% MeOH/ $\text{H}_2\text{O}$ ), which subsequently yielded pure **31** through repetitive NP-HPLC (90% hexanes/EtOAc; 246 x 4.6 mm, 10  $\mu$  Phenomonex Si Column, 1.5 mL/min) by the collection of a peak centered at  $t_{\text{R}} = 6.3$  min detected by UV absorption at 254 nm (354 mg, 27% of total extract).

#### EXTRACTION AND ISOLATION OF TANIKOLIDE (32)

The IPA preserved alga was extracted with  $\text{CH}_2\text{Cl}_2/\text{MeOH}$  (2:1) two times to give a crude extract of 9.4 g. A portion of this (8.6 g) was fractionated using vacuum liquid chromatography (VLC) on Si gel with a stepwise gradient of hexanes/EtOAc/MeOH to give eleven fractions. Fraction four (eluted 50% EtOAc/hexanes), containing molluscicidal activity, was further subjected to VLC ( $\text{CHCl}_3/\text{MeOH}$ ) and collected as six fractions. Fraction 3, the molluscicidal fraction in this series, was purified by HPLC (Versapak Si 10  $\mu$ , 300 x 4.1 mm, 1 mL/min, RI detection, hexanes/EtOAc/IPA, 80:15:5) to yield 70 mg (8.1% of total extract) of tanikolide by collection of a peak centered at  $t_R = 22$  min.

#### EXTRACTION AND ISOLATION OF DEBROMOAPLYSIATOXIN (20)

The IPA preserved alga was extracted with  $\text{CH}_2\text{Cl}_2/\text{MeOH}$  (2:1) two times to give a crude extract of 2.3 g. A portion of this (1.8 g) was fractionated using vacuum liquid chromatography (VLC) on Si gel with a stepwise gradient of hexanes/EtOAc and EtOAc/MeOH to give eight fractions. Because fractions six and seven (eluted with 60%-100% hexanes/EtOAc) both contained **20**, they were recombined and subjected to semi-preparative RP-HPLC (Phenomonex Sphericlone ODS Column, 246 x 10 mm, 5  $\mu$ ) in 90% MeOH/ $\text{H}_2\text{O}$ . Final purification ( $t_R = 26$  min, 0.8 mL/min) was accomplished using RP-HPLC (Phenomonex Sphericlone ODS Column, 246 x 4.6, 5  $\mu$ ) in 70% MeOH/ $\text{H}_2\text{O}$  to yield pure **20** (1.3 mg, 0.07% of total extract).

#### MOLLUSCICIDAL BIOASSAY

Evaluation for molluscicidal activity was performed as previously described, using *Biomphalaria glabrata* as the test organism.<sup>25</sup> Aliquots of a 10 mg/ml (in EtOH) stock solution of were serially diluted using EtOH to achieve a range of concentrations to be tested. To a 20 ml scintillation vial containing 9900 µl of ddH<sub>2</sub>O 100 µl of test solution was added and the contents swirled. To each vial two snails were added (approx. 8 mm each in diameter). After 24 hr the live and dead snails were tallied. Snails were determined alive by visual observation of a heartbeat or a response to foot probing.

#### INHIBITION OF THE PKC PATHWAY

To eventually yield equimolar and 2x molar equivalents of the putative PKC activator, the appropriate quantity of MPKCI (PKC antagonist) was dissolved in EtOH. Into a 20 ml scintillation vial containing 9800 µl ddH<sub>2</sub>O, 100 µl of antagonist was added. To this solution, two snails (as in the standard protocol) were added. After a 2 hr pre-incubation period, 100 µl of test solution (putative activator) was added, and the assay was allowed to proceed in the standard manner for 24 hr. A total of five replicates for each solution were tested.

## REFERENCES

35. Haseeb, M.A. and Eveland, L.K. *Experientia* **1991**, *47*, 970-974.
36. Tingley, G.A. *Trans. R. Soc. Trop. Med. Hyg.* **1988**, 448-452.
37. World Health Organization *The Control of Schistosomiasis: second report of the WHO expert committee* **1993**, WHO Technical Report Series, World Health Organization:Geneva.
38. World Health Organization *The World Health Report 1998; Life in the 21<sup>st</sup> century, a vision for all* **1998**, WHO Technical Report Series, World Health Organization:Geneva.
39. World Bank *World Development Report 1993: Investing in Health* **1993**, Oxford University Press:London, pp. 1-329.
40. WHO Information Fact Sheets, Fact Sheet No. 115, <http://www.who.int/inf-fs/en/fact115.html>, (last accessed, August 2001).
41. WHO Infectious Diseases, Schistosomiasis, <http://www.who.int/ctd/schisto/index.html> (last accessed, August 2001).
42. WHO Infectious Diseases, Schistosomiasis, Burdens and Trends, <http://www.who.int/ctd/schisto/burdens.htm> (last accessed, August 2001).
43. Perrett, S. and Whitfield, P.J. *Parasitology Today* **1996**, *12*, 156-159.
44. Davis, A. In *Manson's Tropical Diseases*, Cook, G.C. Ed.; WB Saunders Co. Ltd.:London, **1996**, pp. 1413-1456.
45. World Health Organization *Bench Aids for the Diagnosis of Intestinal Parasites*, **1994**, WHO Technical Report Series, World Health Organization:Geneva.
46. Fournier, A.; Clement, P. Mimouni, P.; Mingyi, X.; Combes, C. *Ethol. Ecol. Evol.* **1995**, *5*, 477-487.
47. Utzinger, J. *Novel Approaches in the Control of Schistosomiasis: from rapid identification to chemoprophylaxis*, **1999**, <http://www.sti.unibas.ch/pdfs/utzipart1.pdf> and <http://www.sti.unibas.ch/pdfs/utzipart2.pdf>, (last accessed, August 2001).
48. World Health Organization *The Control of Schistosomiasis; Report of a WHO Expert Committee on the Control of Schistosomiasis*, **1985**, WHO Technical Report Series, World Health Organization:Geneva.

49. Fahim, H. *Dams, People and Development: The Aswan High Dam Case*. Pergamon Press: New York, 1981.
50. Invading Species as Agents of Extinction, NRE 220 Lecture 7, <http://www-personal.umich.edu/~dallan/nre220/outline7.htm>, (last accessed August 2001).
51. Haas, W.; Korner, M.; Hutterer, E.; Wegner, M.; Haberl *Parasitol.* **1995**, *110*, 133-142.
52. Haberl, B.; Lakbe, M.; Fuchs, H.; Strobel, M.; Schmalfuss, G.; Haas, W. *Int. J. Parasitol.* **1995**, *25*, 551-560.
53. Haas, W.; Haberl, B.; Schmalfuss, G.; Khayyal, M.T. *J. Parasitol.* **1994**, *80*, 345-353.
54. Thomas, J.D. and Eaton, P. *Comp. Biochem. Physiol.* **1993**, *106C*, 781-796.
55. Sponholtz, G.M. and Short, R.B. *J. Parasitol.* **1975**, *61*, 228-232.
56. Roberts, T.M.; Stibbs, H.H.; Chernin, E.; Ward, S. *J. Parasitol.* **1978**, *64*, 277-282.
57. Monroy, F.P. and Loker, E.S. *J. Parasitol.* **1993**, *79*, 416-423.
58. Haas, W.; Haberl, B.; Kalbe, M.; Korner, M. *Parasitology Today* **1995**, *11*, 468-472.
59. World Health Organization *Bull. WHO* **1965**, *33*, 567-581.
60. Bureson, B.J.; Woodard, F.X.; Moore, R.E. *Chem. Lett.* **1975**, 1111-1114.
61. Singh, I.P.; Milligan, K.E.; Gerwick, W.H. *J. Nat. Prod.* **1999**, *62*, 1333-1335.
62. Cardellina, J.H.; Dalietos, D.; Marner, F.J.; Mynderse, J.S.; Moore, R.E. *Phytochem.* **1978**, *17*, 2091-2093.
63. Mynderse, J.S.; Moore, R.E.; Kashiwagi, M.; Norton, T.R. *Science* **1977**, 538-544.
64. Beutler, J.A. *J. Nat. Prod.* **1990**, *53*, 867-874.
65. Liu, S.Y.; Sporer, F.; Wink, M.; Jourdan, J.; Henning, R.; Li, Y.L.; Ruppel, A. *Trop. Med. Int. Heal.* **1997**, *2*, 179-188.
66. Pechenik, J.A. *Biology of the Invertebrates* **1996**, WCB/McGraw Hill: Boston.

## CHAPTER III.

HALOGENATED MONOTERPENES ISOLATED FROM THE FIJIAN RED ALGA  
*PORTIERIA HORNEMANNI*

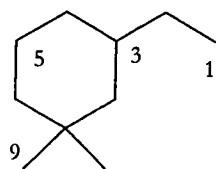
## ABSTRACT

Toxicity to the fresh-water snail, *Biomphalaria glabrata*, led to the re-isolation of the biologically active halogenated monoterpene, chondrocole C, from a Fijian collection of *Portieria hornemanni*. Further investigation of this extract allowed the isolation and identification of four additional halogenated monoterpenes, all lacking molluscicidal activity. Literature searches revealed all but one of the discovered secondary metabolites to have been previously described. The isolation of these metabolites, including the newly discovered taviochtodene, was carried out by preparative liquid chromatography with final purification through repetitive HPLC. Structure elucidation was accomplished utilizing 1D and 2D NMR spectroscopic characterization of the natural products and comparisons with related halogenated monoterpenes. The interpretation of anomalous heteronuclear connectivities, observed within the NMR data acquired with chondrocole C, revealed the necessity for a minor chemical shift re-assignment of chondrocole C.

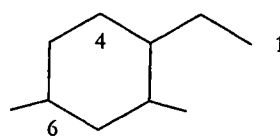
## INTRODUCTION

Red algae, the Rhodophyta, are among the most frequently investigated sources for marine natural products. This is primarily due to their predominance in temperate and tropical locations where most collections occur. A second contributing factor to their popularity for study is that there are approximately 4000 species of red algae, more than the sum of all other algal species.<sup>13,33</sup> Certain members of this division are commercially and pharmaceutically important as producers of important phycocolloids such as carrageenan and agar, which are used in cough syrup, anticoagulants, laxatives, and dental molds.<sup>16-21,26</sup> However, the red algae are also well known for their prolific production of halogenated secondary metabolites, most often terpenes containing chlorine, bromine, and iodine. The Plocamiaceae and Rhizophyllidaceae families, which include *Laurencia*, *Plocamium*, *Portieria*, and *Ochtodes* spp., are particularly adept in utilizing this relatively rare biosynthetic pathway.<sup>67,68</sup> The numerous structures elaborated by these families can be categorized into four predominant skeletal arrangements (Figure III.1), 1-ethyl-3,3-dimethylcyclohexanes (ochtodanes), 1-ethyl-2,4-dimethylcyclohexanes, 1-ethyl-1,3-dimethylcyclohexanes, and 2,6-dimethyloctanes.<sup>69</sup> The *Ochtodes* and *Portieria* spp. are prolific producers of the ochtodane (Figure III.2) and dimethyloctane (Figure III.3) groups, as well as the closely related chondrocoles (Figure III.4).

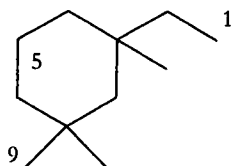
Rather than specializing in the production of any single member of these groups, the producers of halogenated terpenes have displayed a high



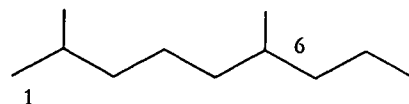
3-ethyl-5,5-dimethylcyclohexanes



3-ethyl-4,6-dimethylcyclohexanes



3-ethyl-3-methyl-5,5-dimethylcyclohexanes



2,6-dimethyloctanes

**Figure III.1.** The four major skeletal arrangements isolated from *Portieria* and *Ochtodes* spp.



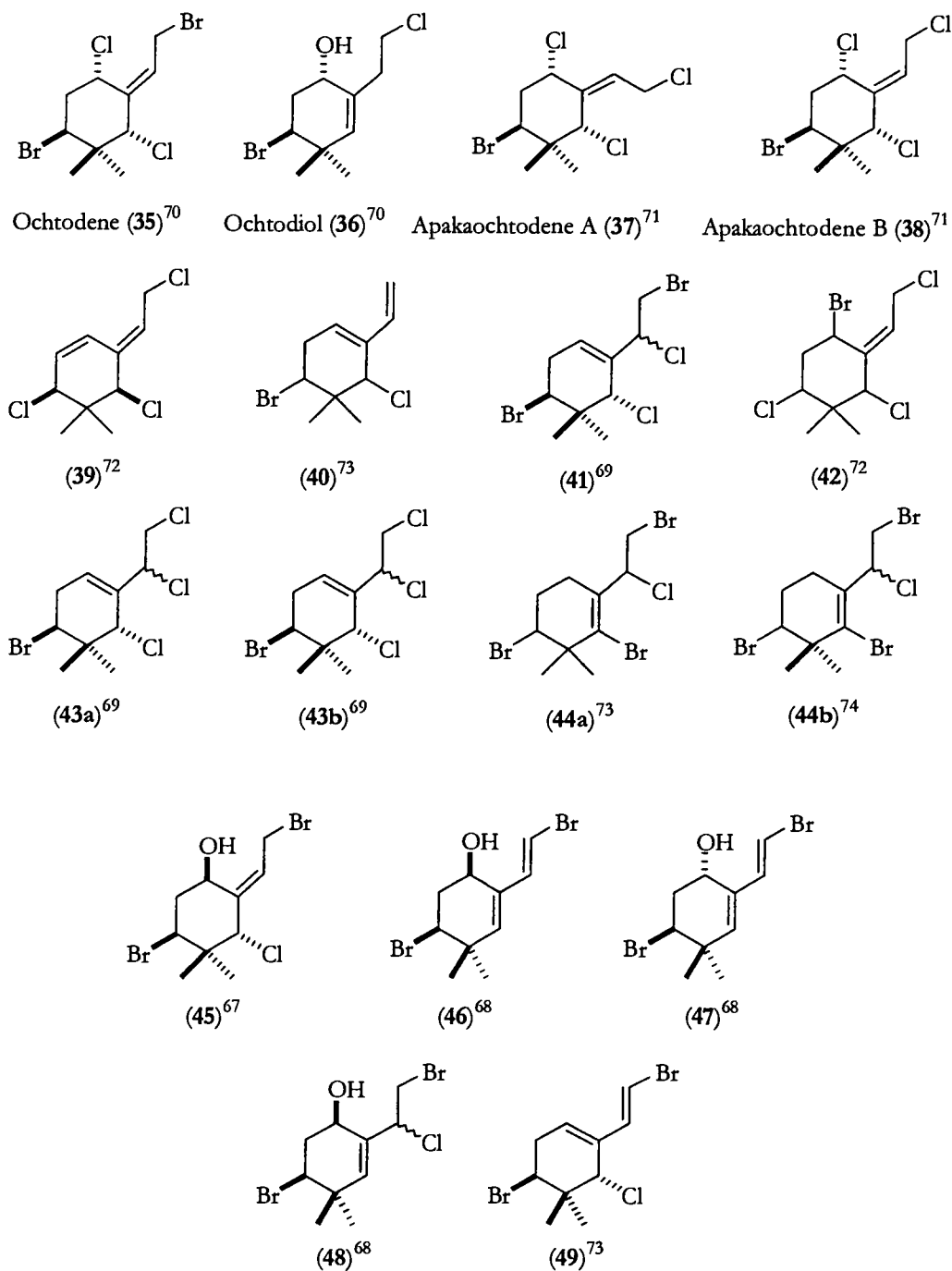


**Figure III.2.** Representative ochtodanes isolated from *Portieria* and *Ochtodes* spp. Structures 43a & 43b and 44a & 44b are stereoisomers that have yet to have their stereochemistries fully elucidated.

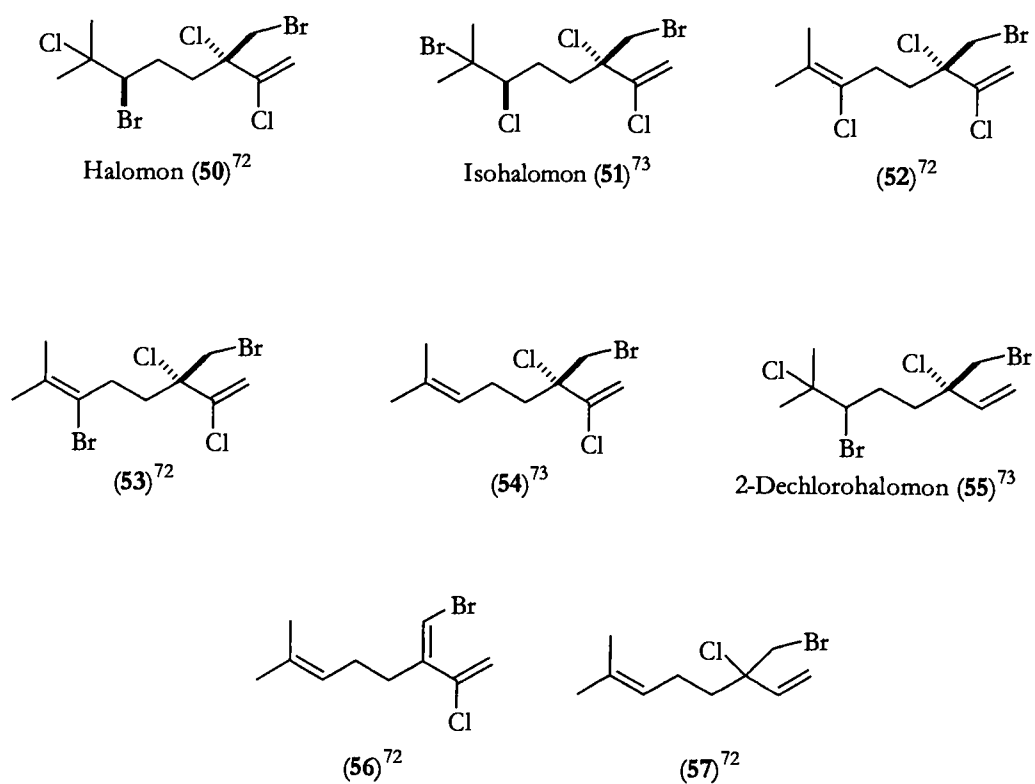


**Figure III.3.** Dimethyloctanes isolated from *Portieria* and *Ochtodes* spp.

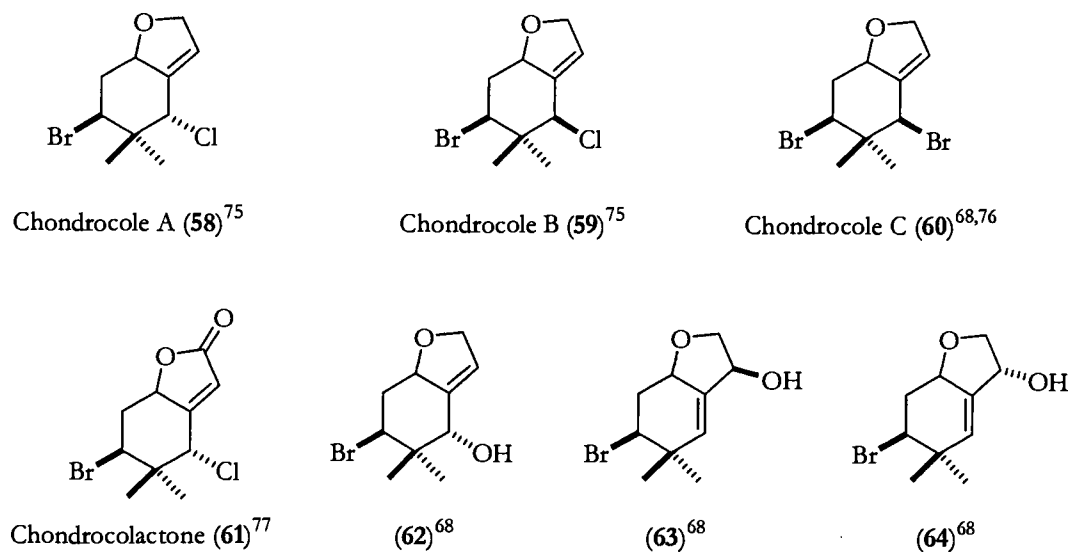


**Figure III.4.** Chondrocoles isolated from *Portieria* and *Ochtodes* spp.

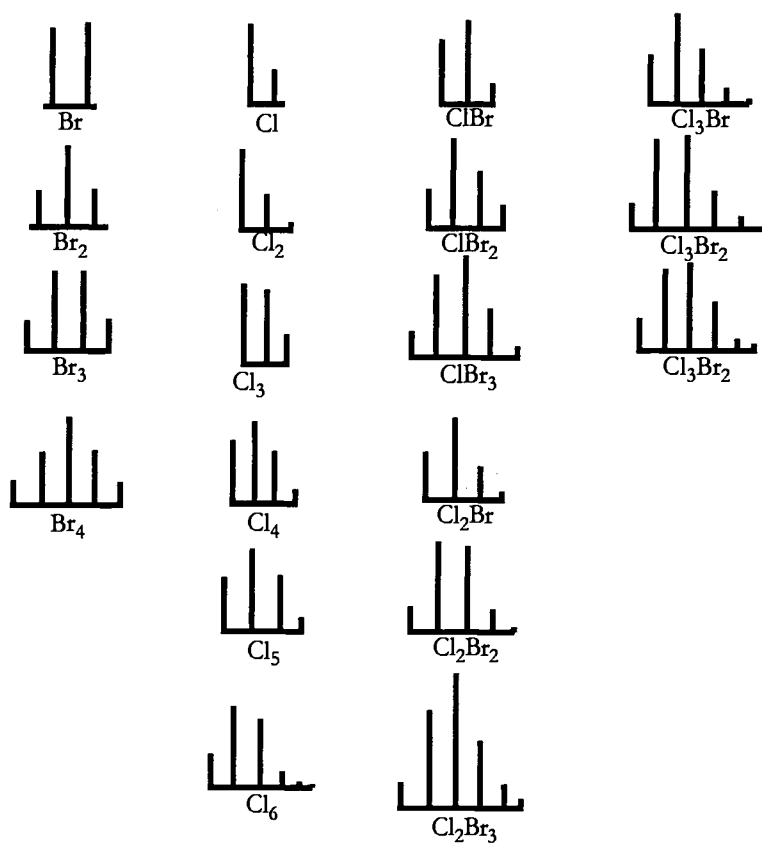


**Figure III.5.** Mass spectral isotope cluster patterns observed for halogenated compounds.

degree of chemical variability, producing suites of related compounds that vary in composition of individual examples and in the proportion of acyclic vs. cyclic metabolites.<sup>71</sup> Geographic, or site-to-site, variability of secondary metabolites has also been observed for these families, at times from samples separated by less than 10 miles.<sup>71,73,78,79</sup> Accepting the available evidence that these suites of compounds confer chemical protection upon their producers, it would seem that the elaboration of numerous modestly active secondary metabolites is energetically less efficient than the production of a single highly potent metabolite.<sup>68,71</sup> However, a current theory concerning the evolution of secondary metabolites suggests that this is a sort of 'bet-hedging' approach.<sup>80</sup> In this manner the producer of a chemical defense distributes its resources widely, protecting itself against the adaptability of the target.<sup>80</sup>

Paul et al., while describing halogenated monoterpenes isolated from a Galapagos *Ochtodes crockeri*, discovered feeding deterrence (to fish) in each compound at the 100 ppm level (46-48, 60, 62-64).<sup>68</sup> Despite the immediate presence of local herbivores, such as marine iguanas, *Ochtodes* grows luxuriantly and seemingly without predation.<sup>68</sup> While further, ecologically relevant, investigation is necessary to prove such defensive utility for these compounds in nature, the evidence is compelling, especially considering the predatory pressure in their local environment and the observation that these metabolites collectively comprise approximately 15,000 ppm of the alga's dry weight.<sup>68</sup>

While such discoveries of biologically active red algal secondary metabolites provide exciting reasons to study the Rhodophyta, the finding of a

potential antitumor red algal compound has further stimulated such pursuits.<sup>72</sup> Halomon (**50**), discovered from *Portieria hornemannii*, exhibited an antitumor profile of high priority at the National Cancer Institutes (NCI).<sup>72</sup> In initial *in vivo* studies, halomon has given rise to a 40% apparent cure rate against the U251 brain tumor cell line (5 doses/day, 50 mg/kg).<sup>72,73</sup> Despite such promising results and selection for preclinical development, halomon has not proceeded through the drug pipeline to the marketplace. Its progress has been hindered by the small quantities found in natural collections and an inability to synthesize the compound efficiently.<sup>72,73</sup> In fact, halomon has only been found on three occasions; as a mixture from a 1975 Hawaiian sample, the original Chanaryan collection (Philippines), and a 1992 re-collection at Chanaryan sites. Attempts to reisolate **50** have led to the discovery of a number of related halogenated monoterpenes, and provided a wealth of structure-activity data for this drug class.<sup>72,73</sup>

Isohalomon (**51**), 7-dechloro-6-dehydrohalomon (**52**), and its brominated isomer (**53**) displayed the characteristic cytotoxicity profile of halomon, with similar potency.<sup>73</sup> Therefore, the presence or absence of a C-7 halogen, the type of halogenation at C-6, and the saturation state of the C6-C7 bond is not of critical importance for activity.<sup>73</sup> However, the presence of a halogen atom at C-6 is important, as **54** displayed only mild toxicity and produced a profile that was not related to halomon or the other active halomon-like compounds.<sup>73</sup> Compounds **55-57** displayed similar profiles and potency to **54**, and were therefore also dissimilar to halomon.<sup>73</sup> The

importance of C-2 chlorination for full potency was thus proven as 2-dechlorohalomon (**55**), differs from halomon only at this single position.<sup>73</sup>

The recollection efforts in search of halomon have not produced a sustainable source of the potential drug.<sup>71,72,73</sup> In fact, they have yet to even provide much additional material, with the exception of the 1992 Chanaryan expedition.<sup>73</sup> However, the structure-activity data gleaned to date has begun to define the active pharmacophore of halomon, and will be invaluable to any future synthetic approaches. Further collection efforts will doubtlessly yield more useful data as well as potentially provide the sought after store of halomon, or an equally active analog.

## RESULTS AND DISCUSSION

Chosen as part of an effort to screen marine algae for molluscicidal activity (Chapter II), the organic extract of a Fijian red alga, *Portieria hornemanni*, demonstrated dramatic activity in this assay with snail death and hemolymph expulsion occurring within minutes at 25 ppm. While pursuing the isolation of the molluscicidal secondary metabolite of this alga, GC/MS and TLC analysis of inactive fractions revealed the presence of a wealth of halogenated small molecules. *P. hornemanni*, a member of the Rhizophyllidaceae family, is known to produce suites of halogenated monoterpenes.<sup>67-79</sup>

The screening of non-polar fractions of this extract of *P. hornemanni* showed a plethora of halogenated compounds, as recognized by characteristic isotope patterns present in the mass spectrometry data (see Figure III.5 for examples). Isotope patterns were also used to make preliminary assessments of the types and number of halogen atoms in these molecules, greatly facilitating the search for compounds of potential interest, such as those displaying unusual halogenation.

The phytochemical investigation of these fractions, guided by GC/MS and TLC, resulted in the isolation of three compounds which have been previously reported in the literature. For one of these, GC/MS analysis revealed a minor compound possessing three bromines and a chlorine atom. Pursuing this metabolite, HPLC isolation yielded the polyhalogenated ochtodene, 2-chloro-1,6 (J),8- tribromo-3-(8)(Z)-ochtodene (**44b**), as a minor metabolite. Previously isolated from a Caribbean *Ochodes secundiramea*, **44b** was the first ochtodane found to possess a cyclic vinyl halide.<sup>74</sup>

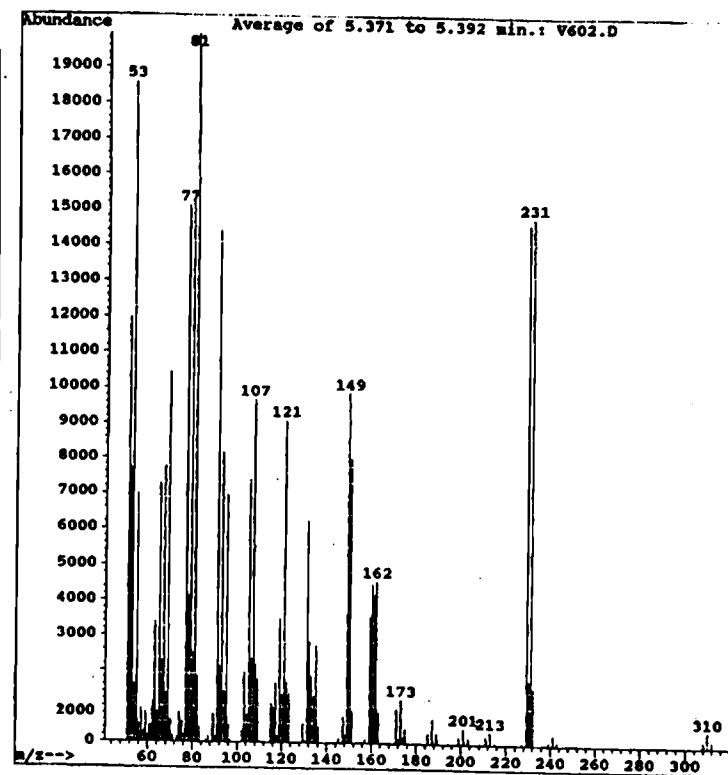
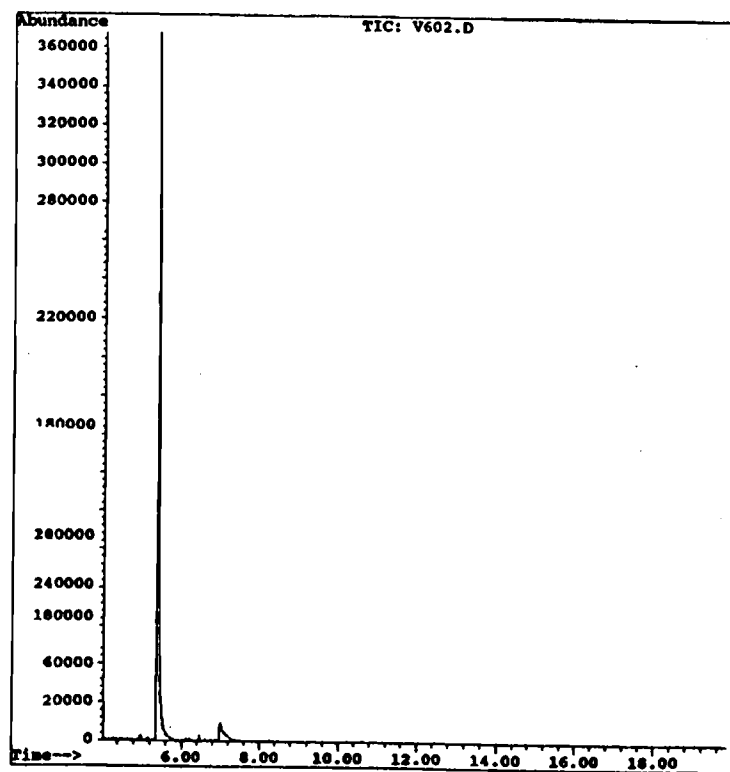


Figure III.6. GC/MS of chondrocole C.



A second known and cyclic monoterpene was also isolated by HPLC from a nonpolar fraction. Displaying a molecular weight by GC/MS of 264 da, with an isotope pattern indicative of a single chlorine and bromine atom, this compound was defined (through 1-D  $^1\text{H}$  NMR and GC/MS) to be chondrocole A (**58**) or its diastereomer, chondrocole B (**59**). Chondrocoles A and B were originally isolated from a Hawaiian *Chondrococcus hornemanni* (synonymous to *P. hornemanni*).<sup>75</sup>

The third known compound discovered in this pursuit was originally thought to be a cyclic monoterpene similar to the chondrocoles or ochtodenes. This assessment was made based on both GC/MS and NMR observations. However, key correlations in the 2-D NMR data sets suggested this to be a linear molecule. The most logical structure, that describing 2-dechlorohalomon, was confirmed by comparisons of 1-D  $^1\text{H}$  and  $^{13}\text{C}$  NMR chemical shifts with published literature values. This metabolite (**55**) is a close structural relative of halomon (**50**), a potential anticancer drug that has proven difficult to obtain from either field collections or by chemical synthesis.

Following the molluscicidal activity through successive tiers of chromatography, the molluscicidal component was isolated as a UV-active non-polar compound that was also the major metabolite of this extract (27%). GC/MS data suggested that this compound had two bromine atoms and a molecular weight of 308 da (Figure III.6). A molecular formula of  $\text{C}_{10}\text{H}_{14}\text{OBr}_2$  was deduced as an initial starting point in the structure elucidation of **60**. The components of this formula were confirmed through 1-D  $^1\text{H}$  (Figure III.7) and  $^{13}\text{C}$  NMR (Figure III.8) experiments,

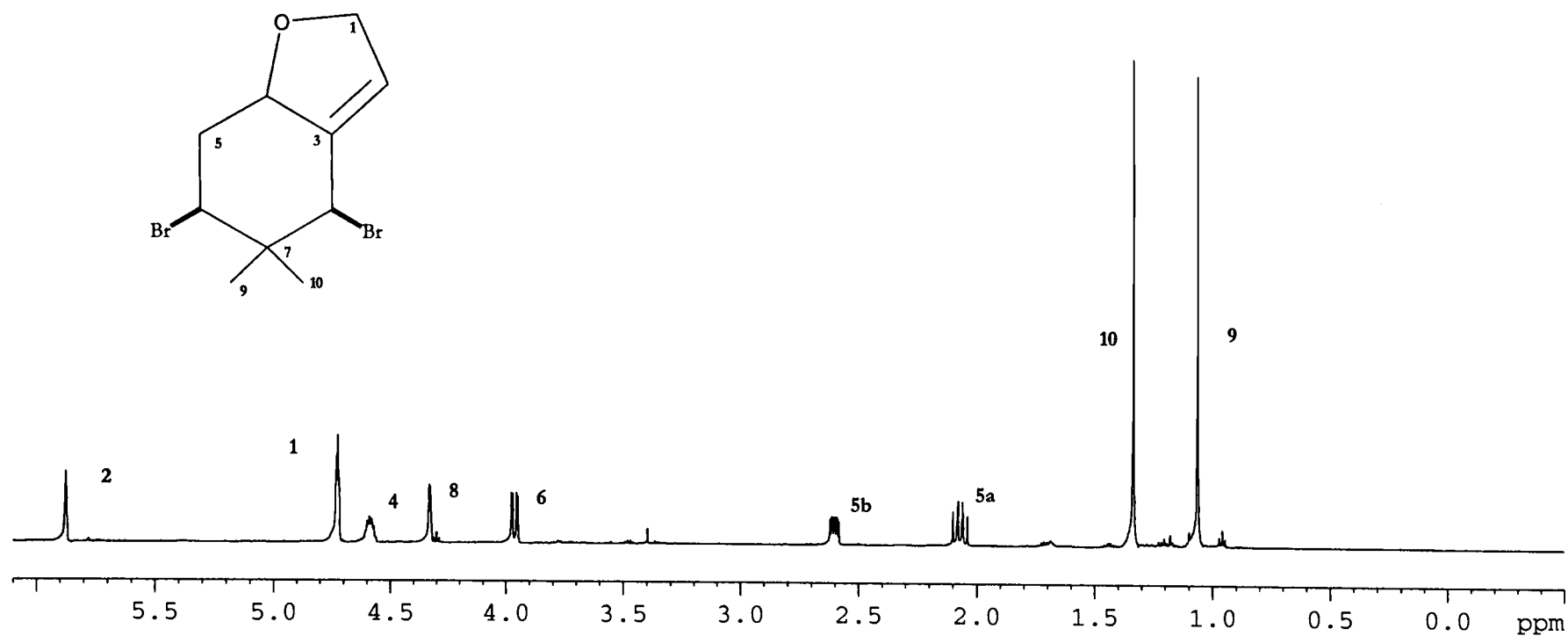


Figure III.7. <sup>1</sup>H NMR of chondrocole C.

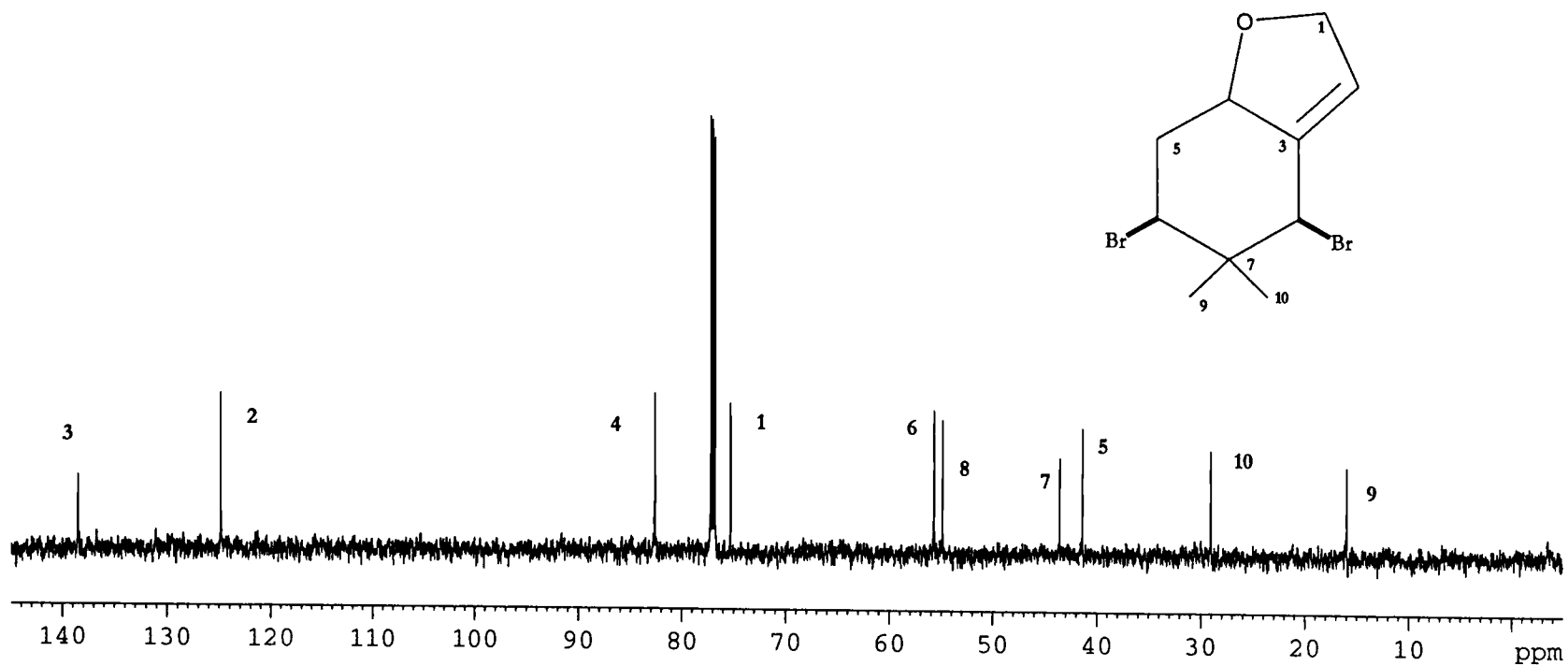


Figure III.8  $^{13}\text{C}$  NMR of chondrocole C.

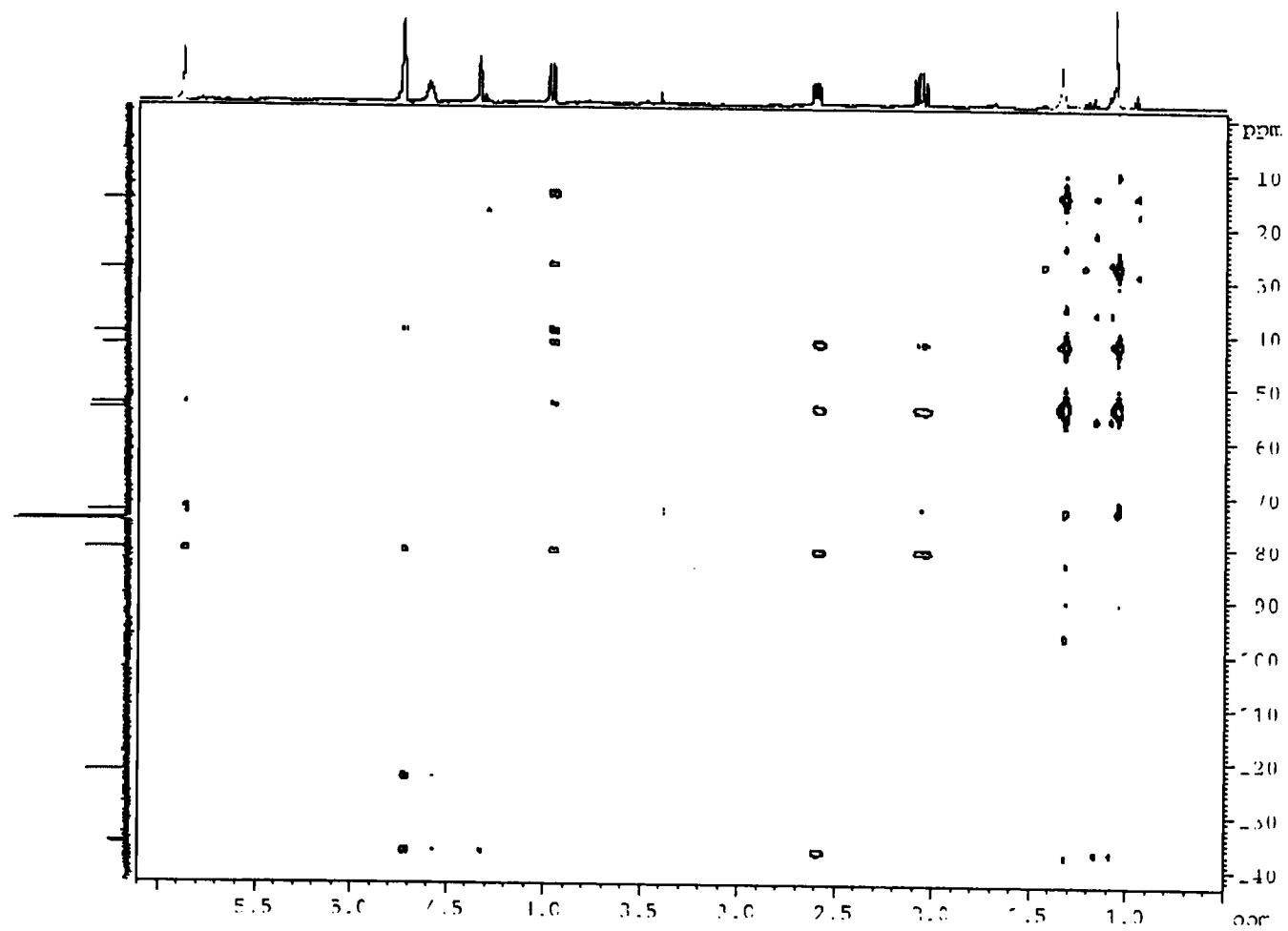
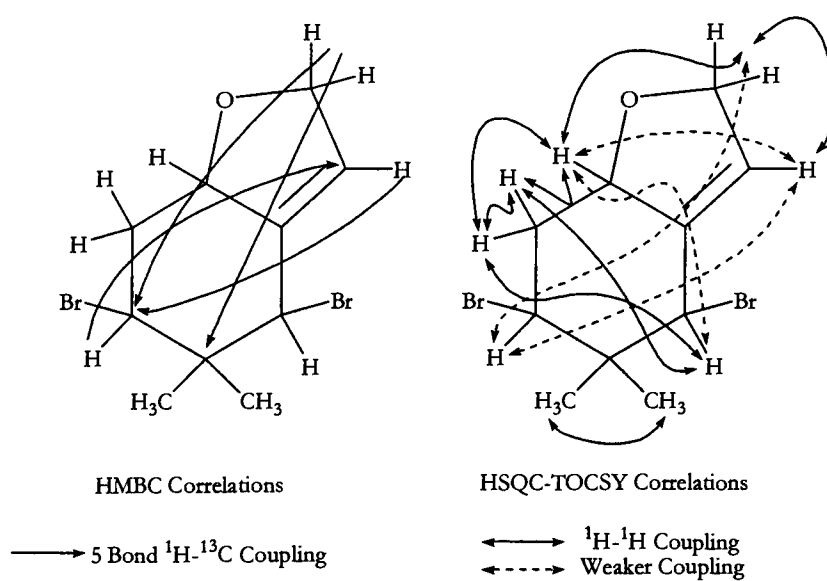


Figure III.9. HMBC of chondrocole C.

which displayed relatively simple spectra consisting of 10 carbon and 14 proton resonances. The only element remaining to be assigned from the molecular formula was a single oxygen atom. A literature search, using the molecular formula, showed that NMR values for chondrocole C matched those for this molluscicidal compound.<sup>68</sup> However, when the carbon and proton assignments from the literature were applied to the molecule, and checked against the HMBC data (Figure III.9) collected for the molluscicidal agent, there was a disparity.

Figure III.10 graphically describes the long range NMR data collected for chondrocole C using the literature values to anchor the placement of the  $^{13}\text{C}$  NMR chemical shifts. Such an inordinate number of unusual couplings in chondrocole C raised questions concerning the reported structure of chondrocole C. However, these questions were fully answered upon closer inspection of the HSQC (Figure III.11) data collected for **60**. Originally unnoticed, the HSQC displayed  $^1\text{J}$  coupling from H-6 to C-8 and from H-8 to C-6 (using the literature values to assign chemical shifts). This pinpointed the problem. Applying this re-assignment provides a much more palatable combination of correlations (Figure III.12). Such data miss-assignments in the literature may exist in more than just this isolated case, as the resolving power of modern NMR spectrometers, and the utility of recently developed pulse sequences, allow more detailed spectroscopic investigations than in the past.

A fifth non-polar and minor metabolite was also isolated from this extract. Analyzing for a molecular weight of 362 da, the isotope pattern appeared to be produced two bromine and two chlorine atoms (Figure III.13). The remaining mass units could be accounted for by  $\text{C}_{10}\text{H}_{14}$ , a fact confirmed by HRCIMS ( $\text{M}^+$  at  $m/z$



**Figure III.10.** Proposed long-range correlations for chondrocole C using the chemical shift assignments as in the literature.<sup>75</sup>

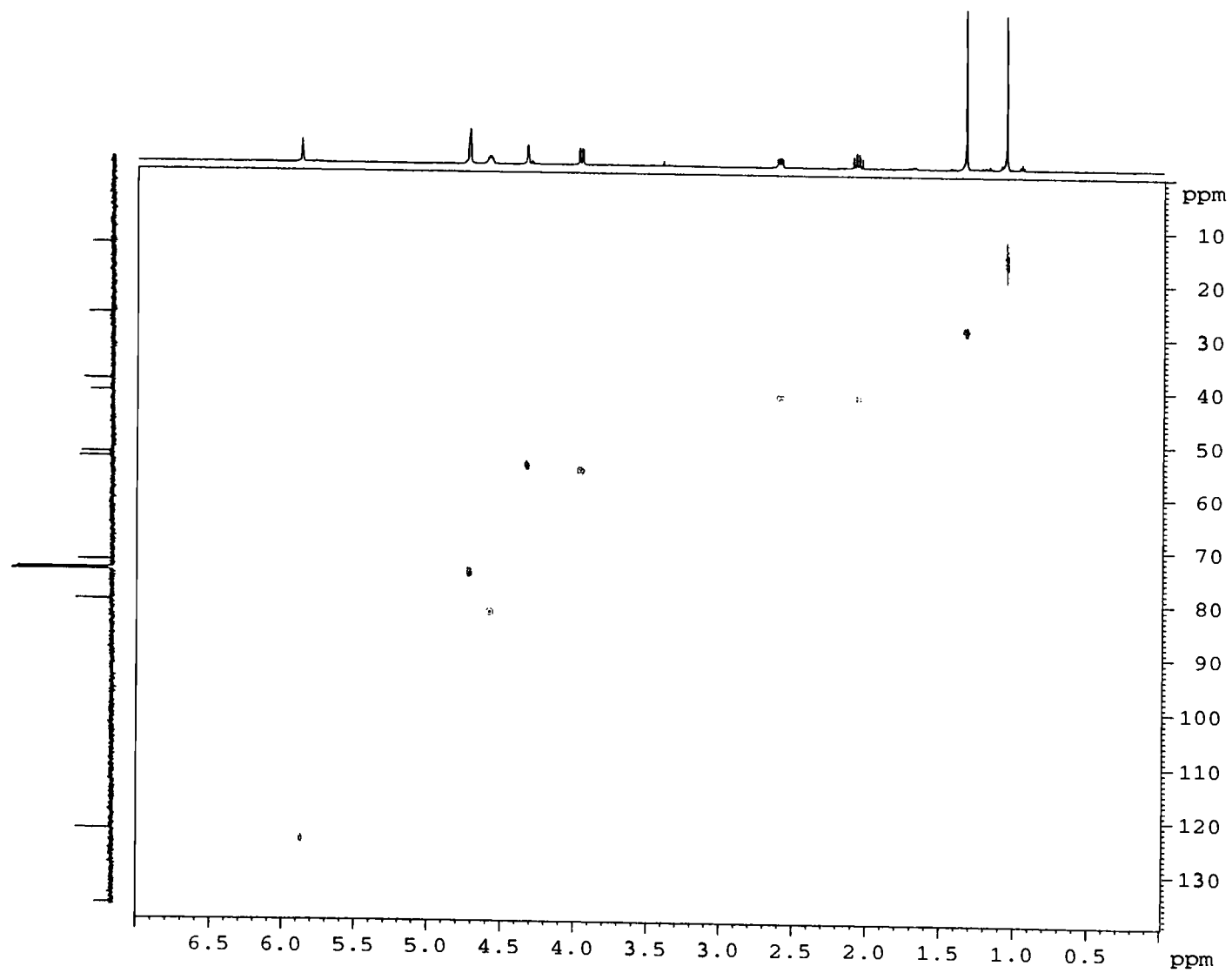
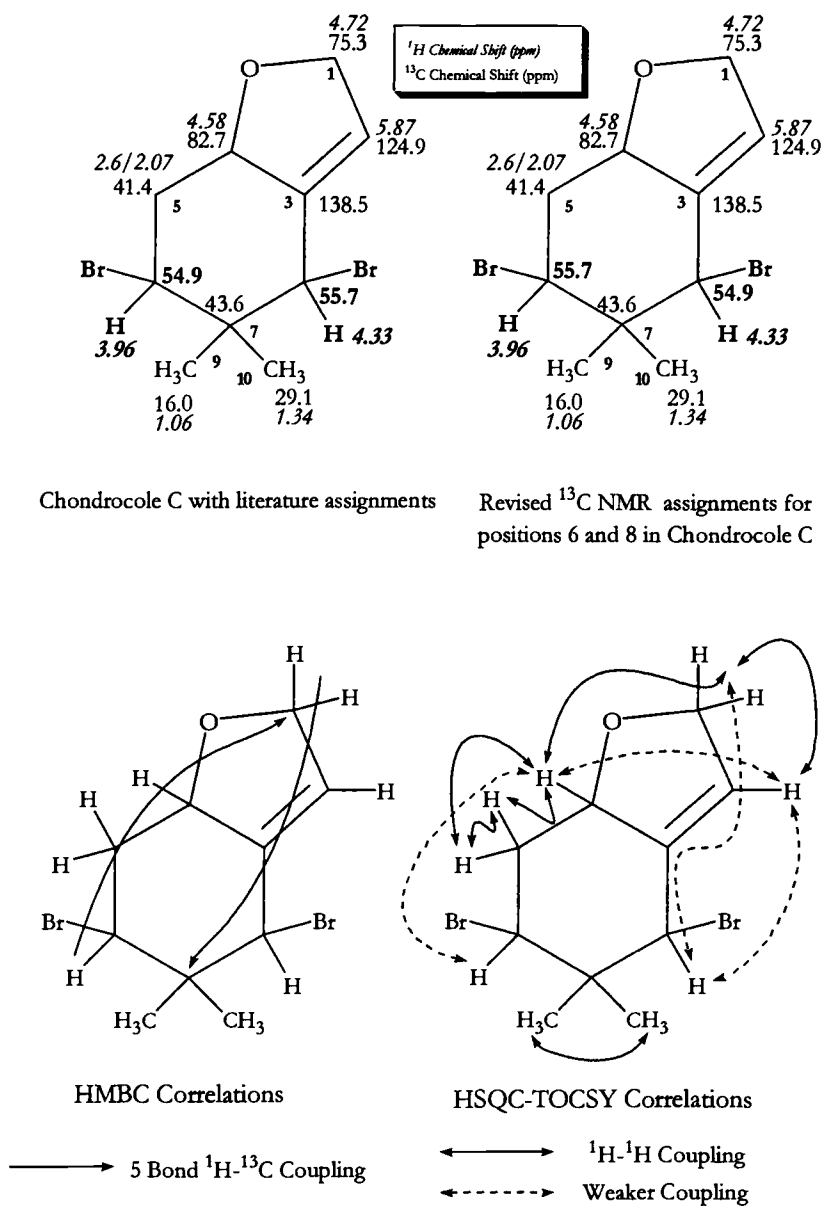


Figure III.11. HSQC of chondrocle C.



**Figure III.12.** Long-range correlations observed for chondrocole C with revised chemical shift assignment.



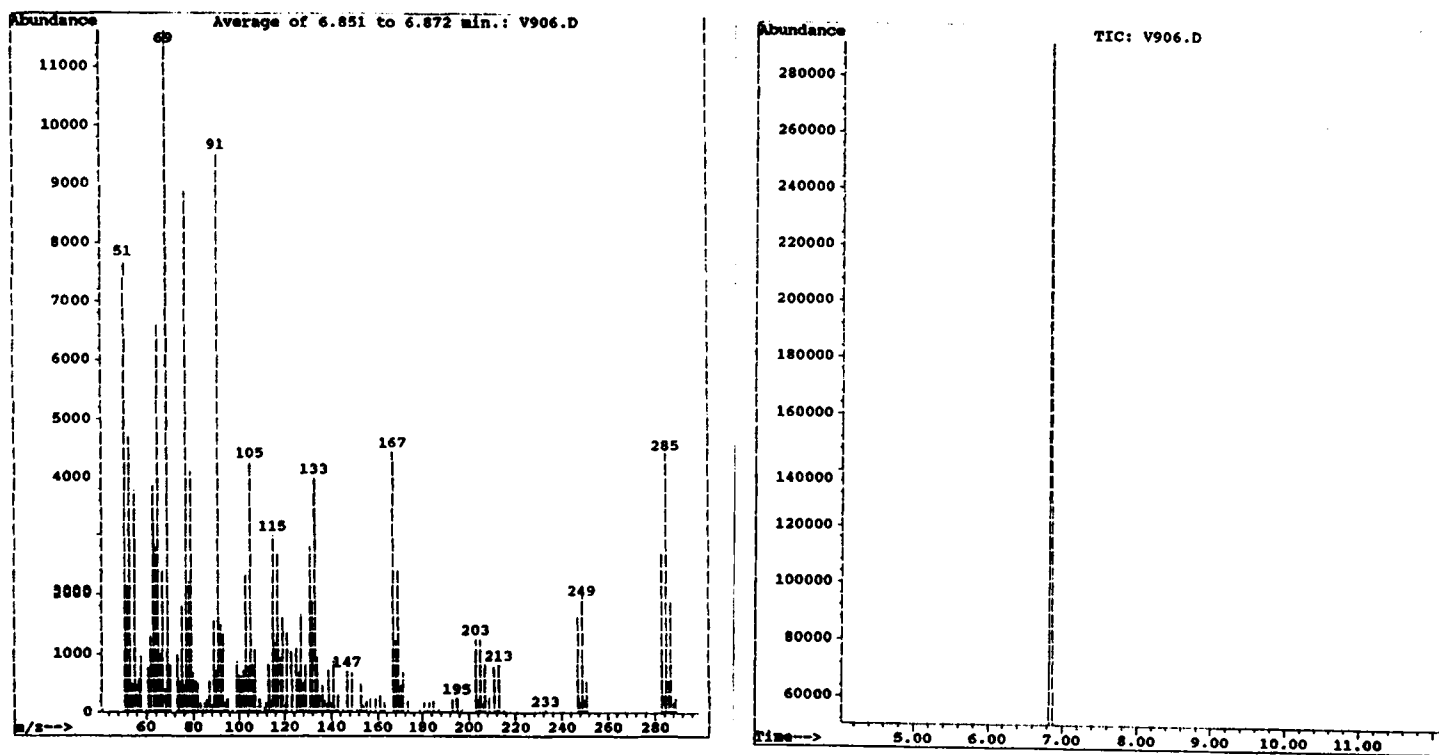
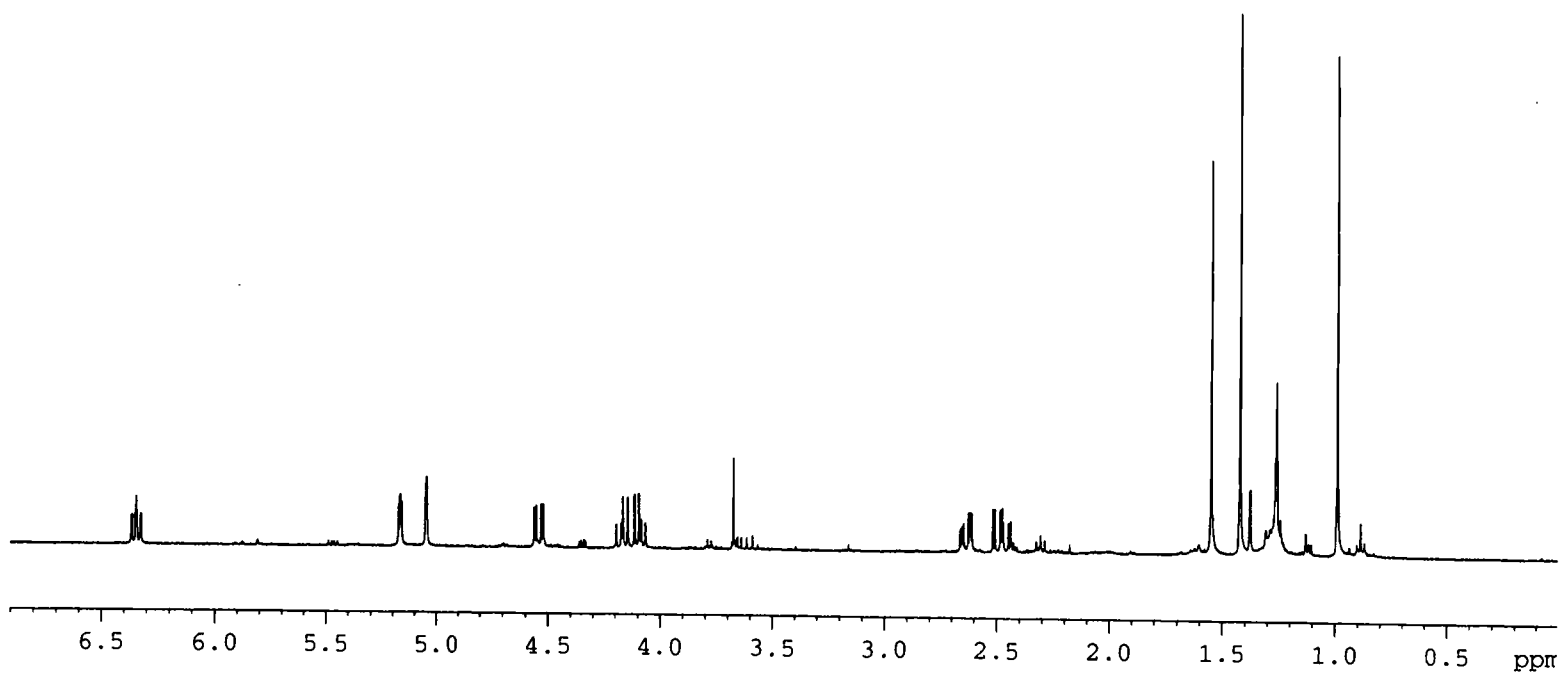


Figure III.13.. GC/MS of taviochtodene.



**Figure III.14.**  $^1\text{H}$  NMR spectrum of taviochtodene.

361.8839;  $\Delta = -0.9$  mmu for  $C_{10}H_{14}Br_2Cl_2$ ). The 1-D  $^1H$  NMR (Figure III.14) displayed a now familiar sample of peaks, including those for *gem*-dimethyl and halomethine protons. Also present was a highly coupled down field signal (H-X) representing an olefinic proton.

HSQC (Figure III.15) allowed the appropriate assignment of protons to their respective carbons (Table III.1). The four halogens expected from the MS data could be further assigned as being a trio of halomethines,  $-CHX$  moieties ( $X = \text{halogen}$ ), and a primary  $-CH_2X$  functionality, by characteristic chemical shifts. The HSQC data confirmed the presence of a single protonated olefinic carbon, indicating that it was trisubstituted. This olefin accounted for one of the two degrees of unsaturation described in the molecular formula. The remaining two carbons, which were the only remaining elements of the molecular formula, were thereby defined as the olefinic partner and the quaternary carbon completing the *gem*-dimethyl system.

HMBC (Figure III.16) correlations, detailed graphically in Figure III.17, confirmed these assignments, as connectivities could be observed between the *gem*-dimethyl protons ( $H_3$ -9 and  $H_3$ -10) and C-7 and from H-2 to the olefinic carbon C-3. Also observed from H-2 was a correlation to the halogen bearing carbon, C-8. Carbon 8 was further defined as being adjacent to the *gem*-dimethyl system because H-8 showed connectivity to C-9. Carbon 9 displayed long range heteronuclear coupling to another of the halomethines as witnessed by a correlation from ( $H_3$ -9 to C-6, as well as to C-8, and a cross-peak from H-6 to C-9). Connectivities from the methylene H-5 protons to both C-6 and C-4 allowed placement of C-5 as being a part of a – halomethine- $CH_2$ -halomethine system. These correlations account for all of the

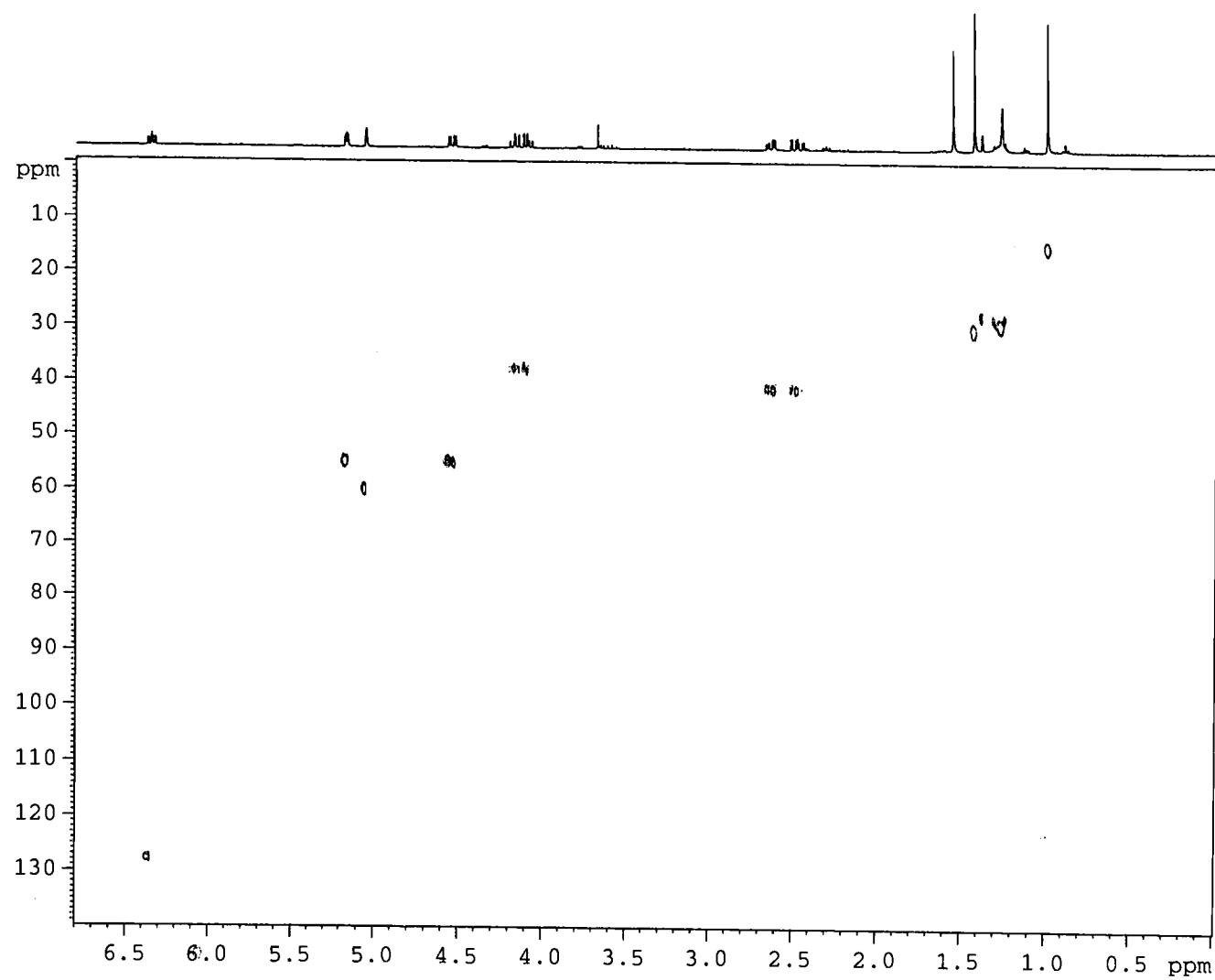


Figure III.15. HSQC of taviochtodene.

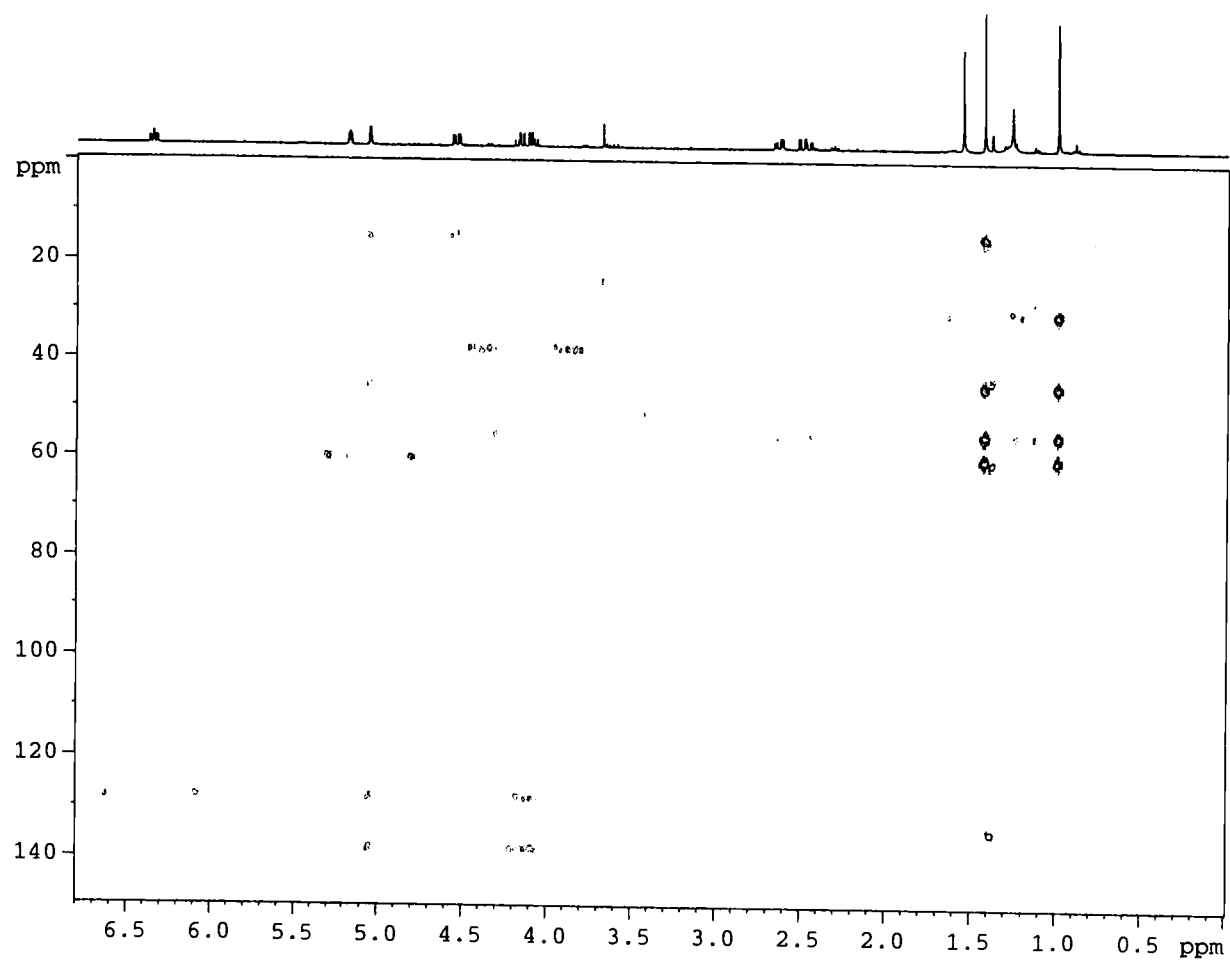
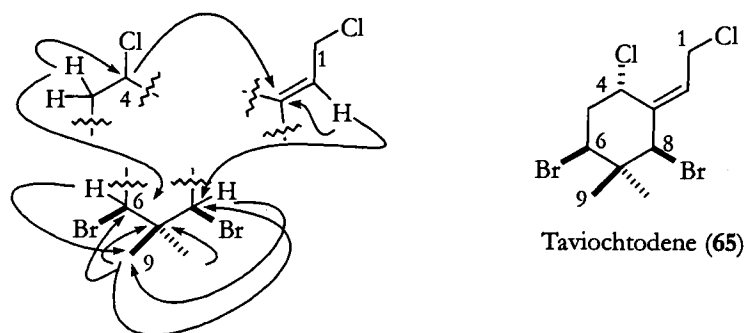


Figure III.16. HMBC of taviochtodene.



**Figure III.17.** Key HMBC correlations used to define taviochtodene (65).

**Table III.1.** NMR data for taviochtodene (65).

Carbon #	$^{13}\text{C}$ $\delta^a$	$^1\text{H}$ $\delta^b$
1	37.82	4.13 dddd (1.7, 7.5, 11.7, 15.0)
2	127.3	6.34 ddd (2.0, 7.5, 8.6)
3	138.18	-
4	54.92	5.17 dd (2.7, 4.0)
5	41.51	2.48 ddd (4.8, 12.8, 15.7) 2.56 ddd (2.6, 3.8, 14.6)
6	55.24	4.54 dd (4.4, 12.4)
7	45.30	-
8	59.88	5.05 bs
9	15.31	0.99 s
10	30.41	1.43 s

<sup>a</sup> Recorded on Bruker DPX 300 (75 MHz) in  $\text{CDCl}_3$ .

<sup>b</sup> Recorded on Bruker DPX 300 (300 MHz) in  $\text{CDCl}_3$ .

elements of the molecular formula; the sole exception being a single degree of unsaturation. This was provided by the logical ring closure at C-4-C-3, and confirmed by an HMBC correlation from H-4 to C-3.

The proper placement of chlorine and bromine atoms was attempted following chemical shift rationale using the representatives of the ochtodene and chondrocole structure classes (Figure III.2 and 4) as evidence. Figure III.18 allows comparison of the  $^1\text{H}$  and  $^{13}\text{C}$  NMR shifts observed for ochtodenes and chondrocoles most closely resembling the new ochtodene, taviochtodene (**65**). Most compelling is the similarity between the *gem*-dimethyl moieties of chondrocole C and taviochtodene. In most of the ochtodenes and chondrocoles, less than 10 ppm separates the peaks of C-9 and C-10. But C-9 and C-10, in chondrocole C and **65**, are separated by 14.9 and 13.1 ppm, respectively. Also, **60** and **65** are the only presented examples that display a C-9 chemical shift which approaches 15 ppm. This observation suggests that both bromines are in the same plane for **65**, and attached at C-6 and C-8.<sup>67</sup> Chemically, the diequatorial positioning of large groups such as bromines is more logical. Of particular note, chondrocole C is the lone representative of these structural classes whose *gem*-dimethyl pair is flanked by two bromine bearing carbons, and was also the major component of this extract. The bromines being placed upon carbons 6 and 8, the chlorides were logically located at C-4 and C-1. Thus the planar structure of taviochtodene was elucidated. Attempts were made to investigate the *E* or *Z* stereochemistry of the C2-C3 double bond using the HSQMBC, NOESY, and DPGSE NOE pulse sequences. No data could be gleaned from any of these experiments, but, presumably due to the limitations of sample size (all other NMR



**Table III.2.** Chemical shift comparisons of selected ochtodenenes and chondrocoles, compound numbers in bold at column tops (a = axial, e = equatorial). <sup>a</sup> Chemical shifts reversed in literature. <sup>b</sup>NMR run in C<sub>6</sub>D<sub>6</sub> as opposed to CDCl<sub>3</sub>.

	<b>35</b>	<b>37</b>	<b>38</b>	<b>42</b>	<b>45</b>	<b>58</b>	<b>60</b>	<b>61</b>	<b>65</b>
C-1	37.6	37.37	37.62	37.6	39.6	75.3	75.3	171.0	37.82
C-2	131.9	131.67	131.89	131.8	125.0	124.8	124.8	115.4	127.3
C-3	137.7	138.22	137.83	137.9	-	137.6	138.3	164.4	138.18
C-4	50.4	59.58	50.44	50.4	73.6	80.7	82.6	76.9	54.92
C-5	41.32	41.80	41.32	41.3	42.6	41.7	41.4	40.0	41.51
C-6	52.70	52.72	52.70	52.7	54.9	54.4	55.7 <sup>a</sup>	51.0	55.24
C-7	41.32	41.03	41.36	41.4	-	41.7	43.6	42.3	45.30
C-8	70.0	60.65	69.98	70.0	68.8	63.8	54.8 <sup>a</sup>	60.8	59.88
C-9	20.4	20.63	20.47	20.5a	21.5	21.0	16.0	20.5	15.31
C-10	28.5	28.60	28.53	28.5a	26.6	27.6	29.1	26.9	30.41

	<b>35</b>	<b>37</b>	<b>38</b>	<b>42</b>	<b>45<sup>b</sup></b>	<b>58</b>	<b>60</b>	<b>61</b>	<b>65</b>
H-1	4.05 4.20	4.02 4.16	4.04 4.18	4.04 4.18	4.3	4.72	4.66	-	4.13
H-2	5.96	6.03	5.95	5.95	5.30	6.97	5.90	6.97	6.34
H-3	-	-	-	-	-	-	-	-	-
H-4	4.99 e	4.65	4.97	4.97	4.47	4.78	4.60	-	5.17
H-5	2.55 2.71	2.50 2.65	2.53 2.68	2.53 2.67	1.86 1.92	1.95 a 2.94 e	2.10 a 2.60 e	1.95 a 2.94 e	2.48 2.56
H-6	4.85 a	4.83	4.83	4.84	4.17	4.40	4.00	4.40	4.54
H-7	-	-	-	-	-	-	-	-	-
H-8	4.40	4.73	4.38	4.38	3.85	4.65	4.46	4.78	5.05
H-9	1.03	1.02	1.01	1.01	0.78	1.07	1.09	1.07	0.99
H-10	1.30	1.33	1.28	1.29	1.0	1.32	1.36	1.32	1.43

experiments were accomplished at a much earlier stage, before experiments destructive to the compound were undertaken). However, an examination of the coupling constants of H-5 of **35** [2.55 (ddd, 4.8, 12.5, 15 Hz), 2.71 (ddd, 1.8, 4.5, 15)], **37** [2.50 (ddd, 2.4, 4.6, 15.0), 2.65 (ddd, 2.4, 12.4, 15.0)], **38** [2.53 (ddd, 5.0, 12.7, 15.3), 2.68 (ddd, 1.8, 4.1, 15.1)], and **65** [2.48 (ddd, 4.8, 12.8, 15.7), 2.64 (ddd, 2.56, 3.8, 14.6)] is potentially enlightening concerning two aspects of taviochtodene's stereochemistry, the relative stereochemistry of C-4 and C-6 and the orientation of the C2-C3 olefin. The chemical shifts of the H-5 pair in all of these examples are nearly identical, suggesting similar chemical environments and further supporting the placement of halogens in **65**. As the structures of **35** and **37** are the same except for a substitution of chlorine for bromine as the primary halogen in **37**. And, because **37** and **38** are geometrical stereoisomers differing only in the orientation of the C2-C3 olefin (**35** and **37** share the same geometry of this moiety) the noted coupling constant differences witnessed between **35/37** and **38** can be reasoned to be due to this altered geometry. While this is somewhat unexpected, and may suggest stereochemical mis-assignment in **38**, the structure of **38** is supported by X-Ray crystallography. As such, **65** displays nearly identical H-5 coupling constants to those of **35** and **37**. Therefore, despite the lack of acquired data to explain these features of **65** it is possible to tentatively assign them as depicted, with an *E* C2-C3 olefin, equatorial H-4, and axial H-6. This analysis is further supported by analyzing the coupling constants H-4,5,6 of **65** without use of the model compounds. With **65** drawn in a pseudo-boat structure it becomes clear that the positioning of H-4 as equatorial will yield two small couplings to the protons of H-5, which is what is observed experimentally (Table III.1). Likewise, for an axial

H-6, one small and one large coupling should be observed, as can also be seen in Table III.1. As stated above, the C-8 bromine was expected, through chemical shift rationale, to be in the same plane as the C-6 bromine, thus suggesting the assignment of H-8 as axial.

Similar to previous reports of the secondary metabolite components of the Rhizophyllidaceae, the extract investigated herein produced a suite of related halogenated monoterpenes.<sup>67-79</sup> In addition to the presented metabolites, GC/MS analyses of this extract suggested the existence of a number of further examples of these same structural classes present, however, as extremely minor components. It is hypothesized that these compounds provide chemical defense against predation.<sup>68</sup> The previous biological activity associated with these structure classes, and the observed molluscicidal activity for chondrocole C, appear to support this hypothesis. The isolation of 2-dechlorohalomon from a Fijian *P. hornemanni* provides a potential new territory in which to explore for the elusive anticancer compound, halomon, and its biologically active derivatives.

The utility of GC/MS analysis in the isolation and structure elucidation of halogenated monoterpenes cannot be overemphasized. During the GC/MS analysis of this extract an empirical observation was made concerning the isotope patterns of polyhalogenated metabolites. The labile nature of halogens under GC/MS conditions can result in their loss in the ionization chamber. In such an instance, analyzing the data could lead to an incomplete understanding of the molecule in terms of molecular weight and halogen content. However, for molecules that possess at least one bromine and chlorine pair, this potential problem can be overcome.

First, identify the two fragment peaks that represent the highest masses and subtract their molecular weights from each other. A difference of 44 mass units [also equal to 79 (Br) minus 35 (Cl)] suggests the loss, prior to mass detection, of a bromine atom. Likewise, a difference of 45 mass units is indicative of a loss of HBr.

Figure III.19 presents this observation using a hypothetical compound with an unknown molecular weight. GC/MS analysis of this molecule reveals two major fragment peaks, 179 and 135 mu. The 179 mu peak has an isotope pattern indicative of a single chlorine atom, while the 135 mu peak suggests a single bromine atom. The difference between these two peaks is equal to 44 mass units. Now add 35 to the 179 mu peak (the highest molecular weight peak) to arrive at the true molecular weight of the compound, 214 mu. From this molecular weight a loss of Br (79 mu) would result in the detection of a 135 mu peak, by GC/MS. The 179 mu peak represents the loss of chlorine (35 mu). Thus, the halogen content suggested by the isotope patterns and the fragmentation pathways to the fragment peaks are logical, and supported by the data.

More complex situations, such as the loss of multiple halogen atoms, can also be understood by the application of this method. The use of this empirical tool can help to deconvolute what are often complex chromatograms filled with useful structural information.

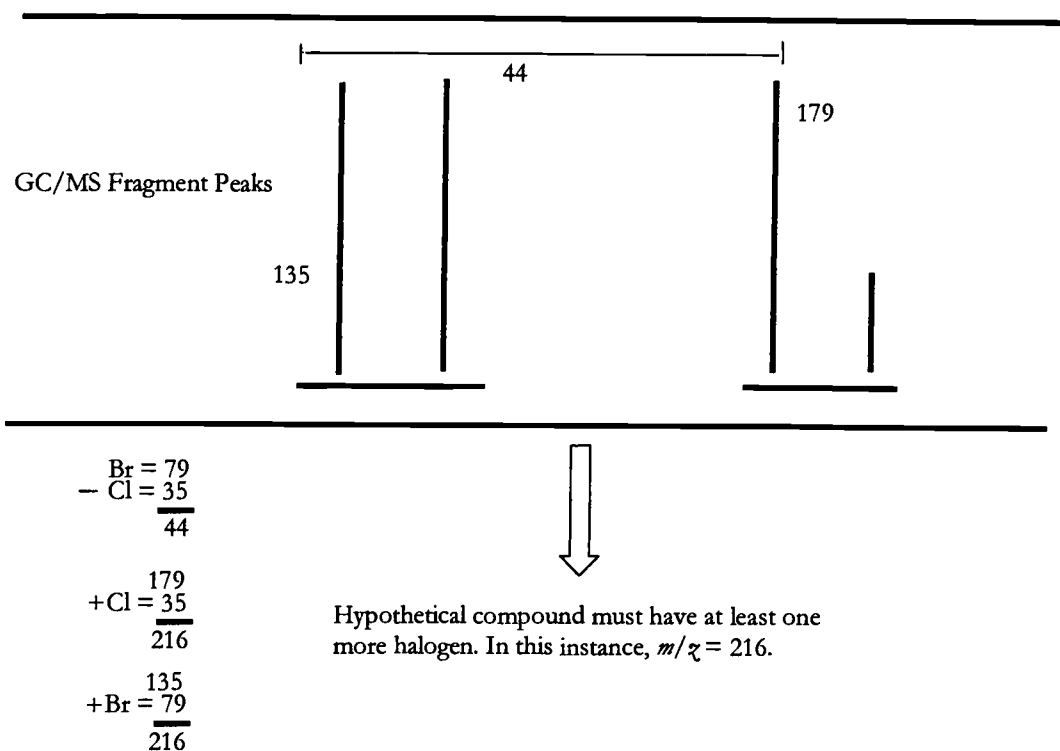


**Figure III.19.** Hypothetical compound ( $m/z = 216$ ) demonstrating the empirical observations that, in GC/MS, structural data can be obtained for halogenated compounds even when the halogen is too labile for mass spectral detection.

## EXPERIMENTAL

### GENERAL

NMR spectra were recorded on Bruker DRX 600 and DPX 300 MHz spectrometers. Mass spectra were recorded on a Kratos MS50TC mass spectrometer. UV spectra were recorded on a Hewlett Packard 8452A diode array spectrophotometer while FT-IR spectra were recorded on a Nicolet 510 spectrophotometer. GC/MS analysis was accomplished on a Hewlett Packard Gas Chromatograph 5890 Series II Gas Chromatograph with a Hewlett Packard 5971 Mass Selective Detector using an HP-1 capillary column. HPLC separation was accomplished with a Waters M-6000A pump, a Rheodyne 7010 injector, and a Waters Lambda-Max 480 spectrophotometer. Optical rotation measurements were recorded on a Perkin-Elmer Model 252 polarimeter.

### BIOLOGICAL MATERIAL

The marine red alga, *Portieria hornemannii*, was collected by hand from shallow water (2-3 m) on 6 April, 1997 at Viti Taveuni, Fiji and stored at -20°C in IPA until workup. The original collection was made by G. Hooper and M. Graber, and a voucher sample is available from WHG as collection number VTI-6 APR 97-1.

### EXTRACTION AND ISOLATION OF CHONDROCOLE C (60) AND TAVIOCHTODENE (65)

The IPA preserved alga was extracted with CH<sub>2</sub>Cl<sub>2</sub>/MeOH (2:1) two times to give a crude extract of 1.5 g. A portion of this (1.3 g) was fractionated using vacuum

liquid chromatography (VLC) on Si gel with a stepwise gradient of hexanes/EtOAc and EtOAc/MeOH to give six fractions. Because fraction two (eluted 5%-10% hexanes/EtOAc) possessed biological activity to *B. glabrata*, it was subjected to RP-Solid Phase Extraction (5mm Varian SEP Cartridge) with a 60-100% MeOH/H<sub>2</sub>O gradient. Molluscicidal activity was observed in fraction 2 (60-70% MeOH/H<sub>2</sub>O), which subsequently yielded pure **60** through repetitive NP-HPLC (90% hexanes/EtOAc; 246 x 4.6 mm 10  $\mu$  Phenomonex Si Column, 1 ml/min) by the collection of a peak centered at  $t_R = 6.3$  min detected by UV absorption at 254 nm (354 mg, 27% of total extract). Fraction 6 from the Solid Phase Extraction above was subjected to preparative NP-HPLC (85% hexanes/EtOAc; 246 x 10 mm 10  $\mu$  Phenomonex Si Column) in a phytochemical pursuit of additional halogenated compounds. Further purification of one of the collected peaks (elution centered at  $t_R = 4.2$  min detected by UV absorption at 254 nm; 4.5 ml/min) was accomplished using NP-HPLC (95% hexanes/EtOAc; 246 x 4.6 mm 10  $\mu$  Phenomonex Si Column) to yield essentially pure **65** (peak centered at  $t_R = 8.1$  min, 0.9 ml/min, 0.3 mg, 0.002% of total extract). Compounds **44b**, **55**, and **59** were purified from fractions of this series.

#### TAVIOCHTODENE (**65**)

Pure taviochtodene showed  $[\alpha]_D^{25} +35$  (CHCl<sub>3</sub>,  $c$  0.1); UV  $\lambda_{max}$  (MeOH) 245 nm (log  $\epsilon = 5,000$ ); IR  $\nu_{max}$  (film) 2964, 2860, 1380, 1365, 897 cm<sup>-1</sup>; LRCIMS (0.1 M oxalic acid/2:1 thioglycerol:glycerol) obs.  $m/z$  (rel int) 362 (10), 327 (75), 283 (100), 247 (50), 211 (15), 203 (25), 167 (45); HRCIMS (0.1 M oxalic acid/2:1

thioglycerol:glycerol) obs.  $[M]^+ m/z$  361.8839 for  $C_{10}H_{14}Br_2Cl_2$  ( $\Delta$  0.9 mmu);  $^1H$  and  $^{13}C$  data see Table III.1.

#### MOLLUSCICIDAL SCREENING PROTOCOL

Evaluation for molluscicidal activity was performed as previously described using *Biomphalaria glabrata* as the test organism. Aliquots of a 10 mg/ml (in EtOH) stock solution of **60** were serially diluted using EtOH to achieve a range of concentrations to be tested. To a 20 ml scintillation vial containing 9900  $\mu$ l of ddH<sub>2</sub>O 100  $\mu$ l of test solution were added. To each vial two snails were added (approx. 8 mm each); after 24 hr the live and dead snails were tallied. Snails was determined to be alive by visual observation of a heartbeat or a response to foot probing. Fractions and pure compounds were, at a minimum, tested in duplicate (in separate scintillation vials).



## REFERENCES

67. Crews, P.; Naylor, S.; Hanke, J.; Hogue, E.R.; Kho, E.; Craslaw, R. *J. Org. Chem.* **1984**, *49*, 1371-1377.
68. Paul, V.J., McConnell, O.J.; and Fenical, W. *J. Org. Chem.* **1980**, *45*, 3401-3407.
69. Crews, P.; Myers, B.L.; Naylor, S.; Clason, E.L.; Jacobs, R.S.; Staal, G.B. *Phytochemistry* **1984**, *23*, 1451-1449.
70. McConnell, O.J. and Fenical, W.F. *J. Org. Chem.* **1978**, *43*, 4238-4241.
71. Gunatilaka, A.A.L.; Paul, V.J.; Park, P.U.; Puglisi, M.P.; Gitier, A.D.; Eggleston, D.S.; Hiltiwanger, R.C.; Kingston, D.G.I. *J. Nat. Prod.* **1999**, *62*, 1376-1378.
72. Fuller, R.W.; Cardellina, J.H.; Kato, Y.; Brinen, L.S.; Clardy, J.; Snader, K.M.; Boyd, M.R. *J. Med. Chem.* **1992**, *35*, 3007-3011.
73. Fuller, R.W.; Cardellina, J.H.; Jurek, J.; Scheuer, P.J.; Alvarado-Lindner, B.; McGuire, M.; Gray, G.N.; Steiner, J.R.; Clardy, J.; Menez, E.; Shoemaker, R.H.; Newman, J.N.; Snader, K.M.; Boyd, M.R. *J. Med. Chem.* **1994**, *37*, 4407-4411.
74. Gerwick, W.H. *Phytochemistry* **1984**, *23*, 1323-1324.
75. Burrenson, B.J.; Woolard, F.X.; Moore, R.E. *Tetrahedron Lett.* **1975**, 2155-2158.
76. Burrenson, B.J.; Woolard, F.X.; Moore, R.E. *Chem. Lett.* **1975**, 1111-1114.
77. Woolard, F.X., Moore, R.E.; Van Engen, D.; Clardy, J. *Tetrahedron. Lett.* **1978**, 2367-2370.
78. Paul, J.V.; Hay, M.E.; Duffy, J.E.; Fenical, W.; Gustafson, K. *J. Exp. Mar. Biol. Ecol.* **1987**, *114*, 249-260.
79. Coll, J.C. and Wright, A.D. *Aust. J. Chem.* **1989**, *42*, 1983-1993.
80. Firn, R.D. and Jones, C.G. *Mol. Microbiol.* **2000**, *37*, 989-994.

## CHAPTER IV.

ISOLATION AND STRUCTURE ELUCIDATION OF THREE NEW  
MALYNGAMIDES FROM THE MARINE CYANOBACTERIUM, *LYNGBYA*  
*MAJUSCULA*

## ABSTRACT

A pair of lipid extracts of *Lyngbya majuscula*, one collected from Curaçao and the other of Malagasy origination, have yielded malyngamides L (**80**, Curaçao), Q, and R (**70** and **71**, Madagascar). All three are amides of 7-methoxytetradec-4-enoic acid, quite common among the malyngamide class of secondary metabolites. Malyngamide L bears resemblance to the cyclohexyl-type subclass, while malyngamides Q and R are most closely related to malyngamide A, a pyrrolidone-type malyngamide. The isolation of these metabolites was carried out by preparative liquid chromatography with final purification through repetitive reversed phase HPLC. Structure elucidation was accomplished utilizing 1D and 2D NMR spectroscopic characterization of the natural products and comparisons with related malyngamides. DPGSE NOE data suggested different geometrical stereochemistry at C-6 in malyngamides Q and R from that observed for other known malyngamides. The Z stereochemistry was confirmed for malyngamide R by measurement of  $^{23}\text{J}_{\text{CH}}$  coupling utilizing the HSQMBC pulse sequence. The absolute stereochemistry of C-4'' of the pyrrolidone ring was defined by chiral GC/MS analysis.

## INTRODUCTION

The malyngamides are the most pervasive class of *L. majuscula* secondary metabolites. Isolated from *L. majuscula* of distinctly varied marine habitats, from locations spanning the globe in tropical locations, 27 malyngamides have now been reported in the literature.<sup>81-95</sup> Of these, our laboratory has identified malyngamides F (76),<sup>86</sup> F-acetate (77),<sup>86</sup> H (86),<sup>88</sup> I (78),<sup>89</sup> J (87),<sup>90</sup> K (75),<sup>90</sup> L (80),<sup>90</sup> Q (70),<sup>93</sup> R (71),<sup>93</sup> and S<sup>94</sup> (92) from Caribbean, Indonesian, Fijian, Malagasy, and New Guinean *L. majuscula*, respectively. While malyngamides have also been reported from sources other than *L. majuscula*, these most likely represent collections including *L. majuscula*, and not *de novo* non-cyanobacterial biosynthesis.<sup>91</sup>

The frequency with which known and novel malyngamides are encountered suggests a demonstrative energetic biosynthetic output by the alga, which often denotes utility in nature. Discovering members of this structure class from diverse habitats and divergent locations intimates an ancient genetic derivation. However, only modest biological activity, pharmaceutical or chemical ecological, has been demonstrated in the malyngamides to date. Regardless of the presence or absence of substantial biological activity, the malyngamides represent a widespread (within the *L. majuscula* species) and structurally interesting series of marine natural product.

## THE MALYNGAMIDE STRUCTURE

In all malyngamides, two molecular 'halves' can be observed, a methoxylated fatty acid tail and an amino acid derived head. Four fatty acid chain lengths have been identified thus far, C-12, -14, -16, and -20, with the vast majority of malyngamides

having a 14 carbon chain. A high degree of fidelity can be seen in two aspects of the fatty acid portion, with all known malyngamides possessing a C-4/C-5 *trans* double bond and a methoxy group at C-7. Malyngamides D (84) and E (85), the only examples with a C-16 chain, are also the only with additional chain functionalization, being methylated at the C-9 position.<sup>84</sup> Collectively, the four malyngamide fatty acid chain variants have been given the trivial name 'lyngbic acids' (Figure IV.1).<sup>33</sup>

A higher degree of variability can be seen in the malyngamide head groups connected to the fatty acid chain by an amide bond. To date, five basic types of amide portions have been discovered, pyrrolidone (Figure IV.2), cyclohexyl (Figure IV.3), non-chlorinated (Figure IV.4.A), acyclic (Figure IV.4.B), and lactone (Figure IV.4.C). The most commonly isolated malyngamides are of the cyclohexyl-type, followed by the pyrrolidone and non-chlorinated types, and the recently discovered acyclic and lactone varieties.

Four motifs are typically seen in cyclohexyl malyngamides, a vinyl chloride (Figure IV.5.A.1), a cyclohexyl ring system (Figure IV.5.A.2), an oxygen bearing C-5' (Figure IV.5.A.3), and a C4'-C9' olefin or epoxide (Figure IV.5.A.4). The pyrrolidone malyngamides are characterized by the vinyl chloride (Figure IV.5.B.1), a conjugated enone system (Figure IV.5.B.2), and what appears to be a cyclized polyketide-extended amino acid (Figure IV.5.B.3). The non-chlorinated malyngamides, obviously lacking the vinyl chloride, possess either an exomethylene moiety adjacent to the cyclohexyl ring (Figure IV.5.C.1) and an additional pre-ring methylene group (Figure IV.5.C.2) in malyngamides H and J, or have functionalization  $\alpha$  to the nitrogen (D, E, and the serinol-derived malyngamides; Figure IV.5.D.1).

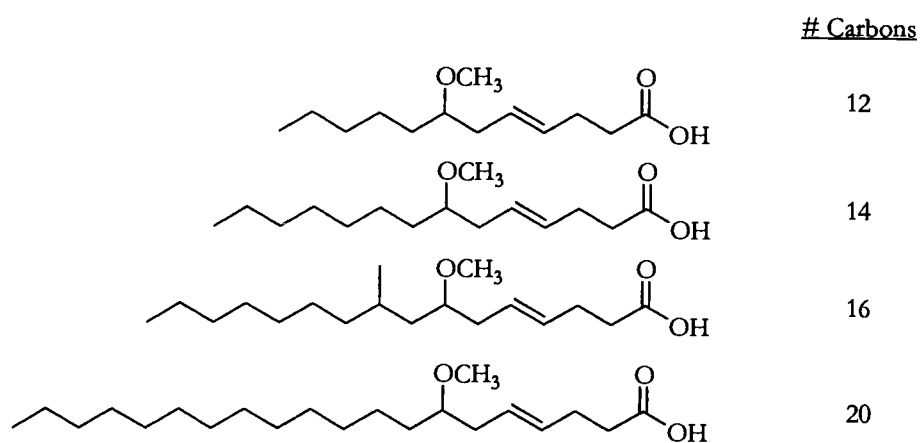


**Figure IV.1.** The lyngbic acids.

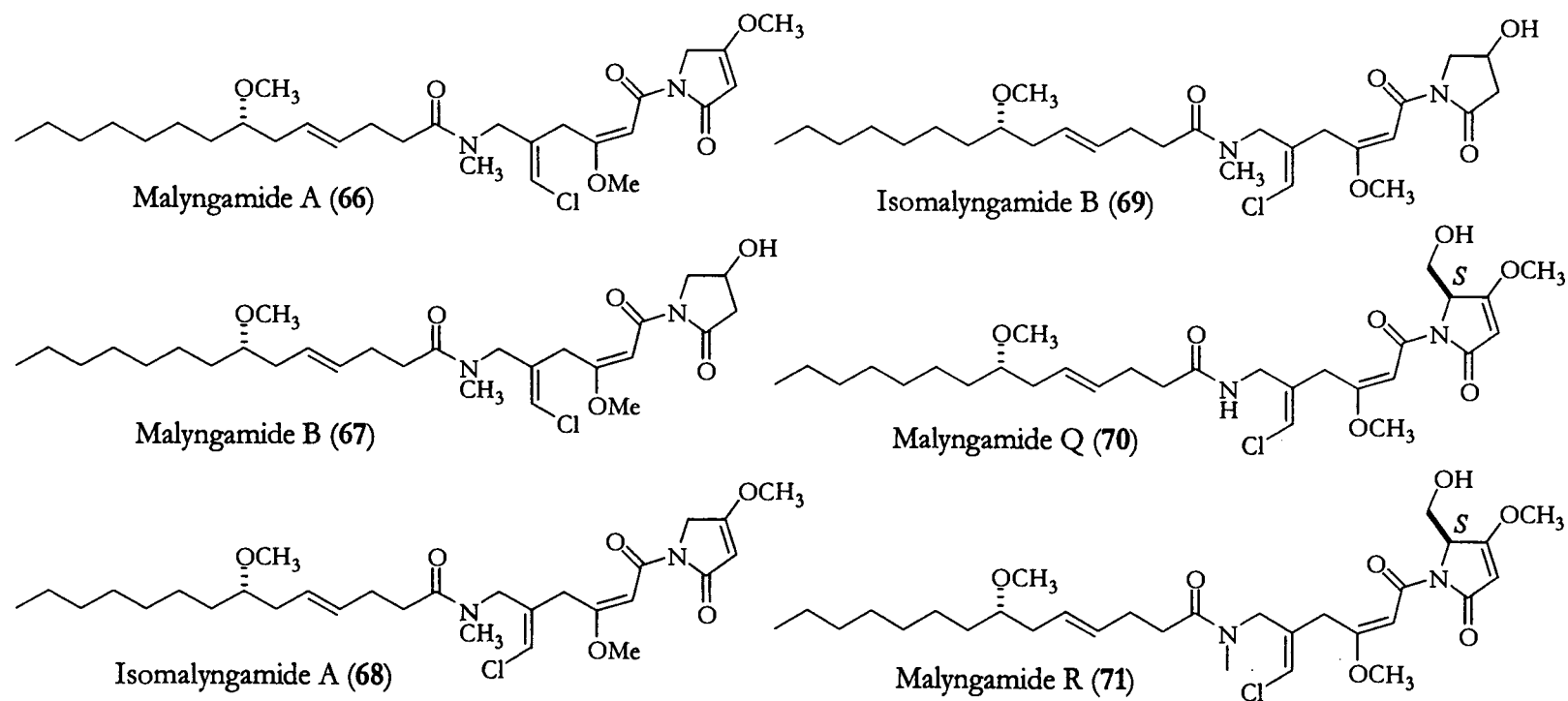


**Figure IV.2.** The pyrrolidone-type subclass of malyngamides.

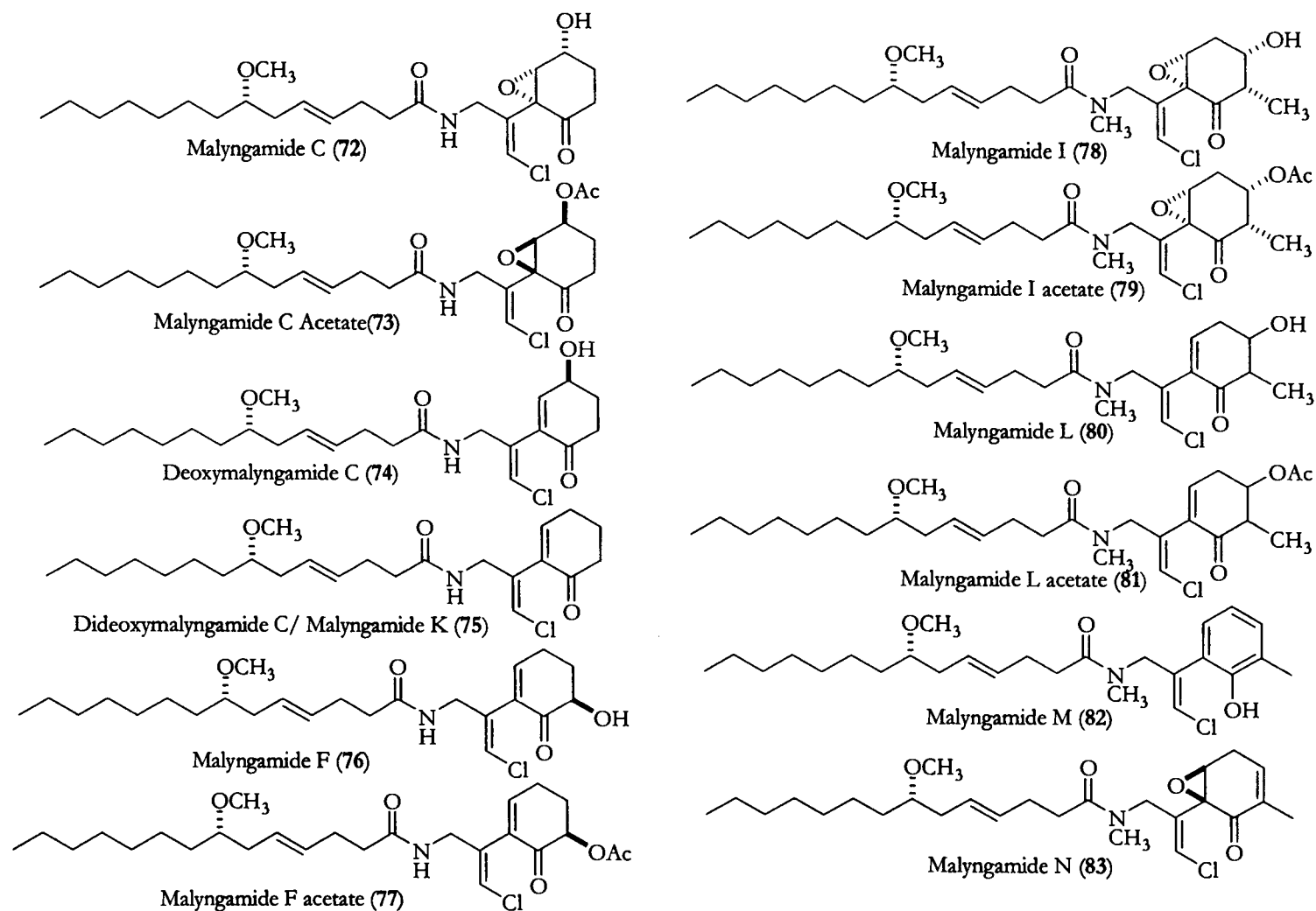
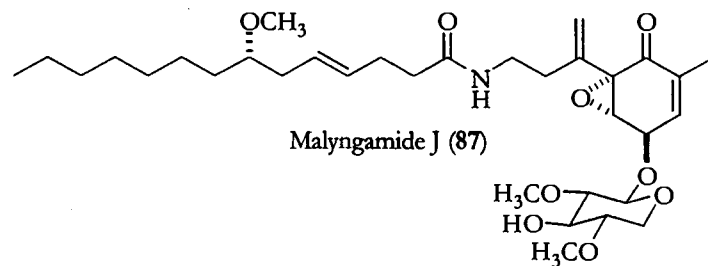
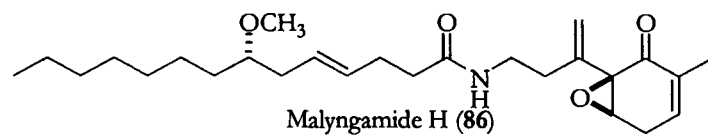
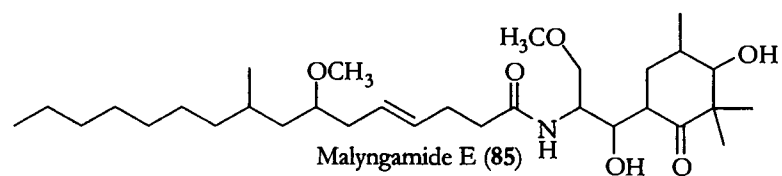
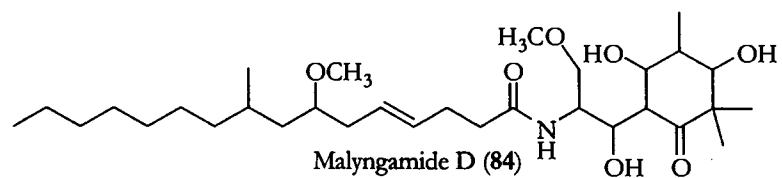
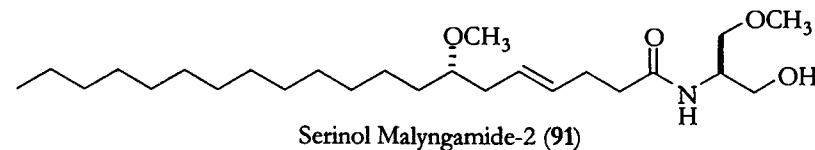
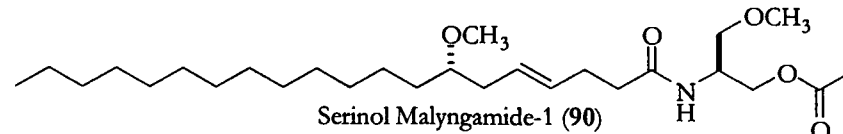
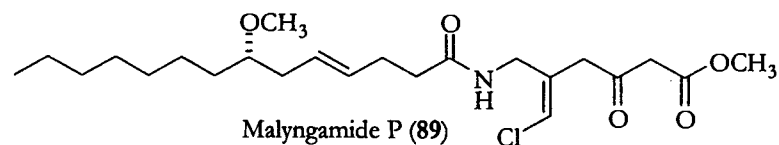
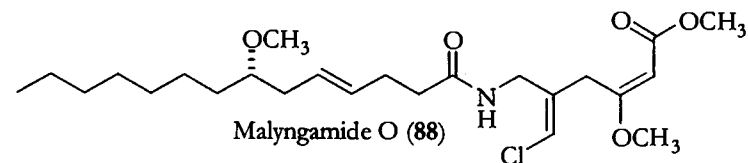


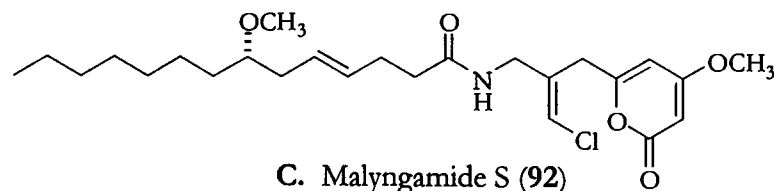
Figure IV.3. The Cyclohexyl Malyngamides



**A. Non-chlorinated malyngamides.**



**B. Acyclic malyngamides.**



**C. Malyngamide S (92)**

**Figure IV.4.** Non-standard malyngamides.



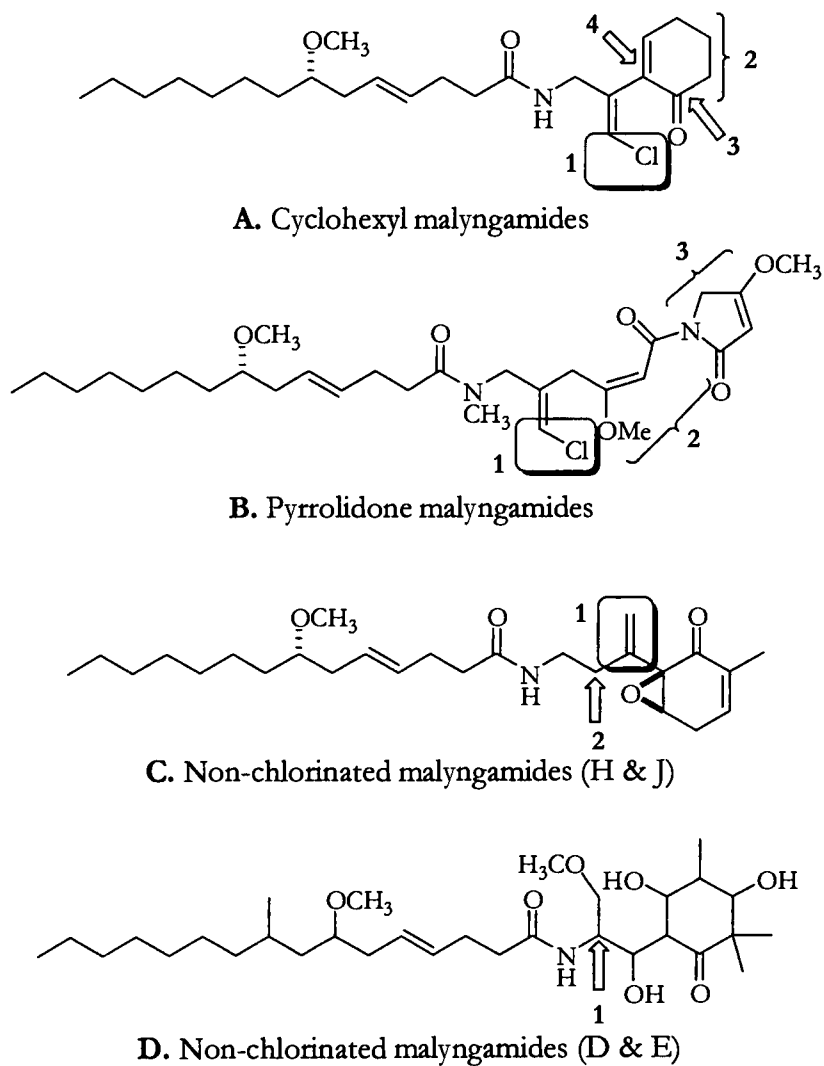


**Figure IV.5.** Common structural motifs of malyngamide amino portion.

Structural trends cannot be established for the remaining malyngamides, the acyclic and lactone types, due to the small number of each that have so far been discovered. The two members of the acyclic subclass of malyngamides appear to be simple analogs of each other, closely resembling the main body of those of the pyrrolidone group. Interestingly, the acyclic and pyrrolidone subclasses are the only having members with altered geometric stereochemistry at the vinyl-chloride carbon, as compared with other malyngamides.

#### CONSIDERING MALYNGAMIDE BIOGENESIS

While no biosynthetic experiments investigating the malyngamides have been reported in the literature, the structural similarities and the ability to form 'family' groupings allows for biogenetic speculation on the malyngamide head group. Similar to the manner used above to simplify the discussion by subdividing the malyngamides into groups, a biogenetic analysis also benefits from forming 'family' groupings.

#### Serine-derived malyngamides

Malyngamides D (84) and E (85), lacking a vinyl chloride and having a functionalized  $\alpha$  carbon and an unusual fatty acid tail, appear biogenetically unusual next to most other malyngamides. The discovery of the serinol malyngamides has added members to the list of non-standard malyngamides, and insight into the biogenesis of the entire structure class. Figure IV.6.A is a biogenetic scheme leading to the creation of 84 and 85 and the serinol derived malyngamides (90 & 91).

Malyngamides D and E could be created by a series of three polyketide extensions proceeding from the serine carboxyl, ultimately terminating in ring closure and functionalization.

#### Pyrrolidone malyngamides

The relationship between the pyrrolidone malyngamides and the acyclic malyngamides O (88) and P (89) is relatively obvious, with 88 merely terminating in a methoxy moiety rather than the standard pyrrolidone ring system. Additionally, the *Z* stereochemistry of the vinyl chloride olefin, as opposed to the *E* stereochemistry present at the same position in other chlorinated malyngamides, can be seen in all but malyngamides A (66) and B (67) of this group. The retained stereochemistry and the presence of most discernable features of the more derivatized malyngamides may suggest 66 and 67 being intermediates leading to the pyrrolidone malyngamides (Figure IV.6.B).

#### Cyclohexyl and non-chlorinated malyngamides

The two previously described groups, the serinols and the pyrrolidones, supply key elements to speculation upon the biogenesis of the cyclohexyl malyngamides. Firstly, viewing the substitution pattern of the typical cyclohexyl ring system brings an immediate comparison to malyngamides O and P, but with what appears to be an additional acetate unit. So, by extension, the as yet undiscovered parent of the cyclohexyl malyngamides can be conceptualized in Figure IV.6.C.

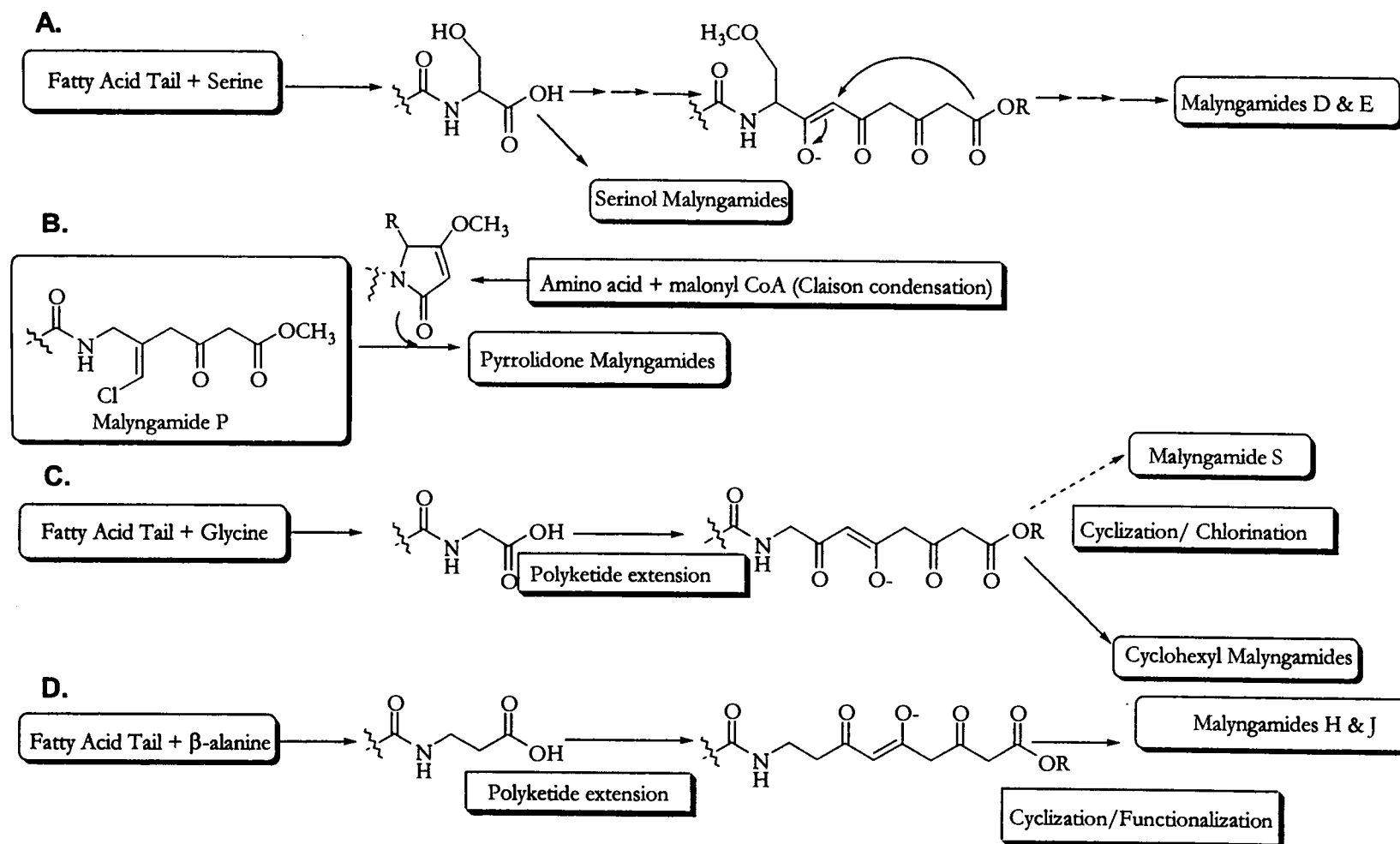


Figure IV.6. Malyngamide biogenesis.

The theory put forth in Figure IV.6.A, with polyketide extension of serine leading to the creation of **85** and **86** allows the possibility of a similar scenario for the cyclohexyl malyngamides. The strongest amino acid candidate, considering the lack of an amino side chain as evidence, would be glycine (Figure IV.6.C). Polyketide extension and tailoring would produce the proposed precursor. Attack by the C-2 of acetate, as seen in jamaicamide biosynthesis, would precede halogenation, leading to the cyclohexyl malyngamides.<sup>96</sup> Glycine would also apparently be the starter unit for polyketide extension in the pyrrolidone malyngamides as well. In parallel, malyngamides H and J, rather than utilizing glycine for polyketide extension, may incorporate  $\beta$ -alanine (Figure IV.6.D), by this analysis. The lack of chlorination in these molecules may suggest some structural impediment to the halogenation mechanism. Malyngamide S (**92**), the only malyngamide with a lactone ring, could be the product of the proposed alternative cyclization pathway proposed in Figure IV.6.C.

## RESULTS AND DISCUSSION

In an effort to discover and identify structurally intriguing and biologically active secondary metabolites from marine algal sources, the crude extracts of two collections of *Lyngbya majuscula* were investigated. The evaluation of NMR data, TLC characteristics, and in-house biological activity assays has lead to the isolation of malyngamides L (**80**), Q (**70**), and R (**71**).<sup>90,92</sup> Malyngamide L is a cyclohexyl malyngamide derived from a Caribbean *L. majuscula*, while **70** and **71** are pyrrolidone malyngamides of Malagasy origination. Modest biological activity has been observed in both malyngamides L (brine shrimp and goldfish) and R (brine shrimp).

## MALYNGAMIDE L

Malyngamide L (**80**) was isolated as an optically active oil ( $[\alpha]_D^{25} = +17^{\circ}$ ,  $c = 0.1$ , EtOH), of modest toxicity (*Artemia salina* LD<sub>50</sub> = 8.0 µg/ml, *Carassius auratus* LD<sub>50</sub> = 15.0 µg/ml) from a Curaçaoan collection of *Lyngbya majuscula*. LRFABMS revealed a molecular ion of 468, with an isotope pattern descriptive of a single chlorine (Figure IV.7). HREIMS analysis of **80** described a molecular formula, (C<sub>26</sub>H<sub>42</sub>NO<sub>4</sub>Cl; [M-Cl]<sup>+</sup> at  $m/z$  432.3096,  $\Delta$  1.7 mmu), suggestive of six degrees of unsaturation. Through the interpretation of 1D and 2D NMR data sets (Figures IV.8-11), a trio of substructures were compiled clearly reflecting some commonly observed motifs of the malyngamides (Figure IV.12). Namely, a 7-methoxytetradec-4-enoic acid chain (Figure IV.12.A), a nitrogen containing vinyl chloride moiety (Figure IV.12.B), and a cyclohexenone ring system (Figure IV.12.C) were observed. Analysis of the 1D <sup>13</sup>C and <sup>1</sup>H NMR spectra also revealed N-methyl [<sup>1</sup>H  $\delta$  2.97 (3H), <sup>13</sup>C  $\delta$  33.48] and

0590 KEN10002.12 RT= 02:23 1C1 SLRP 30-Apr-96 07:48  
TIC= 5391360 100% 373824 PUS EI KEN'S SAMPLE

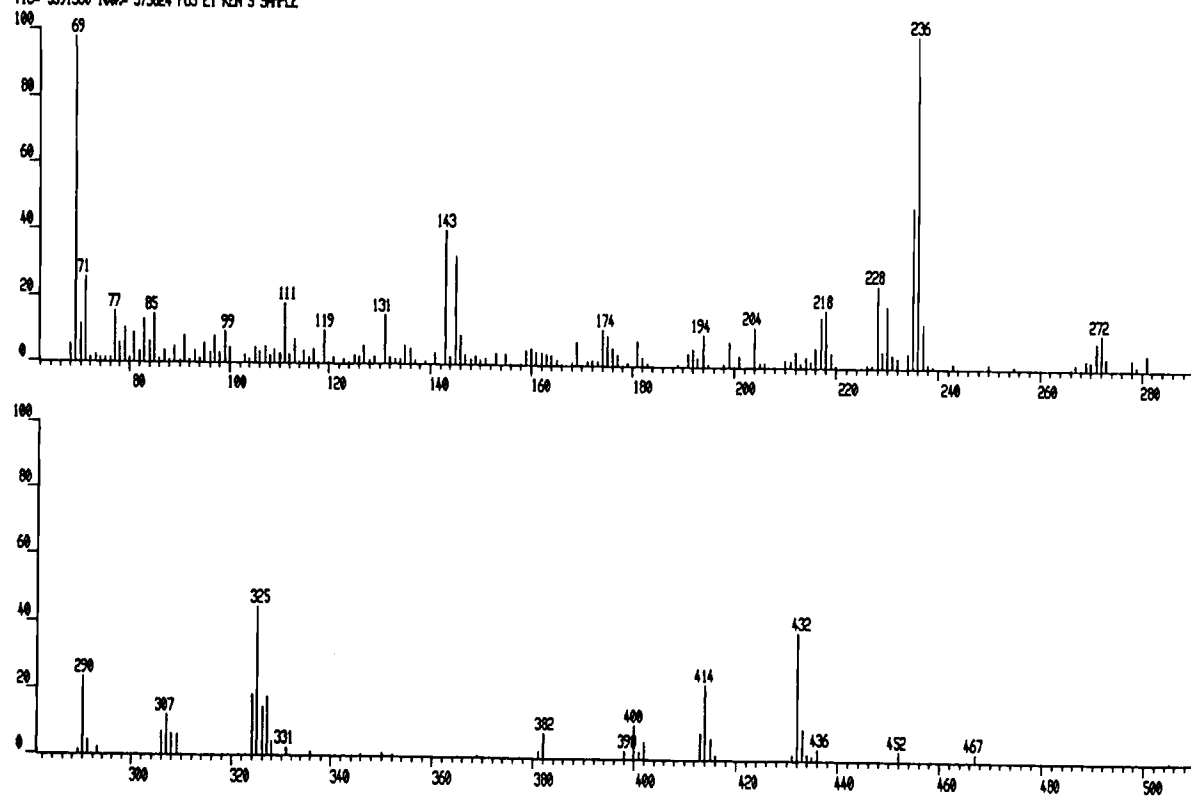
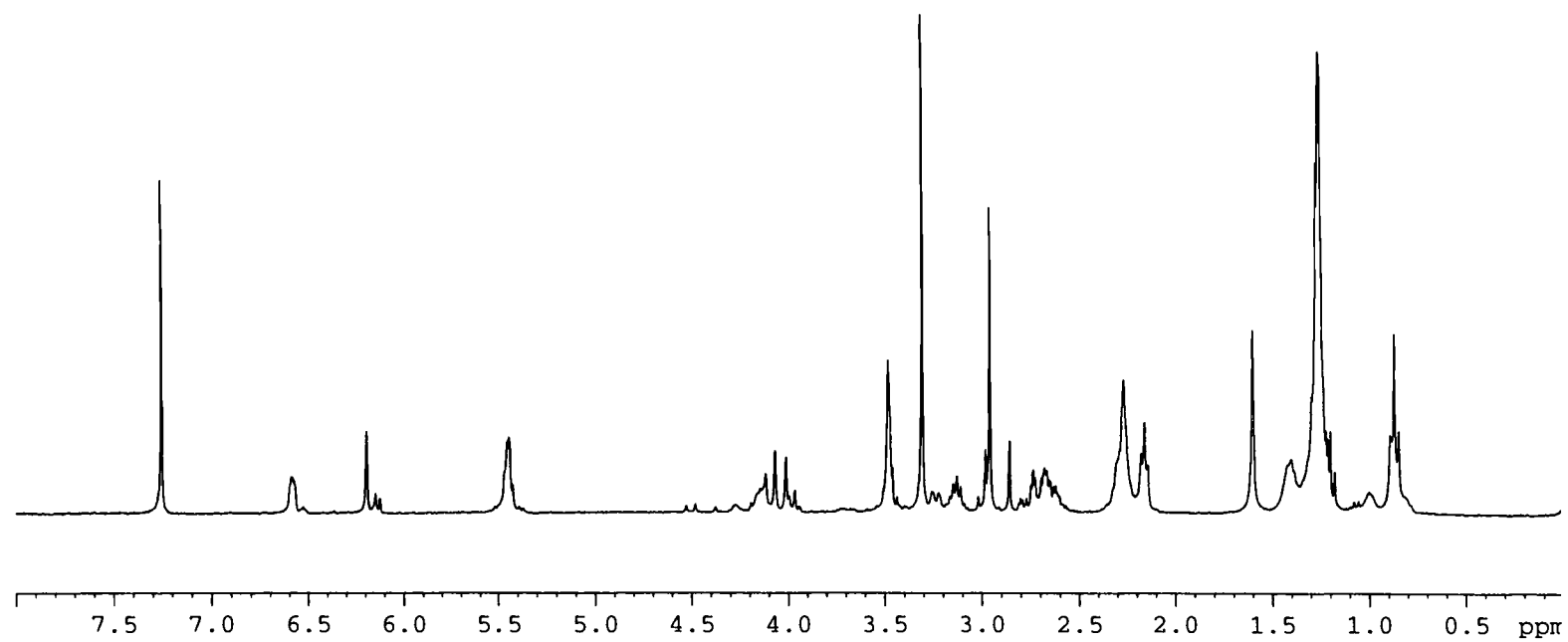


Figure IV.7. LREIMS of malyngamide L.



**Figure IV.8.**  $^1\text{H}$  NMR spectrum of malyngamide L.



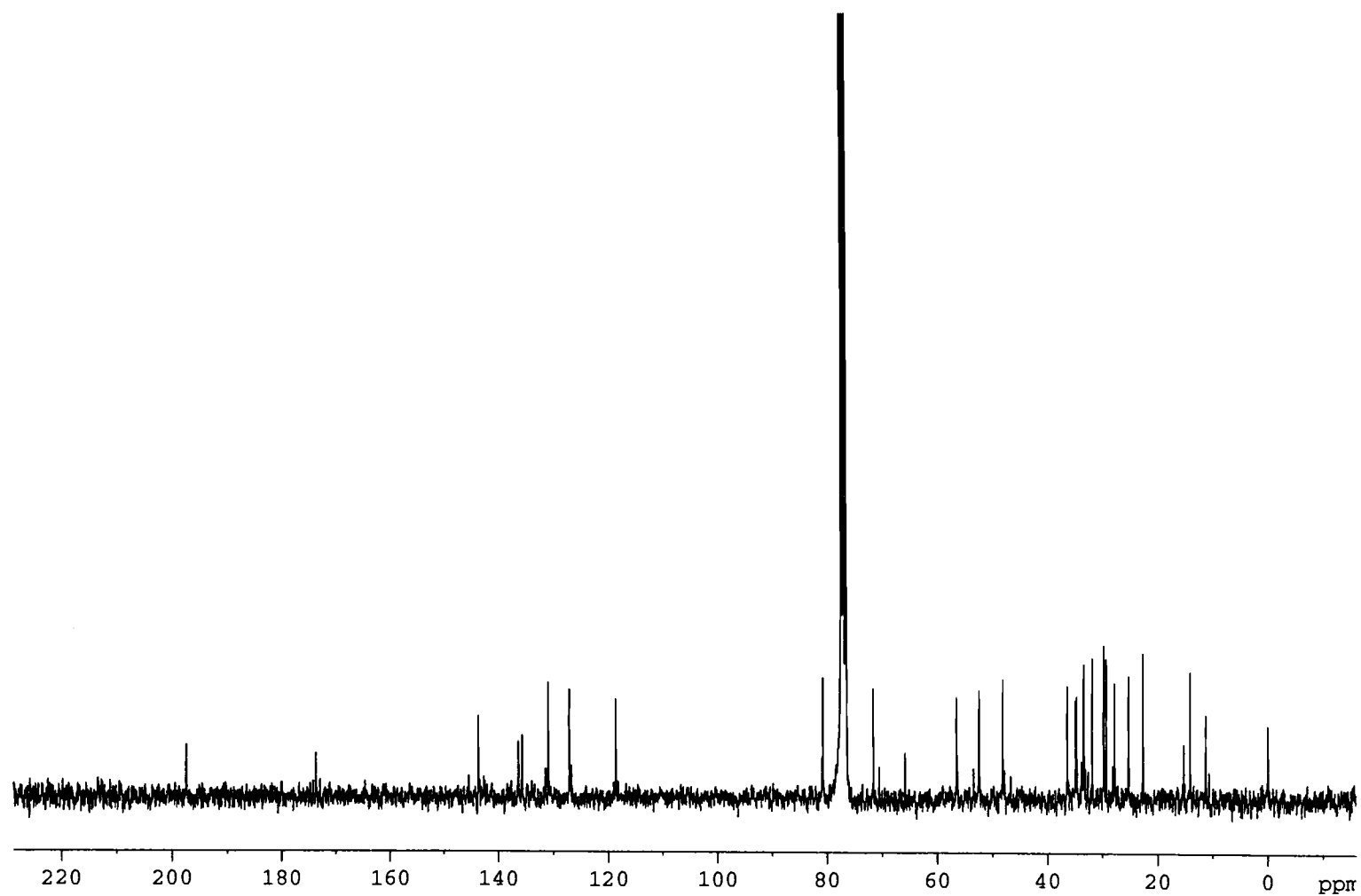


Figure IV.9.  $^{13}\text{C}$  NMR spectrum of malyngamide L.

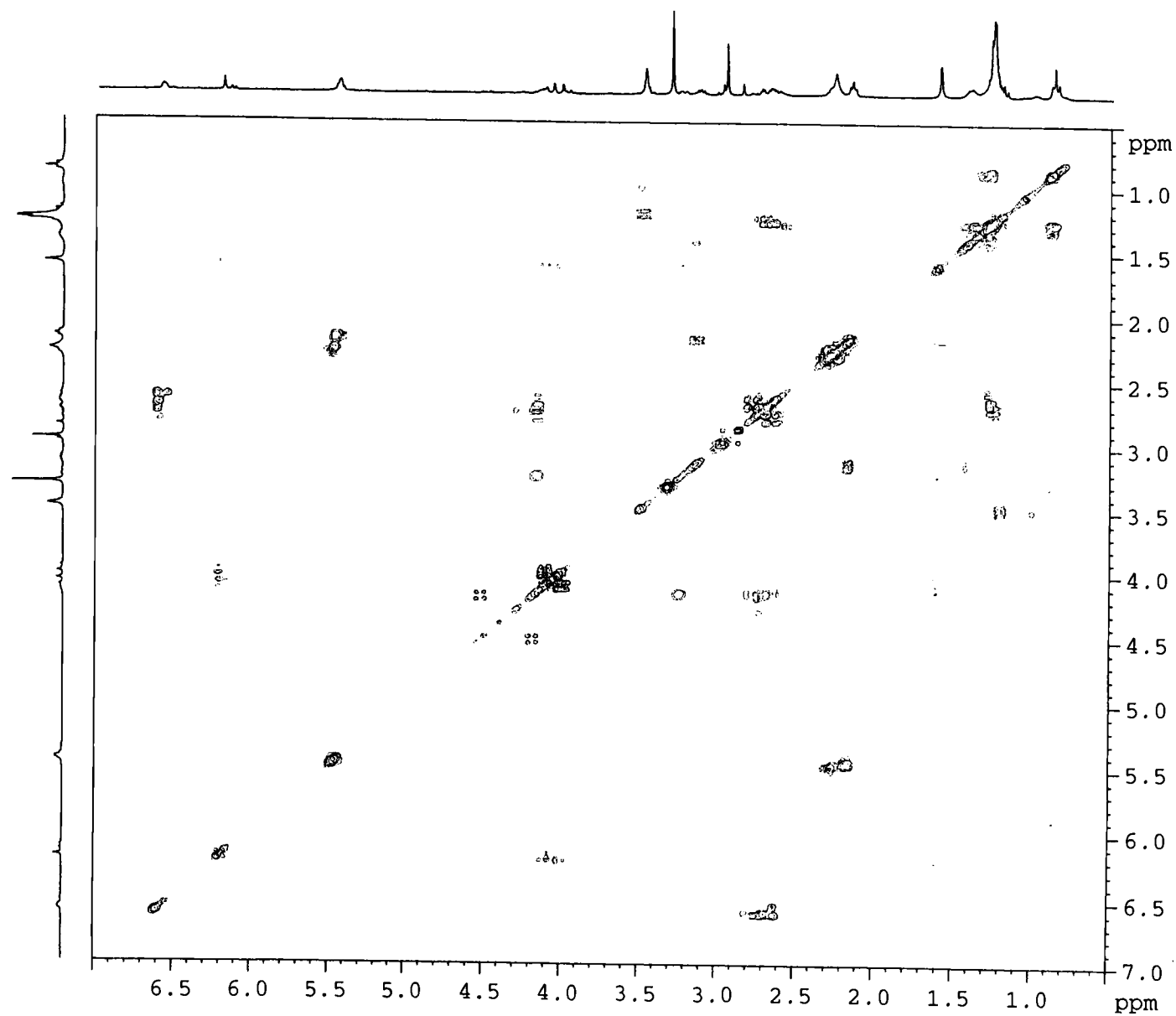


Figure IV. 10.  $^1\text{H}$ - $^1\text{H}$  COSY of malyngamide L.

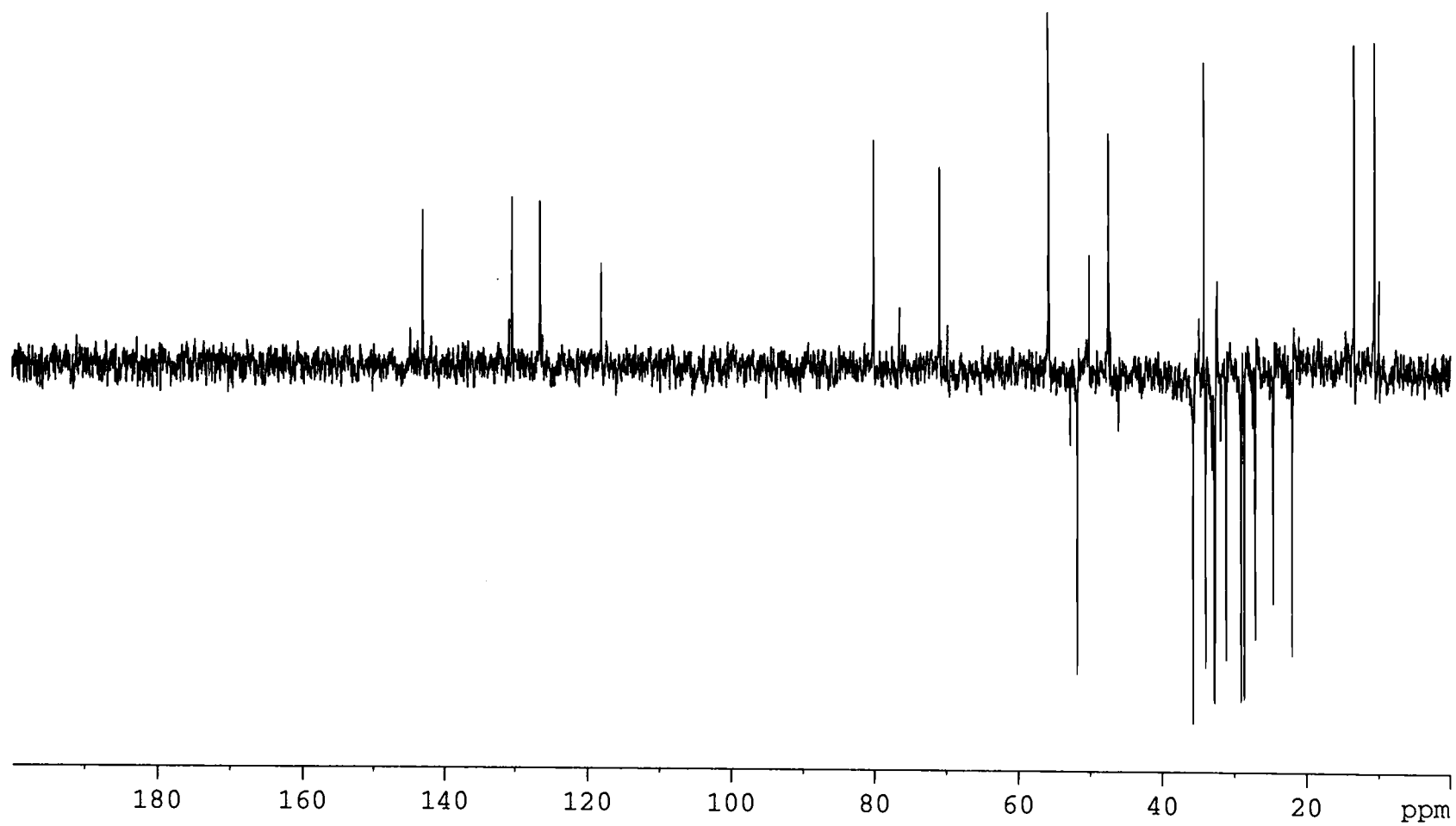
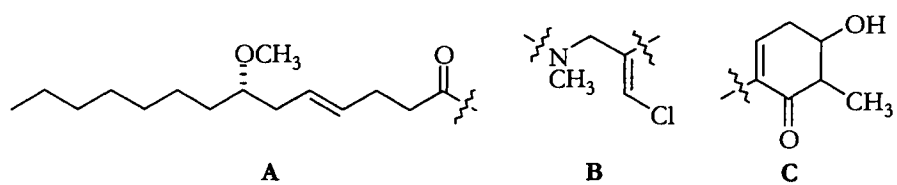


Figure IV. 11. DEPT of malyngamide L.



**Figure IV.12.** Partial structures of malyngamide L.

**Table IV.1. NMR Data for Malyngamide L (80).**

<b><u>Malyngamide L (80)</u></b>		
<b><u>C-atom</u></b>	<b><u><sup>1</sup>H ppm (mult, <i>J</i> in Hz)</u></b>	<b><u><sup>13</sup>C ppm</u></b>
1a	4.0 (d, 14.3)	52.49
b	4.1 (d, 14.3)	
2		136.45
3	6.2 (bs)	118.72
4		135.71
5		197.30
6	2.65 (m)	48.20
7a	4.13 (m)	71.66
b		
8a	2.60 (m)	34.68
b	2.78 (m)	
9	6.57 (m)	143.70
10	1.25 (m)	11.25
1'		173.76
2'	2.26 (m)	34.94
3'	2.28 (m)	27.82
4'	5.45 (m)	131.05
5'	5.45 (m)	127.21
6'	2.15(dd, 5.8,5.5)	36.42
7'	3.15 (m)	80.80
8'	1.41 (m)	33.37
9'	1.27 (m)	25.29
10'	1.27 (m)	29.76
11'	1.27 (m)	29.31
12'	1.27 (m)	31.85
13'	1.27 (m)	22.66
14'	0.88 (t, 6.8)	14.11
15'	3.26 (s)	56.40
NCH <sub>3</sub>	2.97 (bs)	33.48
OH	3.26 (d, 9.6)	
7' OCH <sub>3</sub>	3.29 (bs)	56.54

<sup>1</sup>H chemical shifts referenced to residual CHCl<sub>3</sub> (δ 7.24)

<sup>13</sup>C chemical shifts referenced to CDCl<sub>3</sub> center peak (δ 77.00)

secondary methyl functionalities [ $^1\text{H}$   $\delta$  1.25 (3H),  $^{13}\text{C}$   $\delta$  11.25]. Logically, the N-methyl component was attached to the nitrogen containing portion of Figure IV.12.B).

HMBC connectivities allowed assignment of the secondary methyl group as a substituent of the cyclohexenone ring system, as the methyl protons (H-10) clearly correlated to its carbonyl carbon (C-5,  $^{13}\text{C}$   $\delta$  197.3) and a heteroatom bearing carbon (C-7,  $^{13}\text{C}$   $\delta$  71.66). Possessing the last available position and a chemical shift indicative of heteroatom influence, the remaining hydroxyl component was attached to C-7. By acetylating **80** at the proposed secondary hydroxyl, the expected downfield shift of the proton  $\alpha$  to the acetate group, H-7 ( $^1\text{H}$   $\delta$  4.13 to  $^1\text{H}$   $\delta$  5.23), confirmed this assessment.

The methoxy fatty acid tail (Figure IV.12) was found to form an amide bond with the nitrogen of fragment B through HMBC connectivities to the amide carbonyl (C-1'  $\delta$  173.76) from the N-methyl protons and H-1 ( $^1\text{H}$   $\delta$  4.01 and 4.10). Fragment B was joined with the substituted cyclohexenone by HMBC connectivities from H-3 ( $^1\text{H}$   $\delta$  6.2) to C-4 ( $^{13}\text{C}$   $\delta$  135.71) and from the olefinic H-9 ( $^1\text{H}$   $\delta$  6.57) to the quaternary C-2 ( $^{13}\text{C}$   $\delta$  136.45). Thus, the planar structure of malyngamide L was completed.

#### MALYNGAMIDE Q

Malyngamide Q (**70**) was isolated as a pale yellow oil from the lipid extract of *L. majuscula*, collected near San Christi Island, Madagascar. LRFABMS (Figure IV.13) and HRFABMS showed a pseudomolecular ion ( $\text{M}+\text{H}^+$  at  $m/z$  569.3053) consistent with the molecular formula  $[\text{C}_{29}\text{H}_{46}\text{O}_7\text{N}_2\text{Cl}]$ , indicating a structure with eight degrees

DS90 KEN10001.7 RT= 01:09 fFAB LRP 23-Sep-97 14:16  
TIC= 20909060 100% 411552 POSFAB KEN-11B-83-2 IN 3-NEA

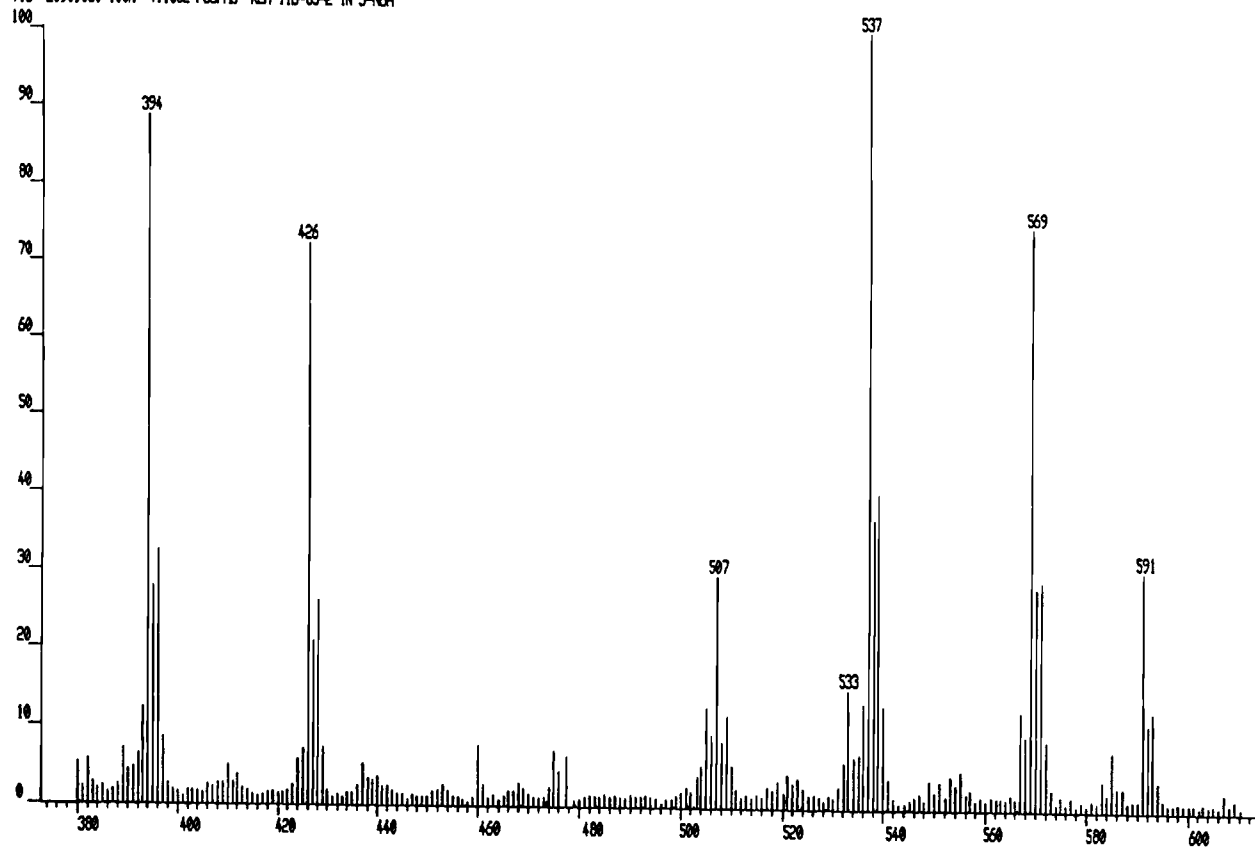


Figure IV. 13. LRFABMS of malyngamide Q.

of unsaturation. The IR spectrum possessed absorptions for NH or OH protons ( $3313\text{ cm}^{-1}$ ) and amide carbonyl groups ( $1713, 1630\text{ cm}^{-1}$ ). A UV maxima was observed at  $264\text{ nm}$ , suggestive of one or more conjugated enone systems.

The structural theme of the 1D NMR spectra (Figure IV.14-15) strongly suggested a malyngamide nature for **70**, with an aliphatic carbon chain, an exomethylene with a vinyl chloride ( $^1\text{H } \delta\ 6.03$ ;  $^{13}\text{C } \delta\ 118.28$ ), three methoxy groups, a trans disubstituted olefin ( $^1\text{H } \delta\ 5.40\ 2\text{H}$ ;  $^{13}\text{C } \delta\ 127.33\text{ and } 130.58$ ), and five resonances in the amide/ester region of the carbon spectrum (Table IV.2). A pair of unusual proton shifts ( $^1\text{H } \delta\ 6.88\text{ and } 5.10$ ) were found to correlate to two equally intriguing carbon resonances ( $^{13}\text{C } \delta\ 95.10\text{ and } 95.38$ , respectively) by HMQC (Figure IV.16). The assignment of these shifts as members of a conjugated enone system corresponded well with chemical shift data reported in the literature for malyngamide A,<sup>81</sup> and began to define **70** as a member of the pyrrolidone-type subclass of the malyngamides.

Similar to nearly all discovered malyngamides, the 1D NMR data and DQF-COSY (Figure IV.17) couplings described an aliphatic chain consistent with a 7-methoxy tetradec-4-enoic acid (Figure IV.19.A). DQF-COSY and HMBC (Figure IV.18) connectivities allowed the elucidation of the amide portion of the molecule, functionalized by an exomethylene with a vinyl chloride (Figure IV.19.B). In this partial structure,  $^1\text{H}$ - $^1\text{H}$  coupling could be observed from the exchangeable proton of the nitrogen to the C-7 methylene protons ( $^1\text{H } \delta\ 3.94\text{ and } 4.10$ ), which in turn showed HMBC cross peaks to the quaternary olefinic carbon (C-5,  $^{13}\text{C } \delta\ 135.20$ ), the vinyl



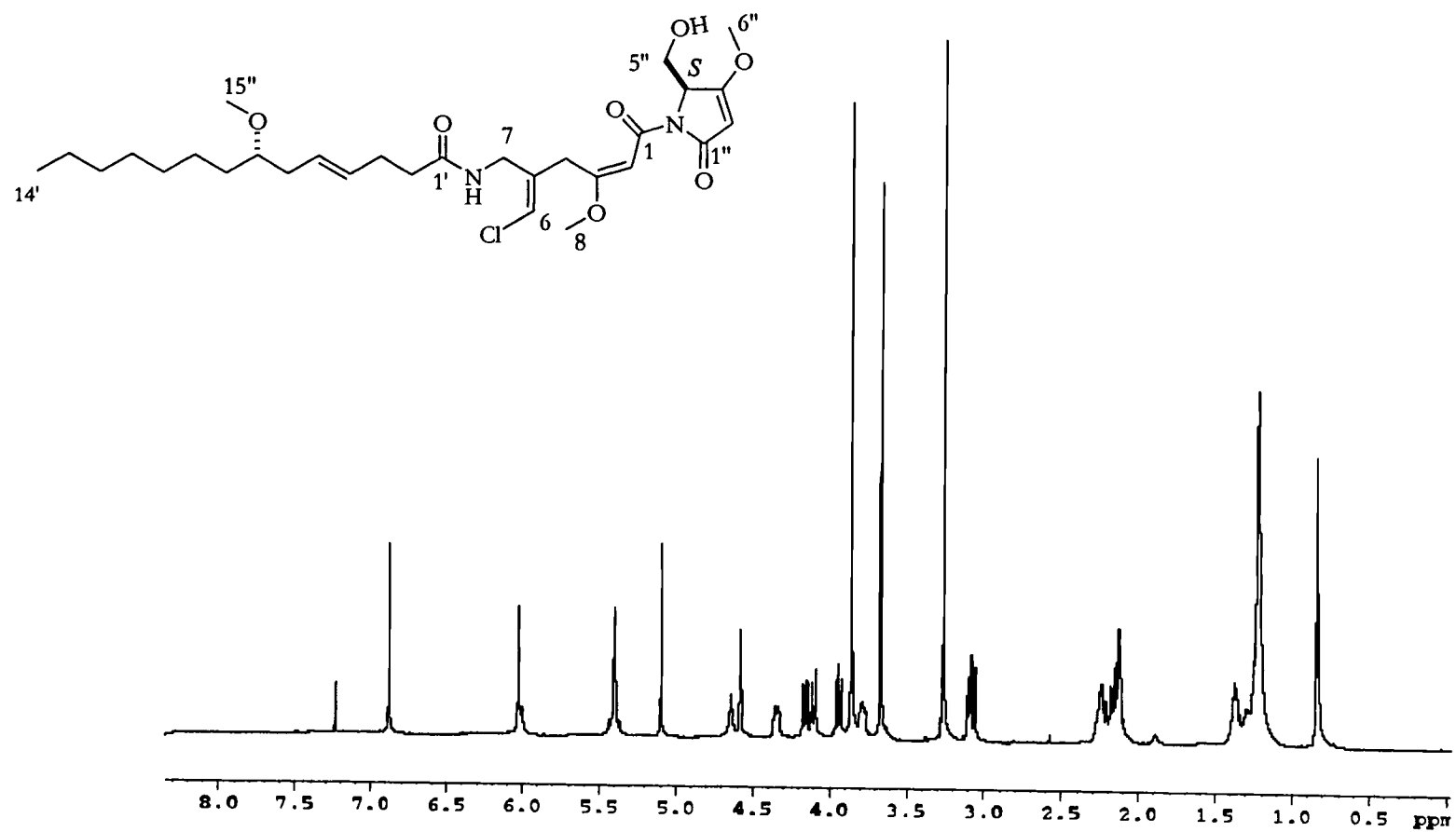


Figure IV.14.  $^1\text{H}$  NMR spectrum of malyngamide Q.

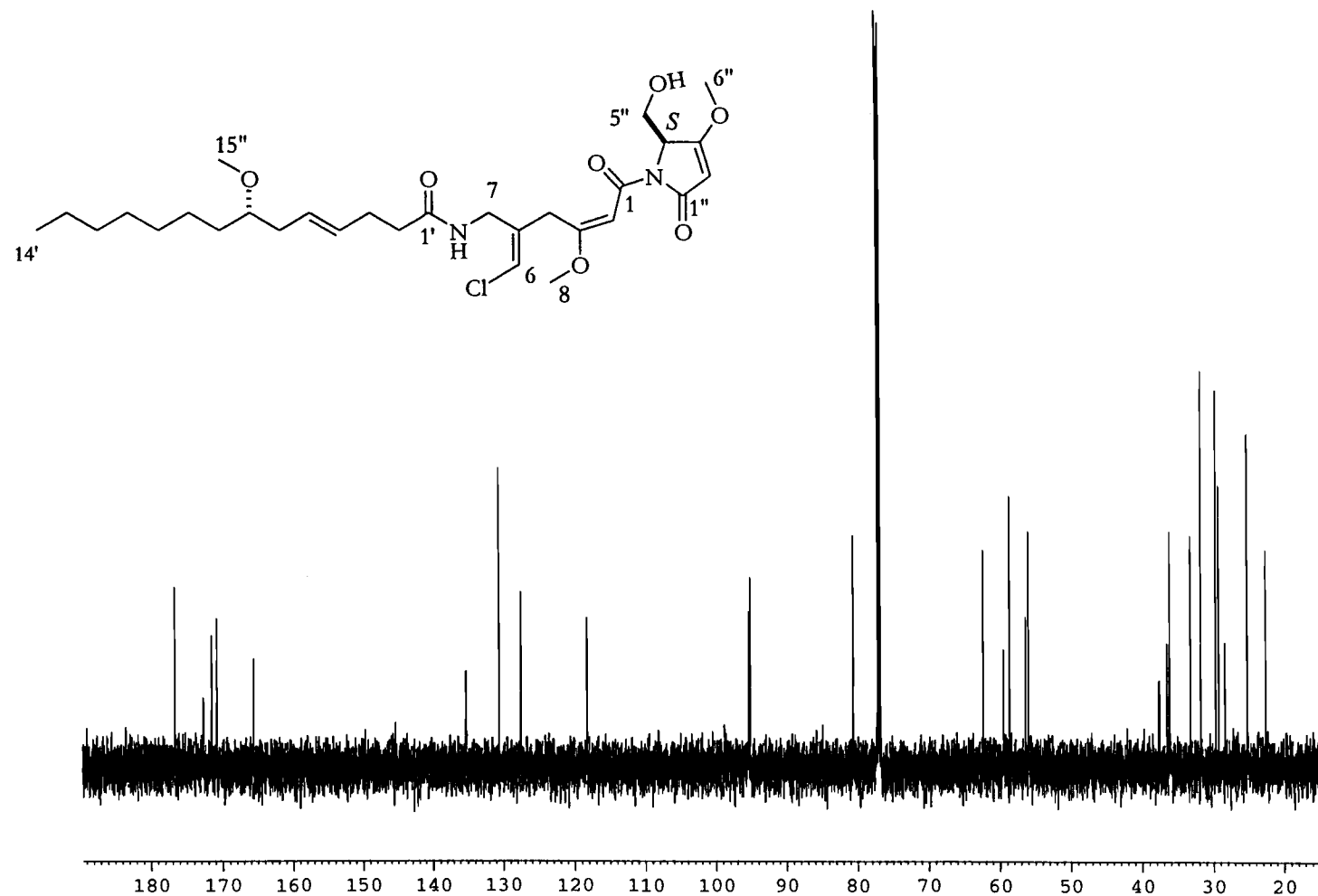


Figure IV.15.  $^{13}\text{C}$  NMR of malyngamide Q.

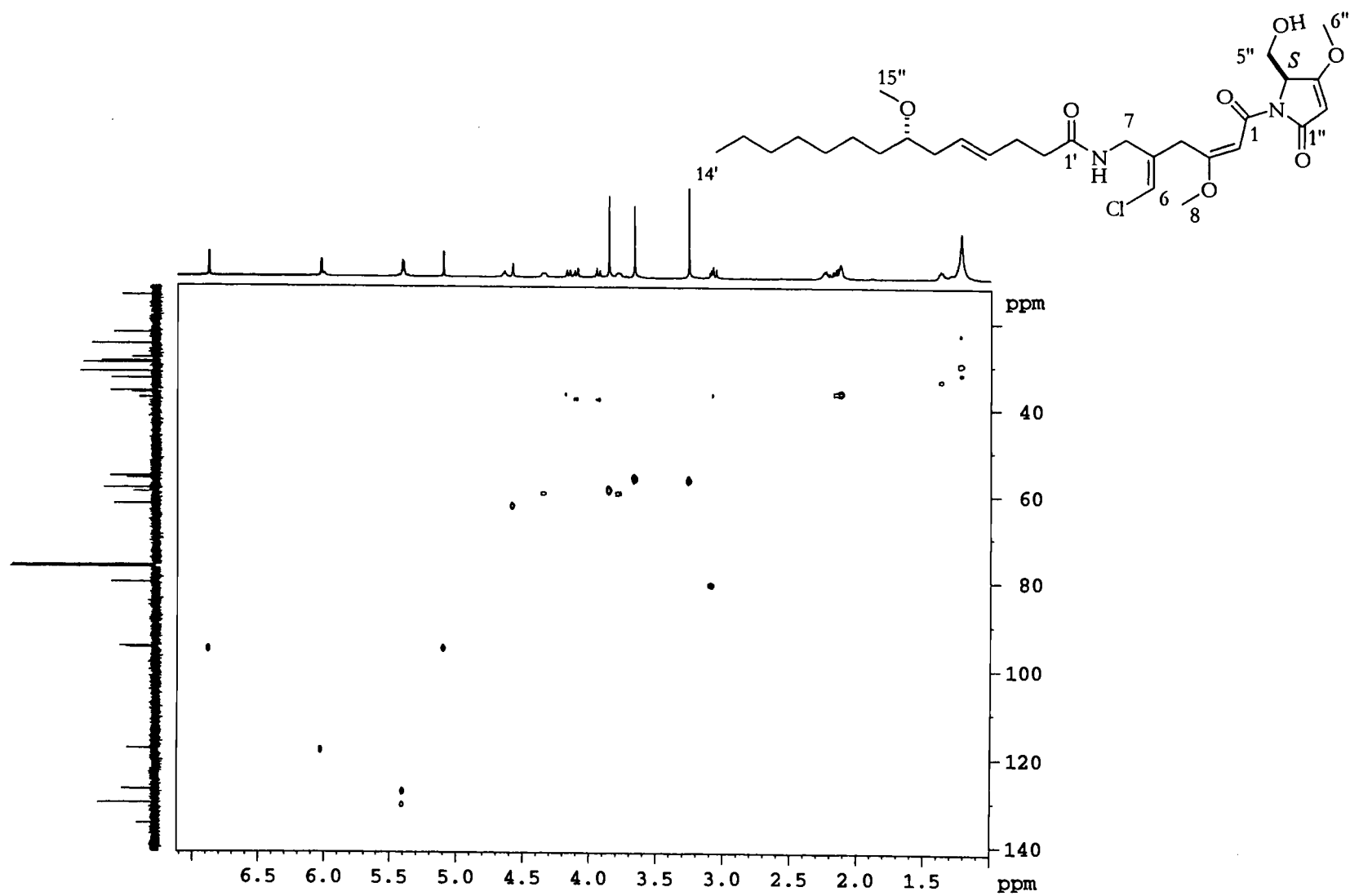


Figure IV.16. HMQC spectrum of malyngamide Q.

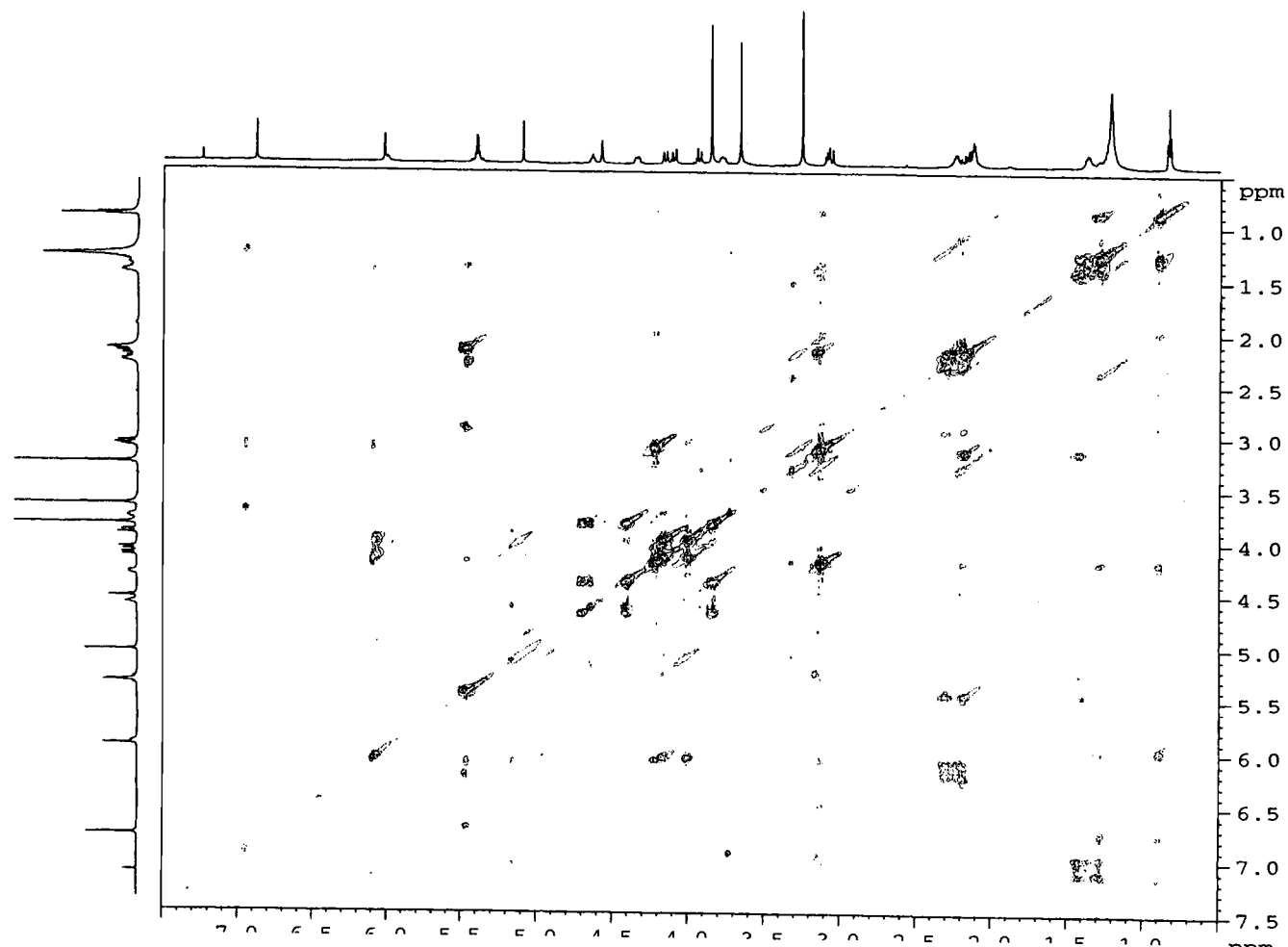


Figure IV.17.  $^1\text{H}$ - $^1\text{H}$  COSY of malyngamide Q.

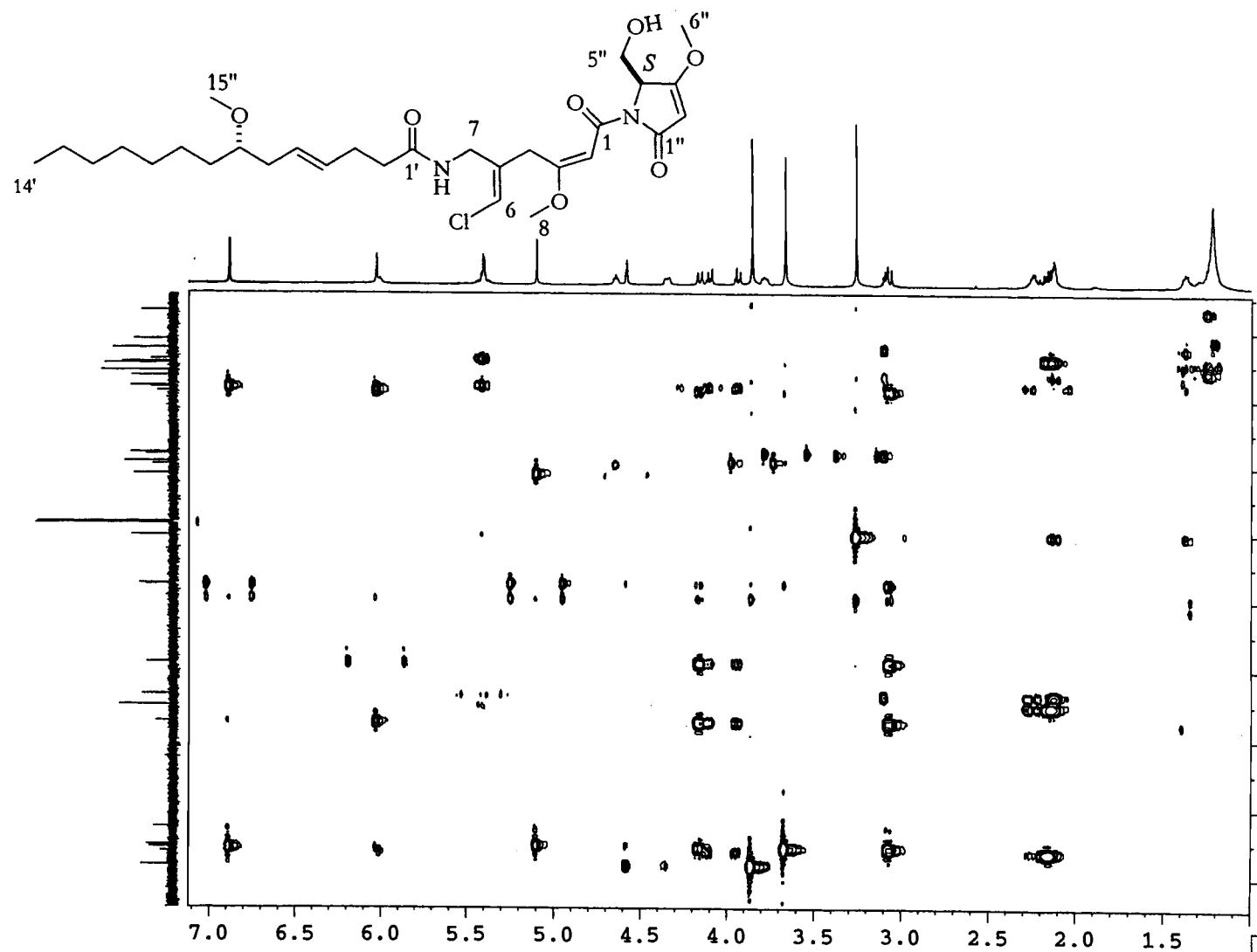


Figure IV.18. HMBC spectrum of malyngamide Q.

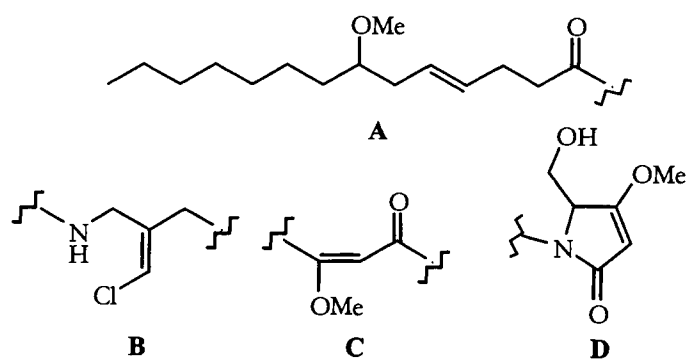


Figure IV.19. Partial Structures of Malyngamide Q (70).

chloride functionalized carbon (C-6,  $^{13}\text{C}$   $\delta$  118.28), and the methylene carbon (C-4,  $^{13}\text{C}$   $\delta$  36.55). The conjugated enone systems of fragments C and D were supported by chemical shift comparisons with the known natural product malyngamide A. This was further delineated, as seen in Figure IV.19.C, by HMBC connectivities from H-2 to C-1 ( $^{13}\text{C}$   $\delta$  165.60) and C-3 ( $^{13}\text{C}$   $\delta$  171.53), the latter of which was also attached to a methoxy group, H-8 ( $^1\text{H}$   $\delta$  3.67, HMBC from H-8 to C-3). Similarly, the pyrrolidone fragment D assignments were corroborated by HMBC correlations from H-2'' ( $^1\text{H}$   $\delta$  5.10) to C-1'' ( $^{13}\text{C}$   $\delta$  170.80), C-3'' ( $^{13}\text{C}$   $\delta$  176.66), and the methine carbon C-4'' ( $^{13}\text{C}$   $\delta$  62.35). This methine carbon (C-4'') was shown to possess a  $\text{CH}_2\text{OH}$  group ( $^{13}\text{C}$   $\delta$  59.51,  $^1\text{H}$   $\delta$  4.35 and 3.79) by DQF-COSY correlations to H-4'' (Figure IV.19.D). Summation of fragments A-D accounted for all components of the molecular formula.

Proton H-4'' of fragment D showed HMBC connectivity to C-1 of fragment C, establishing the C-1 amide bond as present in malyngamides A and B. Attachment of fragment B to C-4 was indicated by the observation of HMBC connectivities from H-2 to C-4 and H-4<sub>ab</sub> to C-3. The linking of the aliphatic chain of fragment A to the rest of the structure was supported by HMBC connectivities between the exchangeable NH proton and C-1' and long range heteronuclear coupling from H-7<sub>ab</sub> to C-1'', thus completing the planar structure of malyngamide Q.

## MALYNGAMIDE R

Modestly brine shrimp toxic ( $LD_{50} = 18.0 \mu\text{g/ml}$ ), malyngamide R (**71**) was also isolated as a pale yellow oil from the lipid extract of a Malagasy *L. majuscula*. LRFABMS (Figure IV.20) of **71** revealed an  $[M+H]^+$  ion cluster characteristic of a single chlorine atom. HRFABMS described a compound with a pseudomolecular weight ( $M+H^+$  at  $m/z$  583.3150) consistent with a molecular formula of  $[C_{30}H_{48}O_7N_2Cl]$ , again indicating eight degrees of unsaturation. The IR spectrum indicated an exchangeable proton ( $3385 \text{ cm}^{-1}$ ) and amide/ester carbonyl groups ( $1713$  and  $1630 \text{ cm}^{-1}$ ). A UV maximum was observed at 258 nm.

The  $^1\text{H}$  and  $^{13}\text{C}$  NMR (Figure IV.21-22) spectra of **71** displayed signals very closely related to **70** (see Table IV.3); however complicated by the presence of a 3:1 pair of conformers owing to an  $\text{NCH}_3$  amide moiety in **71**. As a result, proton signals were doubled for H-2, H-4, H-6, H-7, H-9 and carbons C-2, C-4, C-5, C-6, C-7, C-9, and C-1'. Despite this complexity, HMQC (Figure IV.23) and HMBC (Figure IV.24) allowed facile interpretation of these resonances and, used in conjunction with the data and structure of **70**, allowed complete structural assignment of **71** as shown.

To determine the *cis* or *trans* nature of the C-7' disubstituted olefin in the aliphatic chain a modified Bird Sandwich NMR pulse sequence was employed.<sup>97</sup> By suppressing signals arising from  $^1\text{H}$  bound to  $^{12}\text{C}$ , a 1D  $^1\text{H}$  spectrum was created which clearly allowed observation of only  $^1\text{H}$  bound to  $^{13}\text{C}$ . This greatly deconvoluted spectrum allowed measurement of the  $^3J_{\text{H4-H5}}$  to equal 15.0 Hz; and therefore in the *trans* orientation (Figure IV.25).



**Table IV.2. NMR Data for Malyngamides Q (70) and R (71).**

<b>Malyngamide Q (70)</b>			<b>Malyngamide R (71)</b>		
<b>C-atom</b>	<b><sup>1</sup>H ppm (mult, <i>J</i> in Hz)</b>	<b><sup>13</sup>C ppm</b>	<b>C-atom</b>	<b><sup>1</sup>H ppm (mult, <i>J</i> in Hz)</b>	<b><sup>13</sup>C ppm</b>
1		165.61	1		164.52
2	6.88 (s)	95.38	2	6.82 (s)	95.10
3		171.53	3		170.90
4a	3.07 (d, 14.5)	36.55	4a	2.90 (d, 14.7)	36.71
b	4.16 (dt, 14.5, 1.4)		b	4.44 (m)	
5		135.20	5		133.52
6	6.03 (s)	118.28	6	6.16 (s)	119.97
7a	3.94 (d, 14.2)	37.59	7a	3.96 (d, 13.5)	44.62
b	4.10 (d, 14.2)		b	4.53 (m)	
8	3.67 (s)	55.99	8	3.65 (s)	55.76
9	3.86 (s)	58.67	9	3.86 (s)	58.65
			10	2.82 (s)	33.88
1'		172.73	1'		173.65
2'	2.15 (m)	36.21	2' a	2.21 (m)	33.37
			b	2.29 (m)	
3'	2.24 (m)	28.35	3' a	2.16 (m)	28.12
			b	2.20 (m)	
4'	5.40 (m)	130.58	4'	5.41 (m)	130.80
5'	5.40 (m)	127.33	5'	5.41 (m)	127.37
6'	2.13 (m)	36.25	6' a	2.12 (m)	36.98
			b	2.17 (m)	
7'	3.10 (ddd, 11.5, 12.0, 6.0)	80.62	7'	3.10 (m)	80.76
8'	1.37 (m)	33.24	8'	1.39 (m)	33.39
9' a	1.23 (m)	25.29	9' a	1.24 (m)	25.33
b	1.29 (m)		b	1.32 (m)	
10'	1.22 (m)	29.68	10' a	1.24 (m)	29.58
			b	1.32 (m)	
11'	1.22 (m)	29.25	11'	1.24 (m)	31.86
12'	1.23 (m)	22.60	12'	1.25 (m)	22.72
13'	1.25 (m)	31.77	13'	1.24 (m)	31.84
14'	0.84 (t, 7.0)	14.06	14'	0.85 (s)	14.18
15'	3.26 (s)	56.40	15'	3.29 (s)	56.29
1''		170.80	1''		171.03
2''	5.10 (s)	95.11	2''	5.09 (s)	95.09
3''		176.66	3''		176.98
4''	4.58 (t, 2.4)	62.35	4''	4.56 (m)	62.52
5'' a	3.79 (m)	59.51	5'' a	3.80 (m)	59.16
b	4.35 (m)		b	4.46 (m)	
NH	6.01 (dd, 6.5)				
OH	4.64 (dd, 6.5)		OH	4.65 (bs)	

<sup>1</sup>H shifts referenced to residual CHCl<sub>3</sub> (δ 7.27)<sup>13</sup>C chemical referenced to CDCl<sub>3</sub> (δ 77.00)

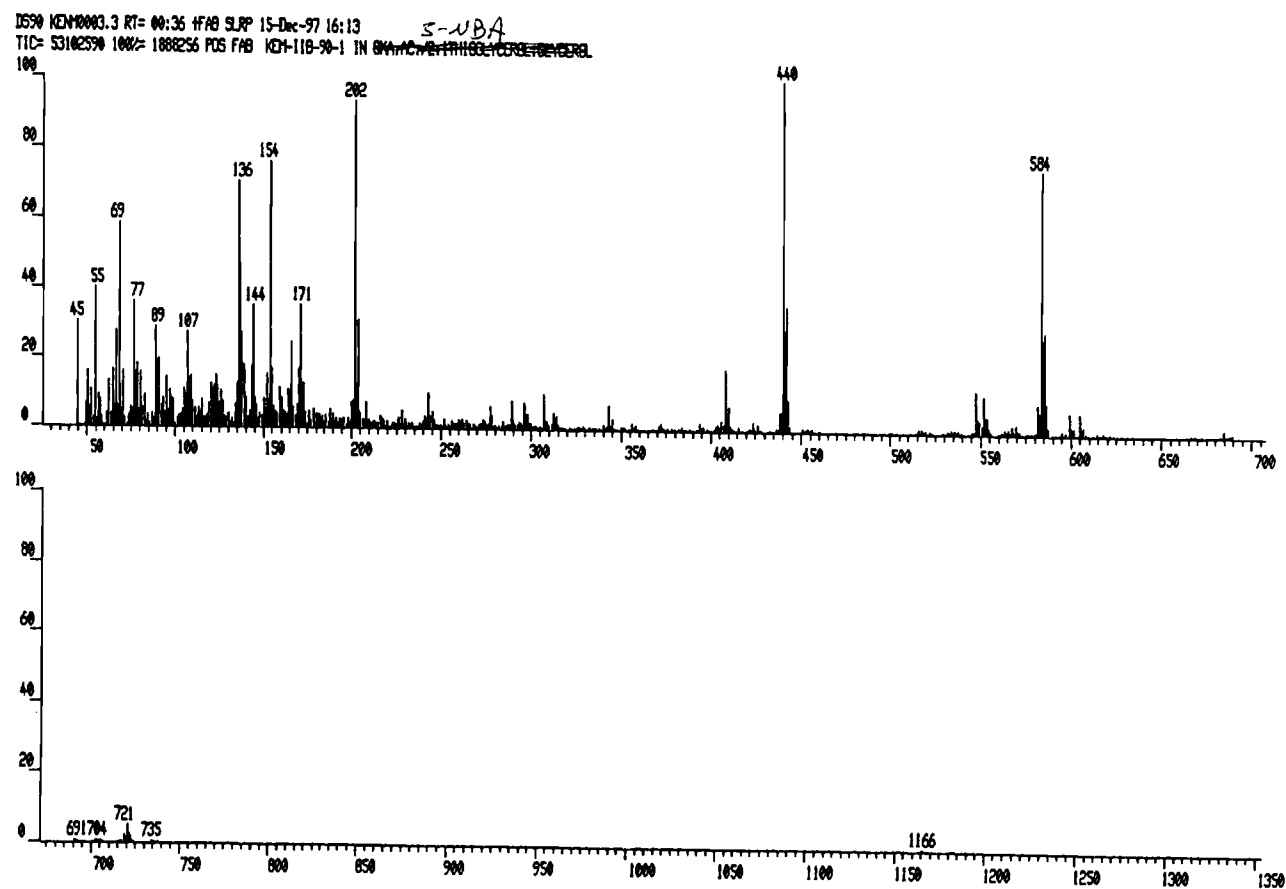


Figure IV.20. LRFABMS of malyngamide R.

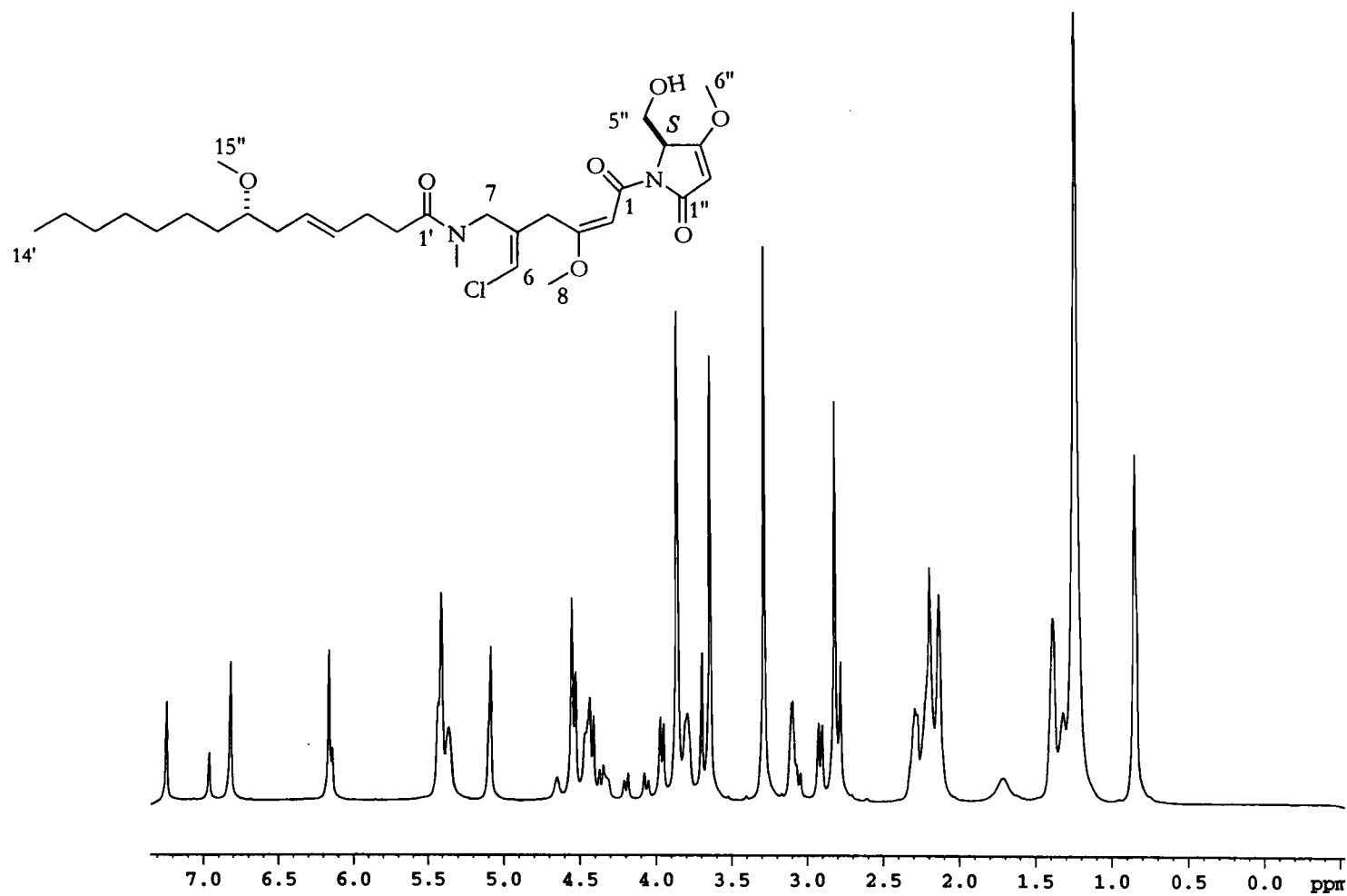


Figure IV.21.  $^1\text{H}$  NMR spectrum of malyngamide R.

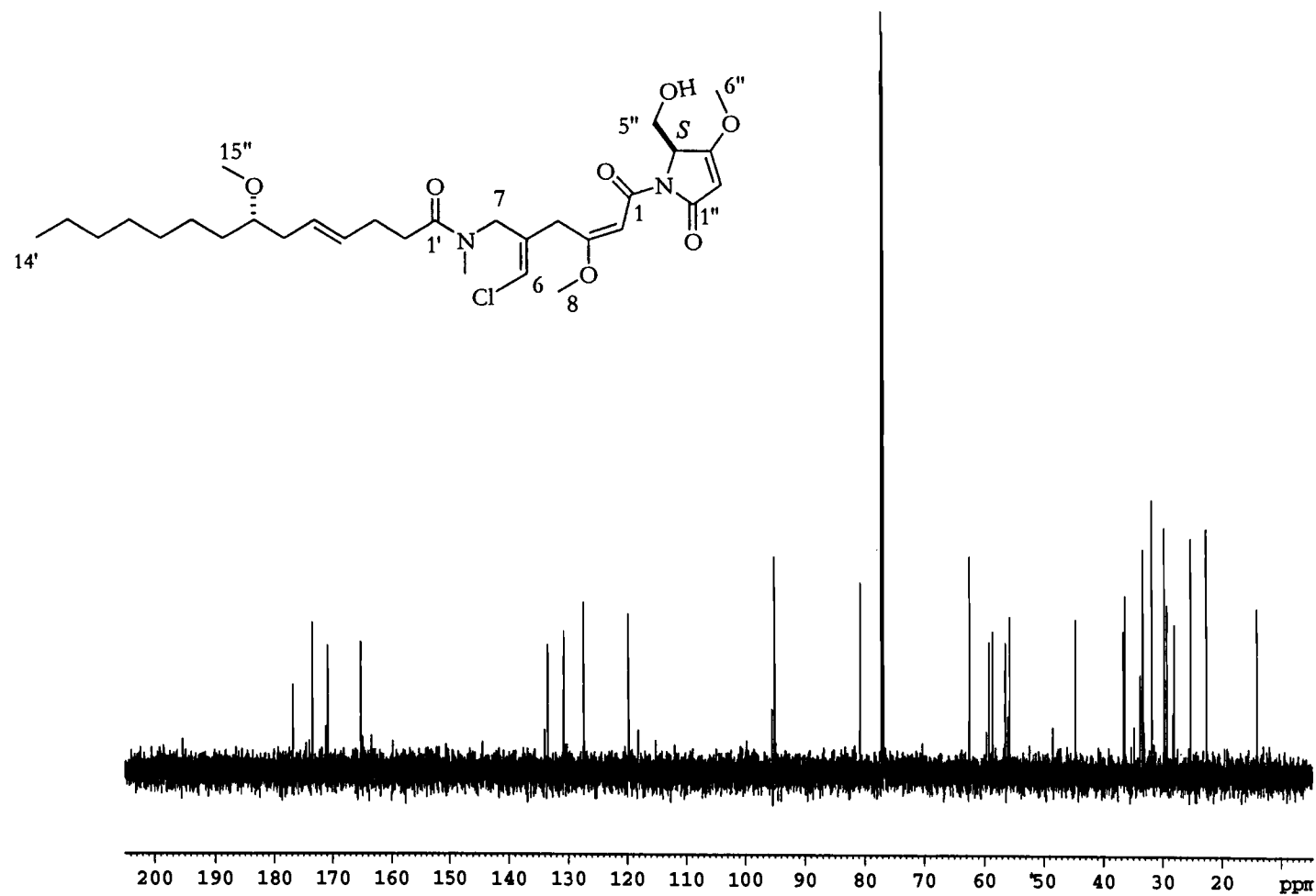


Figure IV.22.  $^{13}\text{C}$  NMR spectrum of malyngamide R.

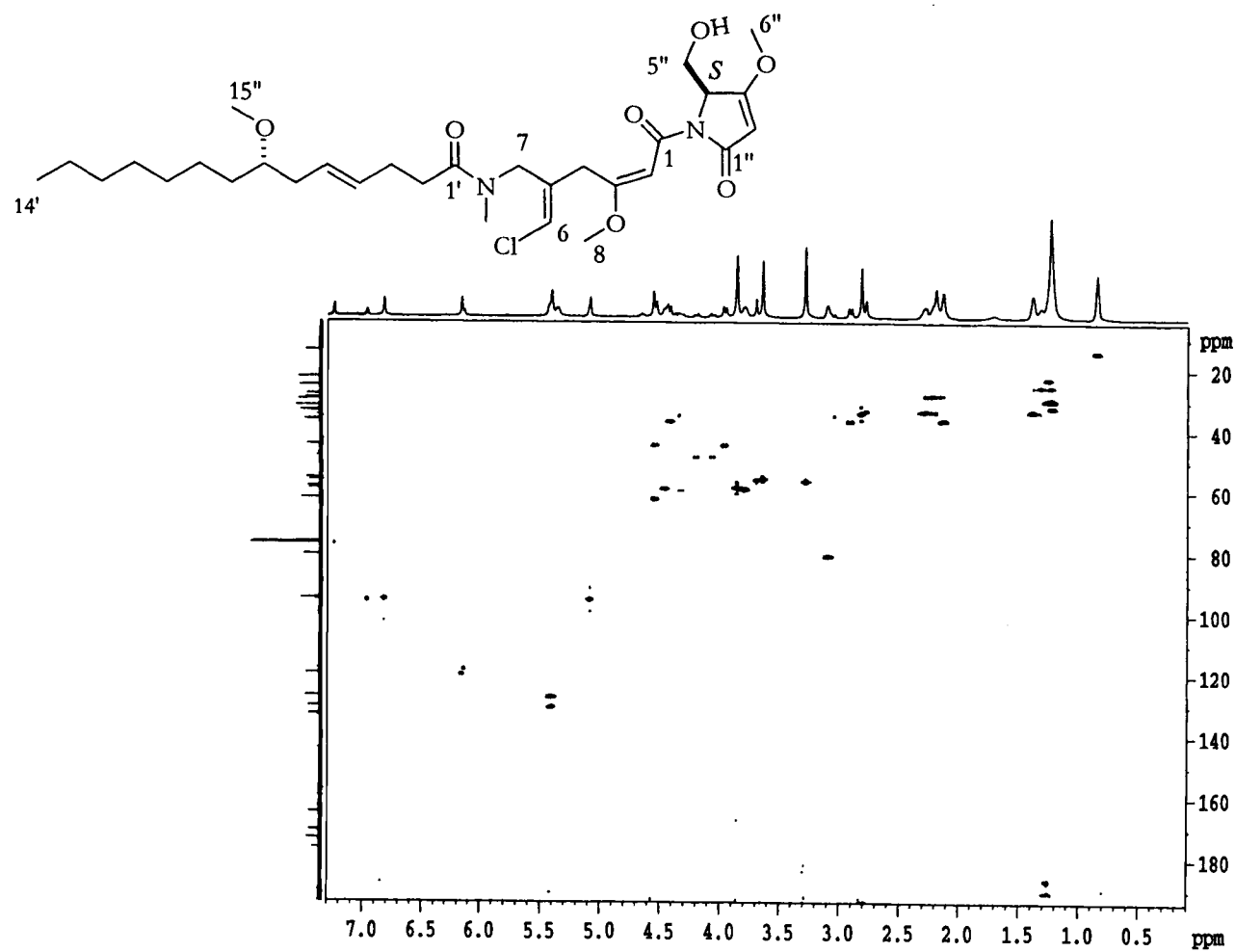


Figure IV.23. HMQC spectrum of malyngamide R.

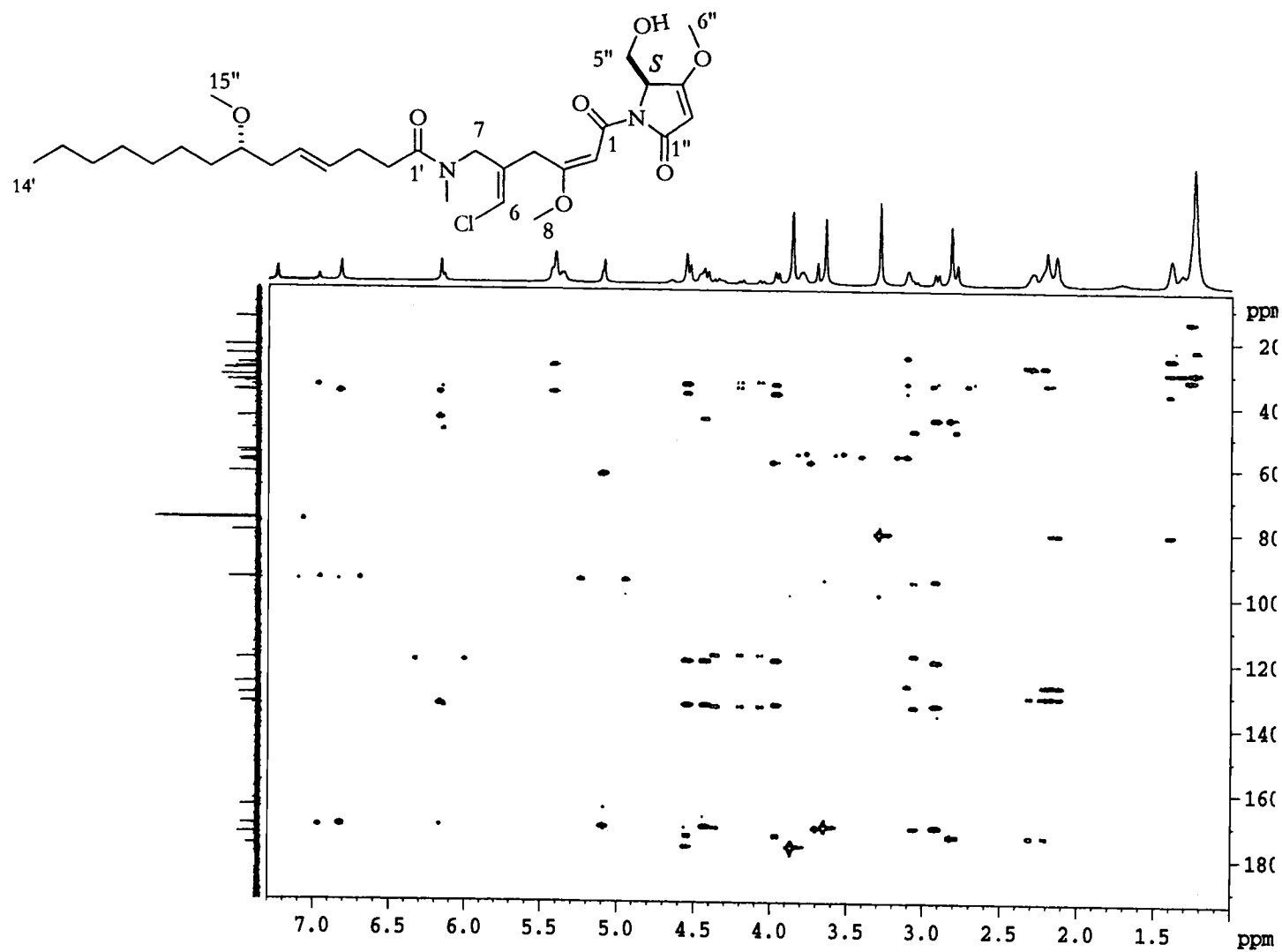
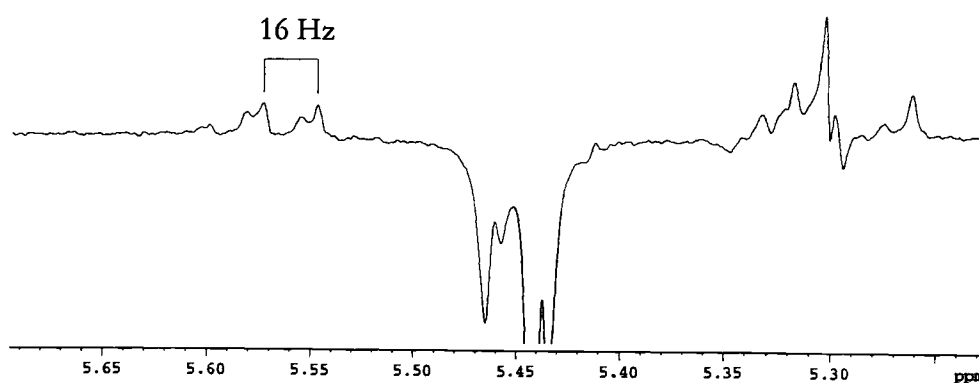
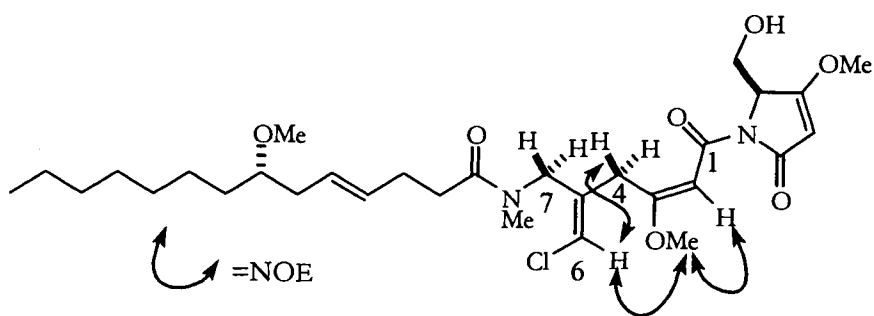


Figure IV.24. HMBC spectrum of malyngamide R.



**Figure IV.25.** Suppression of signals arising from  $^1\text{H}$ - $^{12}\text{C}$  by Bird Sandwich NMR pulse sequence allowing observation of  $^3J_{\text{H}4'\text{-H}5'}\text{H}$ - $^{13}\text{C}$  coupling = 16 Hz, and therefore defining the C4'-C5' olefin as *trans*.



**Figure IV.26.** Malyngamide R (71) with important NOE correlations shown.

Investigation of the geometry of the C5-C6 olefin in **71**, as well as of the acyclic methoxy enone, was accomplished utilizing DPGFSE 1D NOE (Figure IV.26).<sup>98</sup> NOE correlations were seen from H-2 to the protons of the adjacent OMe (H-8), thus defining the C2-C3 olefin to possess an *E* conformation (Figure IV.26-27). Through space interactions were also observed between H-6 and H-4<sub>a</sub> and H-6 and H<sub>3</sub>-8. Correlations were not perceived between H-7<sub>a,b</sub> and H-6, nor between the NCH<sub>3</sub> protons (H-10) and H-6. Malynamide Q (**70**) shared these correlations with the exception that it does not contain an NCH<sub>3</sub> group. From this data we deduced a *Z* stereochemistry in **70** and **71**. This differs from that reported for malynamide A (**66**), which possesses an *E* olefin at this position, as revealed by NOE between the NCH<sub>3</sub> functionality and the vinyl proton.<sup>81</sup>

Because of the unprecedented *Z* geometry of C5-C6 in **71**, we sought to confirm this result through the use of <sup>1</sup>H-<sup>13</sup>C long-range heteronuclear coupling constants. In the past, these coupling constants were difficult to obtain on small samples for a variety of reasons.<sup>99</sup> One approach using a PFG-HMBC experiment with gradient ratios of 5:3:4 selects only the N-type coherence pathways, thereby precluding the acquisition of phase sensitive data with pure absorption lineshapes. Another general difficulty is the mixed phase lineshape resulting from the evolution of <sup>1</sup>H-<sup>1</sup>H couplings during the long delay required for <sup>1</sup>H-<sup>13</sup>C heteronuclear couplings to emanate in HMBC also demands a magnitude mode presentation of the spectra, which results in poor resolution. Because of this lack of pure absorption lineshape, the two most popular ways to obtain long-range coupling constants from HMBC spectra



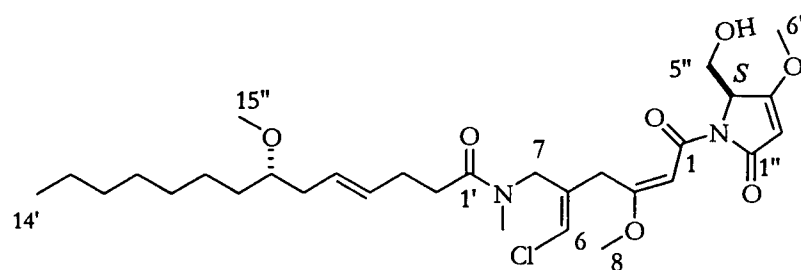
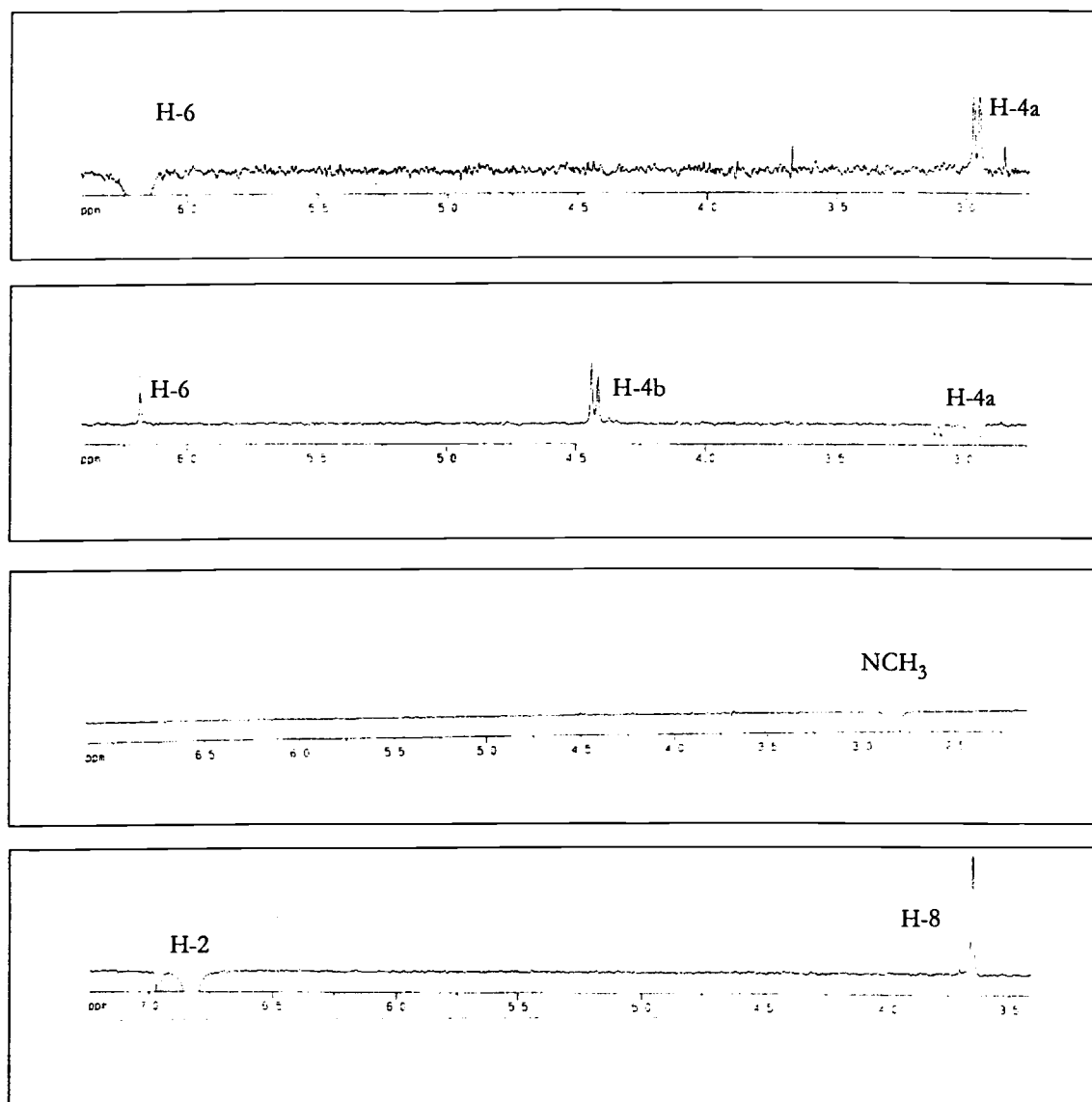


Figure IV.27 HMBC spectrum of malyngamide R.

require the acquisition of a separate reference spectrum and the utilization of an elaborate peak fitting routine; or the acquisition of several HMBC experiments with differing delays for the evolution of long-range coupling and subsequent analysis of the peak intensities for each individual correlation.<sup>100,101</sup> To simplify the detection and measurement of these couplings, an extremely useful new pulse sequence based on the well known HSQC sequence, which provides pure absorption lineshapes and eliminates the phasing problems associated with the evolution of  $^1\text{H}$ - $^1\text{H}$  couplings during the pulse sequence, was developed by Dr. R. Thomas Williamson and Dr. Brian L. Marquez.<sup>99</sup> This method is similar to that presented by Sklenar and coworkers but requires fewer gradient pulses and can be set up with only simple modifications to existing HSQC pulse sequences.<sup>99,102</sup> Using the HSQMBC pulse sequence on malyngamide R, we observed a 7.1 Hz  $^3\text{J}$  coupling from H-6 to C-7 and a 4.7 Hz  $^3\text{J}$  coupling from H-6 to C-4. These coupling constants, obtained directly from the HSQMBC (Figure IV.28) spectrum, were identical to those calculated by the procedure described by Titman and Keeler for the quantitative analysis of coupling constants (data not shown),<sup>101</sup> and unambiguously verified our observations concerning the geometry of C-6, thus indicating that the inherently narrow lineshape of our experiment makes it possible to record accurate heteronuclear coupling constants taken directly from slices along the  $F_2$  dimension, logically excepting the case of exceedingly small couplings.

With the availability of this new methodology for the determination of the  $^1\text{H}$ - $^{13}\text{C}$  heteronuclear coupling constants, we verified the geometry of comparable olefins in two additional malyngamides available from our repository of pure compounds.

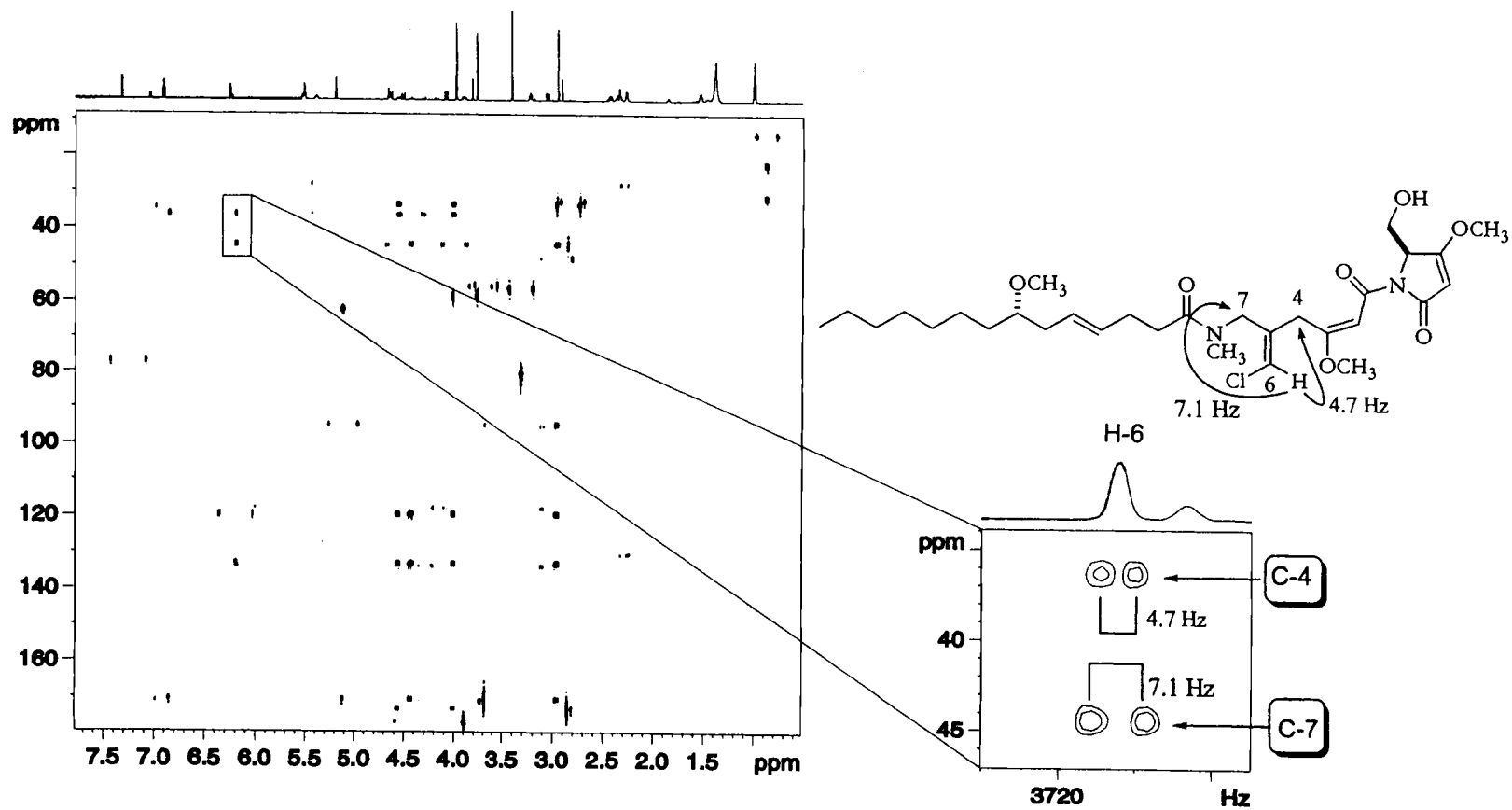
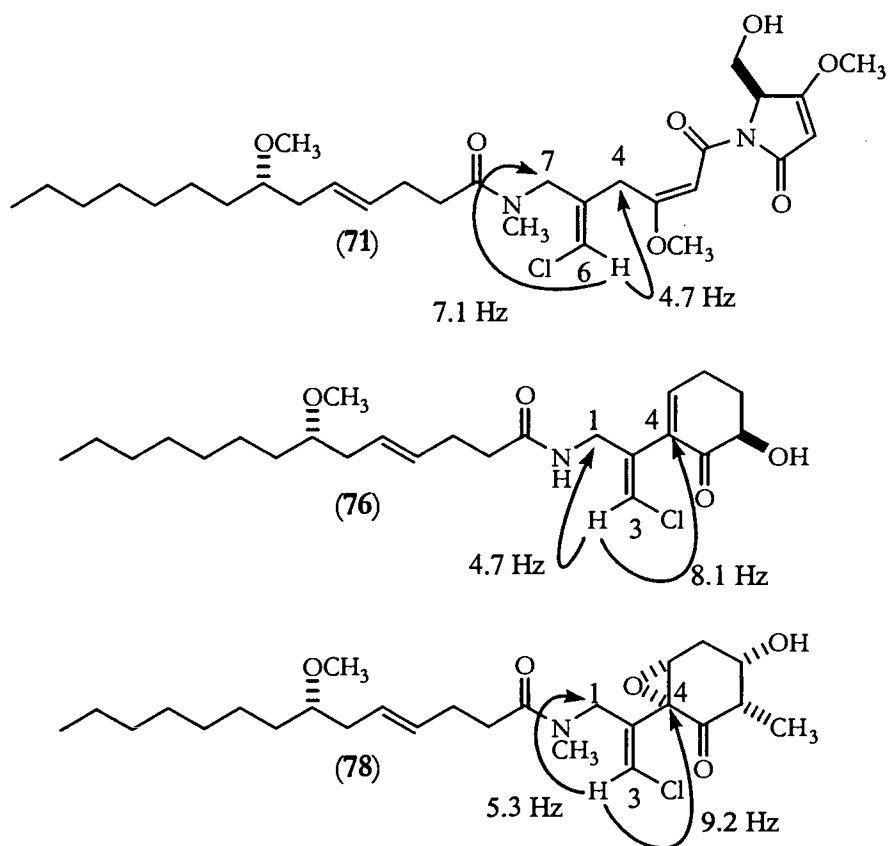


Figure IV.28. HSQMBC spectra highlighting the long range heteronuclear coupling between H-6 and C-4 & 7 of malyngamide R.

When the new pulse sequence was applied to malyngamides F (76) and I (78), the reported *E* geometry was supported (Figure IV.29). That is, the configuration about this  $sp^2$  center is opposite that of the geometry determined for malyngamides Q and R. The methods which we used to define the above stereochemical questions in 70 and 71 exemplify the power of NMR to elucidate molecular subtleties in a non-degradative fashion. This alternate geometrical stereochemistry has subsequently been observed in iso-malyngamides A (68) and B (69) and malyngamides O (88) and P (89).<sup>83</sup>

To elucidate the chirality at the stereogenic C-4'' carbon, we utilized GCMS analysis, employing a chiral column, the two enantiomers of serine methyl ester, and methods commonly used for stereochemical investigations of peptides.<sup>103</sup> By sequentially subjecting malyngamide R to ozonolysis, hydrolysis, and derivatization, we were able to create the pentafluoropropyl serine methyl ester (PFPSME) from C3'-C5'. This PFPSME derivative obtained from malyngamide R coeluted with the similarly derivatized *L*-serine methyl ester standard (16.32 min), displaying a difference in retention time of 0.49 min as compared to the elution of derivitized *D*-serine methyl ester (16.81 min). Thus, the stereochemistry of C-4'' in malyngamide R is defined as *S*.

Definition of the stereochemistry of C-7' of the fatty acid chain was implied by the isolation and investigation of the co-occurring methoxylated free fatty acid. Malyngamides Q and R shared proton resonances with the co-occurring methoxy fatty acid. Also, the methoxy fatty acid displayed an optical rotation ( $[\alpha]_D^{25} = -8.3$ ,  $\text{CH}_2\text{Cl}_2$ ,  $c = 0.8$ ) similar to that reported for malyngamide A ( $[\alpha]_D^{25} = -6.5$ ,  $\text{CH}_2\text{Cl}_2$ ,  $c = 0.8$ ).<sup>81</sup> Precedence for *S* configuration of this stereocenter in all reported



**Figure IV.29.** HSQMB C Correlations for malyn gamide R (71), F (76), and I (78), confirming the geometry of the exomethylene functionalized by a vinyl chloride.

malyngamides, corroborating  $^1\text{H}$  NMR spectra of both **70** and **71** and the co-occurring methoxylated free fatty acid, and the comparable optical rotation of the free fatty acid and malyngamide A suggest that C-7'' also exists in the *S* configuration for malyngamides Q and R.

## EXPERIMENTAL

### GENERAL EXPERIMENTAL PROCEDURES

NMR spectra were recorded on a Bruker DRX 600, AM 400, and ACP 300 NMR spectrometers. Mass spectra were recorded on a Kratos MS50TC mass spectrometer. UV spectra were recorded on a Hewlett Packard 8452A UV/*vis* spectrophotometer while FT-IR spectra were recorded on a Nicolet 510 spectrophotometer. Chiral GCMS analysis was accomplished on a Hewlett Packard Gas Chromatograph 5890 Series II with a Hewlett Packard 5971 Mass Selective Detector, using an Alltech Capillary Column (CHIRASIL-VAL Phase 25 m x 0.25 mm). HPLC separation was accomplished with a Waters M-6000A pump, a Rheodyne 7010 injector, and a Waters Lambda-Max 480 spectrophotometer. Optical rotation measurements were recorded on a Perkin-Elmer Model 141 polarimeter.

### COLLECTION

Malyngamide L was extracted from a Curaçao collection of *L. majuscula* collected by hand (0.5 m) on Aug 9, 1994 from Santa Barbara Beach, Curaçao, and stored in IPA at  $-20^{\circ}\text{C}$  until workup. A voucher sample is available from WHG as collection number NSB-4 AUG 94-3.

Yielding malyngamides Q and R, the marine cyanobacterium, *Lyngbya majuscula*, was collected by hand from shallow water (2 m) on Apr 8, 1997 at San Christí Island, Madagascar ( $48^{\circ}9'\text{E}$   $13^{\circ}18'\text{S}$ ), and stored at  $-20^{\circ}\text{C}$  in IPA until workup. A voucher sample is available from WHG as collection number MNS-8 APR 97-2.

# EXTRACTION AND ISOLATION OF MALYNGAMIDE L, Q, AND R

The defrosted alga was homogenized in  $\text{CH}_2\text{Cl}_2/\text{MeOH}$  (2:1 v/v) and extracted two times to give a crude extract of 1.08 g. This was sequentially fractionated using VLC (1% to 100% EtOAc in hexanes (v/v), Sephadex LH-20 column chromatography (50% MeOH/MeOH, v/v), and Si gel column chromatography (80% EtOAc/hexanes, v/v). Final purification was obtained using HPLC (256 x 4.6 mm Alltech Lichrosorb Diol column, 10  $\mu$ ; 0.5 MeOH/1.5 EtOAc/8.0 hexanes) to yield pure malyngamide L (0.0039 g; 0.36% of total extract).

The IPA preserved alga (16.1 g dry wt) was extracted with  $\text{CH}_2\text{Cl}_2/\text{MeOH}$  (2:1) two times to give a crude extract of 0.75 g. A portion of this (0.70 g) was fractionated using vacuum liquid chromatography (VLC) on Si gel with a stepwise gradient of hexanes/EtOAc and EtOAc/MeOH to give nine fractions. Because fractions seven and eight (eluted 70%-100% hexanes/EtOAc) both contained **70** and **71**, they were recombined and subjected to reversed phase chromatography using an RP-18 Waters Sep-Pak (85% MeOH/ $\text{H}_2\text{O}$ ) and then RP-HPLC (ODS) in 80% MeOH/ $\text{H}_2\text{O}$  to yield pure **70** (0.032 g, 4.6% of total extract) and **71** (0.0091 g, 1.3% of total extract).

## MALYNGAMIDE L (**80**)

Pure malyngamide L showed  $[\alpha]_D^{25} +17$  (EtOH,  $c$  0.1); UV  $\lambda_{\text{max}}$  (MeOH) 206 nm ( $\log \epsilon = 4.49$ ); IR  $\nu_{\text{max}}$  (film) 3416, 2921, 2854, 1680, 1619, 1457, 1090  $\text{cm}^{-1}$ ; FABMS [0.1 N oxalic acid in thioglycerol:glycerol (2:1)] obs.  $m/z$   $[\text{M}+\text{H}]^+$  (rel int) 468



(100), 452 (10), 418 (7), 236 (20), 230 (75), 199 (40), 145 (28); HREIMS obs.  $[M-Cl]^+$  at  $m/z$  432.3096 for  $C_{26}H_{42}O_4N$  ( $\Delta$  1.7 mmu);  $^1H$  and  $^{13}C$  data see Table IV.1.

#### MALYNGAMIDE Q (70)

Pure malyngamide Q showed  $[\alpha]_D^{25} +2$  (MeOH,  $c$  0.8); UV  $\lambda_{max}$  (MeOH) 264 nm ( $\log \epsilon = 4.18$ ); IR  $\nu_{max}$  (film) 3313, 2925, 2848, 1713, 1630, 1451, 1397, 1319, 1248, 1206, 1164, 1069, 961, 854, 776  $cm^{-1}$ ; FABMS (3-NBA) obs.  $m/z$  (rel int) 569 (60), 537 (80), 507 (25), 426 (55), 395 (70); HRFABMS (3-NBA) obs.  $[M+H]^+$   $m/z$  569.3053 for  $C_{29}H_{45}O_7N_2Cl$  ( $\Delta$  -5.9 mmu); obs.  $[M-CH_4O]^+$  at  $m/z$  537.2731 for  $C_{28}H_{41}O_6N_2Cl$  ( $\Delta$  0.0 mmu);  $^1H$  and  $^{13}C$  NMR data see Table IV.2.

#### MALYNGAMIDE R (71)

Pure malyngamide R showed  $[\alpha]_D^{25} +2$  (MeOH,  $c$  0.9); UV  $\lambda_{max}$  (MeOH) 258 nm ( $\log \epsilon = 4.18$ ); IR  $\nu_{max}$  (film) 3385, 2913, 2854, 1713, 1630, 1451, 1385, 1319, 1242, 1200, 1158, 1069, 997, 848, 770  $cm^{-1}$ ; FABMS (3-NBA)  $m/z$  (rel int) 583 (70), 440 (100), 202 (90), 171 (35); HRFABMS (3-NBA) obs.  $[M+H]^+$  at  $m/z$  583.3150 for  $C_{30}H_{47}O_7N_2Cl$  ( $\Delta$  0.0 mmu);  $^1H$  and  $^{13}C$  data see Table IV.2.

#### CHIRAL ANALYSIS OF MALYNGAMIDE R (71)

Malyngamide R was ozonized (1.0 mg 71 in 1.0 ml  $CH_2Cl_2$ , 3 min). The ozonate was immediately dried *in vacuo*, and to this vial 1 ml of 6 N HCl was added and heated in an oven at 110°C for 18 hrs. The hydrolysate was dried under a

constant stream of nitrogen and derivatized using an Alltech PFA-IPA Amino Acid Kit (#18093). The dried hydrolysate was treated with 0.2 N HCl for five minutes at 110°C, then dried under a constant stream of nitrogen. To this vial, 150 µl of acetyl chloride and 500 µl of IPA were added, then the vial was heated for 45 min at 110°C. After drying with a constant stream of nitrogen, the derivatizing agent, pentafluoropropyl isopropionic acid (1 ml in 2 ml CH<sub>2</sub>Cl<sub>2</sub>) was added. The vial was heated to 115°C for 15 min then blown dry with nitrogen. The derivitized product was then solubilized in hexanes. To be used as standards, 1 mg of each of the serine methyl ester enantiomers (*L* and *D*) was weighed into a tared vial and subjected to the identical derivatization sequence as the ozonized hydrolysate of **71**, as detailed above. All samples were gas chromatographed under identical conditions, beginning with a sustained initial oven temperature of 50°C (4 min), a 3°C/min ramp from 50°C to 150°C was followed by a 20°C/min ramp from 150°C to 180°C. The derivitized malyngamide **R** eluted at 16.32 min, as did the derivitized standard *L*-serine methyl ester. The derivitized *D*-serine methyl ester was detected at 16.81 min.

#### BRINE SHRIMP TOXICITY BIOASSAY

Evaluation for brine shrimp toxicity was performed as previously described.<sup>104</sup> using *Artemia salina* as the test organism. After a 24 hr hatching period, aliquots of a 10 mg/ml stock solution of **71** were added to test wells containing 5 ml of artificial seawater and brine shrimp to achieve a range of final concentrations from 0.05-100 ppm. After 24 h the live and dead shrimp were tallied.

#### ICTHYOTOXICITY BIOASSAY

Using *Carassius auratus* (goldfish) as the test organism, the ichthyotoxic potential of our samples were assessed as previously described.<sup>105</sup> Aliquots of a 10 mg/ml stock solution of our samples (in EtOH) were added to 50 ml beakers containing 40 ml of distilled H<sub>2</sub>O to achieve a range of final concentrations from 1-100 ppm. A single test organism was added to each beaker. The experiments were concluded upon death of test organism (floating on surface and lack of respiratory function) or at 1 hr, with 15 min observation intervals.

## REFERENCES

81. Cardellina, J.H.; Marner F.J.; Moore R.E. *J. Am. Chem. Soc.* **1979**, *101*, 240-242.
82. Cardellina, J.H.; Dalietos, D.; Marner, F.J.; Mynderse, J.S.; Moore, R.E. *Phytochemistry* **1978**, *17*, 2091-2095.
83. Kan, Y.; Sakamoto, B.; Fujita, T.; Nagai, H. *J. Nat. Prod.* **2000**, *63*, 1599-1602.
84. Ainslie, R.D.; Barchi, J.J.; Kuniyoshi, M.; Moore, R.E.; Mynderse, J.S. *J. Org. Chem.* **1985**, *50*, 2859-2862.
85. Mynderse, J.S.; Moore, R.E. *J. Org. Chem.* **1978**, *43*, 4359-4362.
86. Gerwick, W.H.; Reyes, S.; Alvarado, B. *Phytochemistry* **1987**, *26*, 1701-1704.
87. Praud, A.; Valls, R.; Banaigs, B. *Tetrahedron Lett.* **1993**, *34*, 5437-5440.
88. Orjala J.; Nagle, D.G.; Gerwick, W.H. *J. Nat. Prod.*, **1995**, *58*:5, 764-768.
89. Todd, J.S.; Gerwick, W.H. *Tetrahedron Lett.*, **1995**, *36*:43, 7837-7840.
90. Wu, M.; Milligan, K.E.; Gerwick, W.H. *Tetrahedron*, **1997**, *53*:47, 15983-15990.
91. Kan, Y.; Fujita, T.; Nagai, H.; Sakamoto, B.; Hokama, Y. *J. Nat. Prod.* **1998**, *61*, 152-155.
92. Gallimore, W.A.; Galaro, D.L.; Lacy, C.; Zhu, Y.; Scheuer, P.J. *J. Nat. Prod.* **2000**, *63*, 1022-1024.
93. Milligan, K.E.; Marquez, B.L.; Williamson, R.T.; Davies-Coleman, M.; Gerwick, W.H. *J. Nat. Prod.* **2000**, *63*, 965-968.
94. Nogle, L.M.; Gerwick, W.H. Manuscript in preparation.
95. Wan, F.; Erickson, K.L. *J. Nat. Prod.* **2001**, *64*, 143-146.
96. Marquez, B.L.; Nogle, L.M.; Williamson, R.T.; Gerwick, W.H. *J. Nat. Prod.* in press.
97. Williamson R.T.; Carney, J.R. and Gerwick, W. H. *J. Nat. Prod.*, (Submitted).
98. Stott, K.; Keeler, J.; Van, Q.N.; Shaka, A.J. *J. Mag. Reson.*, **1997**, *125*, 302-324.

99. Williamson, R.T.; Marquez, B.L.; Kover, K.E.; Gerwick, W.H. *Magn. Reson. Chem.*, **2000**, *38*, 265-273.
100. Willker, W.; Leibfritz, D. *J. Mag. Reson.*, **1995**, *33*, 632.
101. Titman, J.T.; Neuhaus, D.; Keeler, J. *J. Mag. Reson.*, **1989**, *85*, 111-131
102. Marek, R.; Kralik, L.; Sklenar, V. *Tetrahedron Lett.*, **1997**, *38*, 665-668.
103. McDonald, L.A.; Ireland, C.M. *J. Nat. Prod.*, **1992**, *55*:3, 376-379.
104. Meyer, B.N.; Ferrigni, N.R.; Putnam, J.E.; Jacobsen, L.B.; Nichols, D.E.; McLaughlin J.L. *Planta Medica*, **1982**, *45*, 31-34.
105. Bakus, G.J.; Green, G. *Science* **1974**, *185*, 951-953.

## CHAPTER V.

THE ISOLATION AND STRUCTURE ELUCIDATION OF LYNGBYABELLIN B  
AND TORTUGIN: SUPPORT FOR THE CYANOBACTERIAL ORIGIN OF  
SEVERAL MOLLUSCAN CYCLIC DEPSIPEPTIDES

## ABSTRACT

The lipid extract of a *Lyngbya majuscula* collected from the Dry Tortugas, Florida has yielded lyngbyabellin B and tortugin, new biologically active cyclic depsipeptides. Lyngbyabellin B resembles dolabellin, originally derived from the sea hare *Dolabella auricularia*, and lyngbyabellin A, recently isolated from *L. majuscula*. Tortugin is most closely related to the molluscan derived onchidins A and B, kulolide, and kulokainalide-1 and also to the *L. majuscula* derived yanucamides A and B. The discovery of these compounds from a cyanobacterial source further supports cyanobacteria as the primary producers of many secondary metabolites previously attributed to invertebrate *de novo* biosynthesis. Isolation of these metabolites was carried out through preparative liquid chromatography with final purification by repetitive reversed phase HPLC. Structure elucidation was accomplished utilizing 1D and 2D NMR spectroscopic characterization. Chiral analysis of both compounds was accomplished through chiral GC/MS derivatization techniques, Marfey's analysis, and semi-synthesis/menthyl carbonyl chloride (MCC) derivatization.

## INTRODUCTION

Cyanobacteria are phenomenal producers of structurally-intriguing and biologically-active secondary metabolites. Recently, cyclic depsipeptides, many incorporating unusual appendages and presumably arising from the NRPS biosynthetic pathway, have become a dominant theme in cyanobacterial natural products literature. Notable biological activities have been observed for many of these, including antifungal (hormothamnin A, **93**),<sup>106</sup> neurotoxic (antillatoxin, **94**),<sup>107</sup> and antiproliferative [cryptophycin-1 (**23**) and 52 (**24**),<sup>29</sup> lyngbyabellins (**95** & **96**),<sup>108-110</sup> hectochlorin(**97**)<sup>111</sup>] activities (Figure V.1).

Products of the NRPS pathway, common in bacteria and fungi, have been discovered in the marine environment from organisms such as tunicates,<sup>112</sup> sponges,<sup>113</sup> and molluscs.<sup>114</sup> The isolation of yanucamide A (**98**) and B (**99**),<sup>115</sup> lyngbyabellin A (**95**)<sup>108</sup> and B (**96**),<sup>109,110</sup> georgamide (**100**),<sup>116</sup> **23** and **24**, **97**, tortugin (**101**),<sup>117</sup> and carliamide (**102**)<sup>123</sup> from cyanobacterial sources has displayed their ability to utilize this pathway as well (Figure V.1). Such findings have contributed to the debate over the organism responsible for *de novo* synthesis of many marine natural products.

Certain structural motifs, previously derived solely from molluscan secondary metabolite studies, have begun to appear as hallmarks of cyanobacterial biosynthesis, such as the incorporation of  $\beta$ -amino acids,  $\beta$ -hydroxy acids, and unusual amino acid-like residues.<sup>33</sup> As many gastropods (molluscs) are herbivorous grazers, it is conceivable that cyanobacteria would be ingested by the mollusc and the secondary metabolites sequestered (and potentially subjected to biotransformation) by the predator. Cyanobacterial compounds could then proceed further up the food chain

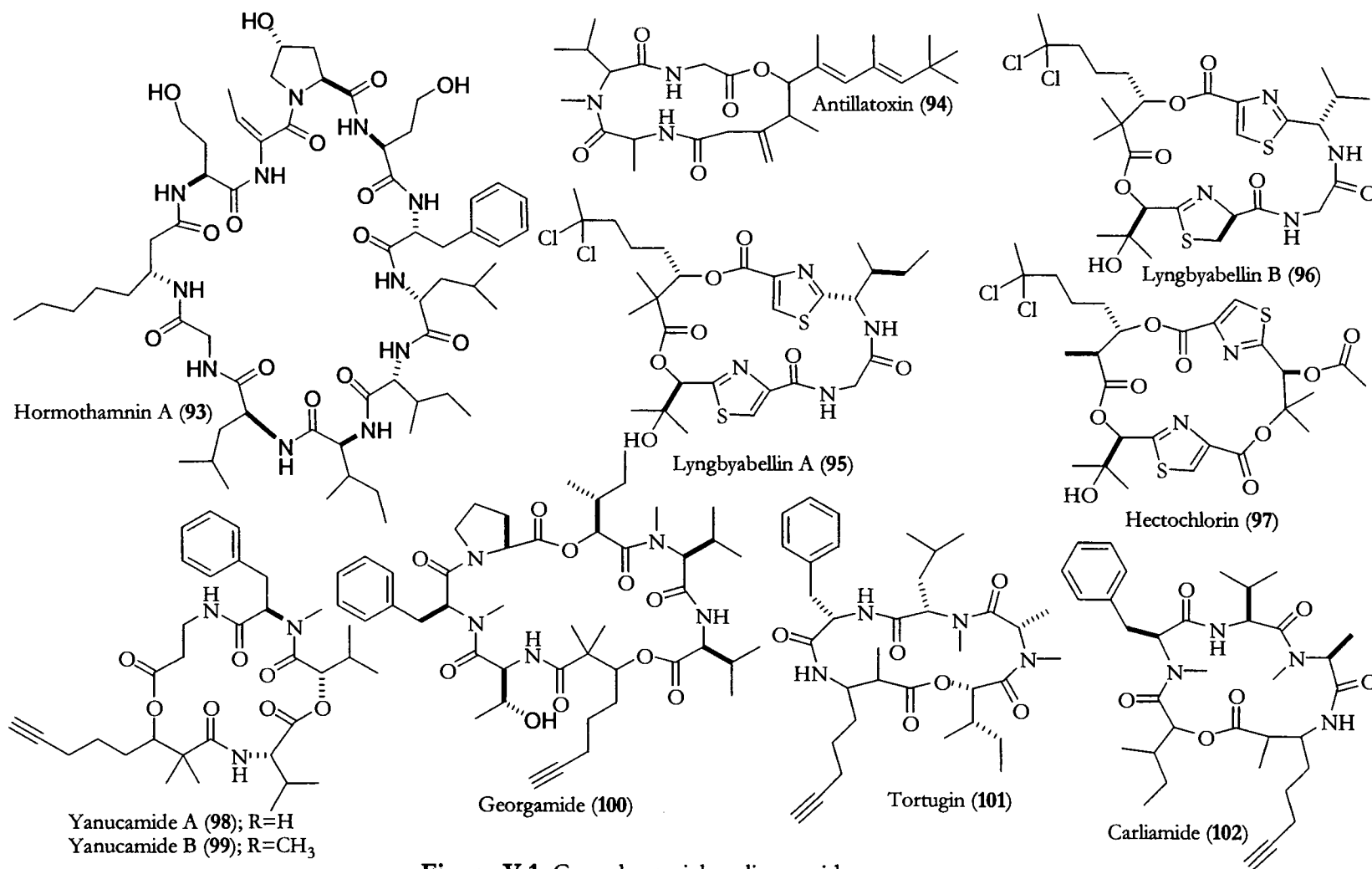
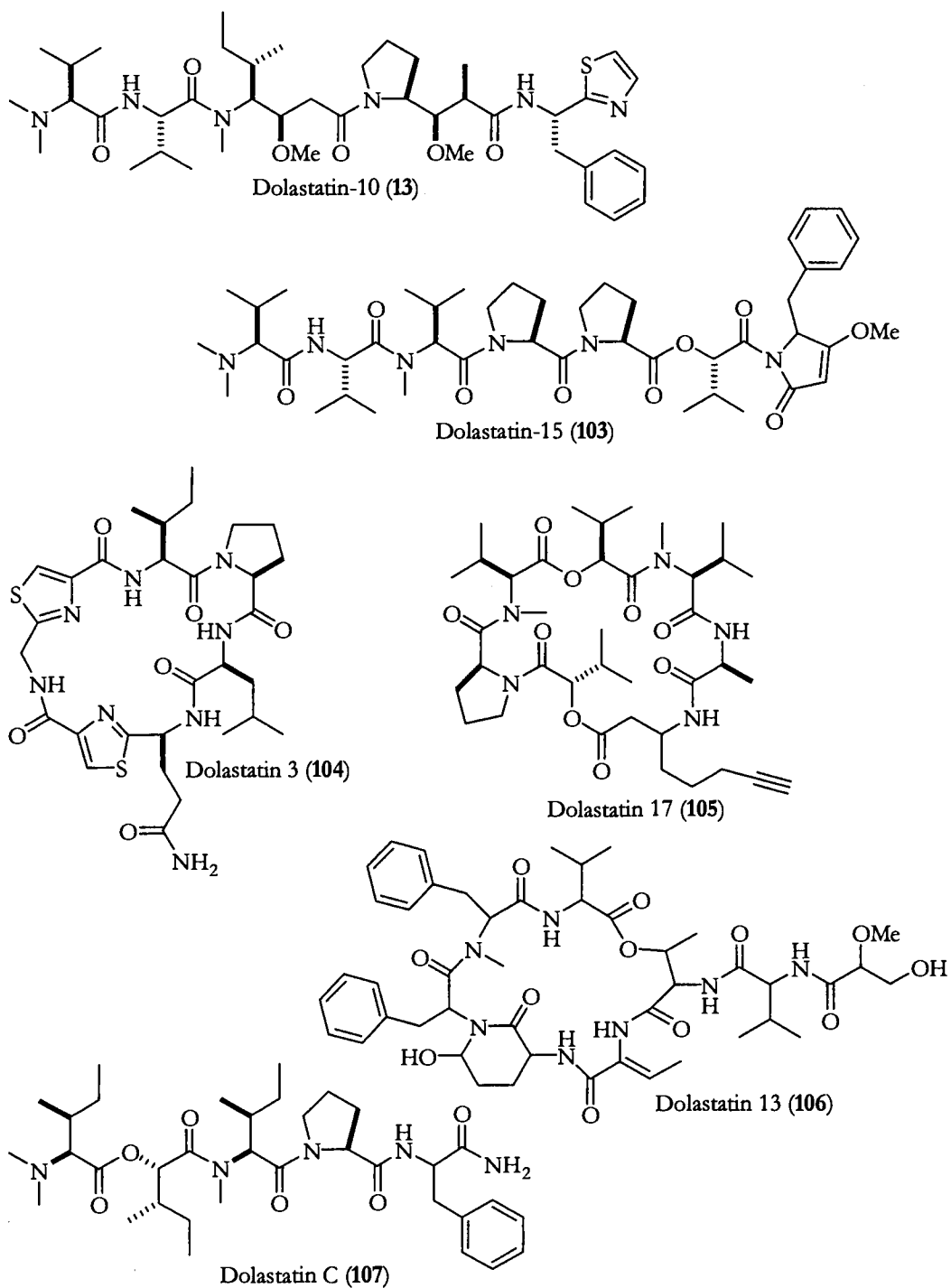


Figure V.1. Cyanobacterial cyclic peptides.



with sequential predation events. Thus, when an herbivore (or predator of that herbivore) is investigated, the secondary metabolites which derived from the cyanobacteria would appear to have been created by the sample organism. A potential example is the sea hare *Dolabella auricularia*, credited in the literature as the producer of some of the fields most recognized and storied natural products, including the dolastatins (**13** and **103-107**) and dolabellin (**108**).<sup>2-6,33</sup> The cyclic depsipeptide dolastatins (some examples in Figure V.2) possess structural motifs that have become recognized as characteristic of cyanobacterial secondary metabolites such as the incorporation of distinctive constellations of atoms (e.g. dolaphine and pyrrolidone units, Figure V.3.A), alternating heterocyclic ring/aliphatic residues (Figure V.3.B),<sup>33</sup> the presence of a  $\beta$ -hydroxy acid containing an acetylenic terminus (Figure V.3.C), the rarely encountered Ahp moiety (3-amino-6-hydroxy-2-piperidone; Figure V.3.D),<sup>33</sup> a lactonized L-Thr (Figure V.3.E),<sup>33</sup> and a high degree of N-methylation (Figure V.3.F). Interestingly, the alternation of heterocyclic rings and aliphatic residues has also been observed in compounds isolated from tunicates (such as the patellamides), which are known to live symbiotically with the prokaryotic *Prochloron* sp.<sup>118</sup> While dolabellin (**108**) is not a cyclic depsipeptide, it bears strong structural semblance to the lyngbyabellins (Figure V.4); maybe most strikingly, sharing the same eight carbon dichlorinated  $\beta$ -hydroxy acid residue.<sup>119</sup>

An unusual terminally acetylated residue incorporated into a growing number of cyanobacterial natural products can be found in a variety of forms, including both  $\beta$ -amino and  $\beta$ -hydroxy acid in  $\alpha$ -methyl/*gem*-dimethylated versions (Figure V.5). The Dhoa (dihydroxy octynoic acid) residue of **98** and **99**, rarely seen in nature, had only



**Figure V.2.** Examples of the dolastatins, invertebrate derived secondary metabolites.

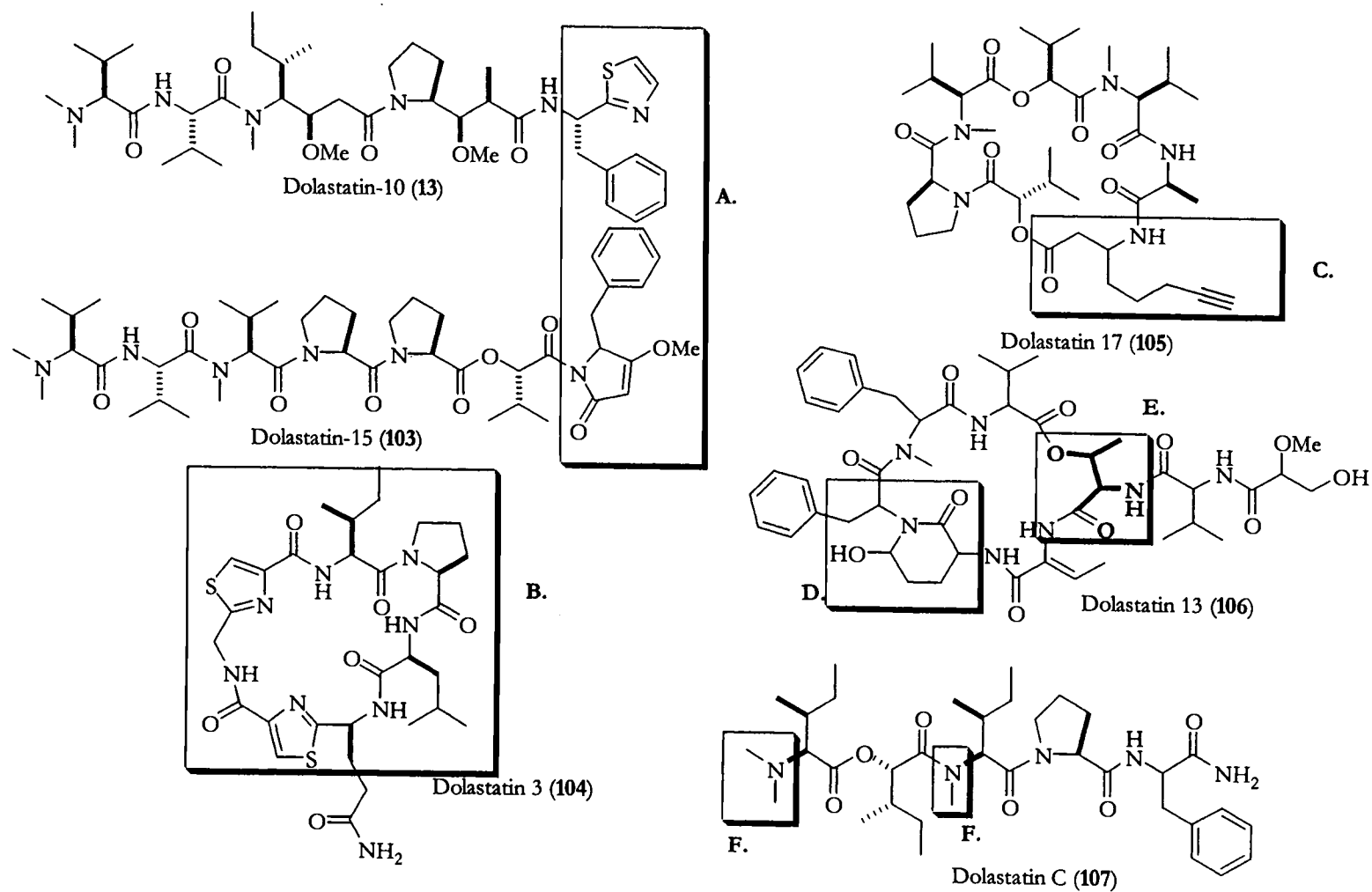


**Figure V.3.** Structural units shared by the dolastatins and cyanobacterial secondary metabolites.

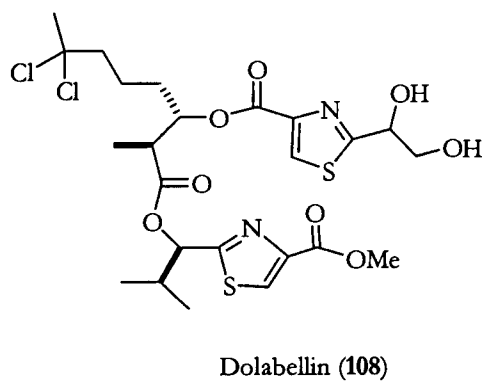
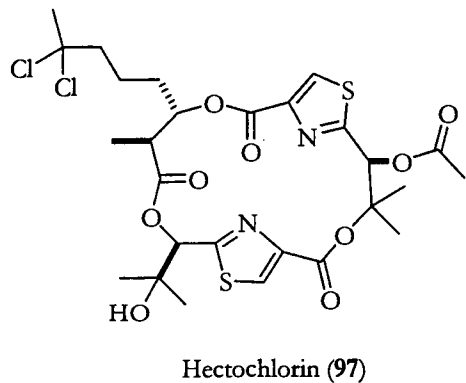
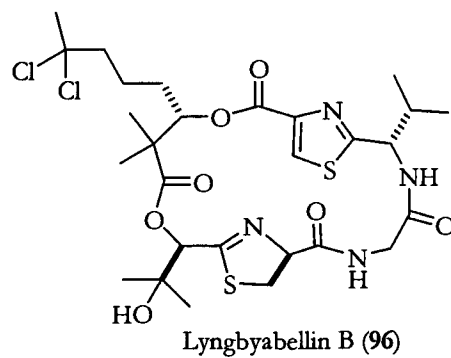
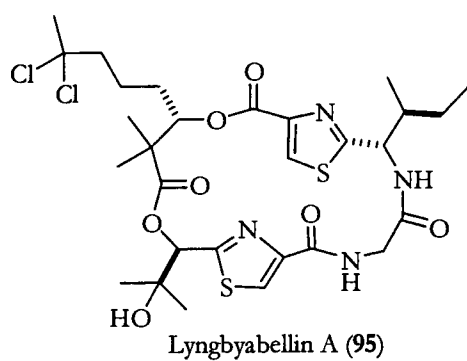
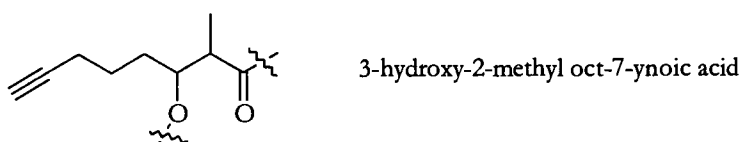
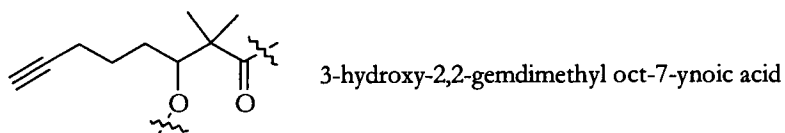


**Figure V.4.** The molluscan derived secondary metabolite dolabellin appears to be closely related to the *L. majuscula* metabolites lyngbyabellin A and B and hectochlorin.

Dihydroxy methyl octynoic acids



Amino methyl octynoic acids

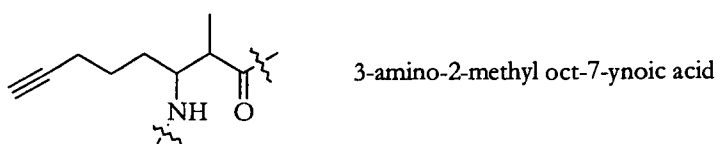
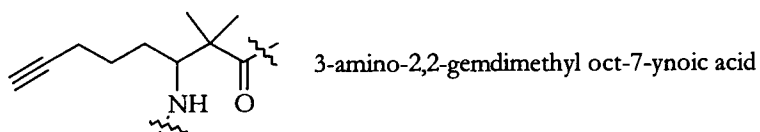


**Figure V.5.**  $\beta$ -hydroxy and amino octynoic acids found in some cyanobacterial cyclic peptides.

been discovered in kulolide (**113**) from the mollusc *Phyllinopsis speciosa*, before the isolation of the yanucamides from a mixed collection of *L. majuscula*/*Schizothrix* sp.<sup>115,120</sup> This residue is also present in the *L. majuscula* derived, georgamide (**100**).<sup>116</sup> The obvious structural similarities between the yanucamides, kulolide, and georgamide suggest the potential of a cyanobacterial origin for these metabolites. A modified version of Dhoa can be seen in the lyngbyabellins and hectochlorin, wherein the terminal acetylene is replaced a dichloromethyl moiety.

*Onchidium* sp., a pulmonate mollusc, is one of the few organisms which has provided secondary metabolites using the Amo moiety (amino methyl octynoic acid); incorporating it into onchidins A (**109**) and B (**110**).<sup>121,122</sup> To date, cyanobacteria have supplied the only other reports of this unusual residue with the discovery of malevamide C from *Symploca laete-viridis*.<sup>128</sup> As in the previous example, cyanobacteria appear responsible for the elaboration of secondary metabolites utilizing the Amo moiety. This line of thought is further strengthened by the discoveries of tortugin (**101**) and carliamide (**102**) which both display the Amo residue observed in onchidin A and B (Figure V.6).<sup>117,121,123</sup>

Additional support for this hypothesis can be gleaned from further investigation of *P. speciosa*. From this organism, tolytoxin 23-acetate (**111**), pupukeamide (**112**), and **113** were isolated.<sup>120,124,125</sup> As in previously discussed examples, **112** contains the 'cyanobacterial' N,O-dimethyltyrosine unit, while **111** has been previously reported as a cyanobacterial secondary metabolite.<sup>124</sup> Also, supporting the reports of secondary metabolite flow through the food chain,

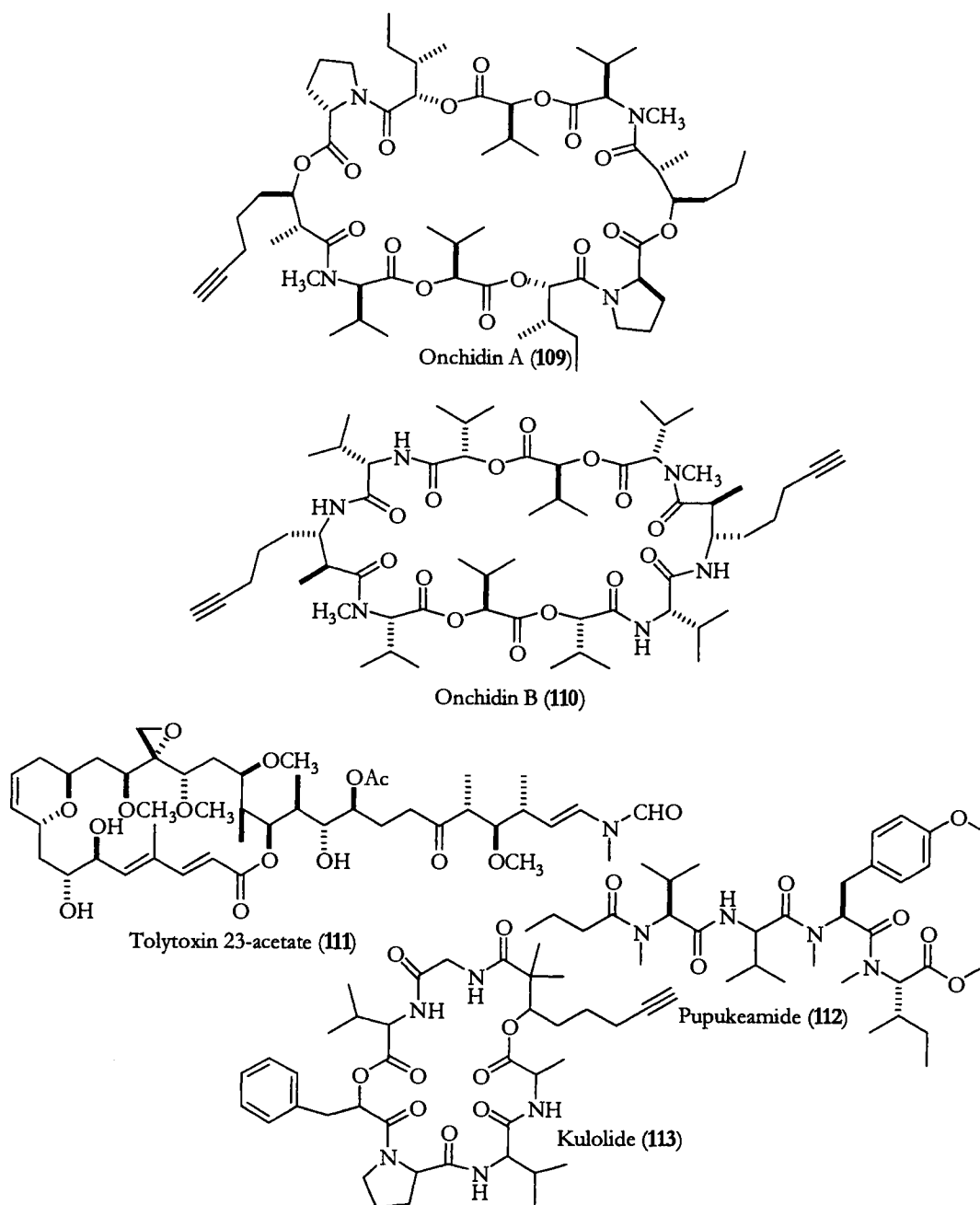


**Figure V.6.** Secondary metabolites isolated from marine invertebrates which either bear strong resemblance to cyanobacterial compounds or have also been isolated from a cyanobacterial source.

laboratory experimentation has revealed that *P. speciosa* is able to feed upon *Stylocheilus longicauda* (a well known grazer of cyanobacteria).<sup>120</sup>



## RESULTS AND DISCUSSION

## LYNGBYABELLIN B

Lyngbyabellin B (**96**) was isolated as a pale yellow oil (0.28% of the organic extract, 7.1 mg) and displayed a UV maximum at 246 nm ( $\log \epsilon$  4.20) and an optical rotation of  $[\alpha]_D^{25} +158^\circ$  ( $\text{CHCl}_3$ ,  $c$  0.1). LRFABMS (Figure V.7) described a compound with a molecular ion at  $[(M+H)^+]$  at  $m/z$  679 and an isotope pattern indicative of the presence of two chlorine atoms. HRFABMS showed a pseudomolecular ion  $[(M + H)^+]$  at  $m/z$  679.1794 consistent with the molecular formula  $\text{C}_{28}\text{H}_{41}\text{O}_7\text{N}_4\text{Cl}_2\text{S}_2$  ( $\Delta$  -2.3 mmu), indicating a structure with ten degrees of unsaturation. The IR spectrum revealed absorptions indicative of NH/OH protons ( $3323\text{ cm}^{-1}$ ), amide/ester carbonyls ( $1718$ ,  $1674\text{ cm}^{-1}$ ), and *gem*-dimethyl moieties ( $1234\text{ cm}^{-1}$ ). Analysis of the 1D  $^1\text{H}$  and  $^{13}\text{C}$  NMR data indicated a short aliphatic chain, two NH protons, three *gem*-dimethyl groups, a *gem*-dichloromethyl functionality, four methines bound to heteroatoms, and six downfield resonances in the amide/ester carbonyl chemical shift range (Table V.1). Interpretation of 1D NMR (Figure V.8-9) data in concert with 2D NMR experiments, including  $^1\text{H}$ - $^{13}\text{C}$  HSQC (Figure V.10),  $^1\text{H}$ - $^{13}\text{C}$  HSQC-TOCSY (Figure V.11),  $^1\text{H}$ - $^{13}\text{C}$  HMBC (Figure V.12), and  $^1\text{H}$ - $^{15}\text{N}$  PEP-HSQC-TOCSY (Figure V.13), defined partial structures A-G (Figure V.14).

Diagnostic chemical shifts and HMBC correlations from the methine proton (H-3) to three quaternary carbons (C-1, 2, and 5) allowed assembly of the thiazole partial structure fragment A. Similarly, in fragment D, connectivity could be observed from the methylene protons (H-17) to a pseudo- $\alpha$  carbon (C-16) and a deshielded

DS90 KEN0005.2 RT= 00:18 #FAB SLRP 15-Dec-97 16:27  
TIC= 44325890 100%= 1798144 POSFAB KEN-11B-94-3 IN OXALIC AC./2:1THIOGLYCEROL:GLYCEROL

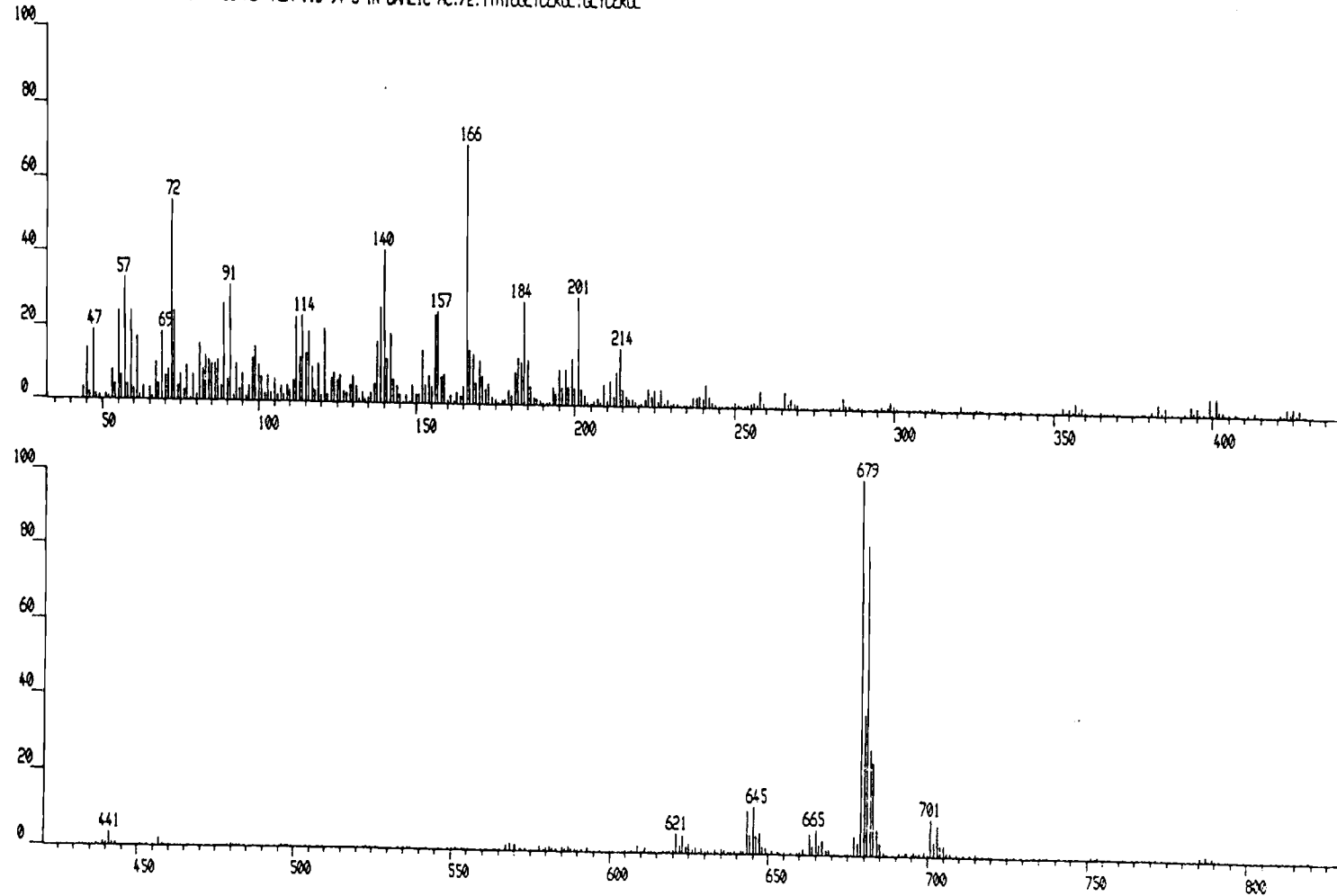


Figure V.7. LRFABMS of lyngbyabellin B.

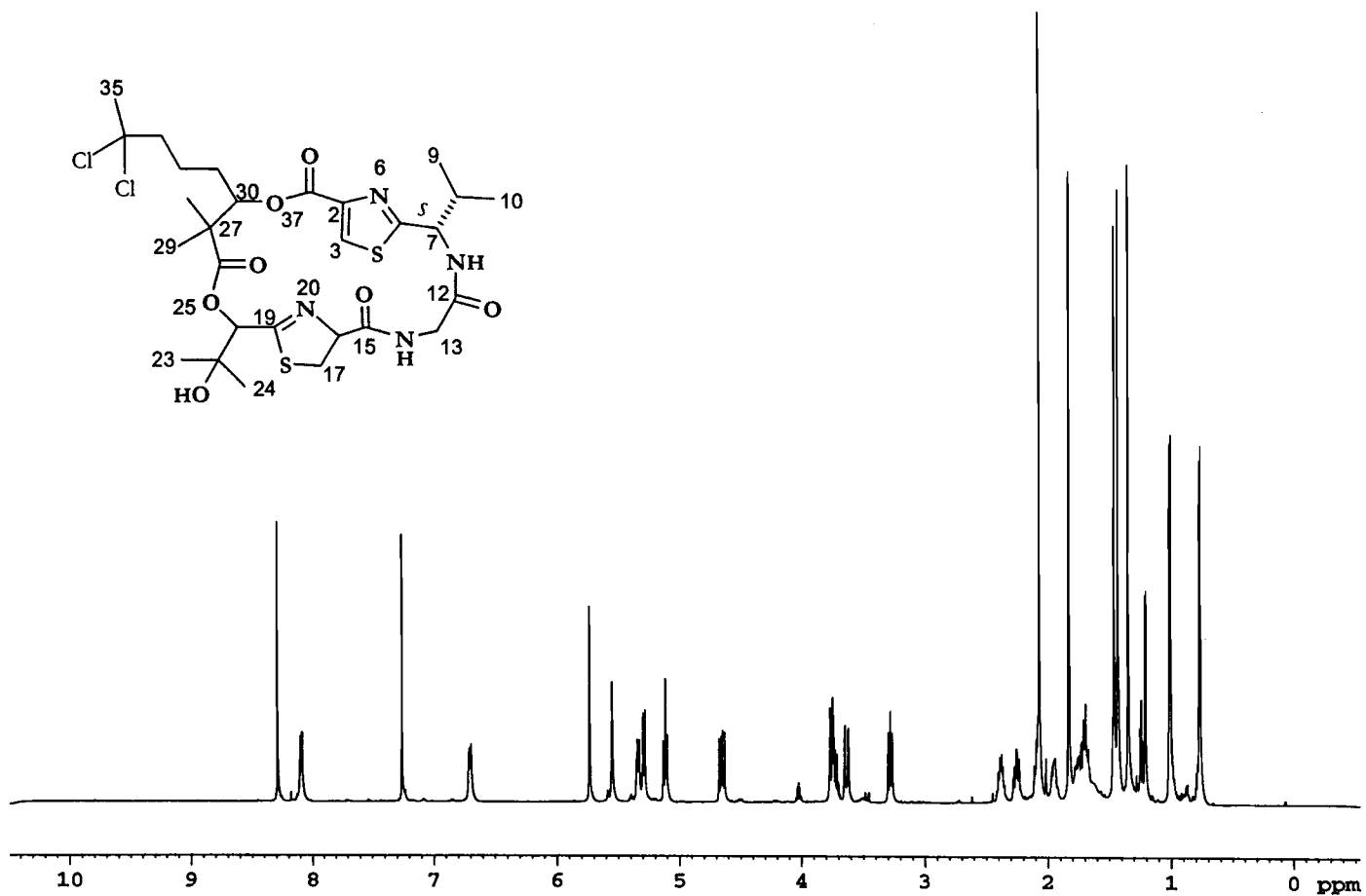


Figure V.8. <sup>1</sup>H NMR spectrum of lyngbyabellin B.

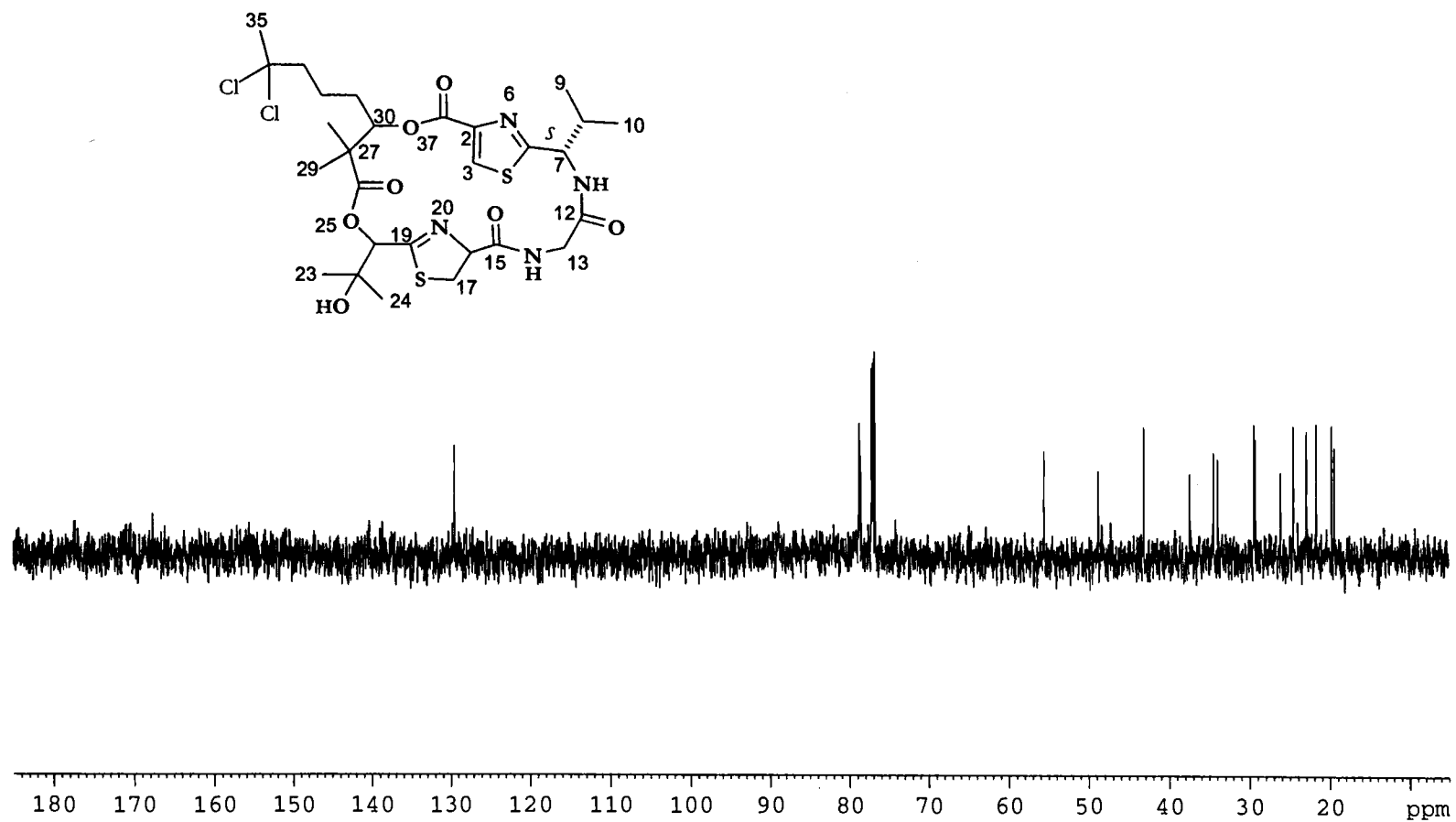


Figure V.9.  $^{13}\text{C}$  NMR spectrum of lyngbyabellin B.

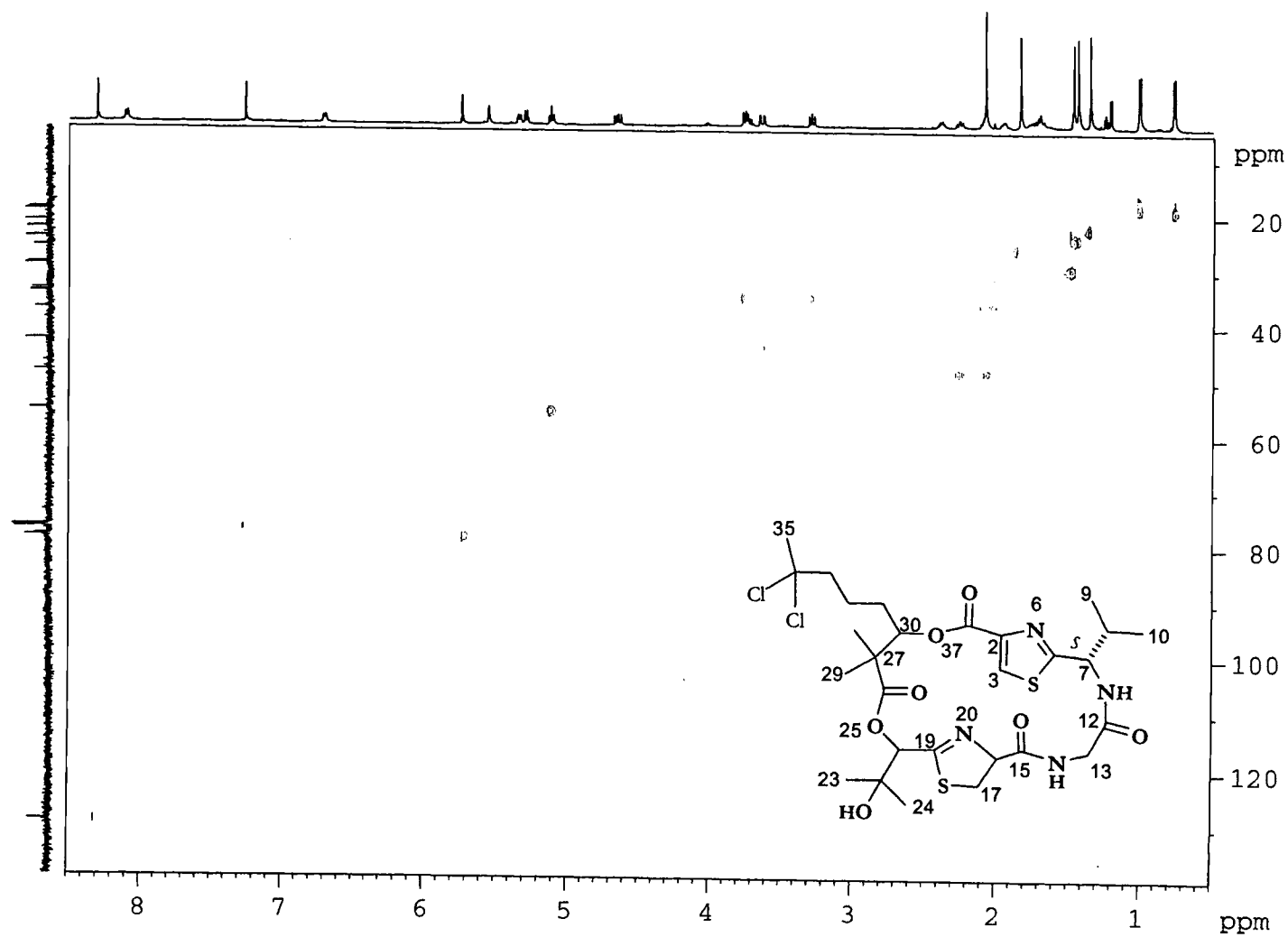
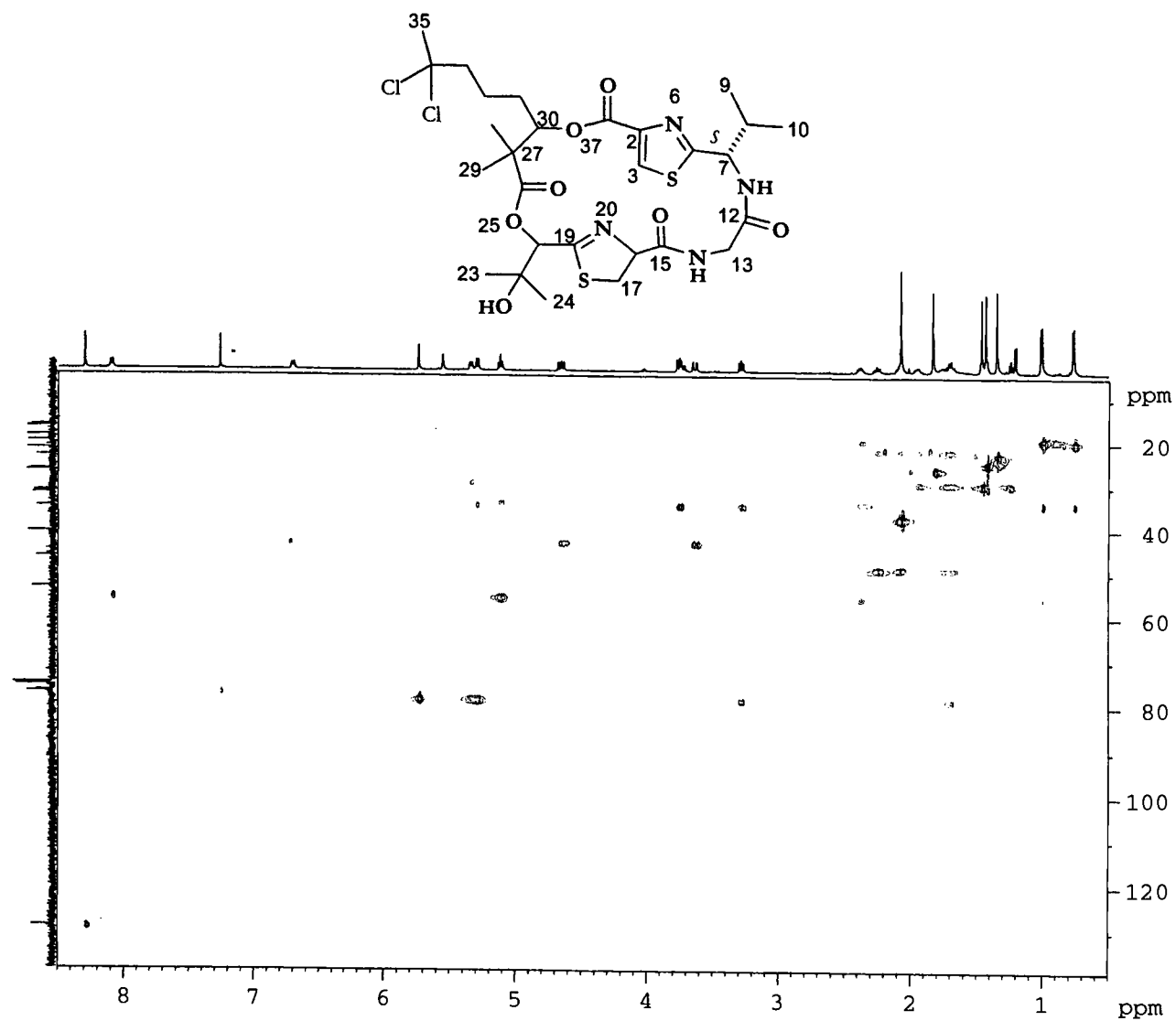


Figure V.10. HSQC spectrum of lyngbyabellin B.



**Figure V.11.**  $^1\text{H}$ - $^1\text{H}$  HSQC-TOCSY spectrum of lyngbyabellin B.

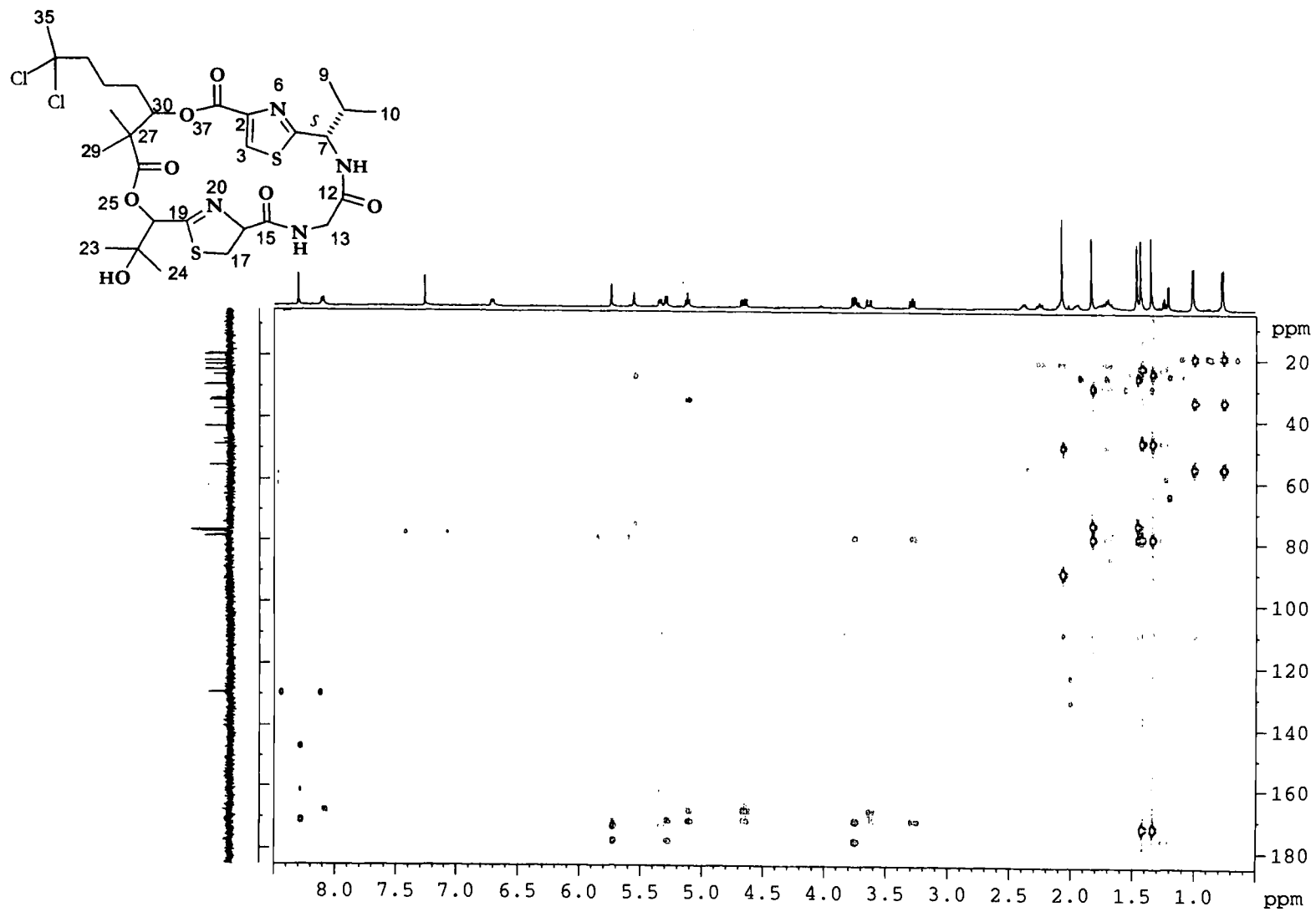


Figure V.12. HMBC spectrum of lyngbyabellin B.

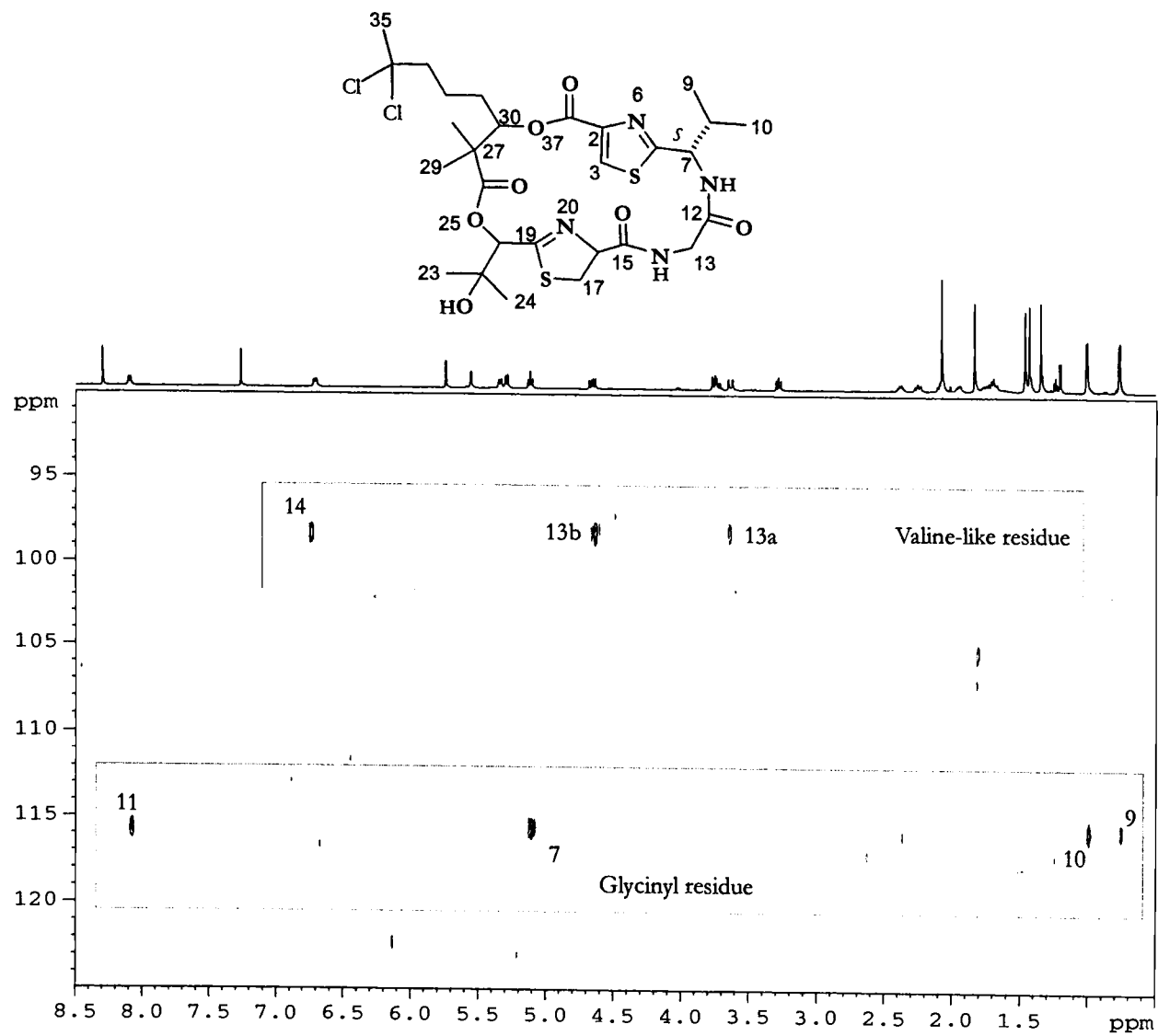


Figure V.13.  $^1\text{H}$ - $^{15}\text{N}$  PEP-HSQC-TOCSY spectrum of lyngbyabellin B.



**Table V.1.** NMR Data for Lyngbyabellin B (96).<sup>a</sup>

Residue <sup>b</sup>	Atom #	<sup>1</sup> H ppm (mult, J in Hz)	<sup>13</sup> C (ppm)	HMBC <sup>c</sup>	<sup>1</sup> H- <sup>15</sup> N PEP-HSQC-TOCSY <sup>d</sup>
Thiazole (A)	1	-	161.10	-	-
	2	-	146.82	-	-
	3	8.27 (s)	129.45	1, 2, 5	-
	4	-	-	-	-
	5	-	171.13	-	-
	6	-	-	-	-
Valine (B)	7	5.10 (t, 9.6)	55.58	5, 8, 9, 10, 12	11
	8	2.36 (dq, 9.7, 6.7)	33.89	7, 10	11
	9	0.74 (d, 6.8)	19.73	7, 8, 10	11
	10	0.99 (d, 6.8)	19.30	7, 8, 9	11
	11	8.07 (bs)	-	12	11
Glycine (C)	12	-	167.69	-	-
	13a	3.61 (dd, 10.0, 2.3)	43.15	12, 15	14
	13b	4.64 (dd, 10.2, 10.0)	43.15	12, 15	14
	14	6.68 (dd, 9.8, 1.6)	-	-	14
Thiazoline (D)	15	-	170.89	-	-
	16	5.27 (d, 9.6)	78.67	15, 19	-
	17a	3.27 (dd, 9.8, 1.8)	34.44	15, 16	-
	17b	3.75 (dd, 10.6, 1.5)	34.44	15, 16, 19	-
	18	-	-	-	-
	19	-	177.63	-	-
	20	-	-	-	-
<i>l</i> -Hydroxy valic Acid (E)	21	5.72 (d, 1.6)	78.58	19, 26	-
	22	-	74.13	-	-
	23	1.81 (s)	26.19	21, 22, 24	-

Table V.1. (Continued) NMR Data for Lyngbyabellin B (96).<sup>a</sup>

DDHO <sup>e</sup> (F & G)	24	1.44 (s)	29.29	21, 22, 23	-
	OH	5.55 (bs)	-	22, 23	-
	25	-	-	-	-
	26	-	172.62	-	-
	27	-	47.24	-	-
	28	1.33 (s)	22.81	26, 27, 29, 30	-
	29	1.41 (s)	24.45	26, 27, 28, 30, 31	-
	30	5.32 (dd, 11.0, 3.3)	78.45	1, 26, 27 <sup>f</sup> , 33	-
	31a	1.68 (m)	21.91	30, 32	-
	31b	1.76 (m)	21.91	30, 32	-
	32a	1.93 (m)	29.23	31	-
	32b	1.70 (m)	29.23	31	-
	33a	2.05 (m, obs)	48.80	31, 32, 34	-
	33b	2.25 (ddd, 14.6, 11.3, 4.4)	48.80	31, 32, 34	-
	34	-	90.01	-	-
	35	2.05 (s)	37.43	33, 34	-

<sup>a</sup> <sup>1</sup>H chemical shifts referenced to residual CHCl<sub>3</sub> (δ 7.27; <sup>13</sup>C chemical shifts referenced to center peak of CDCl<sub>3</sub> (δ 77.00). <sup>b</sup>Residue names given by dominant moiety type. For partial structures see Figure 1.

<sup>c</sup>HMBC data are reported as proton (atom #) displaying connectivity to indicated carbon. <sup>d</sup><sup>1</sup>H-<sup>15</sup>N PEP-HSQC-TOCSY data are reported as proton (atom #) displaying connectivity to indicated nitrogen.

<sup>e</sup>7,7-dichloro-2,2-dimethyl-3-hydroxy octanoic acid. <sup>f</sup>Weak correlation.

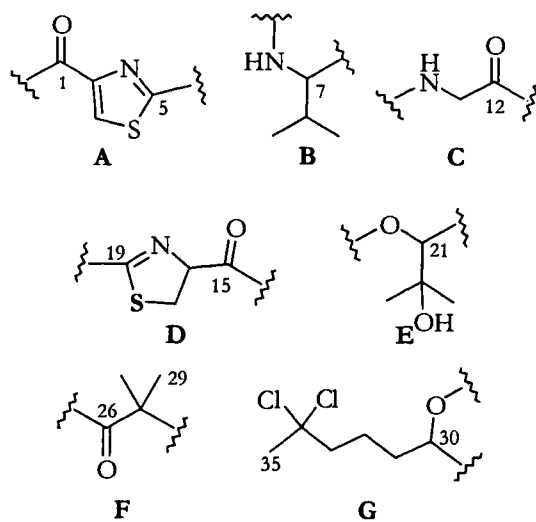


**Figure V.14.** Partial structures of lyngbyabellin B.

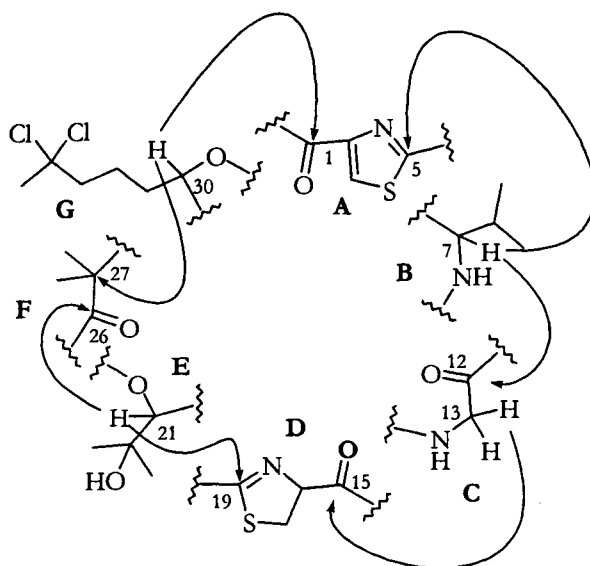


**Figure V.15.** Key HMBC correlations used in the sequencing of partial structures A-G of lyngbyabellin B.

quaternary carbon (C-19), suggesting a thiazoline partial structure. The  $^1\text{H}$ - $^{15}\text{N}$  PEP-HSQC-TOCSY NMR experiment clearly demonstrated connectivity between N-11 and the corresponding  $\alpha$ ,  $\beta$ , and  $\gamma$  protons of fragment B. Likewise, both methylene protons of the glyciny residue correlated to the nitrogen in fragment C (Figure V.13-14). Partial structures E and F were assembled based on their chemical shifts and HMBC data. Particularly revealing for fragment E were HMBC correlations to the pseudo- $\alpha$  carbon (C-21) from both methyl groups of the *gem*-dimethyl pair, as well as connectivity observed from the proton of the tertiary alcohol to the midfield quaternary carbon (C-22) and one of the *gem*-dimethyl pair (C-23). Similarly, fragment F was defined by HMBC cross peaks descriptive of a *gem*-dimethyl functionality adjacent to an amide/ester carbonyl. The aliphatic chain of partial structure G was primarily elucidated by following the  $^1\text{H}$ - $^1\text{H}$  spin system using  $^1\text{H}$ - $^{13}\text{C}$  HSQC-TOCSY. Definition of the *gem*-dichloro arrangement was accomplished by consideration of its  $^{13}\text{C}$  NMR chemical shift (C-34,  $\delta$ 90.01), which is comparable to the *gem*-dichloro functionality in dolabellin (**108**, C-7),<sup>119</sup> and HMBC correlations from the adjacent methyl (C-35) and methylene groups (C-33). These partial structures account for all atoms in the molecular formula of **96**.

Assembly of the planar structure of **96** was accomplished primarily through HMBC correlations (Figure V.15). The thiazole containing partial structure A was placed adjacent to B by HMBC correlations observed between the pseudo- $\alpha$  hydrogen (H-7,  $\delta$ 5.10) of the valine-like residue B to the  $sp^2$  hybridized carbon of residue A (C-5,  $\delta$ 171.13). H-7 also displayed heteronuclear connectivity to the carbonyl terminus, C-

12 ( $\delta$  167.69), of the glycyl residue (Figure V.15.C). The methylene protons of this latter residue ( $H_2$ -13,  $\delta$ 3.61 and 4.64) showed HMBC crosspeaks to C-15 ( $\delta$ 170.89) of partial structure D. Correlations were also observed between C-19 ( $\delta$ 177.63) of partial structure D and the pseudo- $\alpha$  hydrogen of E ( $H$ -21,  $\delta$ 5.72). Substructures E and F were connected through an ester bond by observing long-range heteronuclear coupling between  $H$ -21 and the C-26 carbonyl of F ( $\delta$ 172.62), and consideration of the  $^{13}\text{C}$  NMR chemical shift of C-21 ( $\delta$ 78.58). Correlations between  $H$ -30 ( $\delta$ 5.32) and the quaternary carbon containing a *gem*-dimethyl group (C-27,  $\delta$ 47.24) allowed connection of G and F. The planar structure of **96** was completed by linkage of partial structures G and A by observation of an HMBC correlation between  $H$ -30 and the C-1 carbonyl ( $\delta$ 161.10). The ester nature of this linkage was established by consideration of the chemical shift of C-30 ( $\delta$ 78.45).

The absolute stereochemistry at C-7 was defined using chiral GC/MS analysis (Alltech capillary column, CHIRASIL-VAL Phase 25 m x 0.25 mm). Lyngbyabellin B was ozonized (0.2 mg,  $\text{CH}_2\text{Cl}_2$ , 1 min, ambient temperature), hydrolyzed (6N HCl, 18 hr, 118°C), and derivatized to yield *N*-pentafluoropropionyl isopropyl ester derivatives (Alltech PFP-IPA Amino Acid Kit). The resulting derivatized valine residue of **96**, and identically derivatized valine standards (1 mg each of *L*- and *D,L*-valine) were subjected to chiral GC/MS analysis (see experimental). The valine derivative obtained from **96** eluted at  $t_R = 14.34$  min, as did the standard *L*-valine derivative, thus defining C-7 as having *S* stereochemistry (the *D*-valine derivative eluted with  $t_R = 13.59$  min).

Interestingly, of the 7 partial structures of lyngbyabellin B (Figure V.14.A-G), only one is an underivatized amino acid residue (glycinyll partial structure C). Partial structures A and D may be formed by condensation of cysteine residues to produce thiazole and thiazoline rings, respectively.<sup>126</sup> Partial structures B and E are modified valine residues. Partial structures F and G are similar to the *gem*-dichloro aliphatic chain of dolabellin (108), isolated from the sea hare *Dolabella auricularia*.<sup>116</sup>

Lyngbyabellin B (96) was toxic to brine shrimp (*Artemia salina*)<sup>104</sup> with an LD<sub>50</sub> of 3.0 ppm and active against *Candida albicans* (ATCC 14053) in a disc diffusion assay,<sup>127</sup> giving a 10.5 mm zone of inhibition at 100 µg/disc and a slight halo at 10 µg/disc. The striking structural parallel between lyngbyabellin B (96) and dolabellin (108) strongly supports a cyanobacterial origin for the latter metabolite.

In our laboratory, compound 96 was originally named "tortugamide" to reflect its origin from *L. majuscula* collected in the Dry Tortugas, Florida. However, upon recognition that 96 was discovered simultaneously by both our group and that of Professor R.E. Moore (Univ. of Hawai'i), and in light of the earlier publication of lyngbyabellin A (95),<sup>12</sup> we have adopted the name "lyngbyabellin B" for compound 96.<sup>108-110</sup>

#### TORTUGIN

Tortugin (101) was isolated as a biologically active (brine shrimp LD<sub>50</sub> = 4.0 ppm) pale yellow oil from the lipid extract of *L. majuscula*. LRFABMS (Figure V.16) described a compound with a molecular ion of [(M+H)<sup>+</sup> at *m/z* 625]. HRFABMS showed a pseudomolecular ion (M+H; 625.3965) consistent with a molecular formula

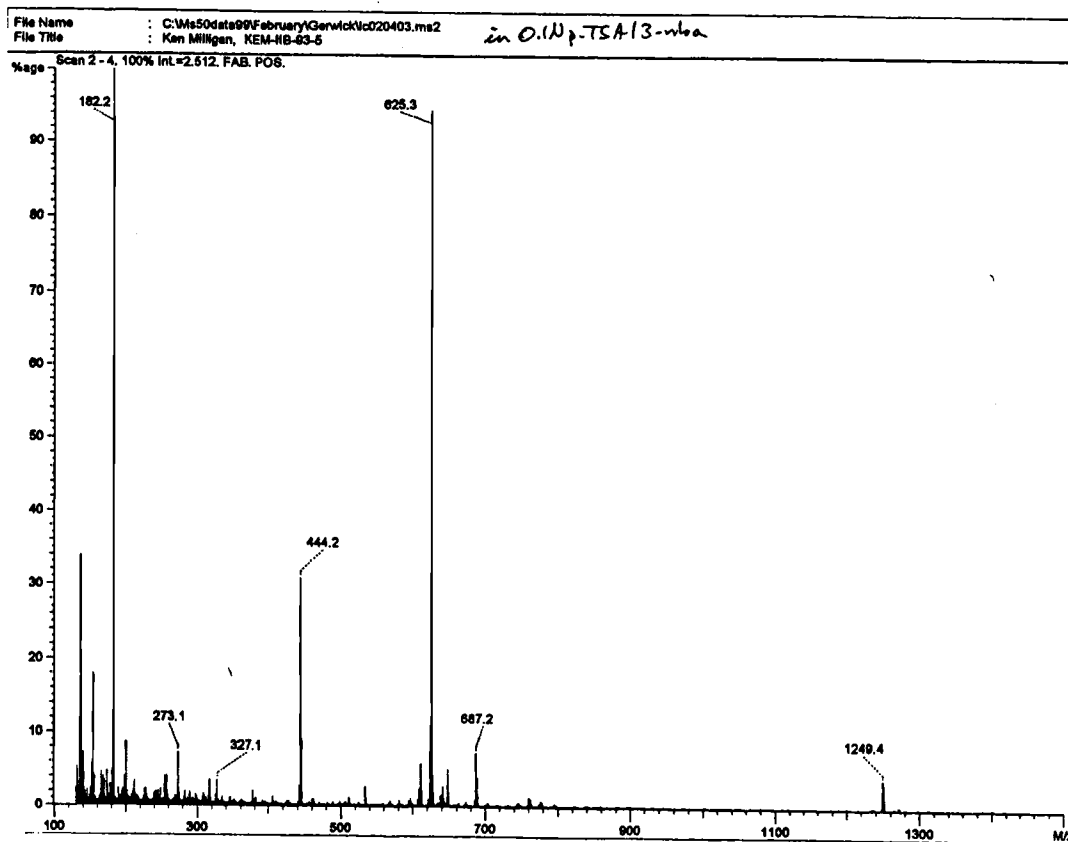


Figure V.16. +FABMS of tortugin.

$[C_{35}H_{52}O_6N_4 + H]^+$ , indicating 12 degrees of unsaturation. The IR spectrum indicated absorptions for NH protons ( $3299\text{ cm}^{-1}$ ), a carbon-carbon triple bond ( $2214\text{ cm}^{-1}$ ), and amide carbonyl groups ( $1735, 1652\text{ cm}^{-1}$ ). A UV maxima was observed at  $210\text{ nm}$ , suggestive of amide bonding.

The 1D  $^1\text{H}$  (Figure V.17) and  $^{13}\text{C}$  NMR (Figure V.18) of **101** is complicated by a near doubling of resonances, as compared to what our molecular weight would suggest, due to the presence of a pair of 3:2 conformers caused by rotation about two NMe amide bonds. In  $\text{C}_6\text{D}_6$  and  $\text{CD}_3\text{OD}$  partial reduction of the conformers was observed. Careful interpretation of 1D and 2D NMR data allows the separation of resonances into conformer sets each forming the complete natural product. Structural analyses were accomplished using the major component.

Interpretation of 1D NMR data and 2D NMR experiments, including  $^1\text{H}$ - $^1\text{H}$  HSQC-TOCSY (Figure V.19),  $^1\text{H}$ - $^{13}\text{C}$  HSQC (Figure V.20),  $^1\text{H}$ - $^{13}\text{C}$  HMBC (Figure V.21), and  $^1\text{H}$ - $^{15}\text{N}$  PEP-HSQC-TOCSY (Figure V.22) defined partial structures A-E (Figure V.23). Partial structure E was confirmed through IR (carbon-carbon triple bond at  $2214\text{ cm}^{-1}$ ) and the HMBC measurement of a  $^1\text{H}$ - $^{13}\text{C}$   $^1J$  coupling constant of  $250\text{ Hz}$ , indicative of a terminal acetylene. Particularly insightful in deciphering the non-NMe amino acids (A and E) was the  $^1\text{H}$ - $^{15}\text{N}$  PEP-HSQC-TOCSY experiment pioneered in our laboratory by Dr. R. Thomas Williamson and Dr. Brian L. Marquez, which allowed visualization of the  $^1\text{H}$ - $^1\text{H}$  spin system “sorted” by their respective nitrogens. Similarly, HSQC-TOCSY was primarily responsible for the development of the remaining partial structures (B,C,D) through the examination of the  $^1\text{H}$ - $^1\text{H}$  coupling of their ‘R’ side chains. The combination of the nitrogen edited and standard





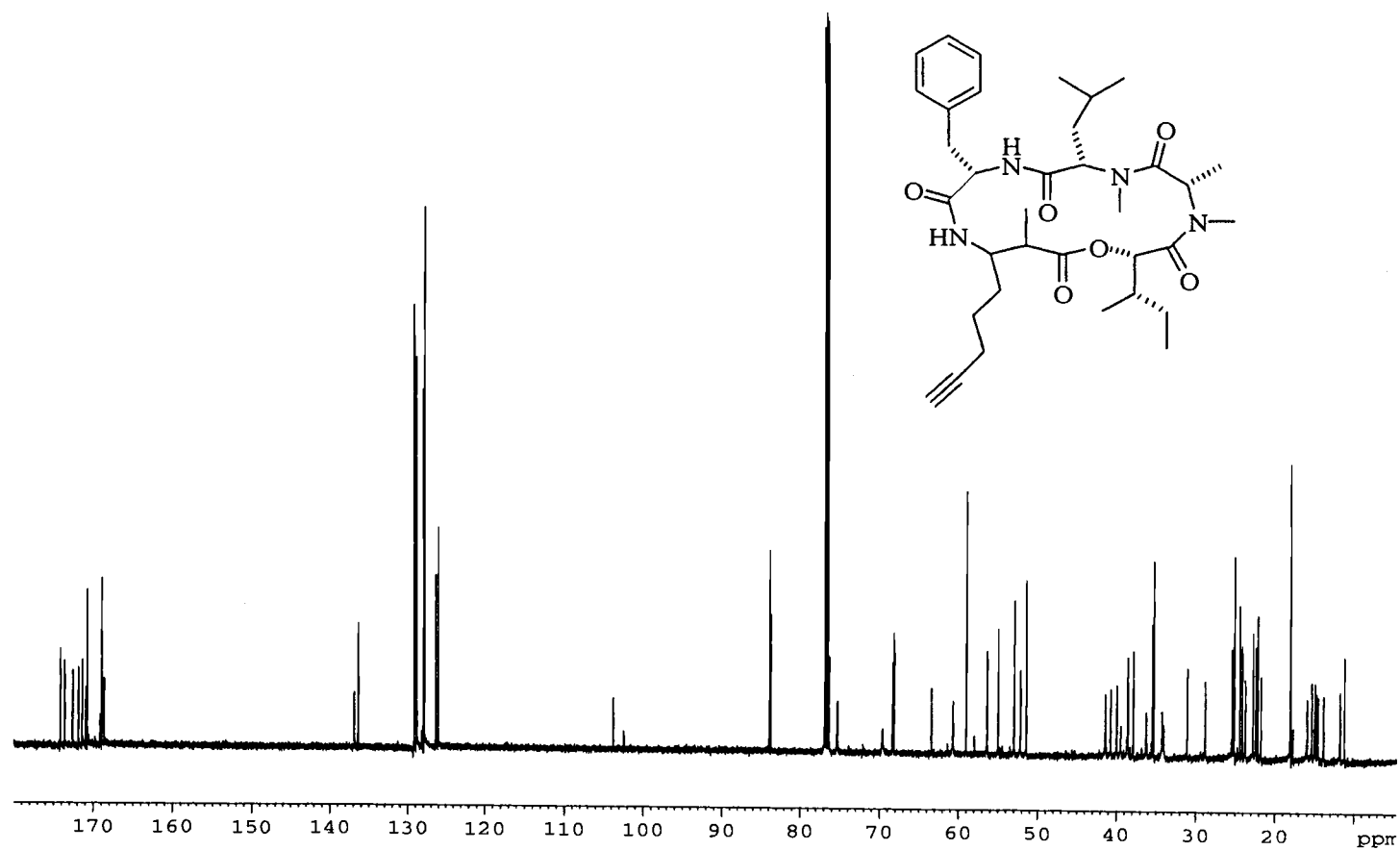


Figure V.18.  $^{13}\text{C}$  NMR spectrum of tortugin.

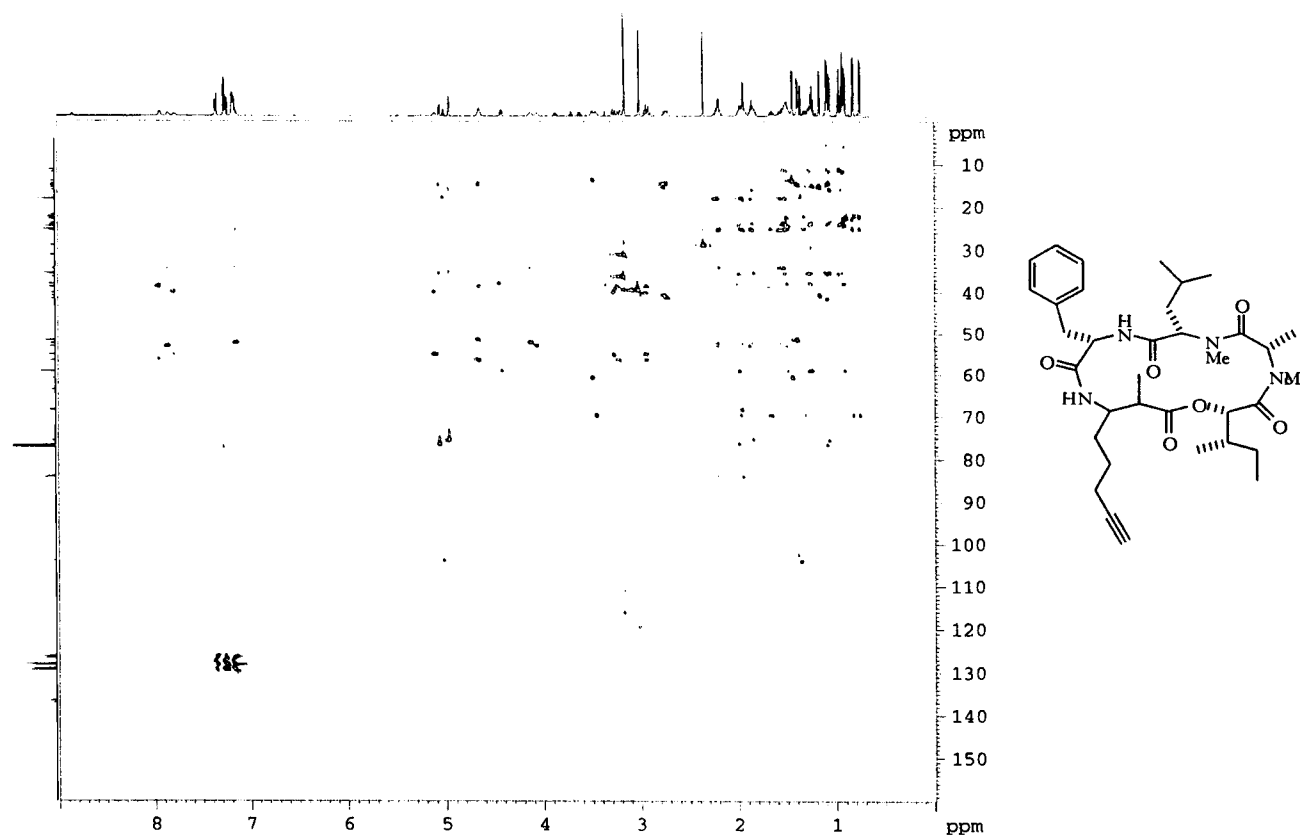


Figure V.19. HSQC-TOCSY of tortugin.

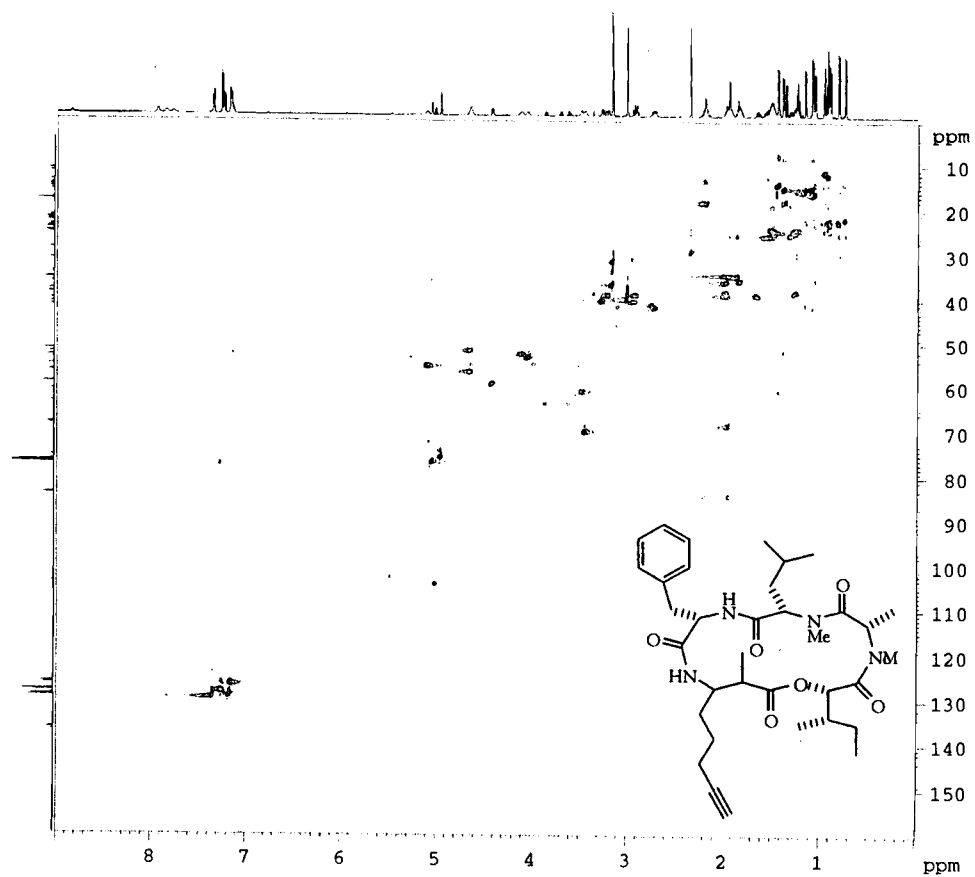


Figure V.20. HSQC of tortugin.

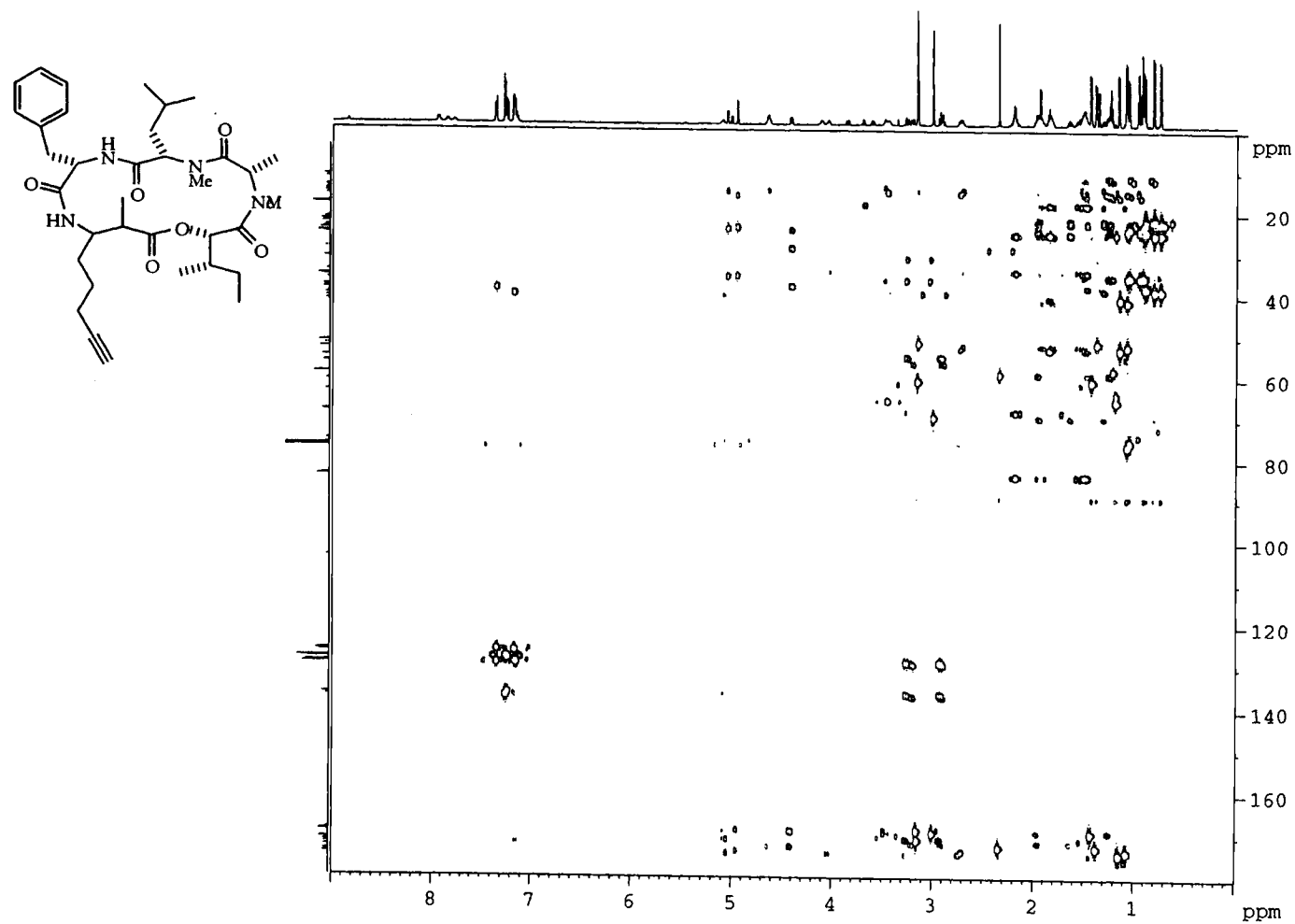
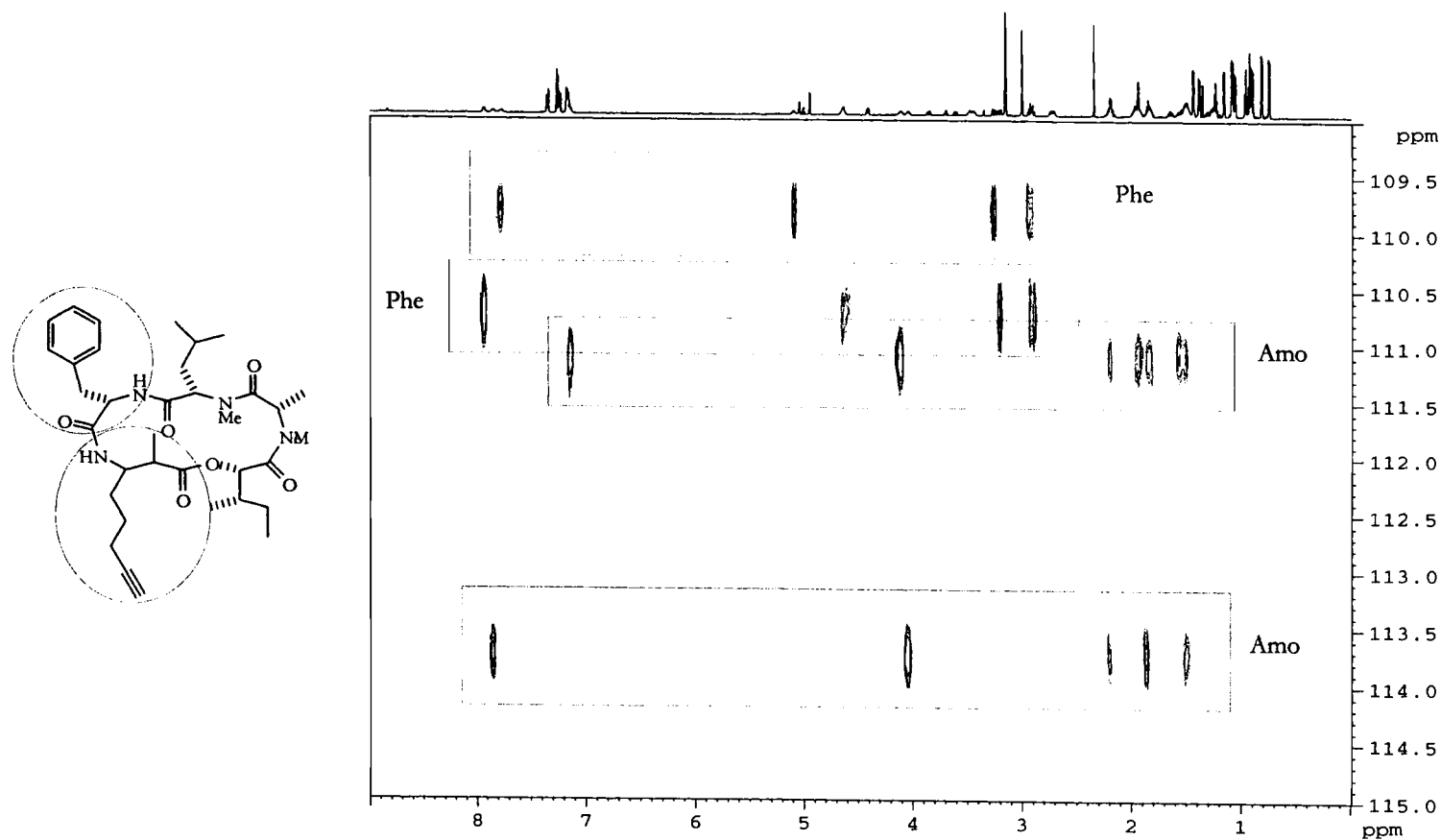


Figure V.21. HMBC of tortugin.



**Figure V.22.**  $^1\text{H}$ - $^{15}\text{N}$  PEP-HSQC-TOCSY of tortugin. The correlations representing the non-NMe amino acid residues of the two conformers are contained within the boxes.

**Table V.2.** NMR Data for Tortugin (**101**)<sup>a</sup>.

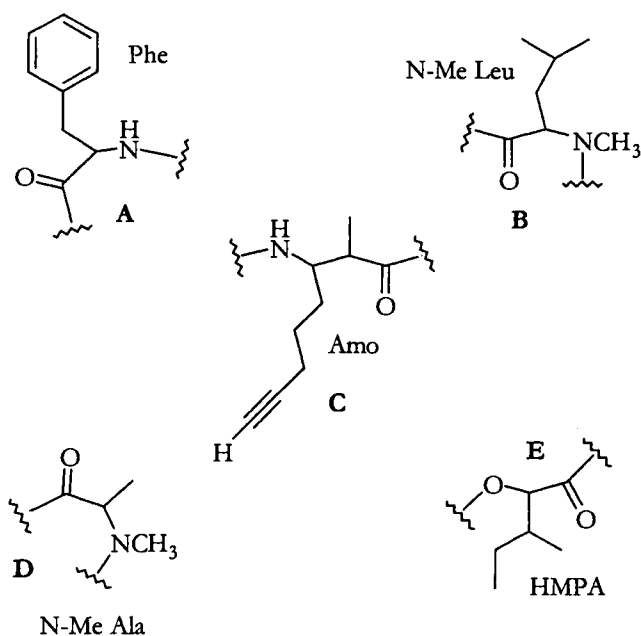
Residue <sup>b</sup>	Atom #	<sup>1</sup> H ppm (mult, J in Hz)	<sup>13</sup> C (ppm)
L-Phe	1		171.11
	2	5.10 (m)	55.27
	3	7.78	
	4a	2.97 (m)-	40.22
	4b	3.27 (dd, 4.7, 14.6)	
	5		137.0
	6	7.18 (m)	129.3
	7	7.15 (m)	126.6
	8	7.35 (m)	128.4
	9	7.25 (m)	126.4
L-NMe-Leu	10	7.26 (m)	128.3
	11		169.3
	12	4.42 (m)	59.29
	13		
	14	1.5 (m)	
	15	1.98 (m)	34.65
	16	1.0 (s)	22.4
	17	1.01 (s)	23.0
L-NMe-Ala	18	2.32 (s)	29.04
	19		172.93
	20	4.65 (m)	51.72
	21		
	22	1.38 (s)	15.19
L-HMPA <sup>c</sup>	23	3.15 (s)	31.30
	24	-	171.32
	25	5.05 (d, 5.8)	76.49

Table V.2. (Continued) NMR Data for Tortugin (101)<sup>a</sup>.

	26		
	27	1.99 (m)	35.76
	28	1.52 (m)	24.35
	29	0.96	11.45
	30	1.08	15.00
Amo <sup>d</sup>	31		174.50
	32	2.75 (m)	40.97
	33	4.05 (m)	53.23
	34	7.84 (bs)	
	35	1.86 (m)	34.51
	36	1.49 (m)	24.65
	37	2.20 (m)	18.32
	38		84.01
	39	1.95 (m)	68.64
	40	1.16 (s)	15.60

<sup>a</sup> <sup>1</sup>H chemical shifts referenced to residual CHCl<sub>3</sub> (δ 7.27); <sup>13</sup>C chemical shifts referenced to center peak of CDCl<sub>3</sub> (δ 77.00). <sup>b</sup>Residue names given by dominant moiety type. <sup>c</sup>HMPA is hydroxy methyl pentanoic acid. <sup>d</sup>Amo is amino methyl octynoic acid.





**Figure V.23.** Partial structures of tortugin.

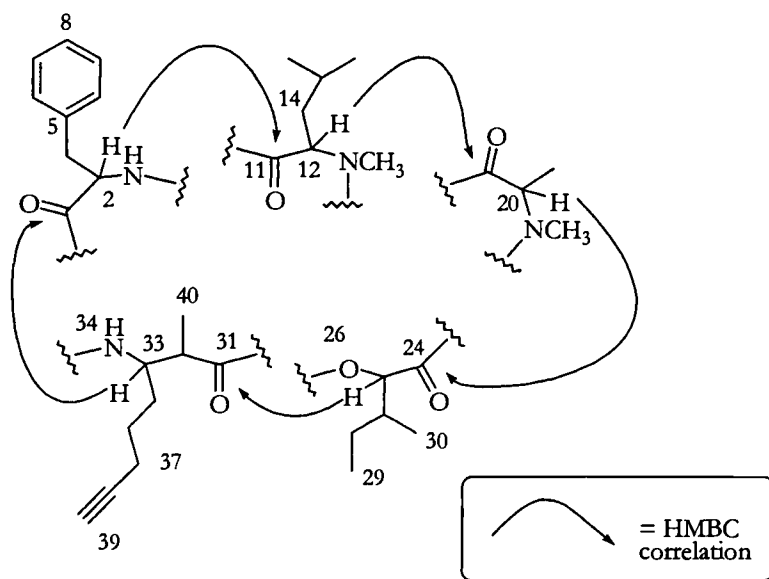


**Figure V.24.** Assembling the partial structures of tortugin.

HSQC-TOCSY experiments allowed relatively facile building of the five partial structures of tortugin. This is due to the structure of **101** (and the predominance of other cyclic peptides and depsipeptides) allowing clear visualization of the  $^1\text{H}$ - $^1\text{H}$  spin system of the amino or hydroxy acid's side chains. Correlations from the  $\alpha$ -proton to protons within other subunits will not typically occur, as the coupling relay must proceed through a protonated carbon (for HSQC-TOCSY) or nitrogen (for  $^1\text{H}$ - $^{15}\text{N}$  PEP-HSQC-TOCSY).

The assembly of the partial structures into the planar structure of tortugin was accomplished primarily through the interpretation of HMBC correlations from the  $\alpha$  or pseudo- $\alpha$  proton to the carboxyl carbon of adjacent subunits (Figure V.24). The Phe  $\alpha$ -H (H-2) displayed HMBC connectivity to the NMe-Leu carbonyl (C-11). From the NMe-Leu  $\alpha$ -H (H-12), a correlation into the NMe Ala residue could be seen through its carbonyl carbon (C-19). HMBC cross-peaks from the NMe-Ala  $\alpha$ -H (H-20) to the HMPA (hydroxy methyl pentanoic acid) carbonyl (C-24) allowed linking of these two residues. The remaining residue was attached to the HMPA, forming an ester bond, owing to heteronuclear connectivity between the HMPA  $\alpha$ -H (H-25) and the Amo carbonyl (C-31). The resulting straight chain depsipeptide partial structure accounted for all of the atoms of the molecular formula for **101**. Cyclization by forming an amide bond between the Amo and Phe residues was accomplished through the observed correlations between the Amo  $\alpha$ -H (H-33) and the Phe carbonyl (C-1), thus completing the planar structure of tortugin.

In order to elucidate the chirality of the Phe  $\alpha$ -carbon, chiral GC/MS analysis was utilized. By subjecting tortugin to acid hydrolysis followed by the appropriate derivatization, the *N*-pentafluoropropyl isopropionyl ester of the phenylalanine derivative (PFPIP-Phe) was created. This PFPIP-Phe derivative of tortugin co-eluted with the similarly derivitized *L*-phenylalanine standard ( $t_R$  16.32 min), and displayed a difference in retention time of 0.49 min as compared to the elution of the derivitized *D*-Phe standard ( $t_R$  16.81 min). The stereochemistry of the NMe-Ala and NMe-Leu residues was deduced using HPLC and Marfey's analysis. HPLC analysis followed acid hydrolysis and Marfey's reagent derivatization, and resulted in the coelution of NMe-Ala with the derivitized standard *L*-NMe-Ala ( $t_R$  26.51 min; *D*-NMe-Ala  $t_R$  27.3 min).<sup>111</sup> The liberated and derivitized NMe-Leu residue also co-eluted with its NMe-*L*-Leu standard ( $t_R$  32.63; *D*-NMe-Leu  $t_R$  34.52). For the HMPA residue, acid hydrolyzed tortugin was reacted with menthoxy carbonyl chloride (MCC) to form the menthyl carbonate of HMPA.<sup>128</sup> Since HMPA has two chiral centers, four standards were required for proper analysis. The *L* and *D*-HMPAs were commercially available and the *L*-allo and *D*-allo-HMPA were synthesized from *L*-allo and *D*-allo-isoleucine, respectively, by a diazotization reaction (Figure V.25 and 26).<sup>129,130</sup> The chemical identity of the synthesized products was confirmed by FABMS. The four derivitized standards were separable from each other by GC/MS. The menthyl carbonate derivative of HMPA obtained from tortugin co-eluted with the derivitized *L*-HMPA standard ( $t_R$  20.7 min;  $t_0=100^\circ\text{C}$  for 0.5 min,  $\Delta t = 3^\circ/\text{min}$  to  $240^\circ\text{C}$ ; *D*-HMPA  $t_R$  20.95, *D*-allo-HMPA  $t_R$  20.80, *L*-allo-HMPA  $t_R$  20.37). The HMPA unit of tortugin could thus be defined as *L*, or *S,S* HMPA.

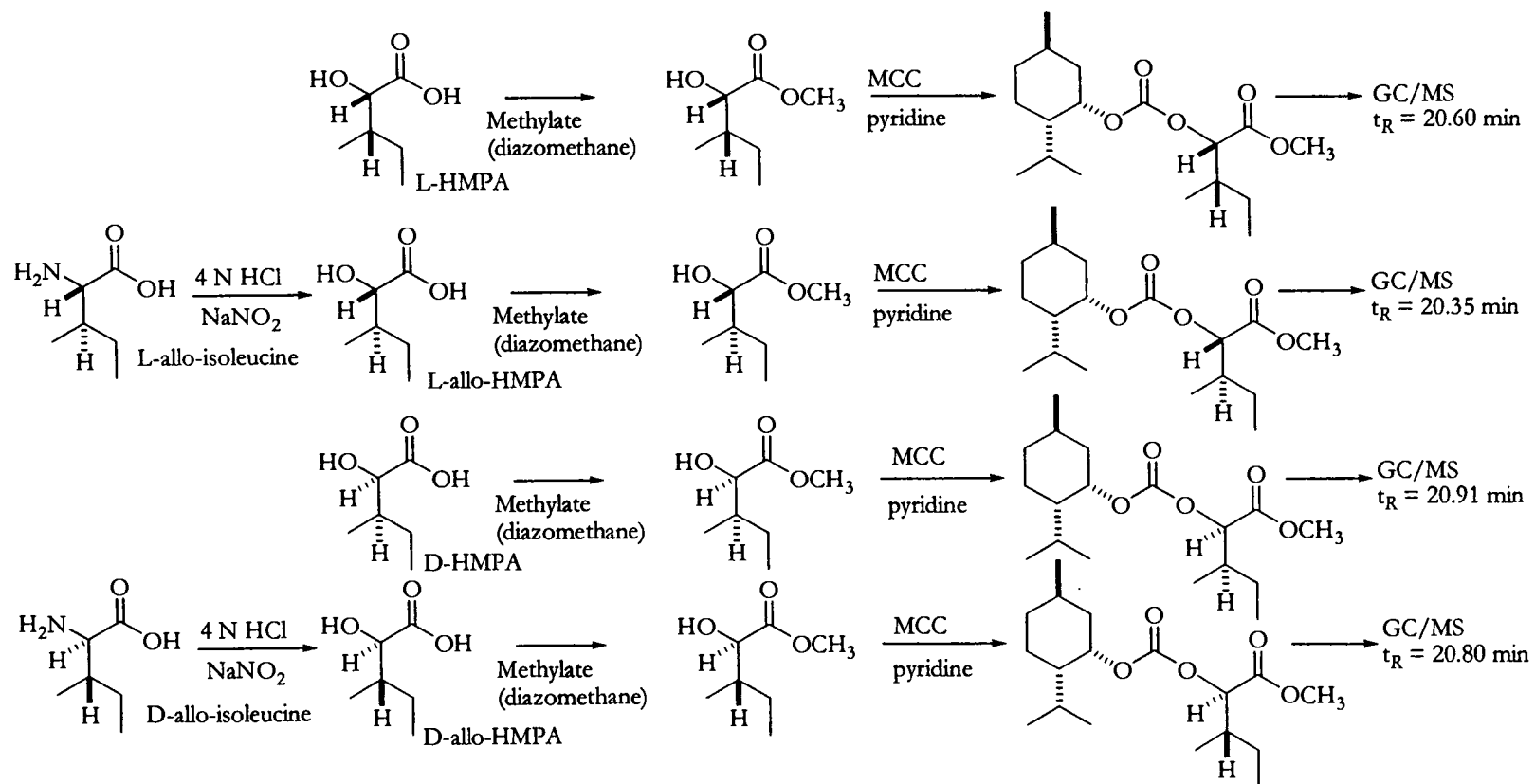


**Figure V.25.** The four stereoisomers of HMPA, the synthesis of L-allo and D-allo-HMPA, and the synthesis of menthyl carbonates for GC/MS analysis (MCC = Menthoxycarbonyl chloride).

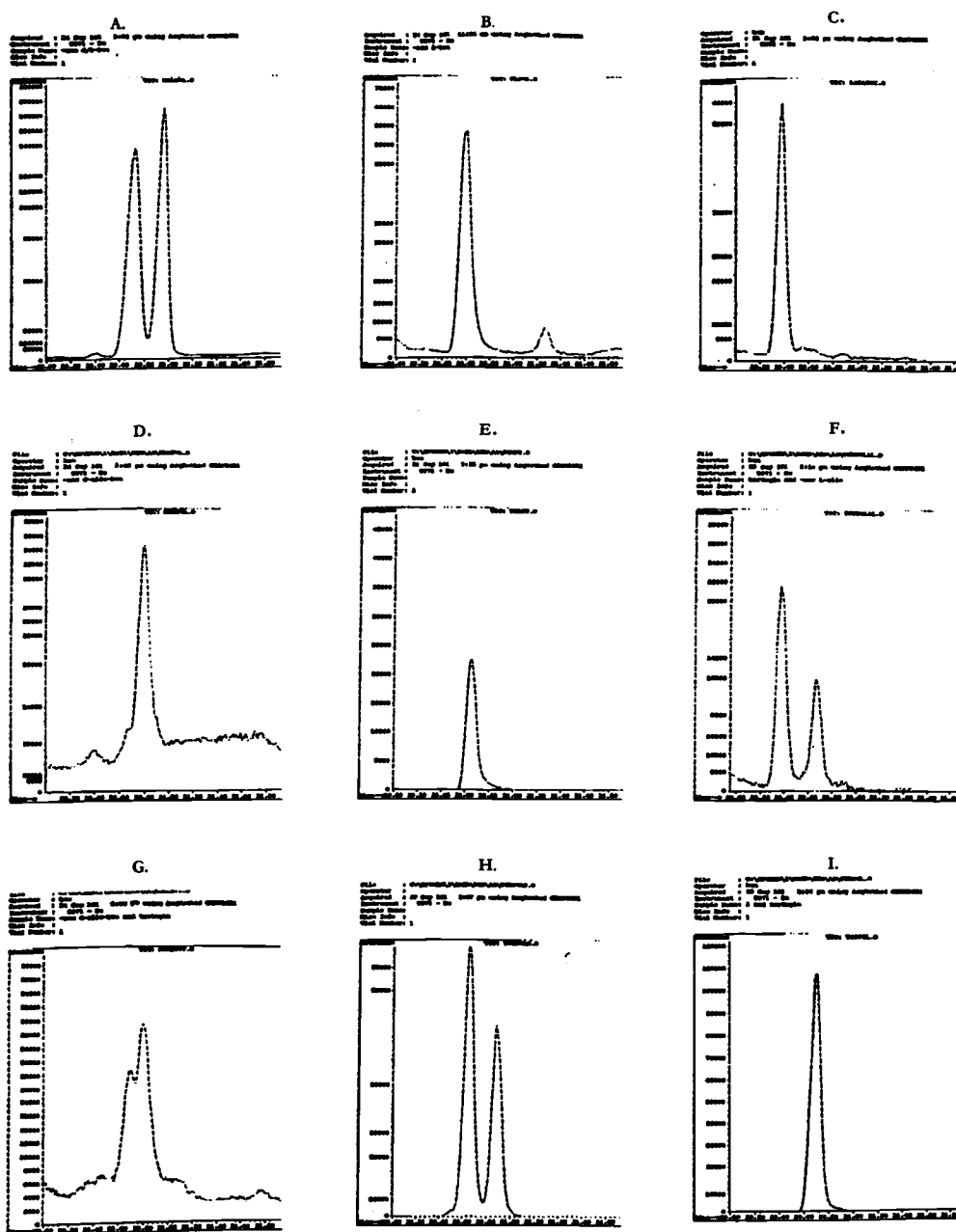


**Figure V.26.** GC/MS analysis of MCC derivatized HMPAs and tortugin ( $t_R$  = retention time). **A.** L and D-HMPA-MCC ( $t_R$  20.70 and 20.95, respectively). **B.** L-HMPA-MCC ( $t_R$  20.70). **C.** L-allo-HMPA-MCC ( $t_R$  20.37). **D.** D-allo-HMPA-MCC ( $t_R$  20.80). **E.** HMPA-MCC (from tortugin,  $t_R$  20.70). **F.** Tortugin HMPA-MCC and L-allo-HMPA-MCC coinjection. **G.** Tortugin HMPA-MCC and D-allo-HMPA-MCC coinjection. **H.** Tortugin-HMPA-MCC and L/D-HMPA-MCC coinjection. Notice the increase in L-HMPA. **I.** Tortugin-HMPA-MCC and L-HMPA-MCC coinjection.

## EXPERIMENTAL

### GENERAL

NMR spectra were recorded on a Bruker DRX 600 MHz spectrometer. Mass spectra were recorded on a Kratos MS50TC mass spectrometer. UV spectra were recorded on a Hewlett Packard 8452A diode array spectrophotometer while FT-IR spectra were recorded on a Nicolet 510 spectrophotometer. Chiral GC-MS analysis was accomplished on a Hewlett Packard Gas Chromatograph 5890 Series II Gas Chromatograph with a Hewlett Packard 5971 Mass Selective Detector using an Alltech capillary column (CHIRASIL-VAL Phase 25 m x 0.25 mm). HPLC separation was accomplished with Waters M-6000A and 515 pumps, a Rheodyne 7010 injector, and Waters Lambda-Max 480 and PDA 1515 spectrophotometers. Optical rotation measurements were recorded on Perkin-Elmer Model 141 and 252 polarimeters.

### BIOLOGICAL MATERIAL

The marine cyanobacterium, *Lyngbya majuscula*, was collected by hand from shallow water (2 m) on 15 November, 1995 at Bush Key, Dry Tortugas, Florida, and stored at -20°C in IPA until workup. A voucher sample is available from WHG as collection number DBK-15 NOV 95-4. The original collection was made by J.V. Rossi.

#### EXTRACTION AND ISOLATION OF LYNGBYABELLIN B (**96**)

- The IPA preserved alga (476 g dry wt) was extracted with  $\text{CH}_2\text{Cl}_2$  (2:1) two times to give a crude extract of 2.6 g. A portion of this (2.5 g) was fractionated using vacuum liquid chromatography (VLC) on Si gel with a stepwise gradient of hexanes/EtOAc/MeOH to give 8 fractions. Because fractions 6 and 7 (eluted 50–75% EtOAc/hexanes) contained **96**, they were recombined and subjected to VLC (hexanes/EtOAc/MeOH) and collected as 7 fractions. Fractions 5 and 6 (60–100% EtOAc/hexanes) both possessed **96** and were recombined. This fraction was further purified over a Waters Sep-Pak  $\text{C}_{18}$  solid phase extraction cartridge (75% MeOH/ $\text{H}_2\text{O}$ ). ODS RP-HPLC (Phenomenex ODS, 250 x 10 mm, 5  $\mu$ ) in 90% MeOH/ $\text{H}_2\text{O}$  afforded a single peak which was further purified using ODS RP-HPLC (Phenomenex ODS, 250 x 4.60 mm, 5 $\mu$ ) in 70% MeOH/ $\text{H}_2\text{O}$  to yield **96** (peak centered at 14 min, 7.1 mg, 0.3% of extract).

#### EXTRACTION AND ISOLATION OF TORTUGIN (**101**)

The IPA preserved alga (125.8 gms dry wt) was extracted with  $\text{CH}_2\text{Cl}_2$ /MeOH (2:1) two times to give a crude extract of 3.0 g. A portion of this (2.5 g) was fractionated using vacuum liquid chromatography (VLC) on Si gel with a stepwise gradient of hexanes/EtOAc and EtOAc/MeOH to give eight fractions. Because fractions six and seven (eluted 60%–100% Hexanes/EtOAc) both contained **101**, they were recombined and subjected to RP-HPLC (ODS) in 90% MeOH/ $\text{H}_2\text{O}$ . Final purification was accomplished using RP-HPLC (ODS) in 70% MeOH/ $\text{H}_2\text{O}$  to yield pure **101** (51 mg, 0.02% of total extract).

## LYNGBYABELLIN B (96)

Pure lyngbyabellin B showed an  $[\alpha]_D^{25} +158^\circ$  ( $\text{CHCl}_3$ ,  $c$  0.1); UV  $\lambda_{\text{max}}$  (MeOH) 246 nm ( $\log \epsilon$  4.20); IR  $\nu_{\text{max}}$  (film) 3323, 2959, 1718, 1674, 1513, 1234, 1145; FABMS (3-NBA) obs.  $m/z$  (rel int) 679 (100), 665 (15), 201 (30), 166 (70); HR FABMS (3-NBA) obs.  $[M + H]^+$   $m/z$  679.1794 for  $\text{C}_{28}\text{H}_{41}\text{O}_7\text{N}_4\text{Cl}_2\text{S}_2$  ( $\Delta -2.3$  mmu);  $^1\text{H}$  and  $^{13}\text{C}$  data see Table V.3

## TORTUGIN (101)

Pure tortugin showed  $[\alpha]_D^{25} -38$  (MeOH,  $c$  1.0); UV  $\lambda_{\text{max}}$  (MeOH) 210 nm ( $\log \epsilon = 15,000$ ); IR  $\nu_{\text{max}}$  (film) 3299, 2948, 2114, 1735, 1652, 1524, 1185, 695  $\text{cm}^{-1}$ ; FABMS (3-NBA) obs.  $m/z$  (rel int) 625 (100), 534 (10), 444 (23), 182 (100); HRFABMS (3-NBA) obs.  $[M+H]^+$   $m/z$  625.3965 for  $\text{C}_{35}\text{H}_{53}\text{O}_6\text{N}_4$  ( $\Delta$  0.8 mmu);  $^1\text{H}$  and  $^{13}\text{C}$  data see Table V.4

## CHIRAL ANALYSIS OF LYNGBYABELLIN B

Lyngbyabellin B was ozonized (0.2 mg of **96** in 1 mL  $\text{CH}_2\text{Cl}_2$ , 1 min, ambient temperature), immediately dried *in vacuo*, and hydrolyzed (1 ml 6 N HCl, 110°C, 18 hr). The hydrolysate was dried under nitrogen and derivatized using an Alltech PFP-IPA Amino Acid Kit (#18093). The dried hydrolysate was treated with 0.2 N HCl (5 min at 110°), and then again dried under nitrogen. To this, 150  $\mu\text{l}$  of acetyl chloride and 500  $\mu\text{l}$  of IPA was added and heated at 110° for 45 min. After drying with nitrogen,



the derivatizing agent, pentafluoropropionic anhydride (1 mL dissolved in 2 mL  $\text{CH}_2\text{Cl}_2$ ), was added and the solution heated at 115 °C for 15 min, blown dry with nitrogen, and then solubilized in hexanes. For standards, 1 mg each of the *L* and *D/L* valine were subjected to the identical derivatization sequence as the ozonized hydrolysate of **96**. All samples were analyzed by gas chromatography under identical conditions, beginning with a sustained initial oven temperature of 50 °C (4 min), a 3 °C/min ramp from 50 °C to 150 °C and concluding with a 2 0°C min ramp from 150 °C to 180 °C. The derivatized lyngbyabellin B fragment as well as the derivatized *L*-valine standard coeluted at  $t_R=14.34$  min. The derivatized *D*-valine eluted at  $t_R=13.59$  min.

#### CHIRAL ANALYSIS OF TORTUGIN

Tortugin was hydrolyzed (1 ml) by incubating in 6 N HCl in an oven at 110 °C for 18 hrs. The hydrolysate was dried under a constant stream of nitrogen. Derivatization was accomplished using an Alltech PFP-IPA Amino Acid Kit (#18093). The dried hydrolysate was treated with 0.2 N HCl for five minutes at 110°C, then dried under a constant stream of nitrogen. To this vial, 150  $\mu\text{L}$  of acetyl chloride and 500  $\mu\text{L}$  of IPA were added, then the vial was heated for 45 min at 110 °C. After drying with a constant stream of nitrogen, the derivatizing agent, pentafluoropropionic anhydride (1 ml in 2ml  $\text{CH}_2\text{Cl}_2$ ) was added. The vial was heated to 115 °C for 15 min then blown dry with nitrogen. The derivatized product was then solubilized in hexanes. To be used as standards, 1 mg of each of the phenylalanine enantiomers (*L* and *D*) was weighed into a tared vial and subjected to the identical

the identical derivatization sequence as the ozonized hydrolysate of **101**, as detailed above. All molecules were gas chromatographed under identical conditions. Beginning with a sustained initial oven temperature of 50 °C (4 min), a 3 °C/min ramp from 50 °C to 150 °C was followed by a 20 °C/min ramp from 150 °C to 180 °C. The derivitized tortugin eluted at 16.32 min, as did the derivitized standard *L*-phenylalanine. The derivitized *D*-phenylalanine was detected at 16.81 min. A portion of the hydrolyzed tortugin was also reacted with Marfey's reagent *N*α-(2,4-dinitro-5-fluoro-phenyl)-*L*-alaninamide (FDAA) in order to examine the NCH<sub>3</sub> amino acids present.<sup>131</sup> HPLC analysis of the derivitized tortugin amino acids and the FDAA-derivitized amino acid standards was accomplished using an aqueous gradient of triethylammonium phosphate (50 mM, pH 3.0)/MeCN 90:10 to 60:40 (UV detection at 340 nm). The tortugin amino acids coeluted with the *L*-Nme Ala (*t*<sub>R</sub> 26.51 min) and *L*-Leu standards (*t*<sub>R</sub> 32.63). An additional portion of the hydrolyzed tortugin sample was methylated with diazomethane then reacted with (1*R*)-(-)-menthyl carbonyl chloride to form the (1*R*)-(-)-menthyl carbonate methyl ester derivatives in preparation for GC/MS analysis. The analytical standards utilized were the commercially available *L*-HMPA and *D*-HMPA and the synthetically produced *L*-allo and *D*-allo-HMPA. To produce the allo acids, 5 mg each of *L* and *D*-isoleucine was solubilized in 1 ml 4*N* HCl in separate vials. To each of these vials 1 ml of a 0 °C solution of NaNO<sub>2</sub> in water (0.5 g/ml) was added and stirred at 0 °C for 4 hr and at room temperature overnight. The solutions were then extracted repeatedly with diethyl ether, dried with MgSO<sub>4</sub> and blown to near dryness with a stream of N<sub>2</sub> gas. All standards and the liberated residues of tortugin were methylated using diazomethane, followed by

creation of the menthyl carbonates. As such, 0.2 mg of derivatized tortugin was reacted with 20  $\mu\text{L}$  of menthyl carbonyl chloride (1.0  $\mu\text{mol}/\mu\text{L}$  (1R)-(-)-menthyl carbonyl chloride in dry benzene) in 120  $\mu\text{L}$  dry benzene and 20  $\mu\text{L}$  dry pyridine for 2 hr at room temperature. The sample was dried under nitrogen and resuspended in 100% hexanes. GC/MS analysis followed using an initial temperature of 100  $^{\circ}\text{C}$ , sustained for 0.5 min and a thermal ramp of 3  $^{\circ}\text{C}/\text{min}$  to a final temperature of 240  $^{\circ}\text{C}$ . Tortugin coeluted with derivatized L-HMPA at  $t_{\text{R}} = 20.60$  min (D-HMPA  $t_{\text{R}}$  20.95, D-allo-HMPA  $t_{\text{R}}$  20.80, L-allo-HMPA  $t_{\text{R}}$  20.37).

#### BRINE SHRIMP TOXICITY BIOASSAY

Evaluation for brine shrimp toxicity was performed as previously described using *Artemia salina* as the test organism.<sup>104</sup> After a 24 hr hatching period, aliquots of a 10 mg/mL stock solution of **96** and **101** were added to test wells containing 5 mL of artificial seawater and brine shrimp to achieve a range of final concentrations from 1.0–50 ppm. After 24 hr the live and dead shrimp were tallied.

#### ANTIMICROBIAL ASSAY

The antimicrobial activity of lyngbyabellin B was evaluated using standard paper sensitivity disk-agar plate methodology (disk diameter, 6 mm).<sup>127</sup> Lyngbyabellin B showed a 10.5 mm zone of inhibition at 100  $\mu\text{g}$  and a slight halo at 10  $\mu\text{g}$  against *Candida albicans* (ATCC 14053). No activity was observed against *Pseudomonas aeruginosa* (ATCC 10145), *Escherichia coli* (ATCC 11775), *Salmonella choleraesuis* subsp. *choleraesuis* (ATCC 14028), *Bacillus subtilis* (ATCC 6051), and *Staphylococcus aureus* (ATCC 12600).

## REFERENCES

106. Gerwick, W.H.; Jiang, Z.D.; Agarwal, S.K.; and Farmer, B.T. *Tetrahedron* **1992**, *48*, 2313-2324.
107. Orjala, J.; Nagle, D.G.; Hsu, V.L.; Gerwick, W.H. *J. Am. Chem. Soc.* **1995**, *117*, 8281-8282.
108. Luesch, H.; Yoshida, W.Y.; Moore, R.E.; Paul, V.J.; Mooberry, S.L. *J. Nat. Prod.* **2000**, *63*, 611-615.
109. Milligan, K.E.; Marquez, B.L.; Williamson, R.T.; Gerwick, W.H. *J. Nat. Prod.* **2000**, *63*, 1440-1443..
110. Luesch, H.; Yoshida, W.Y.; Moore, R.E.; Paul, V.J. *J. Nat. Prod.* **2000**, *63*, 1437-1439.
111. Marquez, B.L. Structure and Biosynthesis of Marine Cyanobacterial Natural Products: Development and Application of New NMR Methods. **2001** Ph.D. Thesis. Oregon State University, Corvallis, OR., **2001**.
112. Fusetani, N.; Matsunaga, S. *Chem. Rev.* **1993**, *93*, 1793-1806.
113. Davidson, B.S. *Chem Rev.*, **1993**, *93*, 1771-1791.
114. Pettit, G.R.; Kamano, Y.; Herald, C.L.; Dufresne, C.; Bates, R.B.; Cerney, R.L.; Schmidt, G.M.; Haruhisa, K. *J. Org. Chem.*, **1990**, *55*, 2989-2990.
115. Sitachitta, N.; Williamson, R.T.; Gerwick, W.H. *J. Nat. Prod.*, **2000**, *63*, 197-200.
116. Wan, F. and Erickson, K.L. *J. Nat. Prod.* **2001**, *64*, 143-146.
117. Milligan, K.E.; Marquez, B.L.; Gerwick, W.H. Manuscript in preparation.
118. Carroll, A.R.; Coll, J.C.; Bourne, D.J.; MacLeod, J.K.; Zabriskie, T.M.; Ireland, C.M.; Bowden, B.F. *Aust. J. Chem.* **1996**, *49*, 659-672.
119. Sone, H.; Kondo, T.; Kiryu, M.; Ishiwata, H.; Ojika, M.; Yamada, K. *J. Org. Chem.* **1995**, *60*, 4774-4781.
120. Reese, M.T.; Gulavita, N.K.; Nakao, Y.; Hamann, M.T.; Yoshida, W.Y.; Coval, S.J.; Scheuer, P.J. *J. Am. Chem. Soc.*, **1996**, *118*, 11081-11084.
121. Rodriguez, J.; Fernandez, R.; Quinoa, E.; Riguera, R.; Debitus, C.; Bouchet, P. *Tet. Lett.*, **1994**, *35*:49, 9239-9242.

122. Fernandez, R.; Rodriguez, J.; Quinoa, E.; Riguera, R.; Munoz, L.; Fernandez-Suarez, M.; Debitus, C. *J. Am. Chem. Soc.*, **1996**, *118*, 11635-11643.
123. Tan, L.T. Bioactive Natural Products from Marine Algae. Ph.D. Thesis. Oregon State University, Corvallis, OR., 2001.
124. Carmeli, S.; Moore, R.E.; Patterson, G.M.L. *J. Nat. Prod.* **1990**, *53*, 1533-1542.
125. Nakao, Y.; Yoshida, W.Y.; Szabo, C.M.; Baker, B.J.; Scheuer, P.J. *J. Org. Chem.* **1998**, *63*, 3272-3280.
126. Williamson, R. T.; Sitachitta, N.; Gerwick W. H. *Tetrahedron Lett.* **1999**, *40*, 175-5178.
127. Gerwick, W.H.; Mrozek, C.; Moghaddam, M.F.; Agarwal, S.K. *Experientia* **1989**, *45*, 115-121.
128. Graber, M.A. Natural Products from Temperate and Tropical Marine Algae. M.S. Thesis. Oregon State University, Corvallis, OR, **1996**.
129. Mamer, O.R. *Meth. Enzymol.* **2000**, *324*, 3-10.
130. Mamer, O.R. and Reimer, M.L.J. *J. Biol. Chem.* **1992**, *267*, 22141-22148.

## CHAPTER VI.

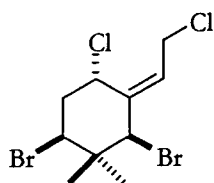
### SUMMARY

To reiterate the "Thesis Statement" presented in Chapter I; Algae are sessile organisms often encountered in areas of intense species diversity and herbivory.<sup>17-19</sup> As such, many have developed methods of defense most suitable for their local habitats. Chemical defense seems to be the defense of choice for smaller slow growing algae.<sup>17-19</sup> Since such secondary metabolites have been honed by evolutionary forces to be biologically active compounds, they represent a downstream stage of the "natural drug discovery process." The investigation of the secondary metabolites present in natural systems has two valuable outcomes, 1) an enhanced understanding and appreciation for the natural environment, with a heightened awareness of the intricate processes that are present yet barely understood and 2) a contribution to the drug discovery process by uncovering both biologically active and inactive secondary metabolites produced by biosynthetic pathways that, while originally protecting more primitive organisms, may lead to the next generation of pharmaceuticals which aid humans.

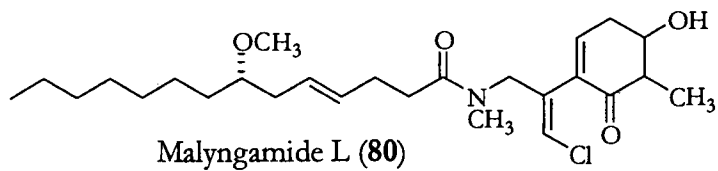
Presented within this thesis are the results of an effort to explore the secondary metabolites of marine algae. The overarching hypothesis of such work is that marine algae produce metabolites, which can be isolated and chemically defined, that will enhance the understanding of marine algae and their ecology and will play a necessary 'front line' role in drug discovery efforts.

The exploration of this hypothesis included the chemical investigation of seven samples of marine algae, a red alga and six cyanobacterial extracts, and the biological activity assessments of nearly 100 examples, representing all the major algal divisions. In total, six compounds new to the literature have been isolated and chemically defined as products of marine algae (Figure VI.1). These secondary metabolites were derived from algae originating from locations circling the globe, including Fiji, Madagascar, Dry Tortugas (Florida), and Curacao.

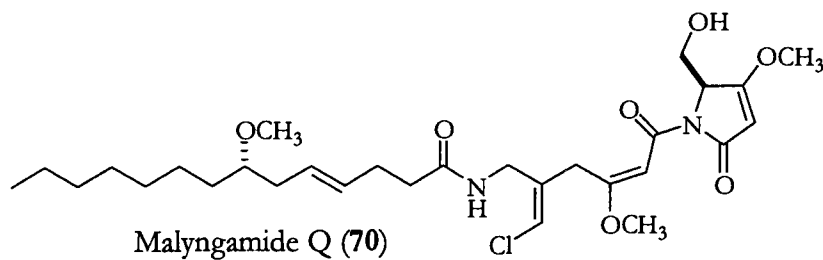
A survey for toxicity against *Biomphalaria glabrata*, was undertaken to examine the molluscicidal activity present in marine algal extracts. It was posited that because snails are a primary marine herbivore, marine algal extracts, if chemically defended against molluscan predation, will display toxicity to freshwater molluscs as well. Molluscicidal pursuits are stimulated in an attempt to control the spread of schistosomiasis by eliminating the intermediate host (*B. glabrata*) of the causative parasite, *Schistosoma mansoni*. The marine algal extracts examined were found to be strongly molluscicidal, with 46% displaying toxicity at 100 ppm and 34% of the extracts active at 50 ppm. Notable activity was observed especially for members of the Rhodophyta and cyanobacteria. As such, the red alga *Portieria hornemanni* and two Malagasy *Lyngbya majuscula* extracts were chemically investigated. Chondrocole C (**60**), previously isolated as a feeding deterrent to fish, was isolated as the major molluscicidal component of the dramatically active *P. hornemanni*.<sup>76</sup> The decreased activity of the pure compound as compared to the more active fractions and crude extract suggests either the susceptibility of **60** to degrade when in a pure state or the synergistic activity of multiple compounds resulting in full toxicity. From two



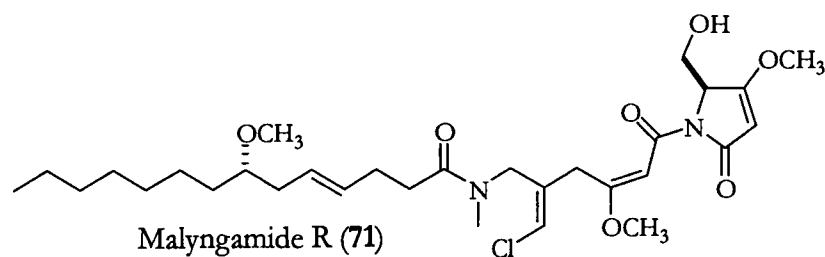
Taviochtodene (65)



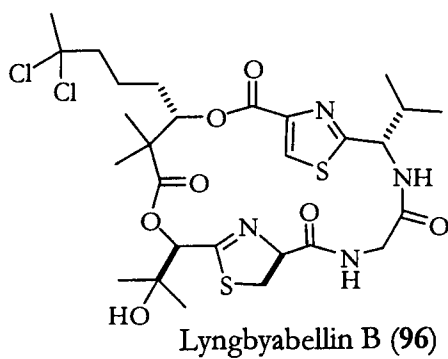
Malyngamide L (80)



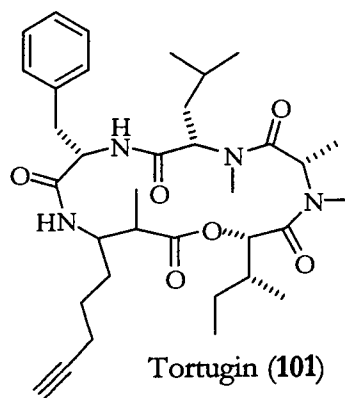
Malyngamide Q (70)



Malyngamide R (71)



Lyngbyabellin B (96)



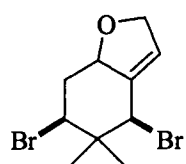
Tortugin (101)

**Figure VI.1.** Newly reported secondary metabolites from marine algae presented within this thesis.

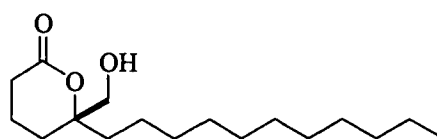


different *L. majuscula* extracts, the molluscicidal metabolites tanikolide (**32**)<sup>61</sup> and debromoaplysiatoxin (**20**)<sup>63</sup> were isolated (Figure VI.2). Active at an LD<sub>50</sub> = 0.003 ppm, debromoaplysiatoxin is one of the most potent molluscicides discovered. Despite the activity of **20** as a PKC activator,<sup>64</sup> such potency may have utility as a molluscicide, especially in artificial waterways such as irrigation channels and rice paddies. The overall frequency of activity observed for marine algal extracts against *B. glabrata*, and the isolation of the active principle in three samples, supports the theory that marine algae produce secondary metabolites that will be toxic to freshwater snails.

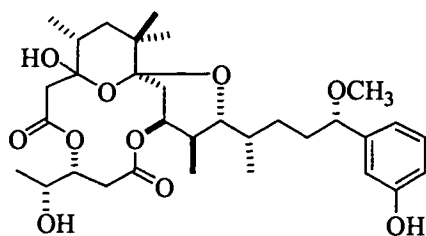
The discovery of chondrocole C as a molluscicidal secondary metabolite inspired the further investigation of *P. bornemanni*. In total five polyhalogenated monoterpenes were isolated, with one being the newly described taviochtodene. Also isolated, in addition to **60**, were chondrocole A/B (**58**, **59**),<sup>75</sup> 2-chloro-1,6 (*S*), 8-tribromo-3-(8)(*Z*)-ochtodene (**44b**),<sup>74</sup> and 2-dechlorohalomon (**55**).<sup>73</sup> The last of these, **55**, is a close structural relative of halomon (**50**), the promising anticancer lead that has thus far remained naturally and synthetically elusive.<sup>72,73</sup> The small size and chemical shift similarities within this structure class necessitate the extensive utilization of mass spectrometry (especially GC/MS) and NMR experiments to accurately determine chemical structures. Such experimentation led to the chemical shift re-assignment of chondrocole C as compared to those made in the literature (Figure VI.3).<sup>76</sup> Also, observations of the GC/MS fragmentation patterns for compounds containing multiple bromine and chlorine atoms allowed for the empirical assessment of the molecular weight of compounds, which lose halogens at ionization, and therefore prior to detection (Figure VI.4). The isolation of this suite of halogenated



Chondrocole C (60)



Tanikolide (32)



Debromoaplysiatoxin (20)

**Figure VI.2.** Molluscicidal metabolites isolated from marine algal extracts.

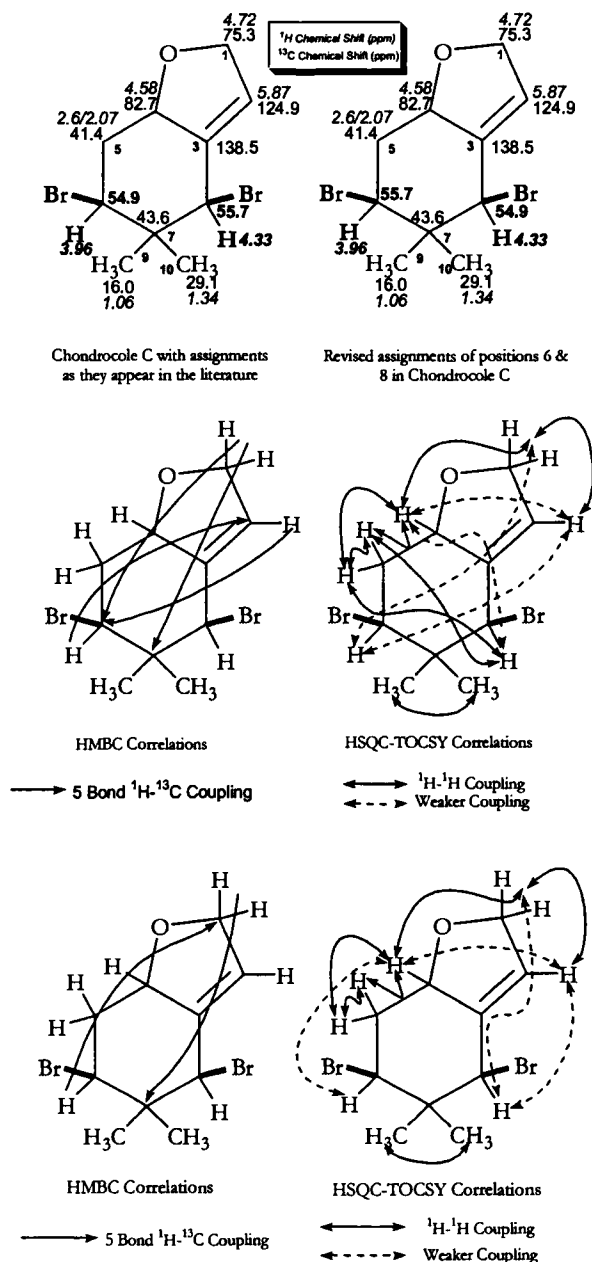


**Figure VI.3** The chemical shift re-assignment of chondrocole C.

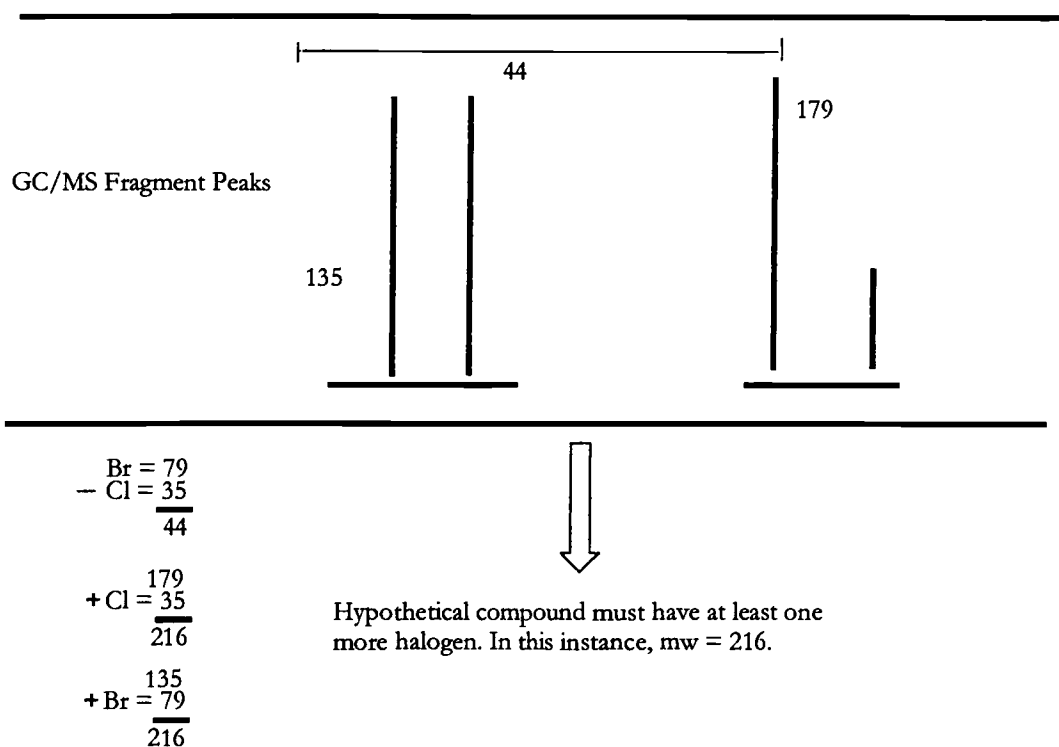


**Figure VI.4.** Hypothetical compound (mw = 216) supporting empirical observation that structural data can be obtained for halogenated compounds even when the halogen is too labile for mass spectral detection.

monoterpenes from a Fijian *P. hornemanni*, suggests a new location to search for red algal metabolites with therapeutic potential against cancer.

Despite lacking significant biological activity, the malyngamides are an intriguing and prominent *Lyngbya majuscula* secondary metabolites structure class. Malyngamides L (80), Q (70), and R (71), isolated from two different collections of *L. majuscula*, are some of the more recent literature additions for this growing structure class. While malyngamide L shares many characteristics with the standardly encountered cyclohexyl-type malyngamide, malyngamides Q and R offered some intriguing differences. Firstly, they show structural similarity to malyngamides A (66) and B (67), members of the less common pyrrolidone-type subclass of malyngamides.<sup>81-83</sup> Also, malyngamides Q and R were the first discovered malyngamides with an alternative stereochemistry at the vinyl-halide carbon (Figure VI.5). The initial observation of this alternate stereochemistry by the 1D DPGSE NOE pulse sequence helped lead to the development of the HSQMBC pulse sequence by Dr. R. Thomas Williamson and Dr. Brian L. Marquez to confirm this unique result by the accurate measurement of heteronuclear (H-C) coupling constants.<sup>99</sup> Following the publication of malyngamides Q and R, further examples of malyngamides were discovered presenting this alternate stereochemistry.<sup>83,92</sup> Also, as a result of the numerous malyngamide structures allowing the observation of molecular trends, hypotheses have been developed which suggest that malyngamide biogenesis proceeds through multiple acetate extensions of an amino acid, or amino acid derived, starter unit, with eventual ring closure and structural tailoring (Figure VI.6).

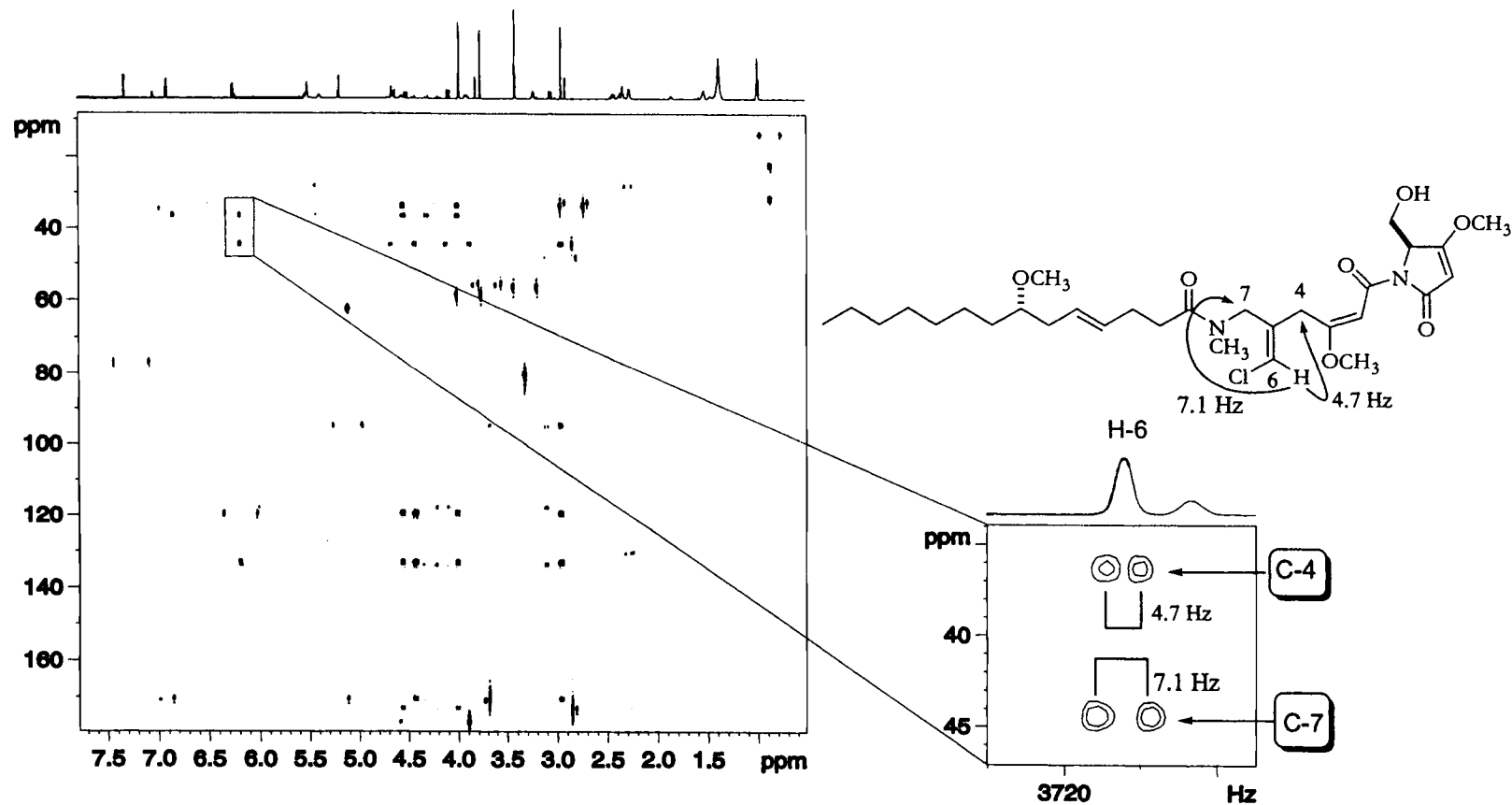


**Figure VI.5** HSQMBC spectra highlighting the long range heteronuclear coupling between H-6 and C-4 & 7 of malyncamide R.

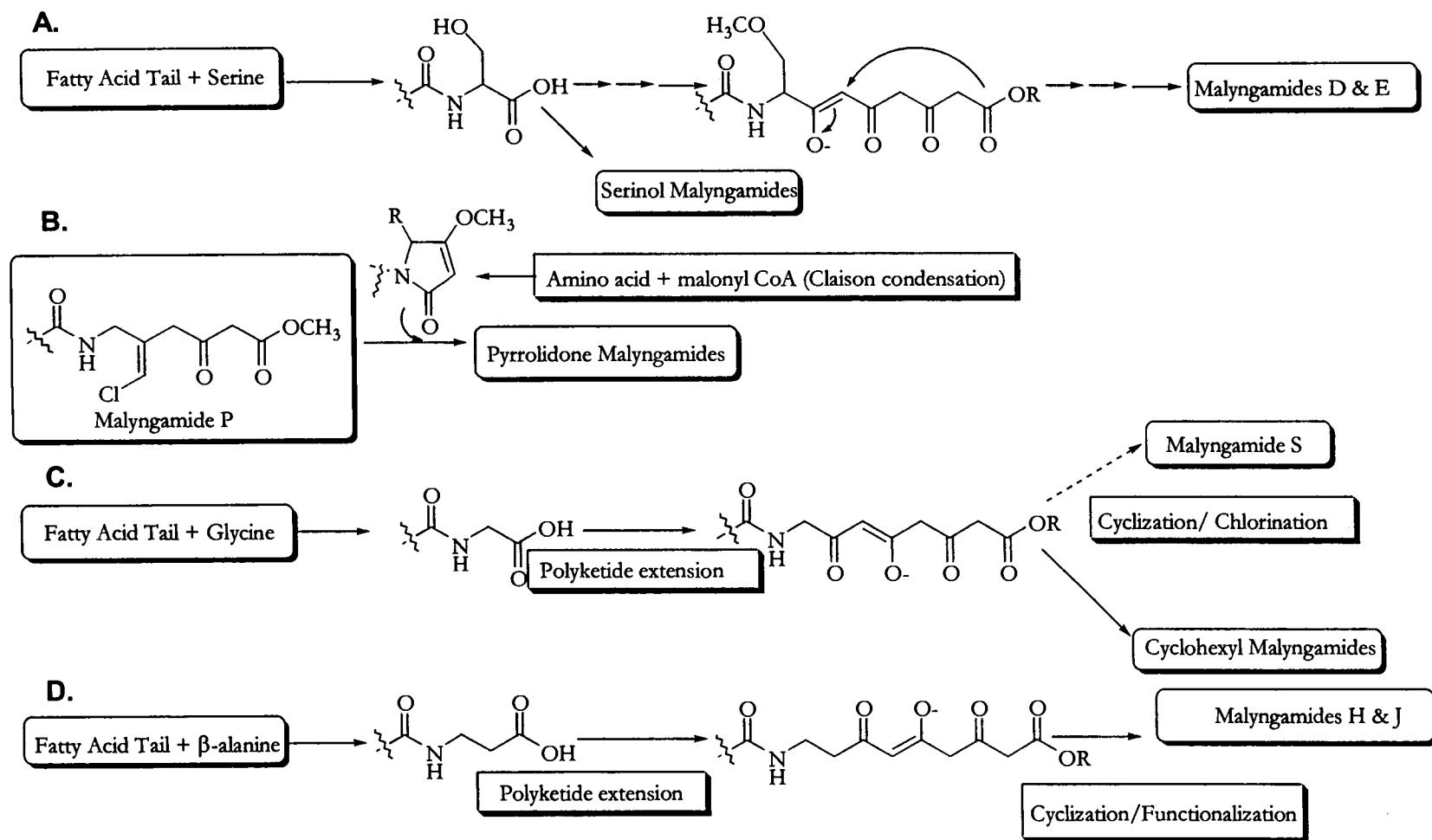
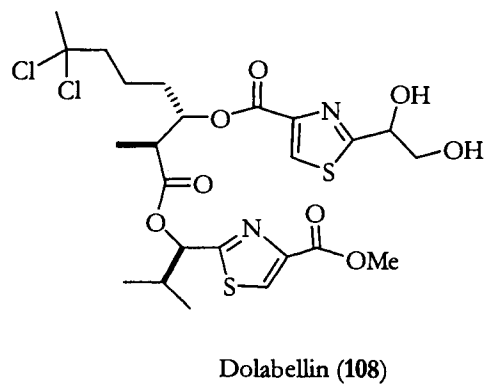
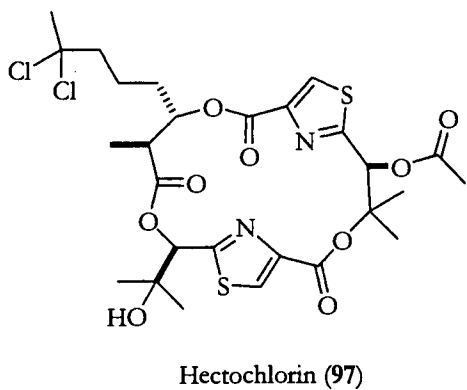
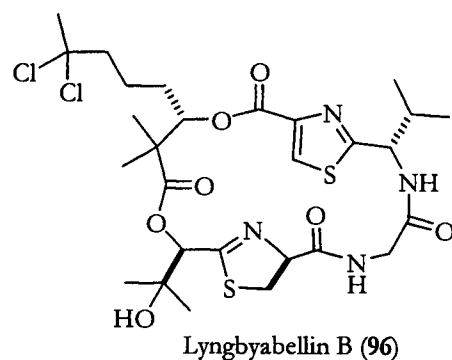
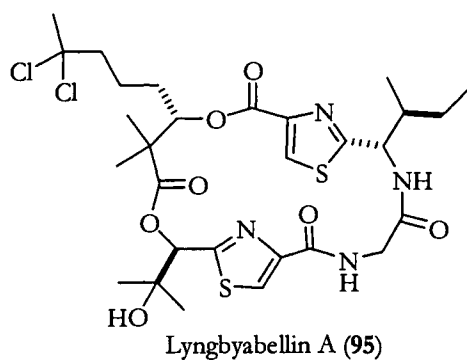
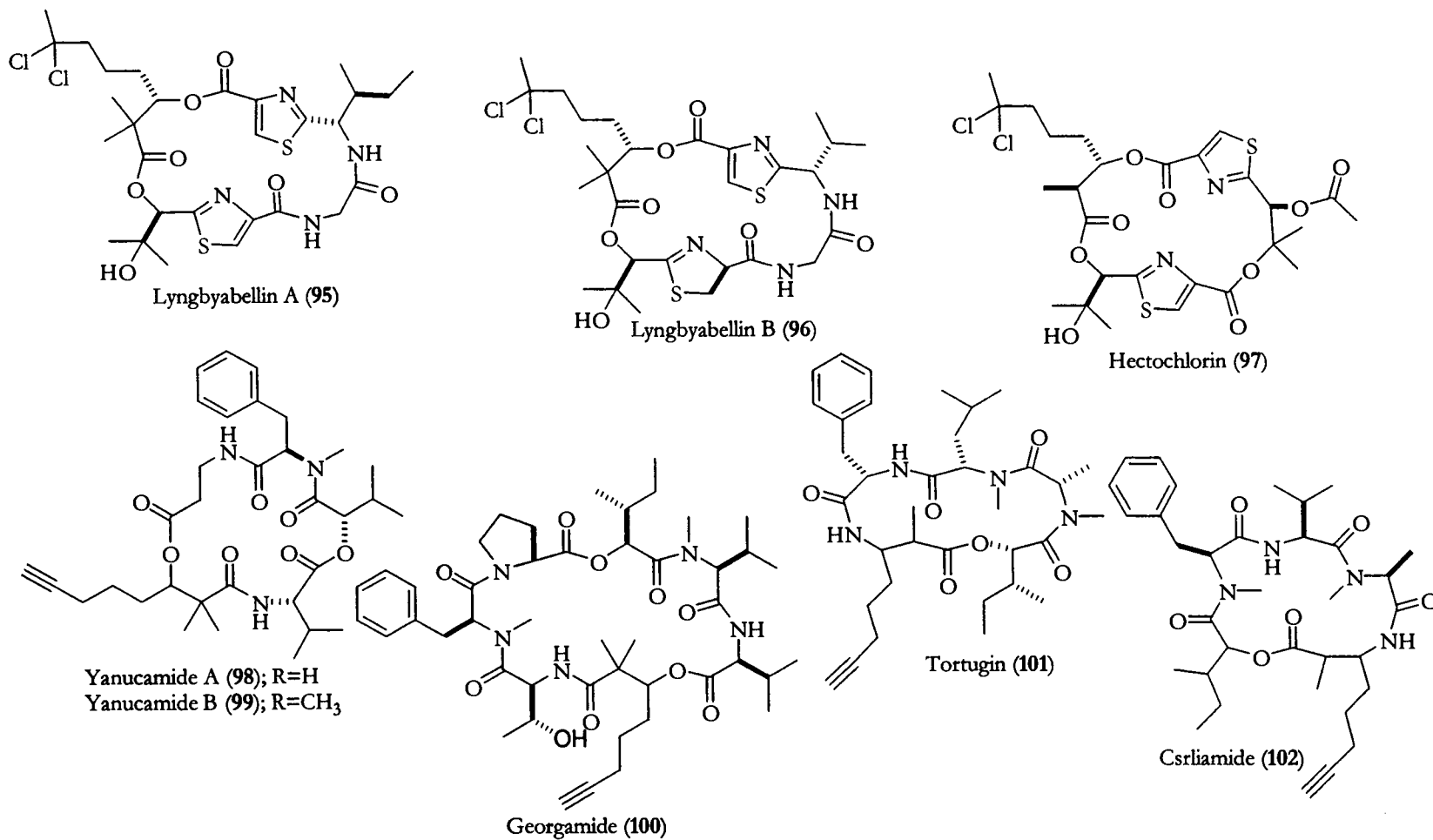


Figure VI.6 Malyngamide biogenesis.



**Figure VI.7.** The molluscan derived secondary metabolite dolabellin appears to be closely related to the *L. majuscula* metabolites lyngbyabellin A and B and hectochlorin.





**Figure VI.8.** Examples of cyanobacterial secondary metabolites possessing unusual octanoic and octynoic acid residues.

From a Dry Tortugas sample of *L. majuscula* two toxic cyclic depsipeptides, lyngbyabellin B (**96**) and tortugin (**101**), were isolated. Lyngbyabellin B, toxic to brine shrimp and *Candida albicans*, is a dichlorinated compound resembling the molluscan derived dolabellin (**108**; Figure VI.7).<sup>116</sup> Tortugin, displaying activity against brine shrimp, incorporates a seldom encountered terminal acetylene residue most commonly observed in a series of molluscan secondary metabolites, but discovered in an increasing number of cyanobacterial compounds (Figure VI.8).<sup>119-122</sup> The unambiguous cyanobacterial derivation of **96** and **101** provide support for the theory that many secondary metabolites attributed to molluscan *de novo* biosynthesis are originally produced by microalgae. The secondary metabolites are subsequently passed up the food chain through either direct or indirect predation. In some cases it appears that the molluscan predator derives chemical protection from the cyanobacterial metabolites through their accumulation and/or biotransformation.

Presented within this thesis are the results of an effort to explore the secondary metabolites of marine algae which support the hypothesis that marine algae produce metabolites which can be isolated and chemically defined and that will enhance the understanding of marine algae. Furthermore, their products have the potential to play a necessary 'front line' role in drug discovery efforts. Marine algae provide the basis for studies that span a wide range of disciplines including natural products chemistry, bioorganic chemistry, biochemistry, chemical ecology, classical ecology, and aquatic botany, among many others. They also provide us with a window into the intricately balanced undersea world, yielding, at once, tools with the potential

to stem diseases which plague humans, and a greater understanding of the natural environment.

## BIBLIOGRAPHY

- 1 Cox, P.A. and Balick, M.J. *Scientific American* **1994**, 4, 82-87.
- 2 McConnell, O.J.; Longley, R.E.; Koehn, F.E. *The Discovery of Natural Products with Therapeutic Potential*; Gullo, V.P., Ed.; Butterworth-Heinemann: Boston, **1994**; pp. 109-174.
- 3 Arasaki, S. and Arasaki, R. *Low Calorie, High Nutrition Vegetables from the Sea to help you look and feel better*, Japan Publications, Inc., Tokyo, **1983**; p. 136.
- 4 National Cancer Institute Cancer Web, Questions and Answers About NCI's Natural Products Branch, <http://www.graylab.ac.uk/cancernet/600733.html>, (accessed August 2001).
- 5 Cragg, G.M.; Newman, D.J.; Snader, K.M. *J. Nat. Prod.* **1997**, 60, 52-60.
- 6 Kelecom, A. *An. Acad. Bras. Ci.* **1999**, 71, 249-263.
- 7 Tsuda, K. and Kawamura, M. *J. Pharm. Soc. Japan* **1952**, 72, 771.
- 8 Kao, C.Y.; Levinson, S.R. *Tetrodotoxin, Saxitoxin, and the Molecular Biology of the Sodium Channel*, Kao, C.Y.; Levinson, S.R., Eds.; The New York Academy of Sciences: New York, **1986**.
- 9 Bergmann, W. and Feeney, R.J. *J. Org. Chem.* **1951**, 16, 981-987.
- 10 Scheuer, P.J. *Med. Res. Rev.* **1989**, 9, 535-542.
- 11 Wallace, R.W. *Molecular Medicine Today* **1997**, 4, 291-295.
- 12 Hay, M.E. and Fenical, W. *Oceanography* **1996**, 9, 10-20.
- 13 El Sayed, K.A.; Dunbar, D.C.; Bartyzel, P.; Zjawiony, J.K.; Day, W.; Hamann, M.T. In *Biologically Active Natural Products: Pharmaceuticals*, Cutler, S.J. and Cutler, H.G., Eds.; CRC Press: New York, **2000**, pp. 233-252.
- 14 Abbott, I.A. and Dawson, E.Y. In *How to Know the Seaweeds*, 2<sup>nd</sup> Ed., WCB McGraw-Hill: Boston, **1978**, pp. 1-19.
- 15 O'Clair, R.M. and Lindstrom, S.C. In *North Pacific Seaweeds*, Plant Press: Alaska, **2000**, pp. 1-8.

- 16 Dixon, G.H. In *Crop Protection Agents from Nature*; Copping, L.G. Ed.; SCI Publications: London, 1996, pp. 114-216.
- 17 Hay, M.E. *J. Exp. Bar. Biol. Ecol.* **1996**, 200, 103-134.
- 18 Hay, M.E. In *Ecological Roles of Marine Natural Products*, Paul, V.J., Ed., Comstock Publishing Associates: Ithaca, 1996, pp. 93-117.
- 19 Cronin, G. and Hay, M.E. *Oecologia* **1996**, 105, 361-368.
- 20 Littler, M.M. and Littler, D.S. *Am. Nat.* **1980**, 116, 25-44.
- 21 Conway, E. and Cole, K. *Phycologia* **1977**, 16, 205-216.
- 22 Gray, G. *Can. Med. Assoc. J.* **1996**; 155, 1613-1614.
- 23 Hatch, M.T.; Ehresmann, D.W.; Deig, F.E. *Mar. Algae Pharm. Sci.* **1979**, 343-363.
- 24 Neushul, D.E. *Hydrobiologia* **1990**, 204/205, 99-104.
- 25 Richards, C.S. *Antimicrob. Agents Chemother.* **1978**, 14, 24-35.
- 26 Thomson, A.W. and Fowler, E.F. *Agents and Actions.* **1981**, 11, 265-273.
- 27 Boyd, M.R.; Gustafson, K.R.; McMahon, J.B.; Shoemaker, R.H.; O'Keefe, B.R.; Mori, T.; Gulakowski, R.J.; Wu, L.; Rivera, M.I.; Laurencot, C.M.; Currens, M.J.; Cardellina, J.H.; Buckheit, R.W.; Nara, P.L.; Pannell, L.K.; Sowder, R.C.; Henderson, L.E. *Antimicrob. Agents Chemother.* **1997**, 41, 1521-1530.
- 28 Blakeslee, D. *JAMA Newslne* [Online] October 27, 1998.
- 29 Panda, D.; Himes, R.H.; Moore, R.E.; Wilson, L.; Jordan, M.A. *Biochemistry* **1997**, 36, 12948-12953.
- 30 Gerwick, W.H.; Proteau, P.J.; Nagle, D.G.; Hamel, E.; Blokhin, A.; Slate, D.L. *J. Org. Chem.* **1994**, 59, 1243-1245.
- 31 Wu, M.; Okino, T.; Nogle, L.M.; Marquez, B.L.; Williamson, R.T.; Sitachitta, N.; Berman, R.W.; Murray, T.F.; McGough, K.; Jacobs, R.; Colsen, K.; Asano, T.; Yokokawa, T.; Shioiri, T.; Gerwick, W.H. *J. Am. Chem. Soc.* **2000**, 122, 12041-12042.

- 32 Simonetti, J. *Rodale's Scuba Diving* 1997, 8.
- 33 Tan, L.T.; Sitachitta, N.; Gerwick, W.H. *Alkaloids*, in press.
- 34 Sze, P. *A Biology of the Algae*, 3<sup>rd</sup> Ed., WCB McGraw-Hill: Boston, 1998.
- 35 Haseeb, M.A. and Eveland, L.K. *Experientia* 1991, 47, 970-974.
- 36 Tingley, G.A. *Trans. R. Soc. Trop. Med. Hyg.* 1988, 448.
37. World Health Organization *The Control of Schistosomiasis: second report of the WHO expert committee* 1993, WHO Technical Report Series, World Health Organization:Geneva.
38. World Health Organization *The World Health Report 1998; Life in the 21<sup>st</sup> century, a vision for all* 1998, WHO Technical Report Series, World Health Organization:Geneva.
39. World Bank *World Development Report 1993: Investing in Health* 1993, Oxford University Press:London, pp. 1-329.
40. WHO Information Fact Sheets, Fact Sheet No. 115, <http://www.who.int/inf-fs/en/fact115.html>, (last accessed, August 2001).
41. WHO Infectious Diseases, Schistosomiasis, <http://www.who.int/ctd/schisto/index.html> (last accessed, August 2001).
42. WHO Infectious Diseases, Schistosomiasis, Burdens and Trends, <http://www.who.int/ctd/schisto/burdens.htm> (last accessed, August 2001).
43. Perrett, S. and Whitfield, P.J. *Parasitology Today* 1996, 12, 156-159.
44. Davis, A. In *Manson's Tropical Diseases*, Cook, G.C. Ed.; WB Saunders Co. Ltd.:London, 1996, pp. 1413-1456.
45. World Health Organization *Bench Aids for the Diagnosis of Intestinal Parasites*, 1994, WHO Technical Report Series, World Health Organization:Geneva.
46. Fournier, A.; Clement, P.; Mimouni, P.; Mingyi, X.; Combes, C. *Ethol. Ecol. Evol.* 1995, 5, 477-487.
47. Utzinger, J. *Novel Approaches in the Control of Schistosomiasis: from rapid identification to chemoprophylaxis*, 1999, <http://www.sti.unibas.ch/pdfs/utzipart1.pdf> and <http://www.sti.unibas.ch/pdfs/utzipart2.pdf>, (last accessed, August 2001).

48. World Health Organization *The Control of Schistosomiasis; Report of a WHO Expert Committee on the Control of Schistosomiasis*, 1985, WHO Technical Report Series, World Health Organization:Geneva.
49. Fahim, H. *Dams, People and Development: The Aswan High Dam Case*. Pergamon Press:New York, 1981.
50. Invading Species as Agents of Extinction, NRE 220 Lecture 7, <http://www-personal.umich.edu/~dallan/nre220/outline7.htm>, (last accessed August 2001).
51. Haas, W.; Korner, M.; Hutterer, E.; Wegner, M.; Haberl *Parasitol.* **1995**, *110*, 133-142.
52. Haberl, B.; Lakbe, M.; Fuchs, H.; Strobel, M.; Schmalfuss, G.; Haas, W. *Int. J. Parasitol.* **1995**, *25*, 551-560.
53. Haas, W.; Haberl, B.; Schmalfuss, G.; Khayyal, M.T. *J. Parasitol.* **1994**, *80*, 345-353.
54. Thomas, J.D. and Eaton, P. *Comp. Biochem. Physiol.* **1993**, *106C*, 781-796.
55. Sponholtz, G.M. and Short, R.B. *J. Parasitol.* **1975**, *61*, 228-232.
56. Roberts, T.M.; Stibbs, H.H.; Chernin, E.; Ward, S. *J. Parasitol.* **1978**, *64*, 277-282.
57. Monroy, F.P. and Loker, E.S. *J. Parasitol.* **1993**, *79*, 416-423.
58. Haas, W.; Haberl, B.; Kalbe, M.; Korner, M. *Parasitology Today* **1995**, *11*, 468-472.
59. World Health Organization *Bull. WHO* **1965**, *33*, 567-581.
60. Bureson, B.J.; Woodard, F.X.; Moore, R.E. *Chem. Lett.* **1975**, 1111-1114.
61. Singh, I.P.; Milligan, K.E.; Gerwick, W.H. *J. Nat. Prod.* **1999**, *62*, 1333-1335.
62. Cardellina, J.H.; Dalietos, D.; Marner, F.J.; Mynderse, J.S.; Moore, R.E. *Phytochemistry* **1978**, *17*, 2091-2093.
63. Mynderse, J.S.; Moore, R.E.; Kashiwagi, M.; Norton, T.R. *Science* **1977**, 538-544.
64. Beutler, J.A. *J. Nat. Prod.* **1990**, *53*, 867-874.
65. Liu, S.Y.; Sporer, F.; Wink, M.; Jourdan, J.; Henning, R.; Li, Y.L.; Ruppel, A. *Trop. Med. Int. Heal.* **1997**, *2*, 179-188.
66. Pechenik, J.A. *Biology of the Invertebrates* **1996**, WCB/McGraw Hill: Boston.

67. Crews, P.; Naylor, S.; Hanke, J.; Hogue, E.R.; Kho, E.; Craslau, R. *J. Org. Chem.* **1984**, *49*, 1371-1377.
68. Paul, V.J., McConnell, O.J.; and Fenical, W. *J. Org. Chem.* **1980**, *45*, 3401-3407.
69. Crews, P.; Myers, B.L.; Naylor, S.; Clason, E.L.; Jacobs, R.S.; Staal, G.B. *Phytochemistry* **1984**, *23*, 1451-1449.
70. McConnell, O.J. and Fenical, W.F. *J. Org. Chem.* **1978**, *43*, 4238-4241.
71. Gunatilaka, A.A.L.; Paul, V.J.; Park, P.U.; Puglisi, M.P. Gitier, A.D.; Eggleston, D.S.; Haltiwanger, R.C.; Kingston, D.G.I. *J. Nat. Prod.* **1999**, *62*, 1376-1378.
72. Fuller, R.W.; Cardellina, J.H.; Kato, Y.; Brinen, L.S.; Clardy, J.; Snader, K.M.; Boyd, M.R. *J. Med. Chem.* **1992**, *35*, 3007-3011.
73. Fuller, R.W.; Cardellina, J.H.; Jurek, J.; Scheuer, P.J.; Alvarado-Lindner, B.; McGuire, M.; Gray, G.N.; Steiner, J.R.; Clardy, J.; Menez, E.; Shoemaker, R.H.; Newman, J.N.; Snader, K.M.; Boyd, M.R. *J. Med Chem.* **1994**, *37*, 4407-4411.
74. Gerwick, W.H. *Phytochemistry* **1984**, *23*, 1323-1324.
75. Burreson, B.J.; Woolard, F.X.; Moore, R.E. *Tetrahedron Lett.* **1975**, 2155-2158.
76. Burreson, B.J.; Woolard, F.X.; Moore, R.E. *Chem. Lett.* **1975**, 1111-1114.
77. Woolard, F.X., Moore, R.E.; Van Engen, D.; Clardy, J. *Tetrahedron Lett.* **1978**, 2367-2370.
78. Paul, J.V.; Hay, M.E.; Duffy, J.E.; Fenical, W.; Gustafson, K. *J. Exp. Mar. Biol. Ecol.* **1987**, *114*, 249-260.
79. Coll, J.C. and Wright, A.D. *Aust. J. Chem.* **1989**, *42*, 1983-1993.
80. Firn, R.D. and Jones, C.G. *Mol. Microbiol.* **2000**, *37*, 989-994.
81. Cardellina, J.H.; Marner F.J.; Moore R.E. *J. Am. Chem. Soc.* **1979**, *101*, 240-242.
82. Cardellina, J.H.; Daliotos, D.; Marner, F.J.; Mynderse, J.S.; Moore, R.E. *Phytochemistry* **1978**, *17*, 2091-2095.
83. Kan, Y.; Sakamoto, B.; Fujita, T.; Nagai, H. *J. Nat. Prod.* **2000**, *63*, 1599-1602.



84. Ainslie, R.D.; Barchi, J.J.; Kuniyoshi, M.; Moore, R.E.; Mynderse, J.S. *J. Org. Chem.* **1985**, *50*, 2859-2862.
85. Mynderse, J.S. and Moore, R.E. *J. Org. Chem.* **1978**, *43*, 4359-4362.
86. Gerwick, W.H.; Reyes, S.; Alvarado, B. *Phytochemistry* **1987**, *26*, 1701-1704.
87. Praud, A.; Valls, R.; Banaigs, B. *Tetrahedron Lett.* **1993**, *34*, 5437-5440.
88. Orjala J.; Nagle, D.G.; Gerwick, W.H. *J. Nat. Prod.*, **1995**, *58*, 764-768.
89. Todd, J.S.; Gerwick, W.H. *Tetrahedron Lett.*, **1995**, *36*, 7837-7840.
90. Wu, M.; Milligan, K.E.; Gerwick, W.H. *Tetrahedron*, **1997**, *53*, 15983-15990.
91. Kan, Y.; Fujita, T.; Nagai, H.; Sakamoto, B.; Hokama, Y. *J. Nat. Prod.* **1998**, *61*, 152-155.
92. Gallimore, W.A.; Galario, D.L.; Lacy, C.; Zhu, Y.; Scheuer, P.J. *J. Nat. Prod.* **2000**, *63*, 1022-1024.
93. Milligan, K.E.; Marquez, B.L.; Williamson, R.T.; Davies-Coleman, M.; Gerwick, W.H. *J. Nat. Prod.* **2000**, *63*, 965-968.
94. Nogle, L.M. and Gerwick, W.H. Manuscript in preparation.
95. Wan, F. and Erickson, K.L. *J. Nat. Prod.* **2001**, *64*, 143-146.
96. Marquez, B.L.; Nogle, L.M.; Williamson, R.T.; Gerwick, W.H. *J. Nat. Prod.* in press.
97. Williamson R.T.; Carney, J.R. and Gerwick, W. H. *J. Nat. Prod.*, (Submitted).
98. Stott, K.; Keeler, J.; Van, Q.N.; Shaka, A.J. *J. Mag. Reson.*, **1997**, *125*, 302-324.
99. Williamson, R.T.; Marquez, B.L.; Kover, K.E.; Gerwick, W.H. *Magn. Reson. Chem.*, **2000**, *38*, 265-273.
100. Willker, W.; Leibfritz, D. *J. Mag. Reson.*, **1995**, *33*, 632.
101. Titman, J.T.; Neuhaus, D.; Keeler, J. *J. Mag. Reson.*, **1989**, *85*, 111-131
102. Marek, R.; Kralik, L.; Sklenar, V. *Tetrahedron Lett.*, **1997**, *38*, 665-668.
103. McDonald, L.A.; Ireland, C.M. *J. Nat. Prod.*, **1992**, *55*:3, 376-379.

104. Meyer, B.N.; Ferrigni, N.R.; Putnam, J.E.; Jacobsen, L.B.; Nichols, D.E.; McLaughlin J.L. *Planta Medica*, **1982**, *45*, 31-34.
105. Bakus, G.J. and Green, G. *Science* **1974**, *185*, 951-953.
106. Gerwick, W.H.; Jiang, Z.D.; Agarwal, S.K.; and Farmer, B.T. *Tetrahedron* **1992**, *48*, 2313-2324.
107. Orjala, J.; Nagle, D.G.; Hsu, V.L.; Gerwick, W.H. *J. Am. Chem. Soc.* **1995**, *117*, 8281-8282.
108. Luesch, H.; Yoshida, W.Y.; Moore, R.E.; Paul, V.J.; Mooberry, S.L. *J. Nat. Prod.* **2000**, *63*, 611-615.
109. Milligan, K.E.; Marquez, B.L.; Williamson, R.T.; Gerwick, W.H. *J. Nat. Prod.* **2000**, *63*, 1440-1443..
110. Luesch, H.; Yoshida, W.Y.; Moore, R.E.; Paul, V.J. *J. Nat. Prod.* **2000**, *63*, 1437-1439.
111. Marquez, B.L. Structure and Biosynthesis of Marine Cyanobacterial Natural Products: Development and Application of New NMR Methods. Ph.D. Thesis. Oregon State University, Corvallis, OR., **2001**.
112. Fusetani, N.; Matsunaga, S. *Chem. Rev.* **1993**, *93*, 1793-1806.
113. Davidson, B.S. *Chem Rev.*, **1993**, *93*, 1771-1791.
114. Pettit, G.R.; Kamano, Y.; Herald, C.L.; Dufresne, C.; Bates, R.B.; Cerney, R.L.; Schmidt, G.M.; Haruhisa, K. *J. Org. Chem.*, **1990**, *55*, 2989-2990.
115. Sitachitta, N.; Williamson, R.T.; Gerwick, W.H. *J. Nat. Prod.*, **2000**, *63*, 197-200.
116. Wan, F.; Erickson, K.L. *J. Nat. Prod.* **2001**, *64*, 143-146.
117. Milligan, K.E.; Marquez, B.L.; Gerwick, W.H. Manuscript in preparation.
118. Carroll, A.R.; Coll, J.C.; Bourne, D.J.; MacLeod, J.K.; Zabriskie, T.M.; Ireland, C.M.; Bowden, B.F. *Aust. J. Chem.* **1996**, *49*, 659-672.
119. Sone, H.; Kondo, T.; Kiryu, M.; Ishiwata, H.; Ojika, M.; Yamada, K. *J. Org. Chem.* **1995**, *60*, 4774-4781.
120. Reese, M.T.; Gulavita, N.K.; Nakao, Y.; Hamann, M.T.; Yoshida, W.Y.; Coval, S.J.; Scheuer, P.J. *J. Am. Chem. Soc.*, **1996**, *118*, 11081-11084.

121. Rodriguez, J.; Fernandez, R.; Quinoa, E.; Riguera, R.; Debitus, C.; Bouchet, P. *Tetrahedron Lett.*, **1994**, 35:49, 9239-9242.
122. Fernandez, R.; Rodriguez, J.; Quinoa, E.; Riguera, R.; Munoz, L.; Fernandez-Suarez, M.; Debitus, C. *J. Am. Chem. Soc.*, **1996**, 118, 11635-11643.
123. Tan, L.T. Bioactive Natural Products from Marine Algae. Ph.D. Thesis. Oregon State University, Corvallis, OR., **2001**.
124. Carmeli, S.; Moore, R.E.; Patterson, G.M.L. *J. Nat. Prod.* **1990**, 53, 1533-1542.
125. Nakao, Y.; Yoshida, W.Y.; Szabo, C.M.; Baker, B.J.; Scheuer, P.J. *J. Org. Chem.* **1998**, 63, 3272-3280.
126. Williamson, R. T.; Sitachitta, N.; Gerwick W. H. *Tetrahedron Lett.* **1999**, 40, 175-5178.
127. Gerwick, W.H.; Mrozek, C.; Moghaddam, M.F.; Agarwal, S.K. *Experientia* **1989**, 45, 115-121.
128. Graber, M.A. Natural Products from Temperate and Tropical Marine Algae. M.S. Thesis. Oregon State University, Corvallis, OR. **1996**.
129. Mamer, O.R. *Meth. Enzymol.* **2000**, 324, 3-10.
130. Mamer, O.R. and Reimer, M.L.J. *J. Biol. Chem.* **1992**, 267, 22141-22148.